



ISSN 2499-9768 print

МОРСКОЙ
БИОЛОГИЧЕСКИЙ
ЖУРНАЛ
MARINE BIOLOGICAL JOURNAL

Vol. 9 No. 1
2024



МОРСКОЙ БИОЛОГИЧЕСКИЙ ЖУРНАЛ
MARINE BIOLOGICAL JOURNAL

Выпуск посвящён 300-летию Российской академии наук.

Журнал включён в перечень рецензируемых научных изданий, рекомендованных ВАК Российской Федерации, а также в базу данных Russian Science Citation Index (RSCI).

Журнал реферируется международной библиографической и реферативной базой данных Scopus (Elsevier), международной информационной системой по водным наукам и рыболовству ASFA (ProQuest), Всероссийским институтом научно-технической информации (ВИНИТИ),

а также Российским индексом научного цитирования (РИНЦ) на базе Научной электронной библиотеки elibrary.ru.

Все материалы проходят независимое двойное слепое рецензирование.

Редакционная коллегия

Главный редактор

Егоров В. Н., акад. РАН, д. б. н., проф., ФИЦ ИнБЮМ

Заместитель главного редактора

Солдатов А. А., д. б. н., проф., ФИЦ ИнБЮМ

Ответственный секретарь

Корнийчук Ю. М., к. б. н., ФИЦ ИнБЮМ

Адрианов А. В., акад. РАН, д. б. н., проф.,
ННЦМБ ДВО РАН

Азовский А. И., д. б. н., проф., МГУ

Васильева Е. Д., д. б. н., МГУ

Генкал С. И., д. б. н., проф., ИБВВ РАН

Денисенко С. Г., д. б. н., ЗИН РАН

Довгаль И. В., д. б. н., проф., ФИЦ ИнБЮМ

Зуев Г. В., д. б. н., проф., ФИЦ ИнБЮМ

Коновалов С. К., чл.-корр. РАН, д. г. н., ФИЦ МГИ

Мильчакова Н. А., к. б. н., ФИЦ ИнБЮМ

Неврова Е. Л., д. б. н., ФИЦ ИнБЮМ

Празукин А. В., д. б. н., ФИЦ ИнБЮМ

Руднева И. И., д. б. н., проф., ФИЦ МГИ

Рябушко В. И., д. б. н., ФИЦ ИнБЮМ

Самышев Э. З., д. б. н., проф., ФИЦ ИнБЮМ

Санжарова Н. И., чл.-корр. РАН, д. б. н., ВНИИРАЭ

Совга Е. Е., д. г. н., проф., ФИЦ МГИ

Стельмах Л. В., д. б. н., ФИЦ ИнБЮМ

Трапезников А. В., д. б. н., ИЭРиЖ УрО РАН

Фесенко С. В., д. б. н., проф., ВНИИРАЭ

Arvanitidis Chr., D. Sc., HCMR, Greece

Bat L., D. Sc., Prof., Sinop University, Turkey

Ben Souissi J., D. Sc., Prof., INAT, Tunis

Kociolek J. P., D. Sc., Prof., CU, USA

Magni P., PhD, CNR-IAS, Italy

Moncheva S., D. Sc., Prof., IO BAS, Bulgaria

Pešić V., D. Sc., Prof., University of Montenegro, Montenegro

Zaharia T., D. Sc., NIMRD, Romania

Zaharia T., D. Sc., NIMRD, Romania

Адрес учредителя, издателя и редакции:

ФИЦ «Институт биологии южных морей имени А. О. Ковалевского РАН».

Пр-т Нахимова, 2, Севастополь, 299011, РФ.

Тел.: +7 8692 54-41-10. E-mail: mbj@imbr-ras.ru.

Сайт журнала: <https://marine-biology.ru>.

Адрес соиздателя:

Зоологический институт РАН.

Университетская наб., 1, Санкт-Петербург, 199034, РФ.

Editorial Board

Editor-in-Chief

Egorov V. N., Acad. of RAS, D. Sc., Prof., IBSS, Russia

Assistant Editor

Soldatov A. A., D. Sc., Prof., IBSS, Russia

Managing Editor

Korneychuk Yu. M., PhD, IBSS, Russia

Adrianov A. V., Acad. of RAS, D. Sc., Prof.,
NSCMB FEB RAS, Russia

Arvanitidis Chr., D. Sc., HCMR, Greece

Azovsky A. I., D. Sc., Prof., MSU, Russia

Bat L., D. Sc., Prof., Sinop University, Turkey

Ben Souissi J., D. Sc., Prof., INAT, Tunis

Denisenko S. G., D. Sc., ZIN, Russia

Dovgal I. V., D. Sc., Prof., IBSS, Russia

Fesenko S. V., D. Sc., Prof., RIRAE, Russia

Genkal S. I., D. Sc., Prof., IBIW RAS, Russia

Kociolek J. P., D. Sc., Prof., CU, USA

Konovalev S. K., Corr. Member of RAS, D. Sc., Prof.,

MHI RAS, Russia

Magni P., PhD, CNR-IAS, Italy

Milchakova N. A., PhD, IBSS, Russia

Moncheva S., D. Sc., Prof., IO BAS, Bulgaria

Nevrova E. L., D. Sc., IBSS, Russia

Pešić V., D. Sc., Prof., University of Montenegro, Montenegro

Prazukin A. V., D. Sc., IBSS, Russia

Rudneva I. I., D. Sc., Prof., MHI RAS, Russia

Ryabushko V. I., D. Sc., IBSS, Russia

Samyshev E. Z., D. Sc., Prof., IBSS, Russia

Sanjharova N. I., Corr. Member of RAS, D. Sc., RIRAE, Russia

Sovga E. E., D. Sc., Prof., MHI RAS, Russia

Stelmakh L. V., D. Sc., IBSS, Russia

Trapeznikov A. V., D. Sc., IPAE UB RAS, Russia

Vasil'eva E. D., D. Sc., MSU, Russia

Zaharia T., D. Sc., NIMRD, Romania

Zuyev G. V., D. Sc., Prof., IBSS, Russia

Founder, Publisher, and Editorial Office address:

A. O. Kovalevsky Institute of Biology of the Southern Seas of Russian Academy of Sciences.

2 Nakhimov ave., Sevastopol, 299011, Russia.

Тел.: +7 8692 54-41-10. E-mail: mbj@imbr-ras.ru.

Journal website: <https://marine-biology.ru>.

Co-publisher address:

Zoological Institute Russian Academy of Sciences.

1 Universitetskaya emb., Saint Petersburg, 199034, Russia.

МОРСКОЙ БИОЛОГИЧЕСКИЙ ЖУРНАЛ

MARINE BIOLOGICAL JOURNAL

2024 Vol. 9 no. 1

Established in February 2016

SCIENTIFIC JOURNAL

4 issues per year

CONTENTS

Scientific communications

Belogurova R.

Morphometric variability in the round goby *Neogobius melanostomus* (Pallas, 1814)
(Actinopterygii, Gobiidae) of the Sea of Azov–Black Sea Basin 3–17

Zaytseva T., Safronova V., Russu A., Kuzikova I., and Medvedeva N.

Nonylphenol biodegradation by the bacterium *Raoultella planticola* strain F8
isolated from the sediment of the Gulf of Finland, the Baltic Sea 18–31

Zakharov D., Manushin I., Jørgensen L., and Strelkova N.

Impact of the red king crab and the snow crab
on the Barents Sea megabenthic communities 32–50

Makarevich P., Vodopyanova V., Bulavina A., Vashchenko P., Namyatov A., and Pastukhov I.

Localization of phytoplankton early spring bloom spots
in the pelagic zone of the Barents Sea 51–69

Markina Zh., Zinov A., and Orlova T.

Experience of growing the microalga *Tisochrysis lutea* (Haptophyta)
under conditions of a Labfors bioreactor
for the production of carotenoids and neutral lipids 70–75

Revkova T. and Sergeeva N.

Stylotheristus paramutilus sp. nov. (Nematoda: Xyalidae),
a new nematode species from the Black Sea 76–85

Ryzhik I., Salakhov D., Makarov M., and Menshakova M.

Analysis of physiological and biochemical parameters of *Acrosiphonia arcta* (Dillwyn) Gain cells
at the early stage of stress reaction formation under the effect of diesel fuel emulsion 86–97

Soldatov A., Rychkova V., and Kukhareva T.

Morphometric characteristics of erythroid elements of *Anadara kagoshimensis* (Tokunaga, 1906)
hemolymph under conditions of hydrogen sulfide loading 98–107

Titlyanov E., Titlyanova T., Belous O., and Tokeshi M.

Marine algal flora of the southern islands of Japan 108–117

Chronicle and information

On the anniversary of Ilkham Khayam ogly Alekperov,
D. Sc., Professor, corresponding member of the Azerbaijan NAS 118–120

SCIENTIFIC COMMUNICATIONS

UDC 597.556.333.1-115-14(262.5+262.54)

**MORPHOMETRIC VARIABILITY IN THE ROUND GOBY
NEOGOBIUS MELANOSTOMUS (PALLAS, 1814) (ACTINOPTERYGII, GOBIIDAE)
OF THE SEA OF AZOV–BLACK SEA BASIN**

© 2024 R. Belogurova^{1,2}

¹A. O. Kovalevsky Institute of Biology of the Southern Seas of RAS, Sevastopol, Russian Federation

²Research Center for Freshwater and Brackish Water Hydrobiology, Kherson, Russian Federation

E-mail: prishchepa.raisa@yandex.ru

Received by the Editor 12.04.2021; after reviewing 08.06.2022;
accepted for publication 09.10.2023; published online 22.03.2024.

The variability of external morphological characters (36 morphometric and 6 meristic ones) of the round goby *Neogobius melanostomus* (Pallas, 1814) from seven regions of the Sea of Azov–Black Sea Basin is considered: the northwestern and southwestern Black Sea coast of the Crimean Peninsula (the Karkinitsky Bay, Donuzlav Liman, and Streletsкая Bay of Sevastopol), the Kazantip Bay of the Sea of Azov, and the Salgir River in the central Crimean Peninsula. As established, the round goby from different catch regions at the age of 2+...3 has different body sizes: the maximum in individuals from the Streletsкая Bay, SL_{av} (136.2 ± 1.97) mm; the minimum in individuals from the Salgir River, SL_{av} (66.8 ± 2.28) mm. With the Mann–Whitney test, statistically significant differences were found between the samples for most morphometric characters. In terms of meristic characters, there were no differences. The greatest contributors to the discrimination of *N. melanostomus* samples were morphometric characters related to the location of fins. According to the results of cluster analysis, based on the totality of all the studied characters of the round goby of the Sea of Azov–Black Sea Basin, the samples from the Karkinitsky Bay (Samarchik Bay and Yarylgachskaya Bay, $D = 28.6$) and from the Bakalskaya Spit water area had the highest similarity. At the level of divergence $D = 47.3$, groups of the round goby from the Streletsкая Bay and Kazantip Bay were united; then, a sample from the Donuzlav Liman adjoined them at the level $D = 215$. The sample from the Salgir River had the most isolated position: the level of divergence was about 475. As found according to the discriminant analysis, the round goby from the Sea of Azov–Black Sea Basin was differentiated into at least three spatial groups: the first one, from the western coast of the Crimean Peninsula (the Karkinitsky Bay and Donuzlav Liman) and the Sevastopol area (the Streletsкая Bay); the second one, from the Kazantip Bay (the Sea of Azov); and the third one, from the Salgir River. The following characters made the greatest contribution to the discrimination of spatial groupings (with the correlation coefficient between characters and coordinate values along the second canonical axis being higher than 0.75): maximum body depth, caudal peduncle depth and width, predorsal and prepelvic distances, and width of pectoral and pelvic fin base. The revealed heterogeneity shows a high paratypical variability of morphometric characters; under different environmental conditions, individuals of the same species form a specific phenotype.

Keywords: round goby, Sea of Azov–Black Sea Basin, morphometric and meristic characters, variability, population

The round goby *Neogobius melanostomus* (Pallas, 1814) is a Ponto-Caspian endemic species with a natural range that includes water areas of the Black, Marmara, and Caspian seas and the Sea of Azov [Boltachev, Karpova, 2017; Manilo, 2014; Pinchuk, Miller, 2003; Smirnov, 1986; Svetovidov, 1964; Vasileva, 2007]. In almost its entire natural range, the round goby is one of the important commercial fish species [Boltachev, Karpova, 2017].

N. melanostomus is a bottom-dwelling fish preferring brackish-water coastal areas of seas and river mouths and one of the widespread goby species off the coast of the Crimean Peninsula [Boltachev, Karpova, 2017; Manilo, 2014]. According to numerous literature data, this species is characterized by high ecological plasticity and invasive potential; it actively spreads in new habitats outside the Ponto-Caspian Basin. Specifically, the round goby penetrated upstream of large European rivers and formed stable freshwater populations in new areas; moreover, the fish was transported with ballast waters into the Baltic Sea Basin and the Great Lakes of North America [Buřič et al., 2015; Crossman et al., 1992; Nyeste et al., 2017; Piria et al., 2011; Roche et al., 2015; Simonović et al., 2001; Skóra, Rzeźnik, 2001; Smirnov, 2001; Strānai, Andreji, 2004; van Beek, 2006; Verreycken et al., 2011; Ćolić et al., 2018].

Gobies are known as low-migratory fish, capable of forming local groups differing morphologically [Manilo, 2014]. Certain publications are focused on the study of intraspecific variability of *N. melanostomus* both in its natural range and under new conditions [Demchenko, Tkachenko, 2017; Diripasko, Zabroda, 2017; Kodukhova et al., 2017; Smirnov, 1986, 2001; Tkachenko, 2012]. However, the morphological structure of the round goby in the coastal area of the Crimea has been poorly studied, while in its inland water bodies, it has generally not been investigated.

The ecological conditions of water bodies and water areas off the Crimean Peninsula are very diverse. On average, the salinity of the Black Sea is 17–18‰, and that of the Sea of Azov is 10–11‰. Anthropogenic load on some areas of the Sea of Azov–Black Sea Basin over the past half century caused changes in both hydrochemical characteristics and composition of the fish fauna. The ichthyofauna of the Karkinitzky Bay and inland water bodies of the Crimea has long been affected by the North Crimean Canal; accordingly, in these areas, representatives of the Dnieper ichthyofauna were recorded [Belogurova et al., 2020; Karpova, 2016; Karpova, Boltachev, 2012]. In the Donuzlav Liman, the modern ichthyofauna has been formed over the past 35 years: since a canal was dug on the Belyaus Spit that separates one of the saltiest Crimean lakes from the Black Sea [Zuev, Boltachev, 1999].

Under different environmental conditions, for example, hydrochemical regime or current speed, in fish of the same species, variations in morphological characters are developed. Studying their variability, one can assess the scale of adaptation of the species to the environmental conditions.

Considering that the round goby actively spreads in new water bodies and is capable of forming local groups which differ morphologically within the area depending on the environmental conditions, the aim of the work was to assess the variability of external morphological characters of *Neogobius melanostomus* from various water areas of the Sea of Azov–Black Sea Basin based on morphometric and meristic characters.

MATERIAL AND METHODS

The material was fish samples fixed with a 4% formaldehyde solution which were obtained during expeditions of IBSS plankton department in 2009–2020. The study sites were several water areas of the Black Sea off the northwestern and southwestern coast of the Crimean Peninsula (the Karkinitzky Bay, 3 samples; the Donuzlav Liman, 1 sample; and the Streletskaya Bay of Sevastopol,

1 sample), the Salgir River (inland water body of the Crimean Peninsula, 1 sample), and the Kazantip Bay (the Sea of Azov, 1 sample) (Fig. 1). Ichthyological material in the Donuzlav Liman and Karkinitzky Bay was sampled with shrimp hoop nets with a mesh size of 6.5–7.5 mm. In the Salgir River (Novogrigorievka village area) and in the Kazantip Bay (the Sea of Azov), sampling was carried out with gill nets with a mesh size of 10–30 mm. In the Streletsкая Bay, a bottom trap was used with a 12-mm mesh. For morphometric analysis, 167 ind. of sexually mature male round goby aged 2+...3 were selected from seven samples. Age was determined analyzing otoliths: those were viewed under a binocular microscope at magnification 20× [Pravdin, 1966].

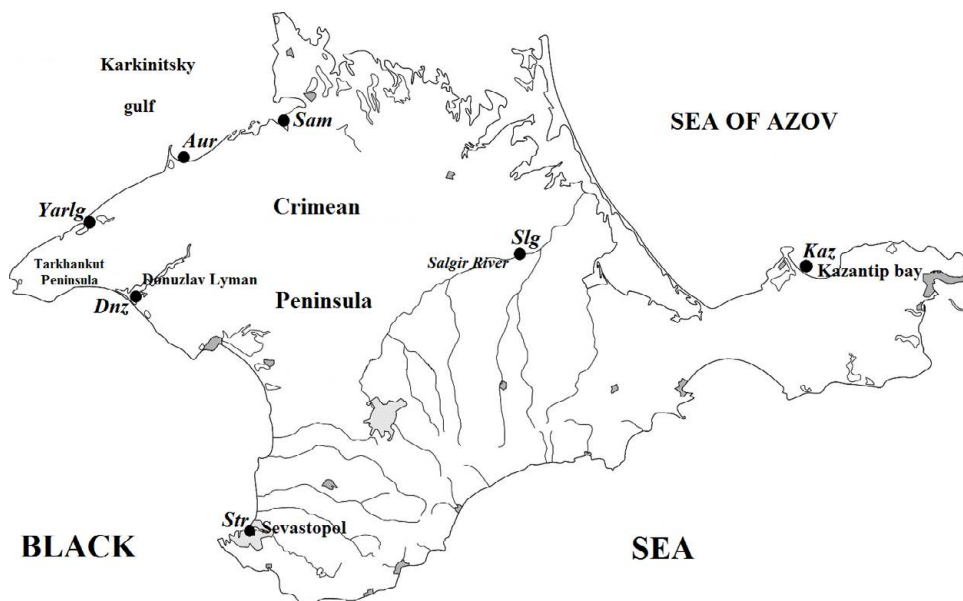


Fig. 1. Schematic map of the round goby *Neogobius melanostomus* sampling sites in the Sea of Azov–Black Sea Basin. Sam, Samarchik Bay; Aur, Bakalskaya Spit (Aurora village area); Yarlg, Yarylgachskaya Bay; Dnz, Donuzlav Liman; Str, Streletsкая Bay; Slg, Salgir River (Novogrigorievka village area); Kaz, Kazantip Bay

In total, 36 morphometric and 6 meristic characters were studied. The measurements were made using a caliper with an accuracy of 0.1 mm according to a standard scheme with additions (Fig. 2) [Pravdin, 1966; Zabroda, Diripasko, 2009]. For further processing, measurements on the body and head of the round goby were converted into character indices expressed as % of the standard length (SL) and head length (HL).

In different samples, fish length varied significantly. Therefore, to level out the factor of size variability in the absolute values of measurements, those were transformed by the Reist formula:

$$\lg \ddot{X}_i = \lg \lg X_i - b(\lg SL_i - \lg SL),$$

where $\lg \ddot{X}_i$ is the transformed value of character X in the *i*-th individual;

X_i is the initial value of the character in the *i*-th individual;

SL_i is the standard length of the *i*-th individual;

SL is the mean length in the sample;

b is the allometric coefficient defined as the tangent of the slope of the regression line for logarithmic measurement values on logarithmic body length values [Reist, 1985, 1986; Thorpe, 1975].

To process the data, we used generally accepted statistical indicators calculated in MS Office Excel. To analyze differences between samples with a small number of specimens, the nonparametric Mann–Whitney test was applied at a significance level of $p \leq 0.05$. The variability of characters in each sample was assessed using the coefficient of variation (*var*) – a standard deviation expressed as a percentage of the arithmetic mean. It was considered that indices varied weakly with $var < 10\%$ and moderately with var of 11–25% [Lakin, 1990]. To determine the divergence in the complexes of the studied characters between fish from different regions, the Kullback–Leibler divergence index (*D*) was used [Andreev, Reshetnikov, 1977]. Methods of univariate and multivariate statistics (discriminant and cluster analysis) were applied, with calculations performed in STATISTICA 10.0 software package [Khalafyan, 2007].

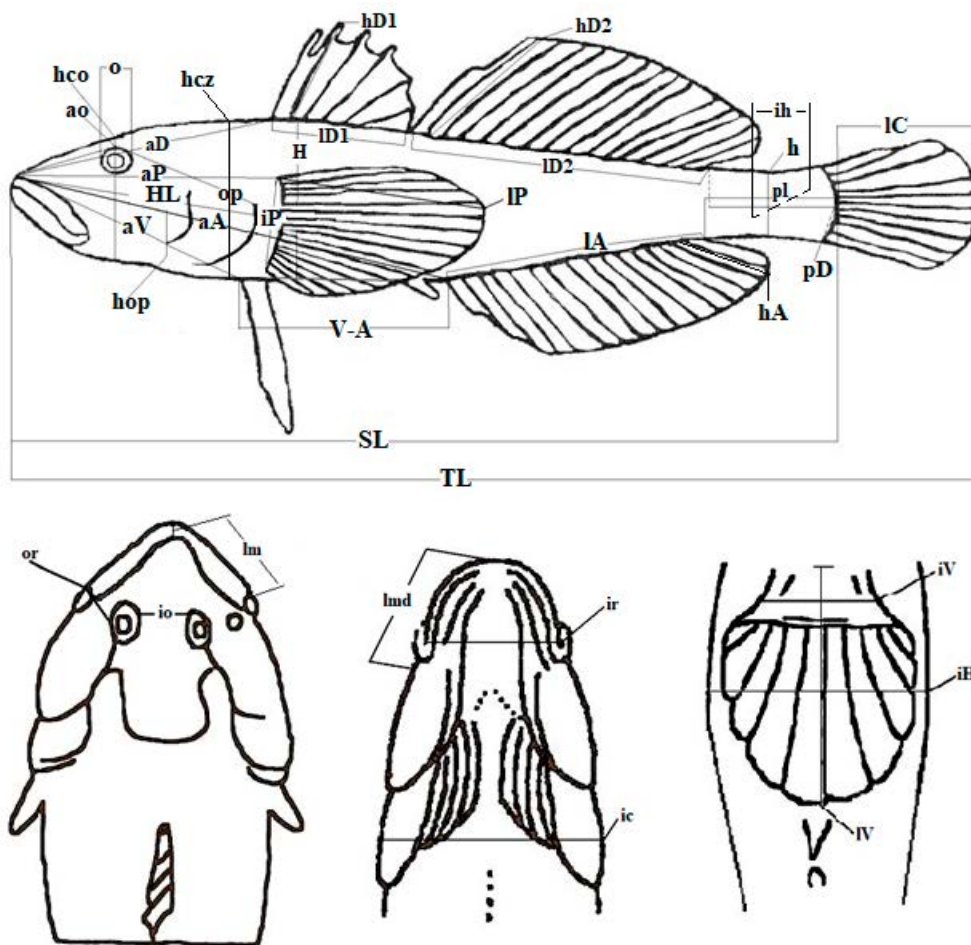


Fig. 2. Scheme of morphometric measurements of the round goby *Neogobius melanostomus*. TL, total length; SL, standard length. Morphometric characters as % of SL: H, maximum body depth; h, minimum body depth (caudal peduncle depth); iH, maximum body width; ih, minimum body width (caudal peduncle width); aD, predorsal distance; pD, postdorsal distance; aP, prepectoral distance; aV, prepelvic distance; aA, preanal distance; V-A, pelvic-anal distance; pl, caudal peduncle length; ID1, length of the first dorsal fin base; hD1, first dorsal fin depth; ID2, length of the second dorsal fin base; hD2, the second dorsal fin depth; IA, length of anal fin base; hA, anal fin depth; IP, pectoral fin length; iP, width of pectoral fin base; IV, pelvic fin length; iV, width of pelvic fin base; IC, caudal fin length; HL, head length. Morphometric characters as % of HL: ic, head width; ao, preorbital distance; o, horizontal eye diameter; op, postorbital distance; io, interorbital distance; lm, upper jaw length; lmd, lower jaw length; or, distance between eye and corner of mouth; hop, cheek depth; ir, mouth width; hco, head depth through middle of eye. Meristic characters: D1, the first dorsal fin spines number; Dr2, the second dorsal fin rays number; Ar, anal fin rays number; P, pectoral fin rays number; V, pelvic fin rays number; C, caudal fin rays number

RESULTS

The results of the morphometric analysis of the round goby from seven study regions of the Sea of Azov–Black Sea basin are given in Table 1.

N. melanostomus from the Streletskaya Bay turned out to be larger on average than specimens from other water areas, SL_{av} was (136.2 ± 1.97) mm. This is likely to result from selectivity of the fishing gear used there. However, the round goby individuals can be large in the bays of Sevastopol because of their low density in the coastal area, and, consequently, better conditions for growth and feeding.

Table 1. Morphometric characters of the male round goby *Neogobius melanostomus* from seven regions of the Sea of Azov–Black Sea Basin, mm (the names of the study regions correspond to those in Fig. 1)

Character	Sam, $n = 21$	Aur, $n = 32$	Yarlg, $n = 23$	Dnz, $n = 22$	Slg, $n = 19$	Kaz, $n = 23$	Str, $n = 27$
SL	$\frac{99.0-129.5}{111.0 \pm 1.87}$	$\frac{100.7-123.1}{109.2 \pm 0.90}$	$\frac{91.9-124.1}{105.0 \pm 1.42}$	$\frac{80.5-107.2}{87.6 \pm 1.27}$	$\frac{55.5-90.8}{66.8 \pm 2.28}$	$\frac{81.0-136.9}{96.6 \pm 3.37}$	$\frac{108.7-153.4}{136.2 \pm 1.97}$
Morphometric characters as % of SL							
H	$\frac{20.5-24.9}{22.2 \pm 0.25}$	$\frac{20.8-26.5}{23.6 \pm 0.24}$	$\frac{19.2-25.1}{22.2 \pm 0.25}$	$\frac{18.0-22.6}{19.9 \pm 0.28}$	$\frac{19.3-24.8}{21.9 \pm 0.36}$	$\frac{18.4-23.4}{20.3 \pm 0.27}$	$\frac{18.8-24.0}{21.2 \pm 0.29}$
h	$\frac{10.3-12.4}{11.1 \pm 0.14}$	$\frac{10.4-13.4}{11.7 \pm 0.11}$	$\frac{10.7-12.5}{11.5 \pm 0.11}$	$\frac{9.8-11.5}{10.5 \pm 0.11}$	$\frac{9.4-12.1}{10.6 \pm 0.17}$	$\frac{8.8-11.4}{10.5 \pm 2.28}$	$\frac{9.3-11.6}{10.5 \pm 0.11}$
iH	$\frac{16.2-20.2}{18.0 \pm 0.25}$	$\frac{18.7-22.0}{20.2 \pm 0.14}$	$\frac{16.7-20.3}{18.4 \pm 0.22}$	$\frac{14.4-19.5}{16.4 \pm 0.32}$	$\frac{17.7-24.4}{20.3 \pm 0.45}$	$\frac{13.5-17.8}{16.1 \pm 0.27}$	$\frac{16.8-21.6}{18.3 \pm 0.24}$
ih	$\frac{5.0-8.0}{6.2 \pm 0.19}$	$\frac{7.0-9.3}{8.3 \pm 0.09}$	$\frac{6.4-10.3}{7.9 \pm 0.18}$	$\frac{6.4-8.2}{7.2 \pm 0.10}$	$\frac{4.0-5.8}{4.8 \pm 0.28}$	$\frac{4.2-6.1}{5.2 \pm 0.10}$	$\frac{4.5-6.1}{5.3 \pm 0.09}$
aD	$\frac{33.7-38.7}{35.8 \pm 0.29}$	$\frac{34.7-38.7}{36.2 \pm 0.16}$	$\frac{26.5-39.2}{35.4 \pm 0.55}$	$\frac{32.6-38.1}{35.6 \pm 0.30}$	$\frac{34.0-37.5}{35.9 \pm 0.30}$	$\frac{32.6-38.3}{35.0 \pm 0.36}$	$\frac{31.4-36.9}{34.5 \pm 0.27}$
pD	$\frac{12.2-16.9}{14.7 \pm 0.25}$	$\frac{12.1-18.5}{15.5 \pm 0.24}$	$\frac{12.8-16.8}{15.1 \pm 0.24}$	$\frac{14.5-18.8}{16.4 \pm 0.18}$	$\frac{13.3-18.4}{15.4 \pm 0.33}$	$\frac{14.6-19.0}{16.6 \pm 0.25}$	$\frac{13.7-17.0}{15.7 \pm 0.19}$
aP	$\frac{27.8-33.5}{31.6 \pm 0.28}$	$\frac{29.4-32.9}{31.1 \pm 0.12}$	$\frac{30.2-32.9}{31.3 \pm 0.15}$	$\frac{26.8-30.8}{28.7 \pm 0.22}$	$\frac{30.9-34.9}{32.8 \pm 0.23}$	$\frac{29.2-33.3}{31.5 \pm 0.18}$	$\frac{29.3-34.8}{32.0 \pm 0.26}$
aV	$\frac{31.0-35.9}{32.9 \pm 0.25}$	$\frac{31.3-34.9}{32.8 \pm 0.15}$	$\frac{30.0-35.3}{32.7 \pm 0.25}$	$\frac{27.8-32.4}{30.5 \pm 0.27}$	$\frac{26.5-32.6}{30.0 \pm 0.37}$	$\frac{29.6-34.7}{32.2 \pm 0.26}$	$\frac{29.1-34.8}{32.1 \pm 0.27}$
aA	$\frac{56.1-63.8}{60.9 \pm 0.39}$	$\frac{31.5-62.6}{58.7 \pm 0.96}$	$\frac{55.0-64.0}{59.6 \pm 0.46}$	$\frac{52.1-61.0}{56.6 \pm 0.41}$	$\frac{54.7-62.2}{57.0 \pm 0.51}$	$\frac{54.1-63.1}{58.1 \pm 0.53}$	$\frac{54.1-64.6}{59.1 \pm 0.52}$
V-A	$\frac{22.6-32.5}{29.5 \pm 0.49}$	$\frac{25.3-32.9}{29.6 \pm 0.32}$	$\frac{26.0-33.4}{29.0 \pm 0.45}$	$\frac{22.0-31.9}{27.4 \pm 0.55}$	$\frac{23.5-30.4}{27.1 \pm 0.44}$	$\frac{24.2-30.9}{26.8 \pm 0.39}$	$\frac{24.7-35.9}{28.8 \pm 0.54}$
pl	$\frac{13.6-17.6}{16.1 \pm 0.24}$	$\frac{12.1-24.4}{16.7 \pm 0.40}$	$\frac{14.2-18.1}{16.0 \pm 0.22}$	$\frac{15.5-24.1}{18.3 \pm 0.35}$	$\frac{13.2-20.1}{17.5 \pm 0.41}$	$\frac{14.8-25.0}{18.3 \pm 0.55}$	$\frac{14.7-19.6}{16.9 \pm 0.26}$
lD1	$\frac{15.4-20.4}{17.9 \pm 0.31}$	$\frac{15.1-21.3}{18.5 \pm 0.24}$	$\frac{16.2-19.5}{18.1 \pm 0.18}$	$\frac{15.3-19.9}{18.1 \pm 0.28}$	$\frac{15.5-20.9}{18.4 \pm 0.29}$	$\frac{14.5-21.4}{17.6 \pm 0.36}$	$\frac{15.6-20.9}{18.3 \pm 0.36}$
hD1	$\frac{12.9-17.1}{15.3 \pm 0.26}$	$\frac{13.7-17.0}{15.8 \pm 0.12}$	$\frac{13.2-18.2}{15.5 \pm 0.26}$	$\frac{14.2-18.2}{16.3 \pm 0.25}$	$\frac{15.0-21.2}{17.9 \pm 0.45}$	$\frac{12.1-18.3}{15.0 \pm 0.31}$	$\frac{14.0-19.4}{16.1 \pm 0.25}$
lD2	$\frac{30.2-35.8}{32.3 \pm 0.32}$	$\frac{18.8-35.1}{32.2 \pm 0.49}$	$\frac{28.9-36.6}{32.3 \pm 0.36}$	$\frac{28.9-36.5}{32.3 \pm 0.46}$	$\frac{30.6-35.3}{32.9 \pm 0.34}$	$\frac{31.1-36.2}{33.7 \pm 0.29}$	$\frac{26.3-38.1}{33.4 \pm 0.42}$

Continue on the next page...

Character	Sam, $n = 21$	Aur, $n = 32$	Yarlg, $n = 23$	Dnz, $n = 22$	Slg, $n = 19$	Kaz, $n = 23$	Str, $n = 27$
hD2	$\frac{13.5-18.6}{15.7 \pm 0.33}$	$\frac{14.0-18.1}{16.0 \pm 0.17}$	$\frac{13.2-17.3}{15.7 \pm 0.22}$	$\frac{13.4-18.7}{16.2 \pm 0.31}$	$\frac{14.9-23.2}{18.3 \pm 0.52}$	$\frac{14.5-18.3}{15.9 \pm 0.21}$	$\frac{12.2-17.3}{14.7 \pm 0.25}$
IA	$\frac{20.7-27.1}{24.5 \pm 0.37}$	$\frac{20.2-28.7}{25.3 \pm 0.25}$	$\frac{23.5-29.1}{26.8 \pm 0.27}$	$\frac{21.1-28.8}{25.6 \pm 0.34}$	$\frac{21.6-28.7}{25.8 \pm 0.45}$	$\frac{22.3-28.6}{26.0 \pm 0.37}$	$\frac{20.8-29.6}{25.9 \pm 0.38}$
hA	$\frac{11.7-16.1}{13.5 \pm 0.25}$	$\frac{11.1-16.2}{14.2 \pm 0.20}$	$\frac{12.9-17.1}{14.4 \pm 0.25}$	$\frac{12.1-15.4}{14.2 \pm 0.16}$	$\frac{13.2-21.9}{16.1 \pm 0.56}$	$\frac{12.6-18.8}{14.7 \pm 0.34}$	$\frac{11.1-15.5}{12.9 \pm 0.20}$
IP	$\frac{21.9-28.5}{25.4 \pm 0.33}$	$\frac{24.0-30.0}{27.1 \pm 0.23}$	$\frac{22.4-29.1}{25.8 \pm 0.34}$	$\frac{23.5-30.3}{27.5 \pm 0.36}$	$\frac{20.2-26.9}{24.4 \pm 0.31}$	$\frac{27.8-33.0}{30.2 \pm 0.30}$	$\frac{22.4-30.2}{26.2 \pm 0.32}$
iP	$\frac{12.5-18.4}{13.6 \pm 0.27}$	$\frac{12.4-14.3}{13.2 \pm 0.08}$	$\frac{13.0-15.4}{13.8 \pm 0.12}$	$\frac{11.0-13.2}{12.1 \pm 0.14}$	$\frac{9.0-12.1}{10.7 \pm 0.18}$	$\frac{11.7-15.2}{13.0 \pm 0.15}$	$\frac{11.8-14.3}{12.9 \pm 0.11}$
IV	$\frac{17.0-20.8}{19.0 \pm 0.23}$	$\frac{19.0-22.0}{19.9 \pm 0.13}$	$\frac{18.1-21.8}{19.5 \pm 0.22}$	$\frac{18.7-23.0}{20.4 \pm 0.25}$	$\frac{20.7-24.2}{22.4 \pm 0.23}$	$\frac{19.2-24.0}{21.3 \pm 0.26}$	$\frac{15.5-20.5}{18.5 \pm 0.24}$
iV	$\frac{7.1-8.9}{8.0 \pm 0.09}$	$\frac{7.2-8.7}{7.9 \pm 0.07}$	$\frac{7.3-9.2}{8.2 \pm 0.08}$	$\frac{6.6-8.0}{7.3 \pm 0.09}$	$\frac{6.1-8.0}{7.2 \pm 0.13}$	$\frac{6.6-8.9}{7.6 \pm 0.09}$	$\frac{6.6-8.9}{7.6 \pm 0.10}$
IC	$\frac{19.8-24.6}{22.7 \pm 0.32}$	$\frac{19.0-25.0}{22.7 \pm 0.22}$	$\frac{20.2-26.7}{22.3 \pm 0.29}$	$\frac{21.6-25.5}{23.5 \pm 0.22}$	$\frac{21.7-27.0}{24.2 \pm 0.33}$	$\frac{23.0-27.8}{25.4 \pm 0.27}$	$\frac{19.1-25.4}{22.8 \pm 0.30}$
HL	$\frac{27.9-31.5}{29.7 \pm 0.21}$	$\frac{28.0-30.4}{29.2 \pm 0.10}$	$\frac{28.9-31.3}{30.0 \pm 0.15}$	$\frac{26.7-29.0}{27.8 \pm 0.15}$	$\frac{27.6-33.7}{30.6 \pm 0.35}$	$\frac{27.0-31.0}{28.8 \pm 0.20}$	$\frac{27.8-31.8}{29.3 \pm 0.19}$
Morphometric characters as % of HL							
hcz	$\frac{71.6-82.8}{77.3 \pm 0.73}$	$\frac{72.9-88.4}{81.7 \pm 0.65}$	$\frac{69.6-87.3}{78.8 \pm 0.91}$	$\frac{64.6-84.6}{76.2 \pm 1.19}$	$\frac{65.2-79.1}{72.1 \pm 0.84}$	$\frac{64.2-79.9}{73.2 \pm 0.81}$	$\frac{67.4-82.6}{74.8 \pm 0.76}$
ic	$\frac{52.2-61.3}{56.3 \pm 0.54}$	$\frac{51.4-61.0}{56.2 \pm 0.43}$	$\frac{49.4-59.6}{55.7 \pm 0.57}$	$\frac{50.2-57.8}{53.9 \pm 0.51}$	$\frac{69.8-81.2}{76.1 \pm 0.75}$	$\frac{49.8-60.2}{54.5 \pm 0.56}$	$\frac{50.8-60.3}{55.0 \pm 0.48}$
ao	$\frac{34.2-39.1}{36.6 \pm 0.29}$	$\frac{34.1-40.3}{38.2 \pm 0.24}$	$\frac{32.4-40.1}{36.4 \pm 0.41}$	$\frac{34.2-39.6}{36.1 \pm 0.27}$	$\frac{28.1-39.6}{34.0 \pm 0.54}$	$\frac{31.1-38.5}{34.9 \pm 0.39}$	$\frac{32.2-39.8}{36.3 \pm 0.33}$
o	$\frac{17.8-22.3}{20.2 \pm 0.25}$	$\frac{18.4-22.6}{20.3 \pm 0.22}$	$\frac{18.7-23.7}{21.3 \pm 0.30}$	$\frac{19.2-24.0}{21.6 \pm 0.31}$	$\frac{20.8-30.6}{24.9 \pm 0.64}$	$\frac{16.9-25.9}{22.4 \pm 0.53}$	$\frac{14.6-21.8}{18.6 \pm 0.32}$
op	$\frac{52.7-58.5}{55.3 \pm 0.37}$	$\frac{54.6-60.7}{57.5 \pm 0.26}$	$\frac{53.9-59.0}{56.4 \pm 0.33}$	$\frac{52.8-60.4}{56.5 \pm 0.36}$	$\frac{50.5-62.1}{56.3 \pm 0.76}$	$\frac{52.4-57.9}{55.3 \pm 0.34}$	$\frac{53.2-59.3}{55.5 \pm 0.31}$
io	$\frac{12.7-16.7}{14.5 \pm 0.23}$	$\frac{11.1-18.1}{15.2 \pm 0.31}$	$\frac{8.7-15.8}{13.5 \pm 0.34}$	$\frac{9.6-15.4}{12.5 \pm 0.34}$	$\frac{10.7-20.3}{14.9 \pm 0.53}$	$\frac{12.2-18.8}{15.3 \pm 0.37}$	$\frac{12.8-19.0}{16.0 \pm 0.30}$
lm	$\frac{30.3-36.2}{32.5 \pm 0.37}$	$\frac{25.8-32.5}{29.8 \pm 0.30}$	$\frac{25.3-34.9}{30.8 \pm 0.50}$	$\frac{24.4-31.3}{27.8 \pm 0.38}$	$\frac{22.3-30.4}{26.6 \pm 0.47}$	$\frac{28.5-39.7}{32.7 \pm 0.58}$	$\frac{30.4-36.9}{33.1 \pm 0.30}$
lmd	$\frac{38.6-48.6}{43.9 \pm 0.50}$	$\frac{35.7-45.4}{42.1 \pm 0.46}$	$\frac{36.9-48.5}{41.7 \pm 0.60}$	$\frac{37.3-44.1}{40.5 \pm 0.36}$	$\frac{30.1-36.7}{33.5 \pm 0.42}$	$\frac{40.4-54.8}{45.7 \pm 0.65}$	$\frac{37.7-47.5}{43.3 \pm 0.48}$
or	$\frac{23.8-33.6}{27.4 \pm 0.56}$	$\frac{23.8-30.6}{27.3 \pm 0.31}$	$\frac{22.5-32.4}{26.8 \pm 0.46}$	$\frac{21.3-29.3}{24.7 \pm 0.43}$	$\frac{16.7-23.9}{27.5 \pm 0.53}$	$\frac{23.5-33.7}{27.5 \pm 0.53}$	$\frac{26.6-35.8}{31.0 \pm 0.38}$
hop	$\frac{40.4-47.4}{43.1 \pm 0.42}$	$\frac{40.7-47.4}{43.6 \pm 0.30}$	$\frac{40.6-48.7}{44.1 \pm 0.43}$	$\frac{40.6-45.8}{43.3 \pm 0.29}$	$\frac{31.9-46.4}{39.9 \pm 0.72}$	$\frac{34.8-50.5}{42.1 \pm 0.73}$	$\frac{37.4-45.2}{42.3 \pm 0.32}$
ir	$\frac{39.1-49.0}{43.8 \pm 0.57}$	$\frac{34.6-46.2}{41.9 \pm 0.43}$	$\frac{35.6-51.9}{41.9 \pm 0.81}$	$\frac{31.8-42.5}{36.7 \pm 0.59}$	$\frac{31.4-45.8}{39.2 \pm 0.86}$	$\frac{38.3-55.3}{44.3 \pm 0.90}$	$\frac{38.7-52.1}{44.4 \pm 0.65}$

Continue on the next page...

Character	Sam, <i>n</i> = 21	Aur, <i>n</i> = 32	Yarlg, <i>n</i> = 23	Dnz, <i>n</i> = 22	Slg, <i>n</i> = 19	Kaz, <i>n</i> = 23	Str, <i>n</i> = 27
hco	$\frac{58.0-69.0}{61.2 \pm 0.60}$	$\frac{54.5-64.2}{60.1 \pm 0.41}$	$\frac{51.4-61.2}{56.5 \pm 0.50}$	$\frac{51.3-59.0}{54.6 \pm 0.35}$	$\frac{47.7-58.8}{52.1 \pm 0.77}$	$\frac{54.7-69.8}{58.5 \pm 0.81}$	$\frac{57.5-68.8}{61.9 \pm 0.55}$
Meristic characters							
D1	$\frac{5.0-7.0}{6.1 \pm 0.08}$	6.0	$\frac{6.0-7.0}{6.1 \pm 0.07}$	6.0	6.0	$\frac{5.0-6.0}{6.0 \pm 0.04}$	6.0
Dr2	$\frac{14.0-15.0}{14.5 \pm 0.11}$	$\frac{14.0-15.0}{14.8 \pm 0.08}$	$\frac{14.0-16.0}{14.9 \pm 0.09}$	$\frac{13.0-16.0}{15.1 \pm 0.13}$	$\frac{15.0-16.0}{15.8 \pm 0.09}$	$\frac{14.0-16.0}{14.9 \pm 0.14}$	$\frac{15.0-16.0}{15.5 \pm 0.10}$
Ar	$\frac{11.0-12.0}{11.6 \pm 0.11}$	$\frac{11.0-13.0}{11.8 \pm 0.10}$	$\frac{12.0-13.0}{12.6 \pm 0.09}$	$\frac{11.0-13.0}{12.2 \pm 0.11}$	$\frac{11.0-13.0}{12.0 \pm 0.09}$	$\frac{11.0-13.0}{12.0 \pm 0.13}$	$\frac{11.0-13.0}{12.5 \pm 0.12}$
P	$\frac{18.0-20.0}{19.1 \pm 0.14}$	$\frac{17.0-20.0}{18.6 \pm 0.16}$	$\frac{18.0-20.0}{18.6 \pm 0.15}$	$\frac{17.0-20.0}{18.6 \pm 0.14}$	$\frac{17.0-18.0}{17.7 \pm 0.11}$	$\frac{17.0-19.0}{17.9 \pm 0.10}$	$\frac{18.0-20.0}{18.8 \pm 0.13}$
V	12.0	12.0	12.0	12.0	12.0	12.0	12.0
C	$\frac{23.0-25.0}{23.7 \pm 0.16}$	$\frac{23.0-26.0}{24.2 \pm 0.15}$	$\frac{23.0-26.0}{24.6 \pm 0.20}$	$\frac{23.0-25.0}{24.1 \pm 0.14}$	$\frac{22.0-24.0}{23.2 \pm 0.20}$	$\frac{24.0-27.0}{25.5 \pm 0.19}$	$\frac{25.0-28.0}{26.2 \pm 0.16}$

Note: the numerator denotes the limiting values of the characters; the denominator, the mean \pm standard error of the mean. Characters for which the value of the coefficient of variation *var* > 10% is recorded are highlighted in color. Indicators with mean values being the highest in samples from seven regions are highlighted in bold.

In catches from the Streletskaya Bay of Sevastopol, the round goby, unlike other fish species, is rare, while in the Karkinitzky Bay and Donuzlav Liman, the population density of all gobies is quite high. For example, in 2017, in Samarchik Bay, the abundance of *N. melanostomus* in catches amounted to 42% of the total abundance of gobies [Prishchepa et al., 2018].

In general, characters in the round goby samples varied slightly. The highest variability (*var* > 10%) was recorded in the caudal peduncle width in fish from Samarchik Bay and Yarylgachskaya Bay and the caudal peduncle length in individuals from the Bakalskaya Spit water area, the Salgir River, and the Kazantip Bay. The anal fin depth was the most variable in fish from the Salgir River and Kazantip Bay. Also, in the round goby from the Salgir River, the first dorsal fin depth and second dorsal fin depth were the most variable characters. Out of head measurements, the most variable in the samples from six regions (except for Samarchik Bay) was the interorbital distance; for *N. melanostomus* from the Salgir River and Kazantip Bay, the most variable characters were the eye diameter and distance between eye and corner of mouth. The Streletskaya Bay was the region for which *var* > 10% were recorded only for the first dorsal fin depth.

The meristic characters of the round goby in the studied samples turned out to be the least variable of all the analyzed characters.

According to the results of comparison with the nonparametric Mann–Whitney test, the indices of morphometric characters of *N. melanostomus* from seven regions of the Sea of Azov–Black Sea Basin significantly differed from each other. Table 2 provides the number of characters studied in the round goby for which noticeable differences were revealed. In meristic characters, there were no significant differences.

In all morphometric characters (24 on the body and 12 on the head), differences were observed between the fish from the Streletskaya Bay and other six regions. Apparently, this is due to the larger size of the round goby from the bay. Differences in the smallest number of characters were recorded

between *N. melanostomus* from three areas of the Karkinitzky Bay, probably due to the significant similarity of conditions because of the geographical proximity of these water areas. Differences were also noted in most of the studied characters between the round goby from three areas of the Karkinitzky Bay and other regions.

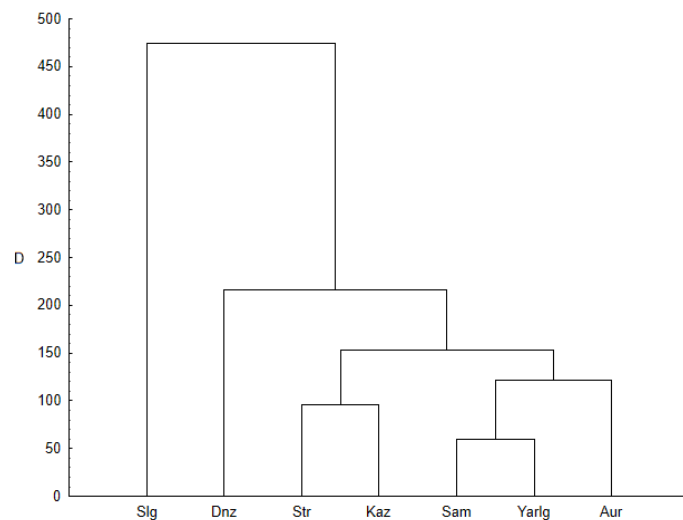
Table 2. Results of assessing differences between samples of the round goby *Neogobius melanostomus* from seven regions of the Black Sea by morphometric characters (the names of the study regions correspond to those in Fig. 1)

Region	Sam	Aur	Yarlg	Dnz	Slg	Kaz	Str
Sam		3	6	12	12	12	12
Aur	3		4	12	12	12	12
Yarlg	9	17		12	12	10	12
Dnz	23	24	24		9	8	12
Slg	24	24	24	24		11	12
Kaz	19	21	19	14	24		12
Str	24	24	24	24	24	24	

Note: differences are observed at a significance level of $p \leq 0.05$. Below the diagonal, the number of significantly different measurements on the body of the round goby is indicated; above the diagonal, on its head.

The degree of similarity of *N. melanostomus* from seven regions of the Sea of Azov–Black Sea Basin for all analyzed characters is shown in the dendrogram (Fig. 3). It is built using cluster analysis according to Kullback–Leibler divergence index (D) in different patterns of combining characters.

Fig. 3. Similarity dendrogram of all studied characters of samples of the round goby *Neogobius melanostomus* from seven regions of the Sea of Azov–Black Sea Basin (the names of the study regions correspond to those in Fig. 1)



Similarity of the round goby samples from Samarchik Bay and Yarylgachskaya Bay is observed at the lowest level of divergence ($D = 28.6$). These samples are adjoined by a group from the Bakalskaya Spit water area. At the level of divergence $D = 47.3$, groups of the fish from the Streletskaya Bay and Kazantip Bay are united. These groups form a cluster with a group of *N. melanostomus* from three areas of the Karkinitzky Bay, and a sample from the Donuzlav Liman adjoins them. The sample from the Salgir River adjoins these groups at the highest level of divergence, about 475. It can be tentatively concluded that such differences are related to the hydrochemical parameters of the studied water bodies. Specifically, fish from marine water areas (bays and bights of the Black Sea and Sea of Azov) form a separate group adjoined by a group of fish from the Donuzlav Liman with a higher salinity; the last in the dendrogram is a group of the round goby from a freshwater basin (the Salgir River).

The divergence of *N. melanostomus* samples from seven regions of the Sea of Azov–Black Sea Basin according to a complex of morphometric characters was obtained by the results of discriminant analysis. Thus, there were 99% of correct classifications of individuals according to catch areas. The studied characters in the samples form clouds of points in the space of two roots of the discriminant functions (Fig. 4A, B).

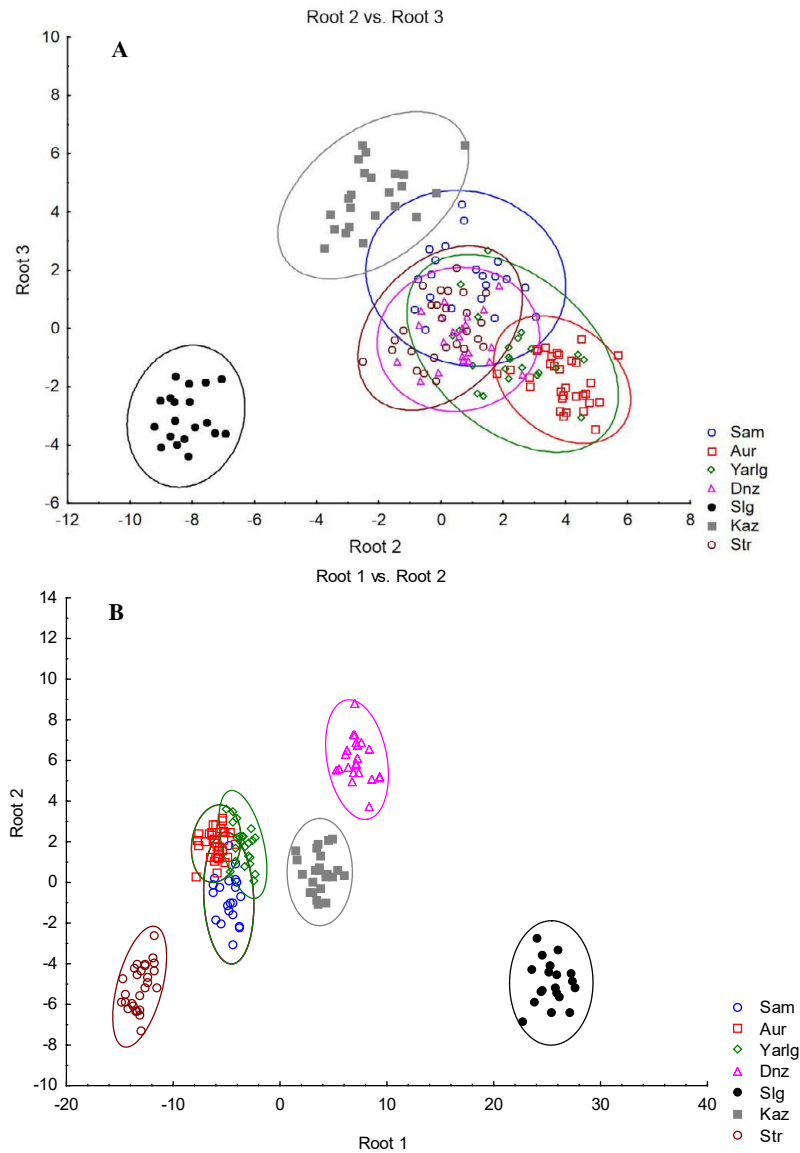


Fig. 4. Scattering diagram of canonical estimates of the indices of morphometric characters of the round goby *Neogobius melanostomus* from seven regions of the Sea of Azov–Black Sea Basin (A) and the values of characters transformed by the Reist formula (B) (results of discriminant analysis) (the names of the study regions correspond to those in Fig. 1)

According to the discriminant analysis, the round goby in the Sea of Azov–Black Sea Basin is differentiated into at least three spatial groupings. The first one is formed by fish from the western coast of the Crimean Peninsula (the Karkinitzky Bay and Donuzlav Liman) and the Sevastopol area (the Streletskaaya Bay); the second one is formed by *N. melanostomus* from the Salgir River; and the third one is formed by the round goby from the Kazantip Bay (the Sea of Azov). Analysis using measurement values transformed by the Reist formula showed a clearer isolation of the samples.

Specifically, fish from geographically close areas of the Karkinitsky Bay form a separate group in the space of the roots of discriminant functions, while *N. melanostomus* from water areas differing in the environmental conditions [from a freshwater basin (the Salgir River) and the Streletskaaya Bay] are isolated from the rest in terms of both canonical variables (Fig. 4B).

Analysis of the correlations of the studied characters of the round goby with the values of canonical variables revealed as follows: the divergence of samples along two axes is ensured by almost all indices of fish body measurements (Table 3) when the correlation coefficient between the characters and coordinate values along the second canonical axis exceeds 0.50. The greatest contributors to discrimination along the first canonical axis (root 2) with correlation coefficients exceeding 0.75 are the characters H, h, ih, aD, aV, iP, and iV.

Thus, the identified differences between the round goby individuals from the studied water areas are determined by the local environmental conditions of fish habitats.

Table 3. Correlations between the characters and coordinate values of two canonical variables for the round goby *Neogobius melanostomus* from seven regions of the Sea of Azov–Black Sea Basin

Character	Root 2	Root 3	Character	Root 2	Root 3
SL	0.56	0.20	ID2	0.66	0.31
H	0.75	0.04	hD2	0.61	0.14
h	0.78	0.10	lA	0.60	0.24
iH	0.68	–0.12	hA	0.51	0.19
ih	0.88	–0.19	lP	0.68	0.46
aD	0.77	0.21	iP	0.77	0.29
pD	0.70	0.35	lV	0.64	0.31
aP	0.67	0.26	iV	0.75	0.22
aV	0.76	0.27	lC	0.63	0.45
aA	0.72	0.25	HL	0.70	0.20
V-A	0.74	0.13	hcz	0.17	0.02
pl	0.54	0.35	ic	0.05	–0.01
ID1	0.70	0.16	ao	0.15	0.03
hD1	0.62	0.07			

Note: significant correlation coefficients are highlighted in bold.

DISCUSSION

Differences in the morphology of populations of invasive species may reflect the processes of adaptive phenotypic change and a unique history of a population [Langerhans, DeWitt, 2004]. At the same time, such differences occur within the native range of the species as well. According to [Smirnov, 1986], in the “Sea of Azov” population of the round goby, compared to the “Black Sea” one, the pectoral and pelvic fin length and the anal fin depth are higher, while the body width and length are lower; this can result from feeding and movement patterns. The round goby from the Dnieper River possesses rheophilic characters: the caudal section of the body is elongated, and the interorbital distance is increased [Smirnov, 1986]. In the Kakhovka Reservoir, *N. melanostomus* has an increased dorsal fin length compared to fish inhabiting bays of the Sea of Azov, while pelvic fin length and width, as well as pectoral, anal, and caudal fin length, are lower, which is related to inhabiting stagnant

water [Demchenko, Tkachenko, 2017; Tkachenko, 2012]. The round goby from the Southeastern Baltic population is characterized by a reduced number of fin rays and number of vertebrae, compared to fish from the native range [Kodukhova et al., 2017]. In *N. melanostomus* from the Great Lakes of North America (an invasive population), a decrease in meristic characters was also revealed: these individuals have reduced number of rays in the second dorsal and caudal fins [Smirnov, 2001].

According to the discriminant analysis, the greatest contribution to the discrimination of the round goby samples from seven areas of the Sea of Azov–Black Sea Basin is made by the maximum body depth, caudal peduncle depth and width, predorsal and prepelvic distance, and width of pectoral and pelvic fin base (the correlation coefficient between these characters and coordinate values along the second canonical axis exceeds 0.75). In fish from the Bakalskaya Spit area, the anterior part of the body and caudal fin length and width are increased. *N. melanostomus* inhabiting areas exposed to strong surf is likely to have a more massive anterior part of the body. The round goby from the Salgir River has higher values of fin depth (the first and second dorsal fins and the anal one) and pelvic fin length, compared to fish from other areas; it is an adaptation for inhabiting spots with constant current.

The indices of head characters turned out to be higher in fish from the Bakalskaya Spit area and Streletskaya Bay. In the first region, compared to other ones, the round goby had a longer preorbital and postorbital distance; in the second, the upper jaw and head were more massive (the interorbital distance, upper jaw length, distance between eye and corner of mouth, mouth width, and head width through middle of eye were the highest). Apparently, the food spectrum of *N. melanostomus* from the Streletskaya Bay includes larger food objects than that of fish from other regions. As shown in [Bogachik, 1967], the structure of the jaw apparatus in the round goby depends on the nature of its feeding. Its food mostly consists of molluscs of the genera *Mytilus* Linnaeus, 1758, *Mytilaster* Monterosato, 1884, *Balanus* Costa, 1778, and *Dreissena* Van Beneden, 1835. *N. melanostomus* has developed specific muscles on the upper jaw allowing it to consume attached forms of molluscs, which are rarely consumed by other fish species.

Conclusion. A significant morphological heterogeneity of *Neogobius melanostomus* groups from different water areas of the Sea of Azov–Black Sea Basin is revealed. The results of the discriminant analysis showed that the spatial groupings of the round goby are combined into at least three groups. The first one is formed by fish from the western coast of the Crimean Peninsula (the Karkinitzky Bay and Donuzlav Liman) and the Sevastopol area (the Streletskaya Bay); the second one, by *N. melanostomus* from the Salgir River; and the third one, by the round goby from the Kazantip Bay (the Sea of Azov). According to the obtained data and analysis of literature, the differences between local groups based on external morphology may be due to various reasons: hydrological, hydrochemical, and environmental, including trophic conditions in certain water areas of the Sea of Azov–Black Sea Basin. Moreover, such differences may be related to the history of formation of the fish population in the studied water areas. In the inland water bodies of the Crimean Peninsula (in particular, the Salgir River), *N. melanostomus* was formed from the ichthyofauna of the Dnieper River Basin, distributing during the period of the North Crimean Canal operation. It is likely to determine the morphological isolation of this local group.

Thus, the round goby within the Sea of Azov–Black Sea Basin has formed morphologically different spatial groupings corresponding to the environmental conditions in this area. The revealed heterogeneity shows high paratypical variability of morphometric characters and the fact that under different environmental conditions, individuals of the same species develop a specific phenotype.

This work was carried out within the framework of IBSS state research assignment “Biodiversity as the basis for the sustainable functioning of marine ecosystems, criteria and scientific principles for its conservation” (No. 124022400148-4) and partly within the framework of RCFBW state research assignment “Studying the features of the structure and dynamics of freshwater ecosystems of the Northern Black Sea Region” (No. 123101900019-5) and “Assessment and development of the fishery potential of promising areas of the Northern Black Sea Region” (No. 124030100137-6).

REFERENCES

1. Andreev V. L., Reshetnikov Yu. S. A study of the intraspecific morphological variation in the whitefish *Coregonus lavareus* (L.) by multivariate statistical analysis. *Voprosy ikhtiologii*, 1977, vol. 17, iss. 5 (106), pp. 862–878. (in Russ.)
2. Bogachik T. A. Morphological adaptations in the digestive apparatus of the Black Sea Gobiidae. *Voprosy ikhtiologii*, 1967, vol. 7, iss. 1 (42), pp. 108–116. (in Russ.)
3. Boltachev A. R., Karpova E. P. *Marine Fishes of the Crimean Peninsula*. 2nd edition, revised & enlarged. Simferopol : Biznes-Inform, 2017, 376 p. (in Russ.). <https://repository.marine-research.ru/handle/299011/1356>
4. Vasil'eva E. D. *Ryby Chernogo morya. Opredelitel' morskikh, solonovatovodnykh, evrigalinnykh i prokhodnykh vidov s tsvetnymi illyustratsiyami, sobrannymi S. V. Bogorodskim*. Moscow : VNIRO, 2007, 238 p. (in Russ.)
5. Zabroda T. A., Diripasko O. A. Otsenka polovykh razlichii v morfometricheskikh priznakakh bychka-kruglyaka *Neogobius melanostomus* (Pallas, 1814) Azovskogo morya. *Visnyk Zaporizkoho natsionalnoho universytetu*, 2009, vol. 2, pp. 41–47. (in Russ.)
6. Zuev G. V., Boltachev A. R. Influence of underwater quarrying of sand on the Donuzlav estuary ecosystem. *Ekologiya morya*, 1999, iss. 48, pp. 5–9. (in Russ.). <https://repository.marine-research.ru/handle/299011/4199>
7. Karpova E. P. Alien species of fish in freshwater ichthyofauna of the Crimea. *Rossiiskii zhurnal biologicheskikh invazii*, 2016, vol. 9, no. 3, pp. 47–60. (in Russ.)
8. Karpova E. P., Boltachev A. R. Dneprovskaya ikhtiofauna v gidrosisteme Severo-Krymskogo kanala. In: *Suchasni problemy teoretychnoi i praktychnoi ikhtiolohii : materialy V Mizhnarodnoi ikhtiolohichnoi naukovy-praktychnoi konferentsii*. Chernivtsi : Knyhy-XXI, 2012, pp. 101–104. (in Russ.)
9. Kodukhova Yu. V., Borovikova E. A., Ezhova E. E., Gushchin A. V. Features of the morphology of round goby (*Neogobius melanostomus*) in the South-Eastern Baltic Sea. *Regional'naya ekologiya*, 2017, no. 3 (49), pp. 65–74. (in Russ.)
10. Lakin G. F. *Biometriya. Uchebnoe posobie dlya biol. spets. vuzov*. Moscow : Vysshaya shkola, 1990, 352 p. (in Russ.)
11. Manilo L. G. *Ryby semeistva bychkovye (Perciformes, Gobiidae) morskikh i solonovatykh vod Ukrainy*. Kyiv : Naukova dumka, 2014, 243 p. (in Russ.)
12. Pravdin I. F. *Rukovodstvo po izucheniyu ryb (preimushchestvenno presnovodnykh) / P. A. Dryagin, V. V. Pokrovskii (Eds) ; 4th edition, revised & expanded*. Moscow : Pishchevaya promyshlennost', 1966, 376 p. (in Russ.)
13. Prishchepa R. E., Boltachev A. R., Karpova E. P. The diversity of gobies (Perciformes: Gobiidae) of the Karkinitsky Gulf (the Black Sea coast of the Crimean Peninsula). In: *Biologicheskoe raznoobrazie: izuchenie, sokhranenie, vosstanovlenie, ratsional'noe ispol'zovanie : materialy Mezhdunar. nauch.-prakt. konf., Kerch, 19–23 September, 2018*. Simferopol : ARIAL, 2018, pp. 259–265. (in Russ.)
14. Svetovidov A. N. *Ryby Chernogo morya*. Moscow ; Leningrad : Nauka, 1964, 551 p. (in Russ.)
15. Smirnov A. I. The round goby *Neogobius melanostomus* (Pisces, Gobiidae) is found outside of its area: Reasons, distribution rate, probable

- after-effects. *Vestnik zoologii*, 2001, vol. 35, no. 3, pp. 71–77. (in Russ.)
16. Smirnov A. I. *Fauna Ukrainy*. Vol. 8. *Ryby*. Iss. 5. *Okuneobraznye (bychkovidnye), skorpenoobraznye, kambaloobraznye, prisoskoperoobraznye, udil'shchikooobraznye*. Kyiv : Naukova dumka, 1986, 320 p. (in Russ.)
17. Tkachenko M. Yu. Morfolohichna minlyvist bychka-kruhliaka *Neogobius melanostomus* (Pallas, 1814) morskykh ta prysnovodnykh vodoim. *Biologichni systemy*, 2012, vol. 4, iss. 4, pp. 525–529. (in Ukr.)
18. Khalafyan A. A. *Statistica 6. Statisticheskii analiz dannykh*. Moscow : OOO “Binom-Press”, 2007, 512 p. (in Russ.)
19. Belogurova R. E., Karpova E. P., Ablyazov E. R. Long-term changes in the fish fauna of the Karkinitzky Gulf of the Black Sea. *Russian Journal of Marine Biology*, 2020, vol. 46, iss. 6, pp. 452–460. <https://doi.org/10.1134/S1063074020060036>
20. Buřić M., Bláha M., Kouba A., Drozd B. Upstream expansion of round goby (*Neogobius melanostomus*) – first record in the upper reaches of the Elbe River. *Knowledge and Management of Aquatic Ecosystems*, 2015, vol. 416, art. no. 32 (5 p.). <https://doi.org/10.1051/kmae/2015029>
21. Ćolić S., Šukalo G., Ćolić V., Kerkez V. First record of round goby *Neogobius melanostomus* Pallas, 1814 (Pisces: Gobiidae) in Bosnia and Herzegovina. *Ecologica Montenegrina*, 2018, vol. 16, pp. 108–110. <https://doi.org/10.37828/em.2018.16.8>
22. Crossman E. J., Holm E., Cholmondeley R., Tuininga K. First record for Canada of the rudd, *Scardinius erythrophthalmus*, and notes on the introduced round goby, *Neogobius melanostomus*. *The Canadian Field-Naturalist*, 1992, vol. 106, no. 2, pp. 206–209.
23. Demchenko V. O., Tkachenko M. Y. Biological characteristics of the round goby, *Neogobius melanostomus* (Pallas, 1814), from different water bodies. *Archives of Polish Fisheries*, 2017, vol. 25, iss. 1, pp. 51–61. <https://doi.org/10.1515/aopf-2017-0006>
24. Diripasko O. A., Zabroda T. A. Morphometric variability in round goby *Neogobius melanostomus* (Perciformes: Gobiidae) from the Sea of Azov. *Zoosystematica Rossica*, 2017, vol. 26, no. 2, pp. 392–405. <https://doi.org/10.31610/zsr/2017.26.2.392>
25. Langerhans R. B., DeWitt T. J. Shared and unique features of evolutionary diversification. *The American Naturalist*, 2004, vol. 164, no. 3, pp. 335–349. <https://doi.org/10.1086/422857>
26. Nyeste K., Nyíri K., Molnár J. First record of the round goby, *Neogobius melanostomus* (Pallas, 1814) in the Water System of Tisza River. *Pisces Hungarici*, 2017, vol. 11, pp. 89–90.
27. Pinchuk V. I., Miller P. J. *Neogobius melanostomus* (Eichwald, 1831). In: *The Freshwater Fishes of Europe*. Vol. 8, pt I. *Mugilidae, Atherinidae, Atherinopsidae, Blenniidae, Odontobutidae, Gobiidae I* / P. J. Miller (Ed.). Wiebelsheim, Germany : AULA-Verlag, 2003, pp. 173–180.
28. Piria M., Šprem N., Jakovlić I., Tomljanović T., Matulić D., Treer T., Aničić I., Safner R. First record of round goby, *Neogobius melanostomus* (Pallas, 1814) in the Sava River, Croatia. *Aquatic Invasions*, 2011, vol. 6, suppl. 1, pp. S153–S157. <https://doi.org/10.3391/ai.2011.6.S1.034>
29. Reist J. D. An empirical evaluation of several univariate methods that adjust for size variation in morphometric data. *Canadian Journal of Zoology*, 1985, vol. 63, no. 6, pp. 1429–1439. <http://dx.doi.org/10.1139/z85-213>
30. Reist J. D. An empirical evaluation of coefficients used in residual and allometric adjustment of size covariation. *Canadian Journal of Zoology*, 1986, vol. 64, no. 6, pp. 1363–1368. <https://doi.org/10.1139/z86-203>
31. Roche K., Janač M., Šlapansky L., Mikl L., Kopeček L., Jurajda P. A newly established round goby (*Neogobius melanostomus*) population in the upper stretch of the river Elbe. *Knowledge and Management of Aquatic Ecosystems*, 2015, vol. 416, art. no. 33 (11 p.). <https://doi.org/10.1051/kmae/2015030>
32. Simonović P., Paunović M., Popović S. Morphology, feeding, and reproduction of the round goby,

- Neogobius melanostomus* (Pallas), in the Danube River Basin, Yugoslavia. *Journal of Great Lakes Research*, 2001, vol. 27, iss. 3, pp. 281–289. [https://doi.org/10.1016/S0380-1330\(01\)70643-0](https://doi.org/10.1016/S0380-1330(01)70643-0)
33. Skóra K. E., Rzeźnik J. Observations on diet composition of *Neogobius melanostomus* Pallas, 1811 (Gobiidae, Pisces) in the Gulf of Gdansk (Baltic Sea). *Journal of Great Lakes Research*, 2001, vol. 27, iss. 3, pp. 290–299. [https://doi.org/10.1016/S0380-1330\(01\)70644-2](https://doi.org/10.1016/S0380-1330(01)70644-2)
34. Stráňai I., Andreji J. The first report of round goby, *Neogobius melanostomus* (Pisces, Gobiidae) in the waters of Slovakia. *Folia Zoologica*, 2004, vol. 53, no. 3, pp. 335–338.
35. Thorpe R. S. Quantitative handling of characters useful in snake systematics with particular reference to intraspecific variation in the ringed snake *Natrix natrix* (L.). *Biological Journal of the Linnean Society*, 1975, vol. 7, iss. 1, pp. 27–43. <https://doi.org/10.1111/j.1095-8312.1975.tb00732.x>
36. van Beek G. C. W. The round goby *Neogobius melanostomus* first recorded in the Netherlands. *Aquatic Invasions*, 2006, vol. 1, iss. 1, pp. 42–43. <https://doi.org/10.3391/ai.2006.1.1.10>
37. Verreycken H., Breine J. J., Snoeks J., Belpaire C. First record of the round goby, *Neogobius melanostomus* (Actinopterygii: Perciformes: Gobiidae) in Belgium. *Acta Ichthyologica et Piscatoria*, 2011, iss. 41 (2), pp. 137–140. <https://doi.org/10.3750/AIP2011.41.2.11>

**МОРФОЛОГИЧЕСКАЯ ИЗМЕНЧИВОСТЬ БЫЧКА-КРУГЛЯКА
NEOGBIUS MELANOSTOMUS (PALLAS, 1814) (ACTINOPTERYGII, GOBIIDAE)
АЗОВО-ЧЕРНОМОРСКОГО БАССЕЙНА**

Р. Е. Белогурова^{1,2}

¹ФГБУН ФИЦ «Институт биологии южных морей имени А. О. Ковалевского РАН»,
Севастополь, Российская Федерация

²ФГБНУ «Научно-исследовательский центр пресноводной и солоноватоводной гидробиологии»,
Херсон, Российская Федерация
E-mail: prishchepa.raisa@yandex.ru

Рассмотрена изменчивость признаков внешней морфологии (36 пластических и 6 меристических) бычка-кругляка *Neogobius melanostomus* (Pallas, 1814) из семи районов Азово-Черноморского бассейна: северо-западного и юго-западного черноморского побережья Крымского полуострова (Каркинитский залив, лиман Донузлав, Стрелецкая бухта Севастополя), Казантипского залива Азовского моря, а также реки Салгир в центральной части Крымского полуострова. Установлено, что бычок-кругляк из разных районов вылова в возрасте 2+...3 имеет разные размеры тела: наибольшие у особей из Стрелецкой бухты, SL_{cp} ($136,2 \pm 1,97$) мм; наименьшие у особей из реки Салгир, SL_{cp} ($66,8 \pm 2,28$) мм. С помощью критерия Манна — Уитни между выборками установлены статистически достоверные различия по большинству пластических признаков. По меристическим признакам они отсутствуют. Наибольший вклад в дискриминацию выборок *N. melanostomus* вносят пластические признаки, связанные с расположением плавников. Согласно результатам кластерного анализа, по совокупности всех изученных признаков у бычка-кругляка Азово-Черноморского бассейна наибольшим сходством обладают выборки из Каркинитского залива (залив Самарчик и Ярылгачская бухта, $D = 28,6$) и из акватории Бакальской косы. На уровне дивергенции $D = 47,3$ объединяются группы бычков из Стрелецкой бухты и Казантипского залива, а затем к ним на уровне $D = 215$ примыкает выборка из лимана Донузлав. Выборка бычка из реки Салгир занимает наиболее обособленное положение: уровень дивергенции составляет около 475. По данным дискриминантного анализа установлено, что бычок-кругляк из Азово-Черноморского бассейна дифференцирован как минимум на три пространственные группировки: первая — из района западного побережья Крымского полуострова (Каркинитский залив и лиман Донузлав) и района Севастополя (бухта Стрелецкая); вторая — из Казантипского залива (Азовское море); третья — из реки Салгир. Наибольший вклад

в дискриминацию пространственных группировок (при коэффициенте корреляции между признаками и значениями координат по второй канонической оси больше 0,75) внесли следующие признаки: высота тела, высота и толщина хвостового стебля, антедорсальное и антевентральное расстояния и ширина грудных и брюшных плавников. Выявленная неоднородность показывает высокую паратипическую изменчивость пластических признаков; в различных экологических условиях у особей одного вида формируется специфический фенотип.

Ключевые слова: бычок-кругляк, Азово-Черноморский бассейн, пластические и меристические признаки, изменчивость, популяция

UDC 579.68:579.222

**NONYLPHENOL BIODEGRADATION
BY THE BACTERIUM *RAOULTELLA PLANTICOLA* STRAIN F8
ISOLATED FROM THE SEDIMENT OF THE GULF OF FINLAND, THE BALTIC SEA**

© 2024 T. Zaytseva¹, V. Safronova², A. Russu¹, I. Kuzikova¹, and N. Medvedeva¹

¹St. Petersburg Federal Research Center of the Russian Academy of Sciences, Scientific Research Centre for Ecological Safety of the Russian Academy of Sciences, Saint Petersburg, Russian Federation

²All-Russia Research Institute for Agricultural Microbiology, Saint Petersburg, Russian Federation

E-mail: zaytseva.62@list.ru

Received by the Editor 11.05.2022; after reviewing 08.11.2022;
accepted for publication 09.10.2023; published online 22.03.2024.

Nonylphenol (NP) is a ubiquitous environmental pollutant of major concern due to its toxicity to hydrobionts, animals, and humans. Moreover, NP is known as an endocrine disruptor. The aim of this study is to isolate from bottom sediments sampled in the southern Gulf of Finland (the Baltic Sea) and identify a highly-efficient NP-degrading bacterial strain and to analyze its NP-degrading capacity at different levels of temperature, initial pH, dissolved oxygen concentrations, and initial NP content. The isolated strain F8 was identified by phenotypic traits using standard methods and by Sanger sequencing of a fragment of the 16S rRNA gene sequence (*rrs*). NP content was determined by high-performance liquid chromatography. The novel NP-degrading bacterium *Raoultella planticola* F8 was isolated from the bottom sediments sampled in the Gulf of Finland. *R. planticola* F8 isolate was deposited in the Russian Collection of Agricultural Microorganisms (RCAM), All-Russia Research Institute for Agricultural Microbiology, as the strain RCAM 05450. The *rrs* sequence of the F8 isolate was deposited in the GenBank database (No. OL831016). This strain is highly efficient for NP degradation in aerobic conditions at different NP concentrations (up to 900 mg·L⁻¹), in the temperature range of +5...+35 °C, the initial pH range of 5–9, and the dissolved oxygen concentration range of 0.8–2.46 mg·L⁻¹. This is the first study to demonstrate the ability of *R. planticola* to degrade NP. Results of this investigation provide useful information for *R. planticola* F8 application in bioremediation processes.

Keywords: *Raoultella planticola* F8, sediments, identification, nonylphenol, biodegradation

Nonylphenol (hereinafter NP), an endocrine disrupting xenobiotic of anthropogenic origin, is a widespread environmental pollutant worldwide. NP is actively used in manufacture of modified phenolic and epoxy resins and non-ionic surfactants, more specifically NP ethoxylates [Bhandari et al., 2021]. NP pollution in aquatic and terrestrial ecosystems occurs mainly due to a massive discharge into the environment of domestic and industrial wastewater, insufficiently treated at wastewater treatment plants [Barber et al., 2015].

NP pollution in the environment is of great concern due to its toxicity to hydrobionts, animals, and humans. Besides, NP is known as an endocrine disruptor [Bhandari et al., 2021; Khalid, Abdollahi, 2021; Uğuz et al., 2009]. For these reasons, NP is referred to in the list of priority hazardous substances under the Environmental Quality Standards Directive 2013/39/EU and in the list of hazardous substances in the Baltic Sea.

Because of its widespread use, NP is frequently detected in all natural environments, *inter alia* rivers, lakes, coastal waters, and bottom sediments. NP concentration in water can reach hundreds of micrograms *per* L [Bhandari et al., 2021; Solé et al., 2000]. Due to its high hydrophobic nature and low solubility in water, NP can be adsorbed on sediment particles, and this leads to its accumulation in bottom sediments of freshwater and marine ecosystems [Soares et al., 2008]. NP concentration in sediments is several orders of magnitude higher than in water, up to several thousand milligrams *per* kg. Considering NP persistence, its half-life in bottom sediments may exceed 60 years [Bhandari et al., 2021; Soares et al., 2008]. Sediments can serve as a secondary NP contamination source for aquatic ecosystems due to the desorption of part of sediment-bound NP fraction followed by its dissolution in the water phase [De Weert et al., 2008].

In the natural environment (soil, water, and bottom sediments), NP may be transformed into less toxic compounds due to abiotic (like hydrolysis and photolysis) and biological processes [Bhandari et al., 2021]. As known, microbial degradation is one of the main strategies to reduce NP pollution in the environment. The rate and extent of the degradation of pollutants, including NP, are largely determined by the physiological activity of microorganisms and conditions of their incubation (temperature, pH, pollutant content, *etc.*) [Abatenh et al., 2017; Khan et al., 2009; Xie et al., 2015]. It is also known that microbial degradation of NP can occur under both aerobic and anaerobic conditions: methanogenic and nitrate- and sulfate-reducing [Mao et al., 2012; Soares et al., 2008; Wang et al., 2015a].

Various microorganisms of different taxonomic groups, such as bacteria [Corvini et al., 2006; Ma et al., 2018; Reddy et al., 2017], blue-green algae [Baptista et al., 2009; Zaytseva, Medvedeva, 2019], microalgae [Feng et al., 2022], yeast [Rajendran et al., 2017; Vallini et al., 2001], and filamentous fungi [Kuzikova et al., 2020; Yang et al., 2018], were reported to be able to degrade alkylphenols, *inter alia* NP.

This finding prompted the search for more bacterial species that may serve as efficient NP biodegraders in bioremediation processes.

The aim of this study is to isolate from the bottom sediments sampled in the southern Gulf of Finland (the Baltic Sea) and identify the highly-efficient nonylphenol-degrading bacterial strain and to analyze its NP-degrading capacity at different levels of temperature, initial pH, dissolved oxygen concentration, and initial NP content.

MATERIAL AND METHODS

The sediments used in this research were sampled in the southern Gulf of Finland, the Baltic Sea (N59.99007°, E28.96475°) in June 2018. The sample (0–10-cm depth) was taken with a Box Corer, placed into a glass jar, and stored at +4 °C.

Technical NP (CAS 84852-15-3) was purchased from Sigma-Aldrich (the USA). Since NP has low solubility in water and mineral salt medium, NP stock solutions in ethanol were used in the tests.

The sediment sample was contaminated with NP (300 mg·kg⁻¹) and incubated in the dark at +25 °C for 240 days.

The sediment sample (5 g, wet weight) was added to 50 mL of minimal mineral medium (hereinafter MMM) containing: (NH₄)₂SO₄, 4.0 g·L⁻¹; KH₂PO₄, 1.5 g·L⁻¹; K₂HPO₄, 1.5 g·L⁻¹; and MgSO₄·7H₂O, 0.2 g·L⁻¹ supplemented with NP (50 mg·L⁻¹) as a selective agent, pH (7.2 ± 0.2). The mixture was incubated on a rotary shaker Certomat BS-1 (230 rpm) at +28 °C in the dark for 7 days and then transferred to a fresh medium with NP and incubated under the same conditions. After that, the cultures were transferred regularly, every 3–4 days.

After 3 times of repeated subculturing, 0.1 mL of culture broth was pipetted and spread on solid MMM containing glucose (5.0 g·L⁻¹), yeast extract (2.0 g·L⁻¹), agar (20 g·L⁻¹), and NP (50 mg·L⁻¹). Single colonies were selected and streaked on nutrient agar supplemented with NP (50 mg·L⁻¹). The cultures were incubated at +28 °C for 3 days. Morphologically different colonies of bacteria were selected for further study of their NP degrading ability.

Selected bacterial isolates were incubated on MMM supplemented with NP (100 mg·L⁻¹) on a rotary shaker at 230 rpm, at +28 °C, in the dark for 7 days. After that, samples were taken to measure NP concentrations.

Phenotypic traits of the strain F8 were determined using standard methods and culture media [Krige, Padgett, 2011].

The isolated strain F8 was identified according to the Bergey's Manual [1994] and the Sanger sequencing method for a 1450-bp fragment of the 16S rRNA gene (*rrs*) using primers fD1 (5'-AGAGTTTGATCCTGGCTCAG-3') and rD1 (5'-CTTAAGGAGGTGATCCAGCC-3') [Weisburg et al., 1991]. Direct sequencing of PCR products was conducted on an ABI PRISM 3500xl genetic analyzer (Applied Biosystems, the USA).

The NCBI GenBank database (<https://www.ncbi.nlm.nih.gov>) and the BLAST program (<https://blast.ncbi.nlm.nih.gov/Blast.cgi>) were used to search for homologous sequences. To construct a phylogenetic tree, we applied the MEGA software v. 6 and used the neighbor joining method [Tamura et al., 2011]. Evolutionary distances were calculated by the Maximum Composite Likelihood method. The statistical reliability of the clusters was assessed with bootstrap analysis (1,000 replicas).

The inoculum was obtained by harvesting the strain F8 grown on solid MMM containing glucose (5.0 g·L⁻¹), yeast extract (2.0 g·L⁻¹), agar (20.0 g·L⁻¹), and NP (50 mg·L⁻¹) for 3 days. Cells were washed three times in 20 mM phosphate buffered saline (pH 7.0) and inoculated into 50 mL of MMM supplemented with NP. The initial cell density was $(3 \pm 1) \times 10^8$ cells·mL⁻¹. The strain F8 was cultivated on MMM with NP in the dark for 7 days. NP was added to the medium in the form of ethanol solutions. Equal amounts of ethanol were added to abiotic controls.

The following cultivation conditions were manipulated in order to investigate their effects on NP biodegradation: temperature (+5, +10, +16, +22, +28, and +35 °C), initial pH (5.0, 6.0, 7.0, 8.0, and 9.0), dissolved oxygen (hereinafter DO) concentration (0.8, 1.08, 1.31, 1.53, and 2.46 mg·L⁻¹), and initial NP content (100, 300, 500, 700, and 900 mg·L⁻¹).

The effects of initial pH, DO concentration, and temperature on NP biodegradation were estimated at 100 mg·L⁻¹ of NP in MMM.

To study the effects of NP content, initial pH, and DO concentration on the biodegradation capacity of the strain F8, cells were cultivated on NP-containing MMM on a rotary shaker Certomat BS-1 in the dark at +28 °C.

Various levels of DO concentration were created during the strain F8 cultivation in the Erlenmeyer flasks with different volumes of MMM (25, 50, 75, 100, and 125 mL). Winkler iodometric method was used to measure DO amount in the medium [Water Quality, 1983].

The effect of temperature on NP biodegradation rate was estimated during the bacteria cultivation under static conditions in the dark.

Non-inoculated variants were kept as blank controls to determine the abiotic loss of NP and incubated throughout the cultivation period. Each treatment in different tests was replicated three times for accuracy.

NP concentrations in the entire content of bacterial culture (cells with medium) and in abiotic controls were measured by high-performance liquid chromatography on an HP1090 chromatograph (Hewlett-Packard, the USA), according to the technique presented earlier [Kuzikova et al., 2020].

The kinetics of NP degradation during its fast phase under different bacterial cultivation conditions was analysed in accordance with the first-order model described by the following equation:

$$\ln(C_t/C_0) = -k \times t,$$

where C_0 is initial NP concentration ($\text{mg}\cdot\text{L}^{-1}$);

C_t is NP concentration at the time t ($\text{mg}\cdot\text{L}^{-1}$);

k is the degradation rate constant, days^{-1} [Baptista et al., 2009].

All statistical analysis was carried out applying PAST 4.0 software. Statistical significance was determined using one-way ANOVA and Tukey's post-hoc test for normally distributed data; differences were considered significant at $p < 0.05$. Shapiro–Wilk and Levene's tests were performed to assess data normality and variance equality. The obtained data are given in tables and graphs as mean values with a standard deviation ($M \pm SD$) of three independent replicates ($n = 3$). Spearman's correlation coefficients (r_s) were used to identify relationships between NP degradation parameters and NP cultivation variables; $p < 0.05$ was considered statistically significant.

RESULTS

Ten bacterial strains isolated from the sample of NP-contaminated bottom sediments had the capacity to degrade NP. Extent of NP ($100 \text{ mg}\cdot\text{L}^{-1}$) degradation after 7 days of cultivation was found to be between 43.1 and 91.5% depending on a bacterial strain (no data provided).

The highest biodegradation capacity (91.5%) was recorded for the strain F8. It should be pointed out that in the abiotic controls (without bacterial cells), NP degradation did not occur in the medium.

Cells of the strain F8 are gram-negative, non-spore-forming, and non-motile rods with capsules. The strain F8 forms circular beige colonies on nutrient agar, with a diameter of 2–3 mm, a smooth edge, smooth and shiny surface, fine-grained structure, and liquid consistency. The strain F8 is catalase-positive and oxidase-negative. It is a facultative anaerobic bacterium. Voges–Proskauer reactions and acid formation are positive; indole is not formed. This strain is capable of using urea, assimilating nitrogen from the atmosphere, performing denitrification, consuming nitrogen from mineral salts, and catabolizing lactose, sucrose, rhamnose, fructose, galactose, mannose, xylose, mannitol, sorbitol, glucose, arabinose, and starch with acid and gas formation; it does not use inositol. The strain shows amylolytic and lipolytic activity. Its cells are capable of growing in a wide range of temperature ($+5\dots+36 \text{ }^\circ\text{C}$) and pH (5–10, but not at pH of 3).

Phenotypically, the isolate F8 is close to the genus *Klebsiella* (Enterobacteriaceae family) [Bergey's Manual of Determinative Bacteriology, 1994].

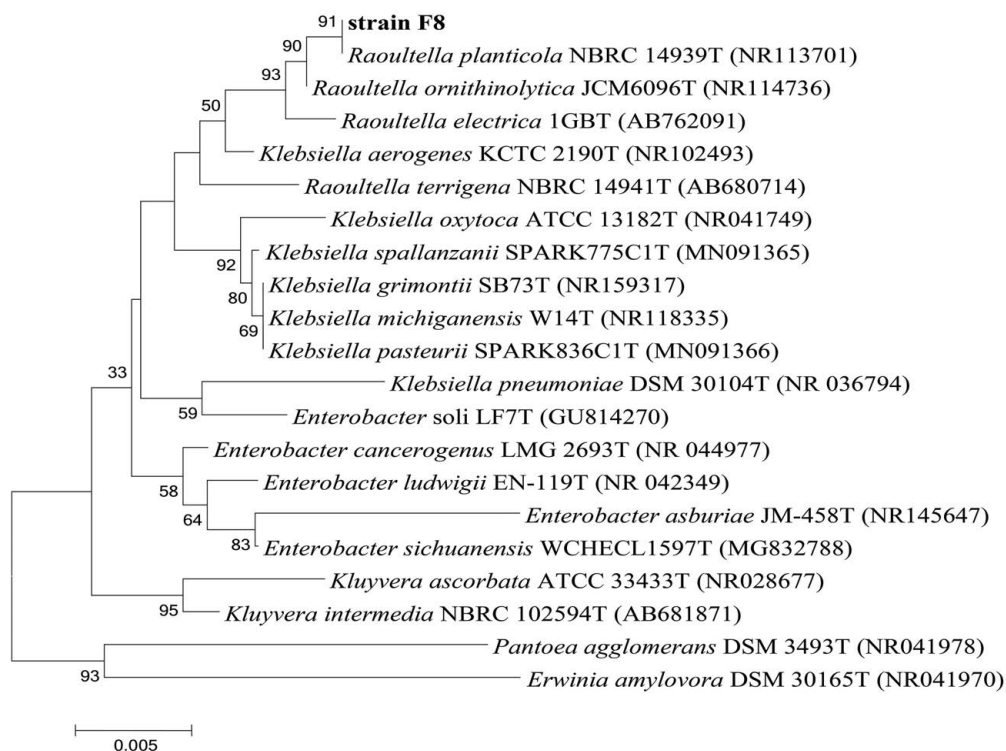
As revealed by sequencing, the *rrs* gene fragment of the isolate F8 has the highest similarity (99.72%) with a similar fragment of the type strain *Raoultella planticola* NBRC 14939, belonging to Enterobacteriaceae family (Table 1).

Raoultella genus was separated from the closely related *Klebsiella* genus on the basis of the *rrs* and *rpoB* gene sequences analysis, DNA–DNA hybridization, and biochemical studies [Drancourt et al., 2001]. Initially, in addition to *R. planticola*, this genus included two species: *R. ornithinolytica* and *R. terrigena* [Drancourt et al., 2001]. Later, the species *R. electrica* was described as well [Kimura, 2014].

Table 1. Similarity between the isolate F8 and the closest type strains belonging to Enterobacteriaceae family based on the 16S rRNA gene sequencing

Type strain	NCBI accession number	Similarity with the isolate F8 (%)
<i>Raoultella planticola</i> NBRC 14939	NR113701	99.72
<i>Raoultella ornithinolytica</i> JCM 6096	NR114736	99.45
<i>Klebsiella aerogenes</i> KCTC 2190	NR102493	99.24
<i>Raoultella electrica</i> 1GB	AB762091	99.16
<i>Raoultella terrigena</i> NBRC 14941	AB680714	98.69
<i>Klebsiella grimontii</i> SB73	NR159317	98.54
<i>Klebsiella oxytoca</i> ATCC 13182	NR041749	98.01
<i>Klebsiella pneumoniae</i> DSM 30104	NR036794	97.80
<i>Enterobacter asburiae</i> JM-458	NR145647	96.46
<i>Erwinia amylovora</i> DSM 30165	NR041970	95.73

A phylogenetic tree based on the *rrs* gene sequences, representing the taxonomic status of the isolate F8 within Enterobacteriaceae family, is shown in Fig. 1. As can be seen, the studied isolate formed a single cluster with the type strain *R. planticola* NBRC 14939T at a high level of statistical support (91%).

**Fig. 1.** Phylogenetic tree generated by the neighbor joining method using partial 16S rRNA gene sequences reflecting the taxonomic position of the strain F8 isolate within Enterobacteriaceae family. The isolated strain is highlighted in bold. Type strains are indicated by the letter T. Bootstrap values of more than 30% are given

Summing all the phenotypic traits with the reported sequence of the 16S rRNA gene fragment, the strain F8 was identified as *R. planticola* F8. The isolate *R. planticola* F8 was deposited in the Russian Collection of Agricultural Microorganisms (RCAM) as the strain RCAM 05450 and stored at -80°C in the automated Tube Store (Liconic Instruments, Liechtenstein). The *rrs* sequence of the isolate F8 was deposited in the GenBank database (No. OL831016).

The results of studying the effect of temperature on NP degradation revealed the capacity of *R. planticola* F8 to degrade NP in a wide range, +5...+35 °C (Fig. 2). A high level of correlation was found between temperature and NP biodegradation rate constant k ($r_s = 0.818$; $p = 0.0038$).

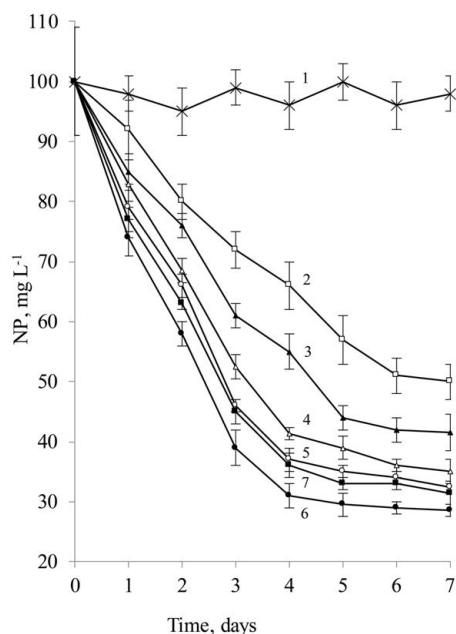


Fig. 2. Dependence of nonylphenol content in the culture liquid of the bacterium *Raoultella planticola* F8 on temperature: 1, abiotic control; 2, +5 °C; 3, +10 °C; 4, +16 °C; 5, +22 °C; 6, +28 °C; 7, +35 °C

At +5 °C, the degradation rate constant k during the fast phase was 0.111 days^{-1} , while half-life t_{50} was 6.2 days. NP degradation by the isolated strain was accelerated with a rise in the incubation temperature up to +28 °C, which resulted in a statistically significant ($p < 0.5$) increase in k and decrease in NP half-life by 2.7 times, as well as in an increase in NP degradation degree from 51 to 71.5%. A further rise in temperature, up to +35 °C, led to a decrease in k and increase in t_{50} by 1.2 times (Table 2).

Table 2. Effect of cultivation conditions on destruction of nonylphenol ($100 \text{ mg}\cdot\text{L}^{-1}$) by *Raoultella planticola* F8

Cultivation condition	T, °C	Dissolved oxygen, $\text{mg}\cdot\text{L}^{-1}$	Initial pH	k , days^{-1}	R^2	t_{50} , days	Nonylphenol degradation degree after 7 days, %
Temperature	+5	0.8	7	0.111 ± 0.004	0.95	6.2 ± 0.2	51 ± 2
	+10	0.8	7	0.161 ± 0.005	0.991	4.3 ± 0.3	58.5 ± 1.9
	+16	0.8	7	0.212 ± 0.011	0.992	3.3 ± 0.1	65 ± 3
	+22	0.8	7	0.251 ± 0.004	0.979	2.8 ± 0.1	67.5 ± 1.2
	+28	0.8	7	0.307 ± 0.005	0.99	2.3 ± 0.2	71.5 ± 1.8
	+35	0.8	7	0.26 ± 0.01	0.995	2.7 ± 0.2	70 ± 2
Dissolved oxygen concentration	+28	0.8	7	0.307 ± 0.006	0.99	2.26 ± 0.01	71.5 ± 1.2
	+28	1.08	7	0.525 ± 0.005	0.999	1.32 ± 0.04	81 ± 2
	+28	1.31	7	0.66 ± 0.01	0.998	1.05 ± 0.03	85 ± 2
	+28	1.53	7	1.15 ± 0.11	0.986	0.6 ± 0.1	91.5 ± 1.9
	+28	2.46	7	0.916 ± 0.005	0.944	0.76 ± 0.03	89 ± 2
Initial pH	+28	1.53	5	0.569 ± 0.003	0.985	1.22 ± 0.14	80 ± 2
	+28	1.53	6	0.655 ± 0.011	0.999	1.06 ± 0.09	82 ± 2
	+28	1.53	7	1.15 ± 0.11	0.986	0.6 ± 0.1	91.5 ± 1.9
	+28	1.53	8	0.886 ± 0.009	0.997	0.78 ± 0.04	88 ± 1
	+28	1.53	9	0.458 ± 0.006	0.998	1.51 ± 0.08	76 ± 2

Taking all data into account, it can be concluded that the maximum biodegradation rate was observed at +28 °C.

As shown, NP degradation by the bacterium *R. planticola* depends on DO concentration (Fig. 3).

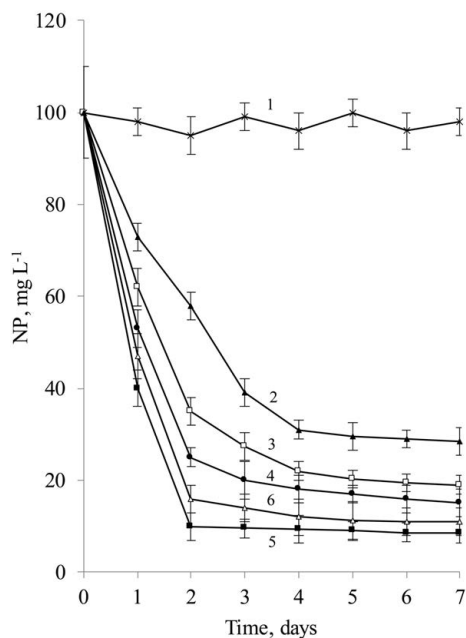


Fig. 3. Dependence of nonylphenol content in the culture liquid of the bacterium *Raoultella planticola* F8 on dissolved oxygen concentration: 1, abiotic control; 2, 0.8 mg·L⁻¹; 3, 1.08 mg·L⁻¹; 4, 1.31 mg·L⁻¹; 5, 1.53 mg·L⁻¹; 6, 2.46 mg·L⁻¹

A rise in DO concentration from 0.8 to 1.53 mg·L⁻¹ led to a statistically significant increase in k and decrease in t_{50} by 3.8 times. The degree of NP degradation after 7 days of cultivation dropped by 1.3 times (Table 2). A further rise in DO concentration, up to 2.46 mg·L⁻¹, resulted in a decrease in NP biodegradation rate constant and an increase in half-life by 1.3 times.

Based on the results, DO concentration for effective NP degradation by *R. planticola* should be within 1.53–2.46 mg·L⁻¹.

The results of studying the effect of initial pH on NP degradation by *R. planticola* revealed that the highest NP degradation degree, 88–91.5%, was reached after 7 days of cultivation in the pH range of 7.0 to 8.0 (Fig. 4, Table 2).

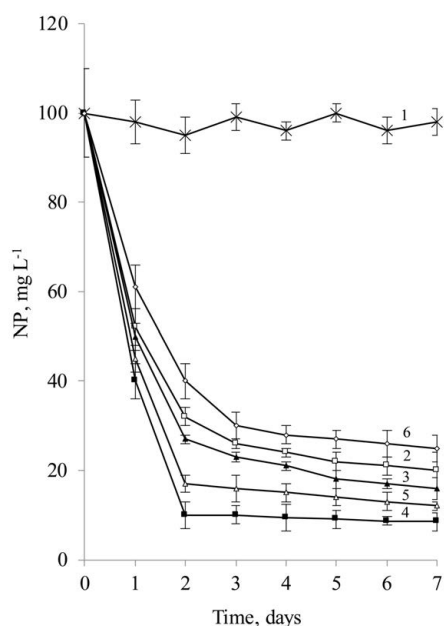


Fig. 4. Dependence of nonylphenol content in the culture liquid of the bacterium *Raoultella planticola* F8 on initial pH: 1, abiotic control; 2, pH 5; 3, pH 6; 4, pH 7; 5, pH 8; 6, pH 9

The highest degradation rate constant k (1.15 days^{-1}) and the lowest half-life t_{50} (0.6 days) were revealed at pH of 7.0. A decrease in pH from 7.0 to 5.0 and an increase to 9.0 resulted in a statistically significant ($p < 0.5$) drop in k and a rise in half-life t_{50} by 2 and 2.5 times, respectively.

Finally, optimal initial pH value for NP biodegradation by *R. planticola* was determined as 7.0–8.0.

As found, the bacterium *R. planticola* F8 degrades NP in a wide range of NP concentrations, from 100 to 900 $\text{mg}\cdot\text{L}^{-1}$ (Table 3).

Table 3. Effect of initial nonylphenol concentration on its destruction by *Raoultella planticola* F8

Nonylphenol, $\text{mg}\cdot\text{L}^{-1}$	k , days^{-1}	R^2	t_{50} , days	Nonylphenol degradation degree after 7 days, %
100	1.15 ± 0.11	0.986	0.6 ± 0.1	91.5 ± 1.9
300	0.866 ± 0.005	0.914	0.8 ± 0.1	84.8 ± 0.6
500	0.292 ± 0.002	0.976	2.4 ± 0.1	84 ± 2
700	0.22 ± 0.01	0.88	3.2 ± 0.4	78.6 ± 1.4
900	0.12 ± 0.01	0.986	5.8 ± 0.5	55.6 ± 1.3

A high level of correlation ($p < 0.001$) was registered between NP biodegradation rate constant and initial NP content ($r_s = -0.983$) and between t_{50} and initial NP concentration ($r_s = 0.999$). A rise in NP content in the medium from 100 to 900 $\text{mg}\cdot\text{L}^{-1}$ led to a statistically significant ($p < 0.05$) decrease in the degradation rate constant k and an increase in half-life t_{50} by 9.6 times. The degree of NP degradation dropped by 1.6 times (Table 3).

DISCUSSION

Recently, one of the main ecological problems was environmental contamination by endocrine disrupting chemicals, in particular NP which affects the endocrine system of living organisms.

NP degradation in natural environments is caused by its abiotic destruction and biodegradation. A wide range of bacteria belonging to different genera are known to have NP-degrading capacity: *Acinetobacter*, *Achromobacter*, *Alcaligenes*, *Arthrobacter*, *Bacillus*, *Burkholderia*, *Citrobacter*, *Corynebacterium*, *Desulfobacterium*, *Klebsiella*, *Pseudomonas*, *Serratia*, *Sphingomonas*, etc. [Corvini et al., 2006; Gabriel et al., 2005; Ma et al., 2018; Reddy et al., 2017; Xie et al., 2015].

The pathways of NP biodegradation by bacteria are widely presented in scientific literature. Previously, it was revealed that aerobic NP degradation by bacteria can be initiated either by oxidative cleavage of the alkyl chain or by oxidative action on an aromatic ring. A putative mechanism for degradation of the alkyl chain includes hydroxylation at the terminal carbon atom (as the first step), oxidation of the resulting alcohol into the corresponding carboxylic acid, and further degradation *via* β -oxidation. NP degradation *via* oxidation of the alkyl chain is characteristic of NP isomers, in which the side chain is linear or at least not highly branched. NP isomers with highly branched side chains can initially be destroyed by hydroxylation phenolic ring. Type II *ipso*-substitution mechanism (hydroxylation at the carbon atom-4) was described as the first step of degradation pathway, which occurs by oxidation and replacement of aromatic carbon atom of NP by an alkyl side chain [Bhandari et al., 2021].

As mentioned earlier, the bacterium *R. planticola* F8, an active NP biodestructor, was isolated from bottom sediments sampled in the southern Gulf of Finland. This strain belongs to Proteobacteria phylum, Gammaproteobacteria class. Gammaproteobacteria, along with Alphaproteobacteria, are known as the most abundant bacterial groups in the microbiome of NP-contaminated bottom sediments [Wang et al., 2015b].

Raoultella representatives have been associated with degradation of various organic contaminants, such as drugs [Palyzová et al., 2019], pesticides [Bhatt et al., 2019], polycyclic aromatic hydrocarbons [Ping et al., 2017], and so on. The ability of *R. planticola* to degrade NP was revealed for the first time.

Two phases of NP biodegradation by *R. planticola* were identified analyzing the degradation curves under test conditions: the fast and the slow one. It should be noted that a similar two-phase nature of a decrease in alkylphenols content was previously found during their destruction by cyanobacteria [Baptista et al., 2009; Zaytseva, Medvedeva, 2019] and micromycetes [Kuzikova et al., 2020]. The limitation of NP degradation process at the end of the fast phase can be caused by a decline in the medium quality which results from formation of metabolites toxic to bacteria [Bai et al., 2017].

Due to their metabolism and capacity to adapt to adverse environmental conditions, microorganisms can degrade a wide range of organic pollutants, including alkylphenols. However, their efficiency depends on many factors, *inter alia* pollutant concentration and physicochemical characteristics of the environment, such as temperature, pH, DO concentration, *etc.* [Abatenh et al., 2017; Watanabe et al., 2012].

This study allowed revealing that the rate of NP degradation by *R. planticola* F8 depends on temperature, initial pH, DO concentration, and initial NP content to a large extent. It is well known that temperature is one of the most relevant abiotic factors affecting the degradation of xenobiotics. Temperature variations can accelerate or decelerate biodegradation by affecting the physiological properties of microbial degraders, in particular *via* direct effect on the biological enzymes involved in the degradation pathway [Abatenh et al., 2017; Khan et al., 2009].

The temperature dependence of NP biodegradation, as well as the optimum temperature (+30 °C), were revealed earlier during NP degradation by bacterial strains *Pseudomonas* sp., *Acidovorax* sp., *Pseudomonas putida*, *Citrobacter freundii*, and complex microorganisms ZJF composed by three strains combined: *Serratia* sp., *Klebsiella* sp., and *Ps. putida* [Ma et al., 2018; Watanabe et al., 2012; Xie et al., 2015].

It is worth noting that previous studies were focused on the ability of bacteria to degrade NP at temperatures above +14 °C [Ma et al., 2018; Watanabe et al., 2012; Xie et al., 2015]. To date, information on NP degradation at lower temperatures is still lacking.

As shown in our tests, NP destruction by *R. planticola* F8 also significantly depends on temperature. This bacterium was found to be highly efficient for NP degradation in a wide temperature range, +5...+35 °C. The fact that *R. planticola* F8 is capable of degrading NP even at such a low temperature, as +5 °C, is of certain interest. Biodegradation rate increases as temperature rises from +5 to +28 °C, reaching its maximum at +28 °C. A rise in temperature from +28 to +35 °C led to a drop in biodegradation rate. It is assumed that contaminant biodegradation is slowed down at relatively high and low temperatures due to a decrease in the activity of bacterial and extracellular enzymes [Xie et al., 2015].

Aeration and pH levels significantly affect the biodegradation of organic pollutants.

Oxygen is the most common electron acceptor in the bacterial respiration. During aerobic biodegradation of aromatic compounds, oxygen acts as an electron acceptor for aromatic pollutants, besides participating in substrate activation *via* oxygenation reactions [Cao et al., 2009]. As known, in aerobic conditions, the bacterial biodegradation of alkylphenols, *inter alia* NP, involves mono- and dioxidases and multicomponent phenol hydroxylases. These enzymes catalyze chemical reactions cleaving chemical bonds and assisting the transfer of electrons from reduced organic substrate (donor) to another chemical compound (acceptor). Oxidases play a key role in metabolism of organic compounds,

increasing their reactivity or water solubility or causing the aromatic ring cleavage. Generally, introduction of O₂ atoms into the organic molecule by oxygenase results in the aromatic ring cleavage [Cao et al., 2009; Karigar, Rao, 2011; Tuan et al., 2011].

We established that *R. planticola* F8 is capable of degrading NP in a wide range of DO concentrations in the medium (0.8–2.46 mg·L⁻¹). The rate of NP degradation by this bacterium was minimal at the lowest DO content used in the tests, 0.8 mg·L⁻¹. An increase in DO concentration up to 1.53 mg·L⁻¹ resulted in a rise in degradation rate. Optimal DO content for NP degradation by *R. planticola* F8 was determined as 1.53–2.46 mg·L⁻¹.

The level of pH is known to affect the physiological properties of microorganisms, thus playing a noticeable role in biodegradation of organic pollutants. Like other proteins, microbial enzymes, *inter alia* those catalysing biodegradation processes, are extremely sensitive to a medium pH. The changes in pH level cause alterations in the electric charge of various chemical groups which are present in enzyme molecules. An imbalance in electrical charges in very acidic and alkaline pH ranges leads to destruction of chemical bonds that support the structure of the enzyme, decrease in enzymatic activity, and denaturation of the enzyme. Consequently, there is a significant deterioration in pollutant biodegradation [Alneyadi et al., 2017].

As previously reported, pH level affects the bacterial degradation of various organic pollutants: polyaromatic hydrocarbons, phenol and its derivatives, antibiotics, *etc.* [Ibrahim et al., 2018; Khan et al., 2009; Lakshmi, Sridevi, 2009; Liu et al., 2017]. As shown earlier, pH value significantly affects NP degradation by the bacteria *Ps. putida* and *C. freundii* with optimal pH levels of 5–7 and 6–7, respectively, and by complex microorganisms ZJF with optimal pH of 6.0 [Ma et al., 2018; Xie et al., 2015].

This work investigated effects of initial pH in the range of 5.0–9.0 on NP degradation by the bacterium *R. planticola* F8, and optimal pH level for NP biodegradation was revealed, 7.0–8.0. Both increasing pH to 9.0 and decreasing it to 5.0 decelerate pollutant biodegradation.

Initial NP concentrations affect the bacterial degradation as well. Earlier studies showed the effect of initial NP content on efficiency of NP removal by different bacteria: *Acidovorax* sp., *C. freundii*, *Serratia* sp., *Klebsiella* sp., and *Ps. putida* [Ma et al., 2018; Xie et al., 2015]. For example, an increase in efficiency of NP degradation by *Ps. putida* and *C. freundii* was recorded when initial pollutant concentration was raised from 1 to 5 µg·L⁻¹. However, a further rise in NP content, up to 9 µg·L⁻¹, caused no statistically significant changes in extent of degradation [Xie et al., 2015]. A rise in initial NP concentration from 5 to 10–15 mg·L⁻¹ also resulted in an increase in efficiency of pollutant degradation by the bacteria *Serratia* sp., *Klebsiella* sp., and *Ps. putida* up to 60%. But a further rise in initial NP concentration, up to 100 mg·L⁻¹, led to a drop in degradation efficiency to 30% [Ma et al., 2018].

Our data show as follows: an increase in NP concentration from 100 to 900 mg·L⁻¹ led to a suppression of degradation efficiency by *R. planticola* F8, a decrease in degradation rate, and an increase in NP half-life. The slowdown in biodegradation of pollutants at high concentrations is explained by their toxic effect on pollutant-degrading microorganisms [Abatenh et al., 2017]. However, it should be noted that the isolated strain *R. planticola* F8, despite a statistically significant drop in the degradation rate constant *k*, a rise in half-life *t*₅₀ by 9.6 times, and a decrease in the degree of NP degradation by 1.6 times, was capable of degrading NP at such a high content, as 900 mg·L⁻¹. The same degradative activity at such a high toxicant concentration was previously registered only in the microbial consortium NP-M2 isolated from bottom sediments, mainly consisting of bacteria of the genera *Sphingomonas*, *Pseudomonas*, *Alicyclophilus*, and *Acidovorax* [Bai et al., 2017].

Conclusion. We isolated the bacterial strain F8 from the nonylphenol-contaminated bottom sediments sampled in the southern Gulf of Finland (the Baltic Sea). *Raoultella planticola* F8 is capable of degrading nonylphenol in aerobic conditions at its different concentrations (up to 900 mg·L⁻¹) and in a wide range of temperature, initial pH, and dissolved oxygen content.

The results of this study provide useful information for the potential application of the bacterium *R. planticola* F8 in bioremediation processes.

This work was supported by the state assignment of the Ministry of Science and Higher Education of the Russian Federation (No. 122041100086-5). Strain identification was supported by the Russian Science Foundation (grant No. 21-16-00084).

REFERENCES

1. Abatenh E., Gizaw B., Tsegaye Z., Wassie M. The role of microorganisms in bioremediation – a review. *Open Journal of Environmental Microbiology*, 2017, vol. 2, iss. 1, pp. 038–046. <https://doi.org/10.17352/ojeb.000007>
2. Alneyadi A. H., Shah I., AbuQamar S. F., Ashraf S. S. Differential degradation and detoxification of an aromatic pollutant by two different peroxidases. *Biomolecules*, 2017, vol. 7, iss. 1, art. no. 31 (18 p.). <https://doi.org/10.3390/biom7010031>
3. Bai N., Abuduaini R., Wang S., Zhang M., Zhu X., Zhao Y. Nonylphenol biodegradation characterizations and bacterial composition analysis of an effective consortium NP-M2. *Environmental Pollution*, 2017, vol. 220, pt A, pp. 95–104. <https://doi.org/10.1016/j.envpol.2016.09.027>
4. Baptista M. S., Stoichev T., Basto M. C. P., Vasconcelos V. M., Vasconcelos M. T. S. D. Fate and effects of octylphenol in a *Microcystis aeruginosa* culture medium. *Aquatic Toxicology*, 2009, vol. 92, iss. 2, pp. 59–64. <https://doi.org/10.1016/j.aquatox.2008.12.005>
5. Barber L. B., Loyo-Rosales J. E., Rice C. P., Minarik T. A., Oskouie A. K. Endocrine disrupting alkylphenolic chemicals and other contaminants in wastewater treatment plant effluents, urban streams, and fish in the Great Lakes and Upper Mississippi River Regions. *Science of the Total Environment*, 2015, vol. 517, pp. 195–206. <https://doi.org/10.1016/j.scitotenv.2015.02.035>
6. *Bergey's Manual of Determinative Bacteriology*. 9th edition / D. H. Bergey, J. G. Holt (Eds). Baltimore : Williams & Wilkins, 1994, 787 p.
7. Bhandari G., Bagheri A. R., Bhatt P., Bilal M. Occurrence, potential ecological risks, and degradation of endocrine disrupter, nonylphenol, from the aqueous environment. *Chemosphere*, 2021, vol. 275, art. no. 130013 (16 p.). <https://doi.org/10.1016/j.chemosphere.2021.130013>
8. Bhatt P., Huang Y., Zhan H., Chen S. Insight into microbial applications for the biodegradation of pyrethroid insecticides. *Frontiers in Microbiology*, 2019, vol. 10, art. no. 1778 (18 p.). <https://doi.org/10.3389/fmicb.2019.01778>
9. Cao B., Nagarajan K., Loh K.-C. Biodegradation of aromatic compounds: Current status and opportunities for biomolecular approaches. *Applied Microbiology and Biotechnology*, 2009, vol. 85, iss. 2, pp. 207–228. <https://doi.org/10.1007/s00253-009-2192-4>
10. Corvini P. F. X., Schäffer A., Schlosser D. Microbial degradation of nonylphenol and other alkylphenols—our evolving view. *Applied Microbiology and Biotechnology*, 2006, vol. 72, iss. 2, pp. 223–243. <https://doi.org/10.1007/s00253-006-0476-5>
11. De Weert J., de la Cal A., van den Berg H., Murk A., Langenhoff A., Rijnaarts H., Grotenhuis T. Bioavailability and biodegradation of nonylphenol in sediment determined with chemical and bioanalysis. *Environmental Toxicology and Chemistry*, 2008, vol. 27, iss. 4, pp. 778–785. <https://doi.org/10.1897/07-367.1>
12. Drancourt M., Bollet C., Carta A., Rousselet P. Phylogenetic analyses of *Klebsiella* species delineate *Klebsiella* and *Raoultella* gen. nov., with description of *Raoultella ornithinolytica* comb. nov., *Raoultella terrigena* comb. nov. and *Raoultella planticola* comb.

- nov. *International Journal of Systematic and Evolutionary Microbiology*, 2001, vol. 51, iss. 3, pp. 925–932. <https://doi.org/10.1099/00207713-51-3-925>
13. Feng Y., Wang A., Fu W., Song D. F. Growth performance, antioxidant response, biodegradation and transcriptome analysis of *Chlorella pyrenoidosa* after nonylphenol exposure. *Science of the Total Environment*, 2022, vol. 806, pt 1, art. no. 150507 (9 p.). <https://doi.org/10.1016/j.scitotenv.2021.150507>
 14. Gabriel F. L., Giger W., Guenther K., Kohler H. P. Differential degradation of nonylphenol isomers by *Sphingomonas xenophaga* Bayram. *Applied and Environmental Microbiology*, 2005, vol. 71, no. 3, pp. 1123–1129. <https://doi.org/10.1128/AEM.71.3.1123-1129.2005>
 15. Ibrahim M., Makky E. A., Azmi N. S., Ismail J. Optimization parameters for *Mycobacteria confluentis* biodegradation of PAHs. *MATEC Web of Conferences*, 2018, vol. 150, art. no. 06035 (5 p.). <https://doi.org/10.1051/mateconf/201815006035>
 16. Karigar C. S., Rao S. S. Role of microbial enzymes in the bioremediation of pollutants: A review. *Enzyme Research*, 2011, vol. 2011, art. no. 805187 (11 p.). <https://doi.org/10.4061/2011/805187>
 17. Khalid M., Abdollahi M. Environmental distribution of personal care products and their effects on human health. *Iranian Journal of Pharmaceutical Research*, 2021, vol. 20, iss. 1, pp. 216–253. <https://doi.org/10.22037/ijpr.2021.114891.15088>
 18. Khan S. A., Hamayun M., Khan A. L., Ahmad B., Ahmed S., Lee I.-J. Influence of pH, temperature and glucose on biodegradation of 4-aminophenol by a novel bacterial strain, *Pseudomonas* sp. ST-4. *African Journal of Biotechnology*, 2009, vol. 8, no. 16, pp. 3827–3831.
 19. Kimura Z., Chung K. M., Itoh H., Hiraishi A., Okabe S. *Raoultella electrica* sp. nov., isolated from anodic biofilms of a glucose-fed microbial fuel cell. *International Journal of Systematic and Evolutionary Microbiology*, 2014, vol. 64, iss. pt_4, pp. 1384–1388. <https://doi.org/10.1099/ijms.0.058826-0>
 20. Krige N. R., Padgett P. J. Phenotypic and physiological characterization methods. In: *Taxonomy of Prokaryotes* / F. Rainey, A. Oren (Eds). London ; San Diego ; Waltham ; Amsterdam : Academic Press, 2011, pp. 15–60. (Methods in Microbiology ; vol. 38). <https://doi.org/10.1016/B978-0-12-387730-7.00003-6>
 21. Kuzikova I., Rybalchenko O., Kurashov E., Krylova Y., Safronova V., Medvedeva N. Defense responses of the marine-derived fungus *Aspergillus tubingensis* to alkylphenols stress. *Water, Air, & Soil Pollution. An International Journal of Environmental Pollution*, 2020, vol. 231, iss. 6, art. no. 271 (18 p.). <https://doi.org/10.1007/s11270-020-04639-2>
 22. Lakshmi M. V. V. C., Sridevi V. Effect of pH and inoculum size on phenol degradation by *Pseudomonas aeruginosa* (NCIM 2074). *International Journal of Chemical Sciences*, 2009, vol. 7, iss. 4, pp. 2246–2252.
 23. Liu Y., Chang H., Li Z., Feng Y., Cheng D., Xue J. Biodegradation of gentamicin by bacterial consortia AMQD4 in synthetic medium and raw gentamicin sewage. *Scientific Reports*, 2017, vol. 7, art. no. 11004 (11 p.). <https://doi.org/10.1038/s41598-017-11529-x>
 24. Ma J., Chen F., Tang Y., Wang X. Research on degradation characteristics of nonylphenol in water by highly effective complex microorganisms. *E3S Web of Conferences*, 2018, vol. 53, art. no. 04016 (7 p.). <https://doi.org/10.1051/e3sconf/20185304016>
 25. Mao Z., Zheng X.-F., Zhang Y.-Q., Tao X.-X., Li Y., Wang W. Occurrence and biodegradation of nonylphenol in the environment. *International Journal of Molecular Sciences*, 2012, vol. 13, iss. 1, pp. 491–505. <https://doi.org/10.3390/ijms13010491>
 26. Palyzová A., Zahradník J., Marešová H., Řezanka T. Characterization of the catabolic pathway of diclofenac in *Raoultella* sp. KDF8. *International Biodeterioration & Biodegradation*, 2019, vol. 137, pp. 88–94. <https://doi.org/10.1016/j.ibiod.2018.11.013>
 27. Ping L., Guo Q., Chen X., Yuan X., Zhang C., Zhao H. Biodegradation of pyrene and benzo[a]pyrene in the liquid matrix and soil

- by a newly identified *Raoultella planticola* strain. *3 Biotech*, 2017, vol. 7, iss. 1, art. no. 56 (10 p.). <https://doi.org/10.1007/s13205-017-0704-y>
28. Rajendran R. K., Huang S.-L., Lin C.-C., Kirschner R. Biodegradation of the endocrine disrupter 4-*tert*-octylphenol by the yeast strain *Candida rugopelliculosa* RRKY5 via phenolic ring hydroxylation and alkyl chain oxidation pathways. *Bioresource Technology*, 2017, vol. 226, pp. 55–64. <https://doi.org/10.1016/j.biortech.2016.11.129>
 29. Reddy M. V., Yajima Y., Choi D. B., Chang Y.-C. Biodegradation of toxic organic compounds using a newly isolated *Bacillus* sp. CYR2. *Biotechnology and Bioprocess Engineering*, 2017, vol. 22, iss. 3, pp. 339–346. <https://doi.org/10.1007/s12257-017-0117-0>
 30. Soares A., Guieysse B., Jefferson B., Cartmell E., Lester J. N. Nonylphenol in the environment: A critical review on occurrence, fate, toxicity and treatment in wastewaters. *Environment International*, 2008, vol. 34, iss. 7, pp. 1033–1049. <https://doi.org/10.1016/j.envint.2008.01.004>
 31. Solé M., López de Alda M. J., Castillo M., Porte C., Ladegaard-Pedersen K., Barceló D. Estrogenicity determination in sewage treatment plants and surface waters from the Catalanian area (NE Spain). *Environmental Science & Technology*, 2000, vol. 34, iss. 24, pp. 5076–5083. <https://doi.org/10.1021/es991335n>
 32. Tamura K., Peterson D., Peterson N., Stecher G., Nei M., Kumar S. MEGA5: Molecular Evolutionary Genetics Analysis using maximum likelihood, evolutionary distance, and maximum parsimony methods. *Molecular Biology and Evolution*, 2011, vol. 28, iss. 10, pp. 2731–2739. <https://doi.org/10.1093/molbev/msr121>
 33. Tuan N. N., Hsieh H.-C., Lin Y.-W., Huang S.-L. Analysis of bacterial degradation pathways for long-chain alkylphenols involving phenol hydroxylase, alkylphenol monooxygenase and catechol dioxygenase genes. *Bioresource Technology*, 2011, vol. 102, iss. 5, pp. 4232–4240. <https://doi.org/10.1016/j.biortech.2010.12.067>
 34. Uğuz C., İşcan M., Togan İ. Alkylphenols in the environment and their adverse effects on living organisms. *Kocatepe Veterinary Journal*, 2009, vol. 2, iss. 1, pp. 49–58.
 35. Vallini G., Frassinetti S., D'Andrea F., Catelani G., Agnolucci M. Biodegradation of 4-(1-nonyl)phenol by axenic cultures of the yeast *Candida aquatextoris*: Identification of microbial breakdown products and proposal of a possible metabolic pathway. *International Biodeterioration & Biodegradation*, 2001, vol. 47, iss. 3, pp. 133–140. [https://doi.org/10.1016/S0964-8305\(01\)00040-3](https://doi.org/10.1016/S0964-8305(01)00040-3)
 36. Wang Z., Yang Y., Dai Y., Xie S. Anaerobic biodegradation of nonylphenol in river sediment under nitrate- or sulfate-reducing conditions and associated bacterial community. *Journal of Hazardous Materials*, 2015a, vol. 286, pp. 306–314. <https://doi.org/10.1016/j.jhazmat.2014.12.057>
 37. Wang Z., Yang Y., He T., Xie S. Change of microbial community structure and functional gene abundance in nonylphenol-degrading sediment. *Applied Microbiology and Biotechnology*, 2015b, vol. 99, iss. 7, pp. 3259–3268. <https://doi.org/10.1007/s00253-014-6222-5>
 38. Watanabe W., Hori Y., Nishimura S., Takagi A., Kikuchi M., Sawai J. Bacterial degradation and reduction in the estrogen activity of 4-nonylphenol. *Biocontrol Science*, 2012, vol. 17, iss. 3, pp. 143–147. <https://doi.org/10.4265/bio.17.143>
 39. *Water Quality – Determination of Dissolved Oxygen – Iodometric Method (ISO Standard No. 5813:1983)*. ISO. International Organization for Standardization, 1983. <https://www.iso.org/standard/11959.html>
 40. Weisburg W. G., Barns S. M., Pelletier D. A., Lane D. J. 16S ribosomal DNA amplification for phylogenetic study. *Journal of Bacteriology*, 1991, vol. 173, no. 2, pp. 697–703. <https://doi.org/10.1128/jb.173.2.697-703.1991>
 41. Xie Y., Pan Y., Bai B., Xu Z., Ding L., Li Q., Xu Y., Zhu T. Degradation performance and optimal parameters of two bacteria in degrading nonylphenol. *Journal of Computational and Theoretical Nanoscience*, 2015, vol. 12, no. 9, pp. 2657–2663. <https://doi.org/10.1166/jctn.2015.4159>

42. Yang Z., Shi Y., Zhang Y., Cheng Q., Li X., Zhao C., Zhang D. Different pathways for 4-n-nonylphenol biodegradation by two *Aspergillus* strains derived from estuary sediment: Evidence from metabolites determination and key-gene identification. *Journal of Hazardous Materials*, 2018, vol. 359, pp. 203–212. <https://doi.org/10.1016/j.jhazmat.2018.07.058>
43. Zaytseva T. B., Medvedeva N. G. Sorption and biodegradation of octyl- and nonylphenols by the cyanobacterium *Planktothrix agardhii* (Gomont) Anagn. & Komárek. *Inland Water Biology*, 2019, vol. 12, iss. 3, pp. 337–345. <https://doi.org/10.1134/s1995082919030192>

**БИОДЕГРАДАЦИЯ НОНИФЕНОЛА
БАКТЕРИЕЙ *RAOULTELLA PLANTICOLA* F8,
ВЫДЕЛЕННОЙ ИЗ ДОННЫХ ОСАДКОВ
ФИНСКОГО ЗАЛИВА БАЛТИЙСКОГО МОРЯ**

Т. Б. Зайцева¹, В. И. Сафронова², А. Д. Руссу¹, И. Л. Кузикова¹, Н. Г. Медведева¹

¹Санкт-Петербургский федеральный исследовательский центр Российской академии наук,
Научно-исследовательский центр экологической безопасности Российской академии наук,
Санкт-Петербург, Российская Федерация

²Всероссийский научно-исследовательский институт сельскохозяйственной микробиологии,
Санкт-Петербург, Российская Федерация
E-mail: zaytseva.62@list.ru

Нонилфенол (НФ) — ксенобиотик антропогенного происхождения — является широко распространённым во всём мире загрязнителем окружающей среды. Попадание НФ в объекты окружающей среды вызывает серьёзную озабоченность вследствие его токсичности для водных организмов, животных и человека. Кроме того, НФ известен как эндокринный деструктор. Цель данной статьи — выделение из донных отложений, отобранных в южной части Финского залива (Балтийское море), и идентификация высокоэффективного штамма бактерий, способного деструктировать НФ, а также изучение его способности к деградации НФ при различных уровнях температуры, pH, концентраций растворённого кислорода и исходных концентраций НФ. Идентификацию выделенного штамма F8 проводили по фенотипическим признакам с использованием стандартных методов, а также методом секвенирования по Сэнгеру фрагмента последовательности гена 16S рРНК (*rrs*). Содержание НФ определяли методом высокоэффективной жидкостной хроматографии. Новая НФ-деструктирующая бактерия *Raoultella planticola* F8 выделена из донных отложений, отобранных в Финском заливе. Изолят *R. planticola* F8 депонирован в Ведомственной коллекции микроорганизмов сельскохозяйственного назначения ВНИИСХМ под регистрационным номером РСАМ 05450. Последовательность гена *rrs* изолята *R. planticola* F8 депонирована в базе данных GenBank под номером OL831016. Этот штамм высокоэффективен для деградации НФ в аэробных условиях при различных концентрациях НФ (до 900 мг·л⁻¹), в диапазоне температур от +5 до +35 °С, начальных значений pH от 5 до 9 и концентраций растворённого кислорода от 0,8 до 2,46 мг·л⁻¹. Данное исследование — первое, демонстрирующее способность *R. planticola* трансформировать НФ. Результаты этой работы предоставляют полезную информацию для применения *R. planticola* F8 в процессах биоремедиации.

Ключевые слова: *Raoultella planticola* F8, донные осадки, идентификация, нонилфенол, биodeградация

UDC 594.58-15(268.45)

IMPACT OF THE RED KING CRAB AND THE SNOW CRAB ON THE BARENTS SEA MEGABENTHIC COMMUNITIES

© 2024 D. Zakharov¹, I. Manushin², L. Jørgensen³, and N. Strelkova²

¹Zoological Institute of Russian Academy of Sciences, Saint Petersburg, Russian Federation

²Polar branch of VNIRO (“PINRO” named after N. M. Knipovich), Murmansk, Russian Federation

³Institute of Marine Research, Bergen, Norway

E-mail: zakharden@yandex.ru

The work is devoted to problems of mutual adaptation of two invasive commercial crab species, the red king crab *Paralithodes camtschaticus* and the snow crab *Chionoecetes opilio*, and the recipient ecosystem of the Barents Sea. Data on the distribution of megabenthic communities obtained for 2006–2020 are provided. The dynamics of invasive crab populations is analyzed, and related changes that occurred in the Barents Sea bottom communities during this period are studied. Mechanisms of the impact of crab species on bottom communities and prospects for their colonization of the Barents Sea are discussed. The research is based on the results of quantitative and taxonomic analysis of bycatch in 6,010 bycatches with a Campelen 1800 trawl performed in the Barents Sea in 2006–2020 during the joint Russian–Norwegian ecosystem survey on RV of the Polar branch of VNIRO and the Institute of Marine Research. The expansion of the range and increase in abundance of the red king crab since the early 1990s led to its colonization of the vast area of the southern Barents Sea. In 2006–2010, this species dominated in megabenthic communities around the Murmansk Rise and Kaninskaya Bank. In 2016–2020, the red king crab spread north and east – up to the Kolguev Island and the southern slope of the Goose Bank. An increase in abundance of the snow crab resulted in its colonization of a huge area in the Barents Sea: from the Pechora Sea to the Franz Josef Land archipelago and from the Novaya Zemlya archipelago to the Spitsbergen archipelago. In 2006–2010, the snow crab abundance started to increase in the Novaya Zemlya archipelago area; there, it was a subdominant species in communities of soft sediments of the Goose Bank. In 2011–2015, the snow crab began to dominate in communities of the Goose and Novaya Zemlya banks and the northern Central Bank. At the same time, it continued to increase its role as a subdominant species in almost all megabenthic communities near the Novaya Zemlya archipelago. Later, in 2016–2020, this species dominated in benthic communities on the boundary with the Kara Sea between the Novaya Zemlya and Franz Josef Land archipelagos, on the slopes of the Novaya Zemlya Bank, near the Central Bank, and in the Southern Novaya Zemlya Trench. Its range increased and covered the area from the Franz Josef Land and Novaya Zemlya archipelagos to the Perseus Bank in the west and to the Pechora Sea in the south. As shown, under current climatic conditions, the red king crab will remain part of megabenthic communities in the southeastern Barents Sea. The snow crab will continue to migrate from the east to the western Barents Sea, up to the Spitsbergen archipelago, where similar benthic communities exist; in case of colder conditions, its migration will occur faster. A scenario is possible in which shallow waters of the Spitsbergen archipelago will be a new reproductive center of the snow crab population in the Barents Sea, along with the current center near the Novaya Zemlya archipelago.

Keywords: Barents Sea, megabenthos, bottom communities, red king crab, *Paralithodes camtschaticus*, snow crab, *Chionoecetes opilio*

Most benthic communities of large marine ecosystems, such as the Barents Sea, are subject to spatial and temporal transformation. Some of the key factors affecting their restructuring are climate fluctuations, interspecific competition, and anthropogenic load.

In the Barents Sea, such changes are studied for quite a long time and identified on the example of macrozoobenthos against the impact of climate and bottom trawling [Denisenko, 2003, 2007, 2013; Manushin, 2021a, b] and pressure from introduced species [Manushin et al., 2021; Strelkova et al., 2021; Zakharov et al., 2021b, 2022b]. Long-term data on bycatch of bottom invertebrates during ichthyological trawling are available, and differences are revealed between this part of the community and macrozoobenthos investigated using bottom grabs and dredges [Zakharov et al., 2021a]. So, the question arises on its response to external effects. In literature, benthos caught in ichthyological trawls is predominantly called megabenthos [Atlas of the Megabenthic Organisms, 2018; Gutt, Starmans, 1998; Jørgensen et al., 2022; Rybakova et al., 2019; Zakharov et al., 2020]; less commonly, it is called trawl macrobenthos [Kolkpakov et al., 2018; Shuntov, Volvenko, 2015].

Recently, the emergence of new species on the Barents Sea shelf has become fairly common [Zakharov, Jørgensen, 2017]. As a rule, these are single findings, and the impact of such invaders on native communities is mostly local and limited. The exceptions are the red king crab *Paralithodes camtschaticus* (Tilesius, 1815) and the snow crab *Chionoecetes opilio* (Fabricius, 1788). Due to their size, these species can be classified as megabenthos; so, the investigation of their bycatch in trawl benthos is of certain interest when studying both their acclimatization and associated dynamics of benthic communities in the Barents Sea.

The introduction of the red king crab into the Barents Sea occurred more than 60 years ago [The Red King Crab, 2021]; the introduction of the snow crab, more than 25 years ago [Kuzmin et al., 1998; Snow Crab *Chionoecetes opilio*, 2016]. The expansion of the range and increase in the abundance of the red king crab since the early 1990s resulted in the fact that this species colonized a vast site of the southern Barents Sea. The range of the snow crab rose from the Goose Bank (one finding in 1996) to a broad area in the Barents and Kara seas and adjacent waters.

The nutrition of the red king crab and snow crab was properly analyzed, and this allowed both to describe their food spectrum in the Barents Sea and identify the most intensively consumed groups of animals [Manushin, 2021b; Snow Crab *Chionoecetes opilio*, 2016; Zakharov et al., 2021b, etc.]. With bycatch data from ichthyological trawls, one can assess the distribution of invasive crabs, their biomass in new areas, and possible effect on other megabenthic species. In this regard, the aim of this study is to reveal changes in the structure of megabenthic communities that have occurred over the past 15 years under the impact of the red king crab and the snow crab.

MATERIAL AND METHODS

Material for this work was sampled during annual Russian–Norwegian ecosystem survey in August–November 2006–2020 (Fig. 1A). The research covered the entire Barents Sea, the northwestern Kara Sea, the eastern sites of the Norwegian and Greenland seas, and adjacent areas of the Arctic Ocean. Trawls were mainly carried out within nodes of the standard grid of stations, with a distance between stations of about 40 nautical miles (Fig. 1B).

The material was sampled with a Campelen 1800 trawl [Atlas of the Megabenthic Organisms, 2018]. Within 2006–2020, 6,010 stations were performed. The material was processed onboard the RV by a unified technique [Zakharov et al., 2020, 2022a]. In total, 1,182 taxa were identified; out of them, 747 taxa were identified down to the species level. Animals were taxonomically identified to the lowest level possible. Material on the snow crab and red king crab was sampled since 2004. Data on nutrition of crabs were taken from previously published works [Manushin, 2021a; Zakharov et al., 2021b].

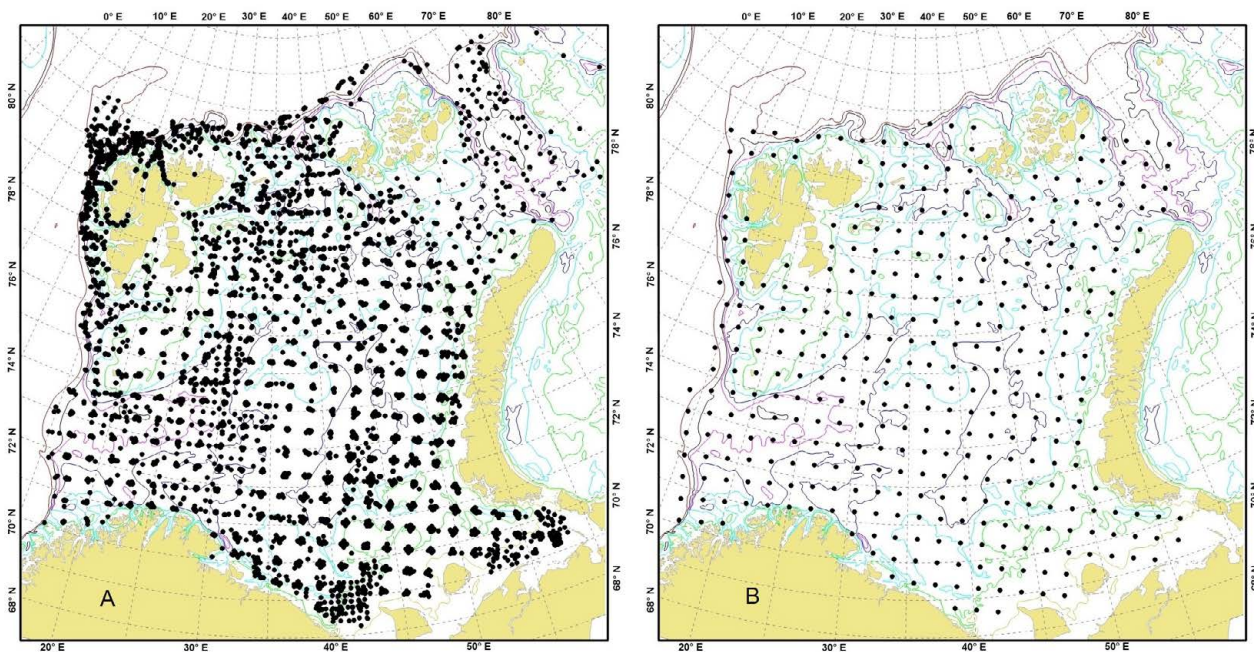


Fig. 1. Position of bottom trawls in 2006–2020 (A) and the standard grid of stations (B) in the joint Russian–Norwegian ecosystem survey

For comparative analysis, biomass values provided in this paper were calculated for a standard trawling distance of 1 nautical mile. Pelagic and benthopelagic species, *e. g.*, the northern shrimp *Pandalus borealis* Krøyer, 1838, were excluded from the dataset.

To estimate the changes in megabenthic communities over 15 years, this period was divided into three ones: 2006–2010, 2011–2015, and 2016–2020. Stations performed during each period and located at a distance of < 35 nautical miles from nodes of the standard grid (Fig. 1B) were combined for subsequent analysis. Stations situated at longer distances and not covered by the standard grid were excluded from the dataset. Each trawl point matched only one node of the standard grid of stations. The variation in depths between stations at nodes of the standard grid for each period averaged about 5 m.

The material obtained in different years during cruises of several RV and processed by researchers of various qualifications differed in the detail of taxonomic processing. Accordingly, to standardize the initial data and analyze it properly, part of the material was not used or was taxonomically grouped. Species and taxa recorded only once during the entire study period were excluded from the dataset. Supraspecific identification of widespread and easily identifiable species was ruled out as well [*e. g.*, *Hyas* sp. against the backdrop of occurrence of two well-recognized species, *Hyas araneus* (Linnaeus, 1758) and *Hyas coarctatus* Leach, 1815]. Animals identified down to the phylum, class, and order levels were excluded from the analysis due to their low abundance or negligible contribution to total biomass. Species with low biomass (bryozoans, hydroids, and amphipods) and difficult to taxonomically identify (sponges and polychaetes) were grouped within family rank.

For each group of stations united within nodes of the standard grid of trawling, a total list of taxa was made, and their ratios in the total biomass were determined. The obtained data were processed by *k*-means clustering using the Bray–Curtis dissimilarity as a station-by-station similarity measure.

The number of clusters was determined for each period based on testing their optimal number by various statistical techniques: elbow method, gap statistic, silhouette method, and clustree.

The data were statistically processed in R applying the following libraries: geosphere, tidyr, tidyverse, ggplot2, clustree, vegan, factoextra, and cluster. Also, MS Office Excel was used. Maps were constructed in Golden Software MapViewer 8.

The names of the morphostructures of the Barents Sea are taken from the publication of A. Zinchenko [2001].

RESULTS

Monitoring which we have begun in 2004–2005 showed that the snow crab and the red king crab were recorded in the survey area at 1% of stations. Then, their occurrence changed. For the snow crab, it increased sharply and rose almost by 30 times by 2020. For the red king crab, it remained almost at the same level of 2% until 2013, started to increase in 2014, and finally reached the value of 4–5% (Fig. 2). This reflects different stages of acclimatization for crab populations during the study period. Specifically, the red king crab was at the last stages of naturalization, while the snow crab was actively exploring the recipient ecosystem expanding its range and increasing the abundance.

In 2004, the distribution area of the snow crab was 20 thousand km²; that of the red king crab was 28 thousand km². By 2020, the range of the snow crab increased by more than 40 times and reached the value of 831 thousand km², while that of the red king crab rose only by 6 times, up to 176 thousand km². The rates of increase in both the frequency of occurrence and range for the snow crab were significantly higher than those for the red king crab (Fig. 2).

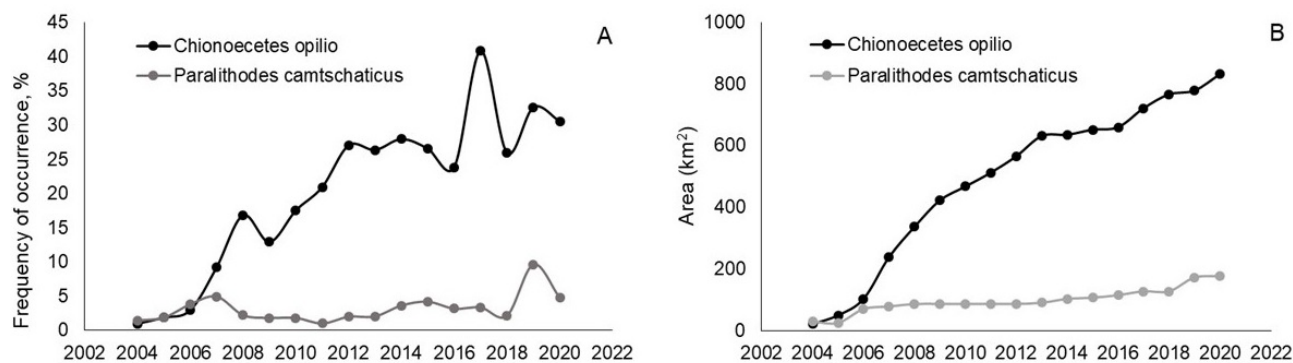


Fig. 2. Frequency of occurrence (%) (A) and range area (km²) (B) of the snow crab and the red king crab in 2004–2020

To analyze the fluctuations in the composition of megabenthos over 15 years, we selected nodes of the standard grid of stations (Fig. 1B) where the snow crab and the red king crab were encountered during the entire study period. The proportion of the snow crab in the total biomass of bycatch in its habitat gradually increased from 0.2% in 2006 to 2% in 2011. In 2012, it rose to 5%; by 2013, the value increased sharply to 15%. In subsequent years, the relative biomass stabilized, varied slightly at one level, and reached 20.6% by 2020. In 2008–2013, the relative biomass of the red king crab in the survey area varied at the level of 1–2%; since 2014, it increased sharply; and by 2020, it amounted to 28.9% (Fig. 3).

In general, in the distribution area of considered invaders, the proportion of almost all megabenthic groups decreased since 2006: ascidians, from 5 to 0.1% in 2020; cnidarians (mainly, sea anemones), from 7 to 1%; crustaceans (excluding introduced species), from 6 to 3%; and molluscs, from 5.2 to 1.3%. The proportion of echinoderms dropped significantly: from 62% in 2006 to 36% in 2020. No changes were recorded in the relative biomass of polychaetes (Annelida in Fig. 3), nemerteans, priapulids, etc. (Varia in Fig. 3). At the same time, an increase in the proportion of sponges was noted in bycatches: from 5 to 10% (Fig. 3).

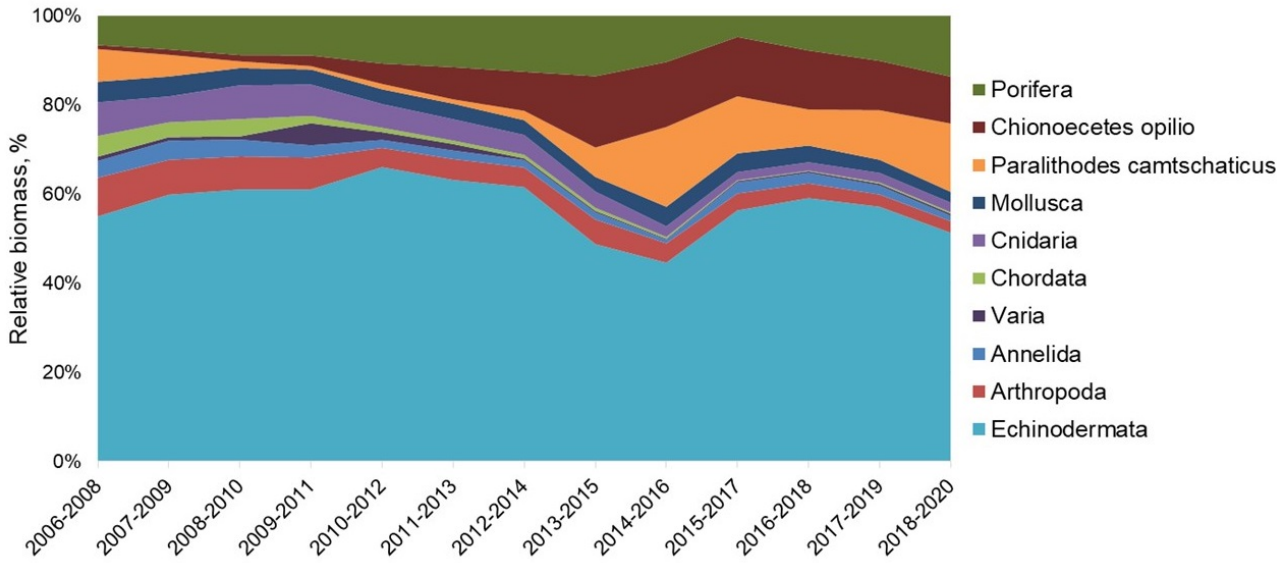


Fig. 3. Dynamics of the ratio of biomass of the main megabenthic groups and two invasive species in their range in the Barents Sea (three-year moving averages)

The dynamics of the relative biomass of the snow crab showed a statistically significant positive trend ($R^2 = 0.69$; $p = 0.0015$) (Fig. 4). When ruling out the data for 2018 and 2019, when the snow crab aggregations were under-surveyed [ICES Working Group, 2020], the coefficient of determination increased to 0.79.

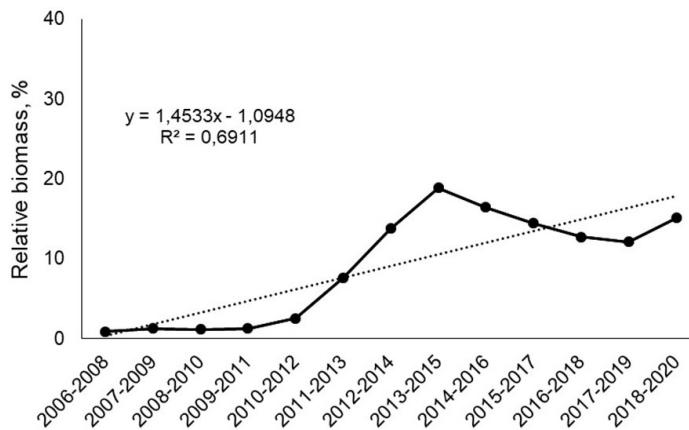


Fig. 4. Dynamics of the snow crab relative biomass in its range. The solid line represents three-year moving averages; the dotted line, linear trend

The moving average of the dynamics of the relative biomass for the snow crab within its distribution area is characterized by a rise, with a slight decrease in recent years (Fig. 4). However, this trend is not typical for all sites of the range. Thus, in the Goose Bank, the linear trend in the dynamics of the relative biomass for the snow crab in 2006–2020 is negative (Fig. 5A); in the Central Bank area and Novaya Zemlya shallows, it is positive (Fig. 5B–D).

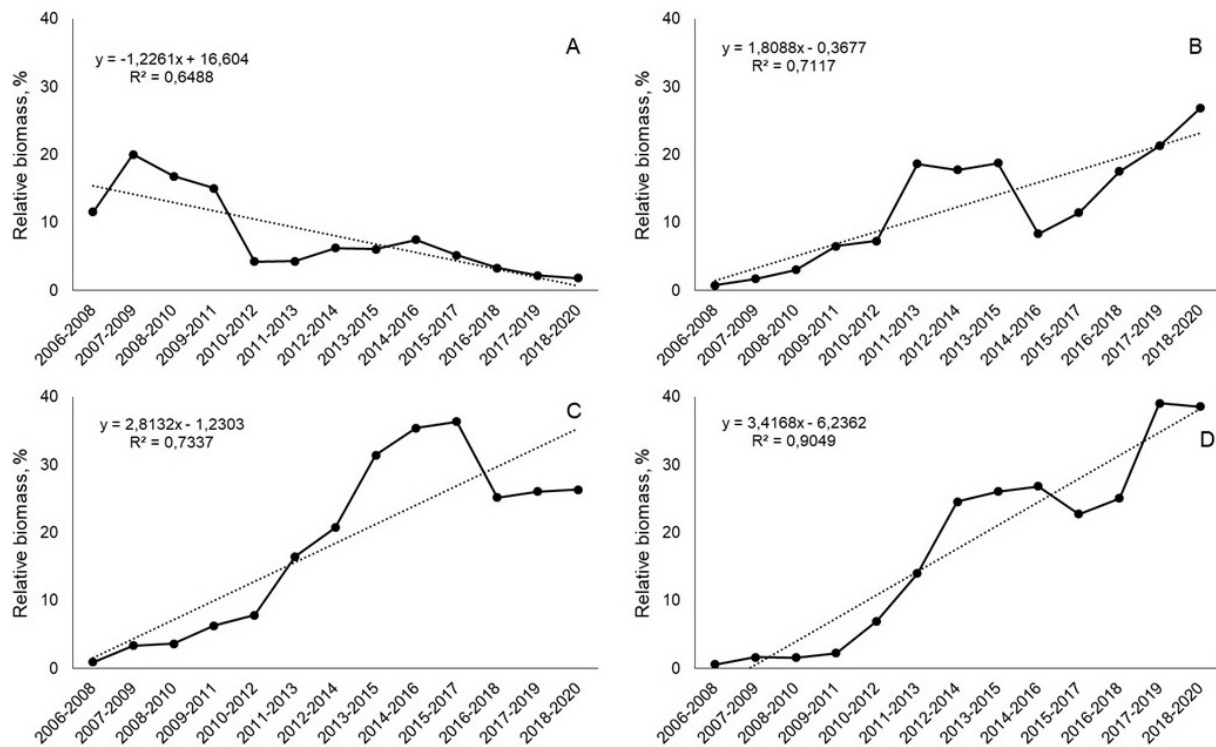


Fig. 5. Dynamics of the snow crab relative biomass in the Goose Bank (A), Central Bank (B), southern Novaya Zemlya Bank (C), and northern Novaya Zemlya Bank (D). The solid line represents three-year moving averages; the dotted line, linear trend (data from all catches in the area are used)

Until 2015, the proportion of the red king crab in the total biomass of megabenthos within its range rapidly increased; then, it stabilized at a fairly high level, with a slight downward trend (Fig. 6). For the red king crab, the trend of the dynamics of the relative biomass was statistically significant ($R^2 = 0.81$; $p = 0.0012$).

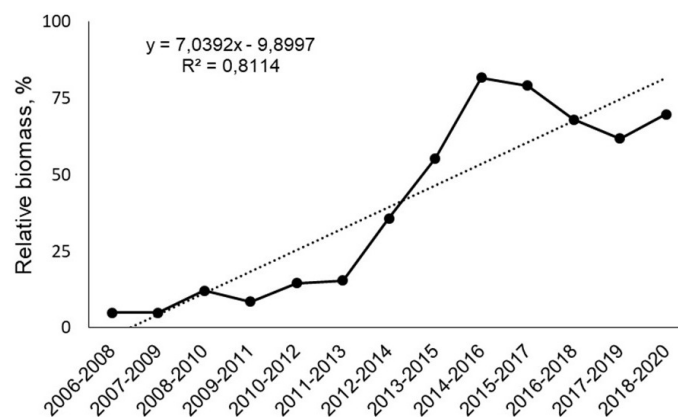


Fig. 6. Dynamics of the red king crab relative biomass in its range

According to the results of *k*-means clustering, 11 clusters were identified in the first analyzed period; 11 clusters were revealed in the second one; and 12 were defined in the third one (Fig. 7, Table 1).

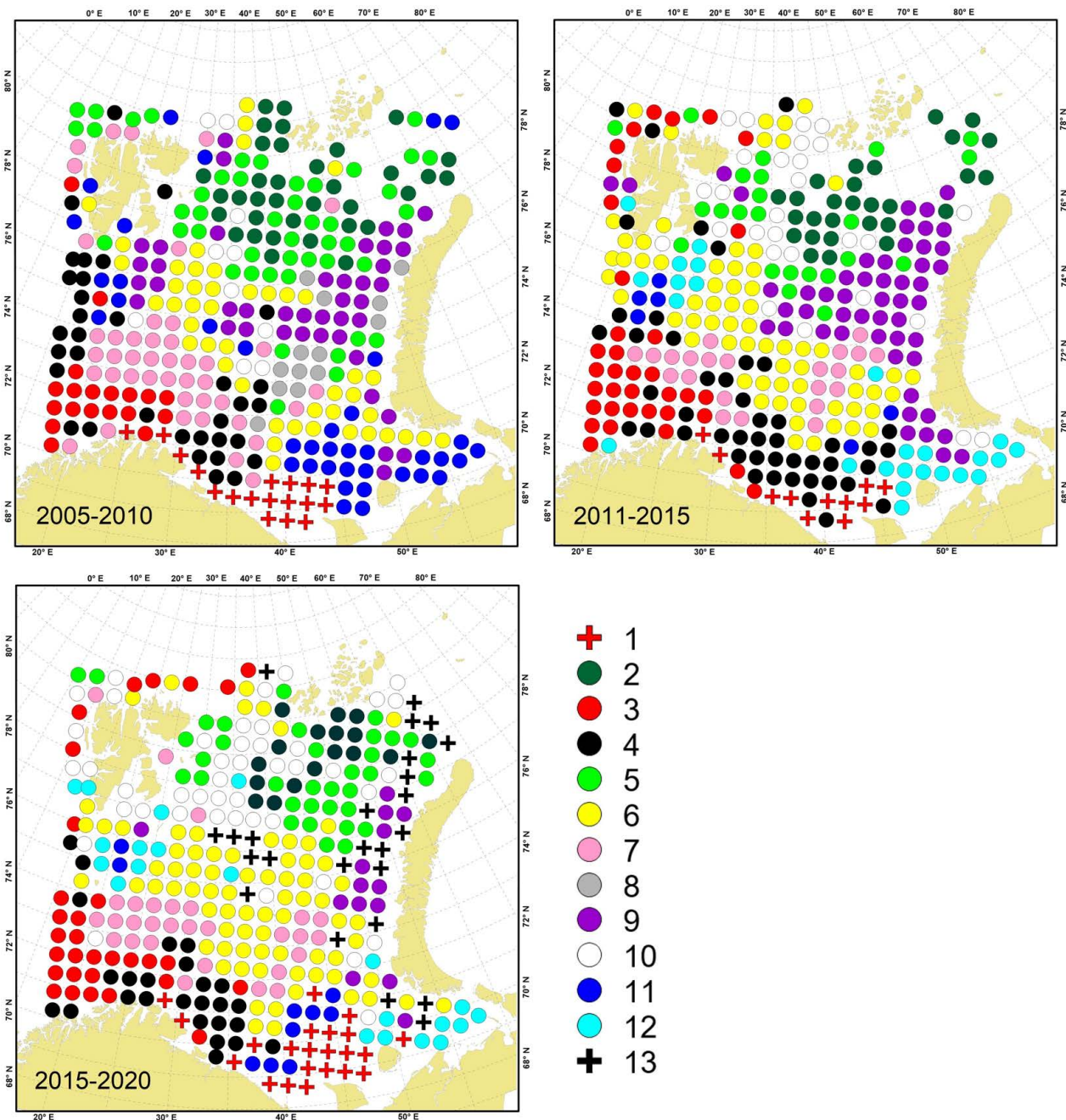





























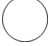






Fig. 7. Megabenthic communities in the Barents Sea and adjacent waters based on the surveys of 2006–2010, 2011–2015, and 2016–2020. Designations of the communities are given in Table 1

In 2006–2010, the biomass of the snow crab rapidly increased in the southeastern Barents Sea. This species became a subdominant one [against the backdrop of the prevalence of the starfish *Ctenodiscus crispatus* (Bruzelius, 1805)] in soft-soil communities in the Goose Bank area [community No. 6 in Fig. 7 and Table 1]. By 2010, the snow crab already locally dominated in the biomass of megabenthic catches in this site [Lyubin et al., 2010a].

Table 1. Megabenthic communities in the Barents Sea based on the surveys of 2006–2010, 2011–2015, and 2016–2020. Designations of the communities are the same as in Fig. 7. Dominant and subdominant species are given with relative biomass indicated (%)

2006–2010		2011–2015		2016–2020	
Com- munity	Dominant and subdominant species	Com- munity	Dominant and subdominant species	Com- munity	Dominant and subdominant species
1 	<i>Paralithodes camtschaticus</i> (55.0) Geodiidae (1.9) <i>Hippasteria phrygiana</i> (1.7)	1 	<i>Paralithodes camtschaticus</i> (41.7) Suberitidae (1.8)	1 	<i>Paralithodes camtschaticus</i> (61.2)
2 	<i>Gorgonocephalus</i> (14.8) <i>Ophiopleura borealis</i> (9.7) <i>Umbellula encrinus</i> (7.6) <i>Heliometra glacialis</i> (7.3) <i>Ophiacantha bidentata</i> (5.8)	2 	<i>Ophiopleura borealis</i> (21.0) <i>Gorgonocephalus</i> (12.9) <i>Molpadia</i> (6.6) <i>Ophiacantha bidentata</i> (5.6) <i>Ophioscolex glacialis</i> (4.5)	2 	<i>Ophiopleura borealis</i> (24.3) <i>Chionoecetes opilio</i> (4.9) <i>Molpadia</i> (4.0) <i>Gorgonocephalus</i> (3.7)
3 	Geodiidae (75.4) <i>Parastichopus tremulus</i> (1.4)	3 	Geodiidae (67.2) Ancorinidae (4.9)	3 	Geodiidae (70.2) Ancorinidae (4.9)
4 	Actiniaria (57.4) Alcyonacea (7.0) Hormathiidae (5.1) <i>Hippasteria phrygiana</i> (3.5)	4 	Hormathiidae (8.7) Actiniaria (6.5) <i>Urasterias lincki</i> (6.2) <i>Ctenodiscus crispatus</i> (5.0)	4 	<i>Bolocera tuediae</i> (10.1) <i>Hippasteria phrygiana</i> (10.1) <i>Parastichopus tremulus</i> (8.2) Hormathiidae (5.0) <i>Molpadia</i> (4.5)
5 	<i>Gorgonocephalus</i> (48.8) Actiniaria (2.9) <i>Heliometra glacialis</i> (2.8) <i>Ctenodiscus crispatus</i> (2.5)	5 	<i>Gorgonocephalus</i> (45.9) <i>Ctenodiscus crispatus</i> (4.2) <i>Sabinea septemcarinata</i> (3.1) <i>Chionoecetes opilio</i> (2.1)	5 	<i>Gorgonocephalus</i> (37.6) <i>Chionoecetes opilio</i> (13.0) <i>Ophiopleura borealis</i> (4.2) <i>Ophioscolex glacialis</i> (4.1)
6 	<i>Ctenodiscus crispatus</i> (23.7) <i>Chionoecetes opilio</i> (7.7) <i>Urasterias lincki</i> (7.0) <i>Icasterias panopla</i> (6.7)	6 	<i>Ctenodiscus crispatus</i> (39.6) <i>Icasterias panopla</i> (18.6) <i>Urasterias lincki</i> (10.0) <i>Sabinea septemcarinata</i> (8.7) Hormathiidae (5.8)	6 	<i>Ctenodiscus crispatus</i> (23.1) <i>Urasterias lincki</i> (9.6) <i>Icasterias panopla</i> (6.9) Polymastiidae (5.0) <i>Chionoecetes opilio</i> (4.4)
7 	Polymastiidae (10.6) Actiniaria (8.3) <i>Molpadia</i> (7.5) <i>Ctenodiscus crispatus</i> (6.2) Theneidae (4.1)	7 	<i>Molpadia</i> (24.8) <i>Ctenodiscus crispatus</i> (11.2) Polymastiidae (3.6) Theneidae (3.6)	7 	<i>Molpadia</i> (22.9) <i>Ctenodiscus crispatus</i> (12.3) <i>Batharca glacialis</i> (7.6) Polymastiidae (7.1)
8 	<i>Ciona intestinalis</i> (13.7) <i>Molpadia</i> (11.5) <i>Ctenodiscus crispatus</i> (4.3) <i>Strongylocentrotus</i> (4.3)				
9 	<i>Strongylocentrotus</i> (35.1) <i>Sabinea septemcarinata</i> (5.7) <i>Gorgonocephalus</i> (5.5) <i>Ctenodiscus crispatus</i> (3.6)	9 	<i>Strongylocentrotus</i> (34.4) <i>Chionoecetes opilio</i> (18.0) <i>Ctenodiscus crispatus</i> (9.2) <i>Urasterias lincki</i> (4.6) <i>Gorgonocephalus</i> (3.6)	9 	<i>Strongylocentrotus</i> (37.9) <i>Chionoecetes opilio</i> (9.9) <i>Gorgonocephalus</i> (1.7)

Continue on the next page...

2006–2010		2011–2015		2016–2020	
Com- munity	Dominant and subdominant species	Com- munity	Dominant and subdominant species	Com- munity	Dominant and subdominant species
10 	<i>Heliometra glacialis</i> (27.6) Actinaria (6.0) <i>Sabinea septemcarinata</i> (3.7)	10 	<i>Gorgonocephalus</i> (7.9) <i>Sabinea septemcarinata</i> (6.4) <i>Heliometra glacialis</i> (6.1) <i>Ophiacantha bidentata</i> (5.0) <i>Strongylocentrotus</i> (4.4) <i>Ctenodiscus crispatus</i> (4.1)	10 	<i>Heliometra glacialis</i> (7.6) <i>Sabinea septemcarinata</i> (6.0) <i>Ctenodiscus crispatus</i> (5.6) <i>Chlamys islandica</i> (5.0) <i>Ophiacantha bidentata</i> (4.7) <i>Gorgonocephalus</i> (4.5)
11 	<i>Sabinea septemcarinata</i> (15.4) <i>Cucumaria frondosa</i> (12.7) <i>Sclerocrangon boreas</i> (7.0) <i>Hyas araneus</i> (6.4) <i>Balanus</i> (5.8) <i>Strongylocentrotus</i> (5.4)	11 	<i>Cucumaria frondosa</i> (32.0) <i>Microcosmus glacialis</i> (4.7) <i>Balanus</i> (1.9)	11 	<i>Cucumaria frondosa</i> (21.2) <i>Paralithodes camtschaticus</i> (13.8) Suberitidae (7.0) Hormathiidae (2.3)
		12 	<i>Strongylocentrotus</i> (13.8) <i>Balanus</i> (10.4) <i>Chlamys islandica</i> (6.9) <i>Alcyonidium gelatinosum</i> (5.6) <i>Hyas araneus</i> (4.7)	12 	<i>Strongylocentrotus</i> (16.2) <i>Balanus</i> (9.1) <i>Chlamys islandica</i> (6.9)
				13 	<i>Chionoecetes opilio</i> (35.3) <i>Ctenodiscus crispatus</i> (4.1) <i>Gorgonocephalus</i> (3.3)

In 2011–2015, the snow crab became a subdominant species in the Novaya Zemlya shallows (community No. 9 in Fig. 7 and Table 1) and the northern Central Bank (No. 5). During this period, it was a subdominant species in almost all communities of the Novaya Zemlya archipelago. The area of several communities shifted. Specifically, for sea urchins, the area decreased (No. 9), and for the mud star *C. crispatus* (No. 6), it increased. The snow crab populations were unstable (see Fig. 5). Thus, the dense aggregation in the Goose Bank dropped greatly, and this is associated with the redistribution of aggregations in general. The snow crab aggregations that moved to the areas of the Central Bank and the southern Novaya Zemlya Bank were increasing their proportions in communities since 2006, and in the northern Novaya Zemlya shallows, since 2009.

In 2016–2020, the snow crab prevailed in communities (No. 13 in Fig. 7 and Table 1) between the Novaya Zemlya and Franz Josef Land archipelagos on the border with the Kara Sea, on the slopes of the Novaya Zemlya shallows and in the Central Bank, and in the Southern Novaya Zemlya Trench. The area of communities with the subdominance of this hydrobiont increased and covered the area from the Franz Josef Land and Novaya Zemlya archipelagos to the Perseus Bank, as well as the northern Pechora Sea (No. 2, 5, and 9). To the south of the Franz Josef Land archipelago, the snow crab was a subdominant species in the community of the brittle star *Ophiopleura borealis* Danielssen & Koren, 1877 (No. 2). In the Novaya Zemlya Bank, in the community dominated by sea urchins of the genus *Strongylocentrotus* Brandt, 1835 (No. 9), mainly *Strongylocentrotus pallidus* (G. O. Sars, 1871), the snow crab was the second most dominant species. In the eastern sea, in the community of brittle stars of the genus *Gorgonocephalus* Leach, 1815 (No. 5) and *O. borealis* (No. 2), the snow crab was on the second position.

In 2006–2010, the red king crab prevailed among megabenthic organisms in coastal waters of the Kola Peninsula, in the Murman Rise, and in waters off the Kanin Peninsula (community No. 1 in Fig. 7 and Table 1). In the community of sponges (No. 3) in the Eastern Murman and warm-water species (No. 4) in the Western Murman, it was a subdominant species.

In 2011–2015, it still dominated in the North Cape area and Eastern Murman waters, but became less common in bycatches in the coastal Western Murman and Murmansk Rise. Dense aggregations of the red king crab on the southern slope of the Kaninskaya Bank expanded eastward, to the Kanin Peninsula.

In 2016–2020, the area of the red king crab dominance expanded noticeably to the northeast: this species prevailed in communities around the entire Kanin Peninsula, north and west of Kolguev Island, off the Kaninskaya Bank, and in the Goose Bank. In the community of the orange-footed sea cucumber *Cucumaria frondosa* (Gunnerus, 1767) (No. 11 in Fig. 7 and Table 1), the red king crab was the first subdominant in the areas of the southern Murmansk Rise, on the slopes of the Kaninskaya Bank, and in the southern Goose Bank. To a limited extent, it was also found in communities of sponges of the genus *Geodia* Lamarck, 1815 (No. 3), warm-water species (No. 4), and shallow-water species (No. 12) in the Pechora Sea. Moreover, it was recorded in the community of the snow crab (No. 13) at the southern tip of the Novaya Zemlya (see Fig. 1 and Table 1).

DISCUSSION

Studies of the dynamics of macrozoobenthic communities in the Barents Sea showed that their alterations under the impact of climatic factors and bottom trawling are registered with a delay of approximately four years [Denisenko, 2013; Lyubina et al., 2012, 2016]. In the case of larger and longer-lived megabenthic organisms, the delay in the recorded response to stress or shifts in environmental conditions should be longer. For these reasons, to analyze changes in the structure of the megabenthic component of benthic communities, we considered not annual data, but data over five-year periods.

In different areas of the Barents Sea, communities are undergoing transformations according to various scenarios (depending on the strength of the effect of prevailing factors).

In the southern Barents Sea, the key factors affecting benthic communities are as follows: the influx of warm Atlantic waters [Denisenko, 2003, 2007, 2013; Zakharov et al., 2022b], active bottom trawling [Lyubin et al., 2010b], predation by the red king crab [Manushin, 2021a, b], and predation by demersal fish (mostly haddock and flounder) [Eriksen et al., 2020]. Importantly, over the past few decades, none of the listed factors has prevented the active acclimatization of the red king crab in the southern Barents Sea, increase in its abundance, and expansion of its range.

The long period of positive temperature anomalies observed in the sea since the late XX century [Boitsov et al., 2012; Trofimov et al., 2018] contributed to the distribution of the crab not only westward, along the coast of Norway, but also eastward, along the Kola Peninsula coast up to the White Sea Gorlo Strait and the Murmansk and Northern Kanin Rise [The Red King Crab, 2021].

Active bottom fishing in the southern Barents Sea has an extremely negative impact on megabenthos [Lyubin et al., 2010b, 2011; Løkkeborg, Fosså, 2011; Zakharov, Lyubin, 2012], but affects the red king crab to a lesser extent. Current fishing regulations in the Russian Federation are aimed at maximum protection of this species – a valuable commercial resource. Bycatch of more than 10 crabs *per* 1 ton of catch is prohibited. If this level of bycatch is exceeded, the vessel must change its position by 5 nautical miles. All caught crabs, regardless of number, sex, and size, must be immediately returned to their

habitat; this is strictly controlled by regulatory agencies. Poaching is localized mostly in coastal waters and has minimal impact on dense commercial aggregations in the open sea. Moreover, bottom trawling provides additional food for crabs (waste from onboard fish processing and discards of substandard parts of the catch) [Manushin, 2021a]. Also, animals injured by trawls become attractive and easy prey [Kedra et al., 2017].

Out of the above-listed factors, the only negative one can be competition with bottom fish. However, commercial fishing actively reduces its pressure on bottom communities, and fish consumption of adult crabs is extremely insignificant [Dolgov, Benzik, 2021]. So, in recent years, in the open, southern Barents Sea, very favorable conditions have developed for the red king crab distribution.

A weakly expressed increase in the frequency of occurrence (see Fig. 2) and distribution area of the red king crab during the study period, compared to indicators of the snow crab, is due to the smaller range area and the fact that a noticeable part of its population is concentrated off the coast. Moreover, trawl catches of the red king crab in open waters (with a rather sparse grid of ecosystem survey stations) are mostly random because of the high mobility of aggregations of large sexually mature males: those perform long and extensive migrations both to find food and reach breeding sites [Berenboim, 2003]. A significant proportion of the red king crab in the total biomass of megabenthos is also explained by the fact as follows: in the southern Barents Sea, the trawl bycatch of megabenthos is quite low, and one of its possible reasons seems to be the long-term negative impact of active trawling [Lyubin et al., 2010b]. Thus, even one commercial male weighing several kilograms caught by trawling can cause the total biomass of megabenthos in the bycatch to be exceeded.

The main groups of macrozoobenthos most actively consumed by the red king crab are echinoderms and molluscs [Strelkova et al., 2021]. Within the distribution area of this species, out of megabenthic organisms, the relative biomass of sea anemones, crustaceans, and ascidians also decreased during the study period. At the same time, an increase in the relative biomass of sponges was noted, the biomass of which negatively correlates with the distribution density of the red king crab. Specifically, in the Western Murman waters (part of the coast west of the Kola Bay), after a drop in the distribution density of the red king crab, a rise in the relative biomass of sponges was recorded – up to formation of local communities with their dominance.

A change in the structure of the benthic population, with the replacement of part of the benthic community by sponges, was previously recorded in the Svyatonos settlement of the Icelandic scallop *Chlamys islandica* (O. F. Müller, 1776), in the area of mass development of the seston-feeding fauna [Nosova et al., 2018; Zolotarev, 2016]. The factor mostly affecting the change in the composition of the community in this area was the long-term fishery of the Icelandic scallop. As a result of overfishing and consequent epizootic, the dominant species, *i. e.*, the Icelandic scallop, was replaced by other seston-feeders, mainly sponges. Unlike more highly organized animals, those are weakly susceptible to pressure from predators, infectious diseases, and damage by commercial dredges. Importantly, after mechanical disruption of the integrity of the sponge body, new individuals can be formed from the body fragments. Under artificial conditions, a fragment of the sponge *Geodia barretti* Bowerbank, 1858 (a species widespread in the Barents Sea) completely regenerated the structure of its body within a year and increased its mass by 40% [Hoffmann et al., 2003]. To date, the probability of a reverse process – a competitive replacement of sponges by scallops when their fishing ceases – is not clear. Apparently, degradation of the scallop population under the impact of fishing is irreversible; therefore, restoration of the stock of this valuable species to its previous level

is impossible. However, for other hydrobionts, this factor can be a positive one: by forming dense settlements, sponges ensure a favorable habitat for many animal species [Kedra et al., 2017; Khalaman, Komendantov, 2011].

A similar picture was noted in areas with mass settlements of the orange-footed sea cucumber in shallow waters of the northwestern and southeastern Barents Sea (the Spitsbergen, Goose, and North Kaninskaya banks and Moller Plateau). In 2006–2010, its community was not isolated during clustering, but was combined with a community characteristic of shallow waters of the southeastern sea and part of the Spitsbergen Bank. In 2011–2015, the relative biomass of *C. frondosa* in the southern sea increased (see Table 1) which may be due to a gradual consumption of certain benthic groups by the red king crab and a restructuring of the community. Previously, similar structural changes – a decrease in the number of main components (taxa) of the red king crab food spectrum and an increase in the abundance of their trophic competitors not consumed by this crab – were recorded in the macrobenthic communities of Motovsky Bay [Strelkova et al., 2021]. A similar picture was registered in several other water basins with the appearance of invaders [Alimov et al., 2000].

The ethological aspects of the biology of the red king crab and snow crab differ significantly. The first species, whose breeding and feeding areas are spatially separated, performs long and extensive migrations. As already mentioned, this mainly concerns sexually mature males of commercial size. Females and juveniles are more sedentary and stick to a narrow coast almost all year round [The Red King Crab, 2021]. So, in the open, southern Barents Sea, the bycatch is dominated by large male red king crabs – grazing predators. In contrast, the snow crab has noticeably less pronounced migratory activity. Throughout its range, catches include individuals of both sexes and all age groups with slight differentiation by depth [Zakharov et al., 2021b].

The growth of the snow crab population has led to its colonization of a huge area in the eastern and northern Barents Sea: from the Pechora Sea to the Franz Josef Land archipelago and from the Novaya Zemlya archipelago to Spitsbergen. In general, its distribution largely copies the distribution within the Barents Sea of Pacific-origin species, *e. g.*, whelks [Zakharov, 2013]. To date, Pacific species are recorded throughout the Barents Sea, but they form a stable faunal complex in the Novaya Zemlya, Kanin–Pechora, and Medvezhin–Nadezhdin shallows only. The faunal similarity of the benthic population indicates the similarity of living conditions in these remote areas.

The habitat of the snow crab continues to expand westward, to the Spitsbergen archipelago. There, the benthos is similar in terms of species composition and quantitative characteristics to communities widespread in the area of the densest concentrations of the snow crab.

However, modern data indicate that the expansion of its range westward is much slower than eastward, into adjacent areas of the Kara Sea [Zalota et al., 2018, 2019, 2020; Zimina, 2014]. Apparently, the main factor inhibiting its westward distribution is now the warming of the Barents Sea waters observed in the last few decades [ICES Working Group, 2022]. Obviously, in case of a cold snap, colonization of the snow crab in the western sea may accelerate [Bakanev, 2017], and a new center of its reproduction may be formed in the Spitsbergen archipelago area – in addition to the existing one off the Novaya Zemlya archipelago.

In some years within 2006–2010, in the Goose Bank, the bycatch of the snow crab reached 30–40% of the catch mass. In subsequent years, there were a decrease in its abundance in this site and formation of new dense settlements much further north, in the area of the Novaya Zemlya Bank and eastern slopes of the Central and Perseus banks. A drop in the abundance of the snow crab and its importance

in the megabenthic part of the benthic community in the Goose Bank area may be associated both with the impact of warm waters of one of the North Cape Current branches and with a decrease in the food supply after the explosive growth in the abundance of the invader.

Interestingly, in 2006–2010, in the Central Basin area, there was a community dominated by the ascidian *Ciona intestinalis* (Linnaeus, 1767) (No. 8 in Fig. 7 and Table 1). During next two periods, it was no longer distinguished: it was absorbed by a community dominated by holothurians of the genus *Molpadia* Cuvier, 1817. This may be partly due to the fact that the growing population of the snow crab feeds on ascidians. Their large size, soft cylindrical body with no protective shell, and attached lifestyle – apparently, all these characteristics made ascidians vulnerable to the invasive predator occurring in mass, in contrast to *Molpadia* representatives burrowing into the ground.

Undoubtedly, as mentioned above, against the backdrop of a cold snap, the frequency of occurrence and range of the snow crab will increase [Bakanev, 2017]. However, a rise in the abundance of the invader in already explored areas is unlikely, since the main limiting factor in this case is not the ambient temperature, but the food supply. Apparently, after the colonization of certain areas, there will be a redistribution of aggregations into adjacent communities suitable for the species and a reduction in the abundance of the invader down to an optimal level. To date, a similar picture is observed in the Goose Bank and partly in the southern Novaya Zemlya Bank, where the growth in the abundance of the invasive species is slowing down or has already stopped. Most likely, new productive generations will arise locally in areas that are being explored by the invader for the first time, for example, off the Spitsbergen and Franz Josef Land archipelagos and in elevations of the northern and central Barents Sea.

Like the red king crab, the snow crab displaces or replaces native species by consuming them or competing for food. However, due to its smaller size, the snow crab seems to be unable to eat larger individuals of megabenthos; so, this species affects *via* eating their juveniles. The pressure from the invader on megabenthos may be partially reduced by the consumption of macrozoobenthos by the crab.

In recent years, the proportion of the snow crab in catches within the area it has explored long ago remains at a level of about $\frac{1}{5}$ of the total biomass of trawl megabenthos. It can be assumed as follows: under conditions of the Barents Sea, this proportion is optimal, and in the future, it will be maintained within the entire area inhabited by this species.

Obviously, the occurrence of the snow crab and red king crab in the Barents Sea ecosystem does not lead to an increase in the total bioproductivity of the water basin, since the latter is completely determined by the level of food resources available to bottom population [Zenkevich, 1970], *i. e.*, primary production. In case of the invaders considered, we are talking only about the redistribution of energy flows and an increase in their biomass due to native species. Being exclusively carnivores, these two species do not introduce new or uninvolved sources of nutrients into the food pyramid (for example, unclaimed detritus or plankton); those just exploit and transform existing benthic communities [Biological Invasions, 2004; Shadrin, Anufrieva, 2019].

Under current conditions, both crab species will definitely continue to expand their ranges against the backdrop of comfortable conditions and availability of sufficient food supply. The red king crab will continue to integrate into the communities of the Pechora Sea and adjacent waters. However, its distribution northward will most likely be limited to the Goose Bank and Moller Plateau, and eastward, to shallow waters subject to winter cooling. The range of the snow crab will cover the entire northern and eastern sea, with the exception of areas under the impact of warm Atlantic waters. Its distribution

will not be uniform, but the area of megabenthic communities with its dominance will increase. Apparently, competition between invaders will be minimal; it will be observed only at the junction of habitats. With climate fluctuations, the ranges of crabs will change in antiphase: with warming, the range of the red king crab will expand, and the range of the snow crab will decrease, and *vice versa*.

Thus, the benthic communities of the Barents Sea are currently in a state of transformation caused by a long period of warming and emergence of new invasive species. The presented results suggest as follows: while the red king crab and the snow crab explore accessible waters, the bottom population of the Barents Sea will undergo significant structural changes within the entire distribution area.

The material for this work was sampled within the framework of the state research assignments of the Polar branch of VNIRO (Murmansk) and Institute of Marine Research (Bergen). The paper was prepared within the framework of the state research assignment of the Zoological Institute of the Russian Academy of Sciences No. 122031100275-4.

Acknowledgement. We are grateful to all colleagues and staff onboard the RV, in laboratories, and in offices for their work in the joint Russian–Norwegian ecosystem survey of the Barents Sea. We are extremely grateful to the reviewers for their comments and positive final assessment of our paper.

REFERENCES

1. Alimov A. F., Orlova M. I., Panov V. E. Posledstviya introduktsii chuzherodnykh vidov dlya vodnykh ekosistem i neobkhodimost' meropriyatii po ikh predotvrashcheniyu. In: *Vidy-vselentsy v evropeiskikh moryakh Rossii* : sbornik nauchnykh trudov. Apatity : Izd-vo Kol'skogo nauchnogo tsentra RAN, 2000, pp. 12–23. (in Russ.)
2. *Atlas of the Megabenthic Organisms of the Barents Sea and Adjacent Waters*. Murmansk : PINRO, 2018, 534 p. (in Russ.)
3. Bakanev S. V. Prospects of snow crab *Chionoecetes opilio* fishery in the Barents Sea. *Voprosy rybolovstva*, 2017, vol. 18, no. 3, pp. 286–303. (in Russ.)
4. Berenboim B. I. Sezonnaya migratsiya kamchatskogo kraba v Barentsevom more. In: *Kamchatskii krab v Barentsevom more*. Murmansk : PINRO, 2003, pp. 70–78. (in Russ.)
5. *Biological Invasions in Aquatic and Terrestrial Ecosystems* / A. F. Alimov, N. G. Bogutskaya (Eds). Moscow ; Saint Petersburg : KMK Scientific Press Ltd., 2004, 436 p. (in Russ.)
6. Denisenko S. G. Mnogoletnie izmeneniya donnoi fauny Barentseva morya i gidrologicheskie flyuktuatsii vdol' razreza "Kol'skii meridian". In: *Materialy simpoziuma, posvyashchennogo 100-letiyu okeanograficheskikh nablyudenii na razreze "Kol'skii meridian" (Murmansk, 1999)*. Murmansk : Izd-vo PINRO, 2003, pp. 65–76. (in Russ.)
7. Denisenko S. G. Zoobentos Barentseva morya v usloviyakh izmenyayushchegosya klimata i antropogennogo vozdeistviya. In: *Dinamika morskikh ekosistem i sovremennyye problemy sokhraneniya biologicheskogo potentsiala morei Rossii*. Vladivostok : Dal'nauka, 2007, pp. 418–511. (in Russ.)
8. Denisenko S. G. *Biodiversity and Bioresources of Macrozoobenthos in the Barents Sea: Structure and Long-Term Changes*. Saint Petersburg : Nauka, 2013, 284 p. (in Russ.)
9. Dolgov A. V., Benzik A. N. Kamchatskii krab kak ob"ekt pitaniya donnykh ryb. In: *The Red King Crab in the Barents Sea* : 3rd edition, revised and expanded. Moscow : VNIRO, 2021, pp. 347–359. (in Russ.)

10. Zakharov D. V. *Raspredelenie, ekologiya i promyslovoe znachenie mollyuskov semeistva Buccinidae v Barentsevom more i sopredel'nykh vodakh.* (dissertation). Murmansk, 2013, 162 p. (in Russ.)
11. Zakharov D. V., Luybin P. A. Fauna, ecology and distribution of molluscs Buccinidae (Mollusca, Gastropoda) in the Barents Sea and adjacent waters. *Vestnik Murmanskogo gosudarstvennogo tekhnicheskogo universiteta*, 2012, vol. 15, no. 4, pp. 749–757. (in Russ.)
12. Zakharov D. V., Manushin I. E., Strelkova N. A. Sravnitel'nyi analiz bentosnykh materialov, sobrannykh raznymi orudiyami lova v vostochnoi chasti Barentseva morya. In: *Chteniya pamyati K. M. Deryugina : materialy XXII yubileinogo nauchnogo seminara "Kafedre ikhtiologii i gidrobiologii 90 let"*. Saint Petersburg : St Petersburg University, 2021a, pp. 52–68. (in Russ.)
13. Zakharov D. V., Manushin I. E., Strelkova N. A., Zimina O. L., Khacheturova K. S., Blinova D. J., Jørgensen L. L. Guidance for the assessment of the megabenthos bycatch in the bottom trawl in the course of research surveys. *Voprosy rybolovstva*, 2022a, vol. 23, no. 3, pp. 179–192. (in Russ.). <https://doi.org/10.36038/0234-2774-2022-23-3-179-192>
14. Zakharov D. V., Strelkova N. A., Manushin I. E., Khacheturova K. S., Blinova D. Yu., Kudryashova A. S. Changes in benthic communities in the Kola Peninsula bays in the 21st century. In: *Marine Research and Education (MARESEDU-2022) : proceedings of the XI International Conference*. Tver : PoliPRESS, 2022b, vol. 3 (4), pp. 102–105. (in Russ.)
15. Zenkevich L. A. Donnaya fauna okeana. In: *Programma i metodika izucheniya biogeotsenozov vodnoi sredy. Biogeotsenozy morei i okeanov*. Moscow : Nauka, 1970, pp. 213–227. (in Russ.)
16. Zinchenko A. G. Geomorfologicheskaya osnova kompleksnykh landshaftno-geoekologicheskikh issledovaniy Barentseva morya. In: *Opyt sistemnykh okeanologicheskikh issledovaniy v Arktike*. Moscow : Nauchnyi mir, 2001, pp. 476–481. (in Russ.)
17. Zolotarev P. N. *Biology and Fishery of the Icelandic Scallop *Chlamys islandica* in the Barents and White Seas*. Murmansk : PINRO, 2016, 289 p. (in Russ.)
18. *The Red King Crab in the Barents Sea : 3rd edition, revised & expanded*. Moscow : VNIRO, 2021, 712 p. (in Russ.)
19. Kolpakov N. V., Korneichuk I. A., Nadtochy V. A. Current data on composition and distribution of trawl macrozoobenthos in the Russian waters of the Japan Sea. *Izvestiya TINRO*, 2018, vol. 193, pp. 33–49. (in Russ.). <https://doi.org/10.26428/1606-9919-2018-193-33-49>
20. *Snow Crab *Chionoecetes opilio* in the Barents and Kara Seas*. Murmansk : PINRO, 2016, 242 p. (in Russ.)
21. Lyubin P. A., Anisimova N. A., Jørgensen L. L., Manushin I. E., Prokhorova T. A., Zakharov D. V., Zhuravleva N. E., Golikov A. V., Morov A. V. Megabentos Barentseva morya. In: *Nature of the Shelf and Archipelagos of the European Arctic. Complex Investigations of the Svalbard Archipelago Nature : proceedings of the International Scientific Conference*, Murmansk, 27–30 October, 2010. Moscow : GEOS, 2010a, iss. 10, pp. 192–199. (in Russ.)
22. Lyubin P. A., Anisimova N. A., Manushin I. E., Zhuravliova N. E. Additional catch of macrozoobenthos in the ichthyological over-trawling as a mark of trawling intensity. *Vestnik Murmanskogo gosudarstvennogo tekhnicheskogo universiteta*, 2010b, vol. 13, no. 4 (spec. iss.), pp. 641–646. (in Russ.)

23. Lyubina O. S., Strelkova (Anisimova) N. A., Lubin P. A., Frolova E. A., Dikaeva D. R., Zimina O. L., Akhmetchina O. Yu., Manushin I. E., Nekhaev I. O., Frolov A. A., Zakharov D. V., Garbul E. A., Vyaznikova V. S. Modern quantitative distribution of zoobenthos along on the transect “Kola Section”. *Trudy Kol'skogo nauchnogo tsentra RAN*, 2016, no. 2 (36), pp. 64–91. (in Russ.)
24. Manushin I. E., Zakharov D. V., Strelkova N. A., Lyubin P. A., Zhuravleva N. E., Vyaznikova V. S., Nosova T. B., Blinova D. Yu., Khacheturova K. S. Otsenka vozdeistviya kamchatskogo kraba na bentos raionov Vostochnogo Murmana. In: *The Red King Crab in the Barents Sea*. Moscow : VNIRO, 2021, pp. 651–660. (in Russ.)
25. Manushin I. E. Pitanie kamchatskogo kraba v yuzhnoi chasti Barentseva morya. In: *The Red King Crab in the Barents Sea*. Moscow : VNIRO, 2021a, pp. 283–337. (in Russ.)
26. Manushin I. E. Potreblenie pishchi kamchatskim krabom. In: *The Red King Crab in the Barents Sea*. Moscow : VNIRO, 2021b, pp. 337–342. (in Russ.)
27. Nosova T. B., Manushin I. E., Zakharov D. V. Structure and long-term dynamics of zoobenthos communities in the areas of scallop *Chlamys islandica* beds at Kola Peninsula. *Izvestiya TINRO*, 2018, vol. 194, pp. 27–41. (in Russ.). <https://doi.org/10.26428/1606-9919-2018-194-27-41>
28. Strelkova N. A., Manushin I. E., Zakharov D. V., Vyaznikova V. S. Otsenka vozdeistviya kamchatskogo kraba na bentos raionov Zapadnogo Murmana. In: *The Red King Crab in the Barents Sea*. Moscow : VNIRO, 2021, pp. 600–650. (in Russ.)
29. Trofimov A. G., Karsakov A. L., Ivshin V. A. Climate changes in the Barents Sea over the last half century. *Trudy VNIRO*, 2018, vol. 173, pp. 79–91. (in Russ.)
30. Shadrin N. V., Anufrieva E. V. Lake ecosystems and invasive species: All are not so simple. In: *Lakes of Eurasia: Problems and Solutions* : proceedings of the II International Conference, 19–24 May, 2019. Kazan : Izd-vo Akademii nauk Respubliki Tatarstan, 2019, pt 2, pp. 355–359. (in Russ.)
31. Shuntov V. P., Volvenko I. V. Generalized assessments of composition, quantitative distribution and biomass of benthic macrofauna on the shelf and slope in the North-West Pacific. *Izvestiya TINRO*, 2015, vol. 182, no. 3, pp. 3–22. (in Russ.). <https://doi.org/10.26428/1606-9919-2015-182-3-22>
32. Boitsov V. D., Karsakov A. L., Trofimov A. G. Atlantic water temperature and climate in the Barents Sea, 2000–2009. *ICES Journal of Marine Science*, 2012, vol. 69, iss. 5, pp. 833–840. <https://doi.org/10.1093/icesjms/fss075>
33. Eriksen E., Benzik A. N., Dolgov A. V., Skjoldal H. R., Vihtakari M., Johannesen E., Prokhorova T. A., Keulder-Stenevik F., Prokopchuk I., Strand E. Diet and trophic structure of fishes in the Barents Sea: The Norwegian–Russian program “Year of stomachs” 2015 – establishing a baseline. *Progress in Oceanography*, 2020, vol. 183, art. no. 102262 (17 p.). <https://doi.org/10.1016/j.pocean.2019.102262>
34. Hoffmann F., Rapp H. T., Zöller T., Reitner J. Growth and regeneration in cultivated fragments of the boreal deep-water sponge *Geodia barretti* Bowerbank, 1858 (Geodiidae, Tetractinellida, Demospongiae). *Journal of Biotechnology*, 2003, vol. 100, iss. 2, pp. 109–118. [https://doi.org/10.1016/s0168-1656\(02\)00258-4](https://doi.org/10.1016/s0168-1656(02)00258-4)
35. ICES Working Group on the Integrated Assessments of the Barents Sea (WGIBAR). *ICES Scientific Reports*, 2020, vol. 2,

- iss. 30, 206 p. <https://doi.org/10.17895/ices.pub.5998>
36. ICES Working Group on the Integrated Assessments of the Barents Sea (WGIBAR). *ICES Scientific Reports*, 2022, vol. 4, iss. 50, 235 p. <https://doi.org/10.17895/ices.pub.20051438>
37. Jørgensen L. L., Logerwell E. A., Strelkova N. A., Zakharov D. V., Roy V., Nozères C., Bluhm B. A., Ólafsdóttir S. H., Burgos J. M., Sørensen J., Zimina O., Rand K. International megabenthic long-term monitoring of a changing arctic ecosystem: Baseline results. *Progress in Oceanography*, 2022, vol. 200, art. no. 102712 (20 p.). <https://doi.org/10.1016/j.pocean.2021.102712>
38. Kedra M., Renaud P. E., Andrade H. Epibenthic diversity and productivity on a heavily trawled Barents Sea bank (Tromsøflaket). *Oceanologia*, 2017, vol. 59, iss. 2, pp. 93–101. <https://doi.org/10.1016/j.oceano.2016.12.001>
39. Khalaman V. V., Komendantov A. Y. Structure of fouling communities formed by *Hali-chondria panicea* (Porifera: Demospongiae) in the White Sea. *Russian Journal of Ecology*, 2011, vol. 42, no. 6, pp. 493–501. <https://doi.org/10.1134/S1067413611050080>
40. Kuzmin S. A., Akhtarina S. M., Menis D. T. The first findings of snow crab *Chionoecetes opilio* (Decapoda, Majidae) in the Barents Sea. *Zoologicheskii zhurnal*, 1998, vol. 77, no. 4, pp. 489–491.
41. Gutt J., Starman A. Structure and biodiversity of megabenthos in the Weddell and Lazarev seas (Antarctica): Ecological role of physical parameters and biological interactions. *Polar Biology*, 1998, vol. 20, iss. 4, pp. 229–247. <https://doi.org/10.1007/s003000050300>
42. Lyubin P. A., Anisimova N. A., Manushin I. E. Long-term effects on benthos of the use of bottom fishing gears. In: *The Barents Sea: Ecosystem, Resources, Management. Half a Century of Russian–Norwegian Cooperation* / T. Jakobsen, V. K. Ozhigin (Eds). Trondheim : Tapir Academic Press, 2011, pp. 768–775.
43. Lyubina O. S., Frolova E. A., Dikaeva D. R. Current zoobenthos monitoring at the Kola Transect in the Barents Sea. In: *Arctic Marine Biology: A Workshop Celebrating Two Decades of Cooperation Between Murmansk Marine Biological Institute and Alfred Wegener Institute for Polar and Marine Research* / G. Hempel, K. Lochte, G. Matishov (Eds). Bremerhaven : Alfred Wegener Institute for Polar and Marine Research, 2012, pp. 177–189. (Berichte zur Polar- und Meeresforschung = Reports on Polar and Marine Research ; no. 640).
44. Løkkeborg S., Fosså J. H. Impacts of bottom trawling on benthic habitats. In: *The Barents Sea: Ecosystem, Resources, Management. Half a Century of Russian–Norwegian Cooperation* / T. Jakobsen, V. K. Ozhigin (Eds). Trondheim : Tapir Academic Press, 2011, pp. 760–767.
45. Rybakova E., Kremenetskaia A., Vedenin A., Boetius A., Gebruk A. Deep-sea megabenthos communities of the Eurasian Central Arctic are influenced by ice-cover and sea-ice algal falls. *PLoS One*, 2019, vol. 14, iss. 7, art. no. e0211009 (27 p.). <https://doi.org/10.1371/journal.pone.0211009>
46. Zakharov D. V., Jørgensen L. L. New species of the gastropods in the Barents Sea and adjacent waters. *Russian Journal of Biological Invasions*, 2017, vol. 8, iss. 3, pp. 226–231. <https://doi.org/10.1134/S2075111717030146>
47. Zakharov D. V., Jørgensen L. L., Manushin I. E., Strelkova N. A. Barents Sea megabenthos: Spatial and temporal distribution and production. *Morskoj biologicheskij zhurnal*, 2020, vol. 5, no. 2, pp. 19–37. <https://doi.org/10.21072/mbj.2020.05.2.03>

48. Zakharov D. V., Manushin I. E., Nosova T. B., Strelkova N. A., Pavlov V. A. Diet of snow crab in the Barents Sea and macrozoobenthic communities in its area of distribution. *ICES Journal of Marine Science*, 2021b, vol. 78, iss. 2, pp. 545–556. <https://doi.org/10.1093/icesjms/fsaa132>
49. Zalota A. K., Spiridonov V. A., Vedenin A. A. Development of snow crab *Chionoecetes opilio* (Crustacea: Decapoda: Oregonidae) invasion in the Kara Sea. *Polar Biology*, 2018, vol. 41, iss. 10, pp. 1983–1994. <https://doi.org/10.1007/s00300-018-2337-y>
50. Zalota A. K., Zimina O. L., Spiridonov V. A. Combining data from different sampling methods to study the development of an alien crab *Chionoecetes opilio* invasion in the remote and pristine Arctic Kara Sea. *PeerJ*, 2019, vol. 7, art. no. e7952 (25 p.). <https://doi.org/10.7717/peerj.7952>
51. Zalota A. K., Spiridonov V. A., Galkin S., Pronin A. A. Population structure of alien snow crabs (*Chionoecetes opilio*) in the Kara Sea (trawl and video sampling). *Oceanology*, 2020, vol. 60, iss. 1, pp. 83–88. <https://doi.org/10.1134/S0001437020010257>
52. Zimina O. L. Finding the snow crab *Chionoecetes opilio* (O. Fabricius, 1788) (Decapoda: Majidae) in the Kara Sea. *Russian Journal of Marine Biology*, 2014, vol. 40, iss. 6, pp. 490–492. <https://doi.org/10.1134/S1063074014060224>

ВЛИЯНИЕ КАМЧАТСКОГО КРАБА И КРАБА-СТРИГУНА ОПИЛИО НА СООБЩЕСТВА МЕГАБЕНТОСА БАРЕНЦЕВА МОРЯ

Д. В. Захаров¹, И. Е. Манушин², Л. Л. Йоргенсен³, Н. А. Стрелкова²

¹Зоологический институт Российской академии наук, Санкт-Петербург, Российская Федерация

²Полярный филиал ФГБНУ «ВНИРО» («ПИНРО» имени Н. М. Книповича),

Мурманск, Российская Федерация

³Институт морских исследований, Берген, Норвегия

E-mail: zakharden@yandex.ru

Работа посвящена проблемам взаимной адаптации двух чужеродных видов промысловых крабов — камчатского краба *Paralithodes camtschaticus* и краба-стригуна опилио *Chionoecetes opilio* — и реципиентной экосистемы Баренцева моря. Представлены данные о распределении сообществ мегабентоса, полученные за период с 2006 по 2020 г. Проанализированы динамика численности крабов и связанные с ней изменения, произошедшие в донных сообществах Баренцева моря за указанные годы. Проведено обсуждение механизмов воздействия крабов на донные сообщества и перспектив освоения ими акватории Баренцева моря. Исследование основано на результатах количественно-таксономического анализа прилова беспозвоночных в 6010 тралениях стандартным учётным тралом Sampelen 1800, выполненных в акватории Баренцева моря в 2006–2020 гг. в ходе проведения совместной российско-норвежской экосистемной съёмки на судах Полярного филиала ФГБНУ «ВНИРО» и Института морских исследований (Institute of Marine Research, Bergen, Trømsø). Расширение ареала и увеличение численности камчатского краба с начала 1990-х гг. привели к его расселению в обширной акватории южной части Баренцева моря. В 2006–2010 гг. камчатский краб доминировал в сообществах мегабентоса Мурманской и Канинской банок. К 2016–2020 гг. область его доминирования расширилась на север и восток — до острова Колгуев и южного склона Гусиной банки. Рост численности краба-стригуна опилио привёл к заселению им огромной акватории в Баренцевом море — от Печорского моря до архипелага Земля Франца-Иосифа и от архипелага Новая Земля до архипелага Шпицберген. В 2006–2010 гг. численность краба-стригуна опилио начала расти у архипелага Новая Земля, где он выступал в качестве субдоминанта в сообществах мягких грунтов Гусиной банки.

В 2011–2015 гг. краб-стригун опилио стал доминировать в сообществах Гусиной банки, Новоземельской банки, северной части Центральной возвышенности. В то же время он продолжал увеличивать свою роль как вид-субдоминант практически во всех сообществах у архипелага Новая Земля. Позднее, в 2016–2020 гг., краб-стригун опилио доминировал в бентосных сообществах на границе с Карским морем между архипелагами Новая Земля и Земля Франца-Иосифа, на склонах Новоземельской банки, у Центральной банки и в Южно-Новоземельском жёлобе. Его ареал увеличился и в итоге охватил акваторию от архипелагов Земля Франца-Иосифа и Новая Земля до возвышенности Персея на западе и до Печорского моря на юге. Показано, что камчатский краб будет и дальше входить в состав сообществ юго-восточной части Баренцева моря. Краб-стригун опилио продолжит миграцию с востока в западную часть моря вплоть до архипелага Шпицберген, где существуют сходные сообщества бентоса; в случае похолодания миграция пойдёт более быстрыми темпами. Возможен сценарий, при котором мелководье архипелага Шпицберген станет новым центром воспроизводства популяции краба-стригуна опилио в Баренцевом море вместе с нынешним центром у архипелага Новая Земля.

Ключевые слова: Баренцево море, мегабентос, донные сообщества, камчатский краб, *Paralithodes camtschaticus*, краб-стригун опилио, *Chionoecetes opilio*

UDC 581.526.325(268.45.02)

**LOCALIZATION
OF PHYTOPLANKTON EARLY SPRING BLOOM SPOTS
IN THE PELAGIC ZONE OF THE BARENTS SEA**

© 2024 **P. Makarevich, V. Vodopyanova, A. Bulavina, P. Vashchenko,
A. Namyatov, and I. Pastukhov**

Murmansk Marine Biological Institute of the Russian Academy of Sciences, Murmansk, Russian Federation

E-mail: makarevich@mmbi.info

Received by the Editor 01.04.2022; after reviewing 26.07.2022;
accepted for publication 09.10.2023; published online 22.03.2024.

Atlantification of the Barents Sea leads to a decrease in the area of ice cover and an increase in the ice-free period. This process affects the entire pelagic ecosystem of the Barents Sea, where the main part of the annual primary production of phytoplankton is formed during the spring bloom. Chlorophyll *a* concentration reflects changes in phytoplankton biomass and can serve as an indicator of its production characteristics. In the spring of 2021, hydrological characteristics of water masses, as well as the distribution of concentrations of chlorophyll *a* and nutrients, were studied in the ice-free water area of the Barents Sea. The year of 2021 was characterized by negative ice cover anomalies. The location and length of the areas of increased (or decreased) chlorophyll *a* concentrations were consistent with the alternation of water masses. Separate spots of early spring bloom were identified – in coastal waters in the southeastern and southwestern Barents Sea. In late March and early April 2021, maximum chlorophyll *a* concentrations in coastal waters reached values of about $1 \text{ mg}\cdot\text{m}^{-3}$. At the same time, in the Barents Sea and Arctic waters, the maximum content did not exceed $0.20 \text{ mg}\cdot\text{m}^{-3}$. The distribution of nutrients corresponded to that for the winter period when the vertical gradients of these parameters were not formed yet. The values of water saturation with oxygen exceeding 100% (to varying degrees throughout the studied area) characterized the activation of the photosynthesis process in the phytoplankton community. Analysis of long-term data showed that the subsequent active spring phytoplankton bloom in years with negative ice cover anomalies occurred already in the second or third decade of April in the Barents Sea water masses of various types – in Arctic, Atlantic, and coastal waters (maximum chlorophyll *a* concentration reached the value of $5.69 \text{ mg}\cdot\text{m}^{-3}$ in Arctic waters). In May, this process covered various types of water masses throughout the Barents Sea (maximum chlorophyll *a* content was of $5.08\text{--}5.77 \text{ mg}\cdot\text{m}^{-3}$). In abnormally cold years, the low position of the ice edge in March–April limited the possible area of phytoplankton development, and the active phase of its bloom (according to satellite data) occurred much later, in May. Atlantification of the Barents Sea contributes to the formation of several bloom spots and the distribution of spring bloom over a larger area, which might affect the annual production indicators of the entire pelagic zone.

Keywords: chlorophyll *a*, spring bloom, water masses, Atlantification, Barents Sea

Climate change affects and is expected to significantly affect Arctic marine ecosystems with consequences at different levels: pelagic, benthic, and sympagic. The observed sharp warming in the Arctic Basin that began in the 1980s under the effect of global climate anomalies [Barber et al., 2008; Comiso, Hall, 2014] resulted in alterations in climatic and hydrological parameters of the Barents Sea. Recently, there has been a rise in volume and temperature of Atlantic waters entering the Barents Sea, as well as associated unprecedented reduction in sea ice and an increase in the ice-free period [Alekshev, 2015; Boitsov et al., 2012; Zhichkin, 2015].

The term “Atlantification” was first used to characterize the periodic change in the vertical structure of waters in the central Barents Sea [Reigstad et al., 2002]. Further, this concept was expanded to the entire Barents Sea, and the term was defined as an increase in the influx of Atlantic waters leading to reduction in sea ice in the sea. To date, this term is applied to the entire Nansen Basin. Intensification of Atlantification in the Arctic Ocean consists of expanding the zone of effect of Atlantic waters on its hydrological and ice regime [Aksenov, Ivanov, 2018]. The Barents Sea, being a sort of heat exchanger for the Arctic Ocean, releases most of ocean heat entering from the North Atlantic. The resulting heat exchange between air and sea is critical both for regulating climate and determining deep circulation in the Arctic Ocean and beyond. According to climate model projections, in a warming climate, the cooling role of the Barents Sea is likely to expand to the Kara Sea and then to the Arctic Basin. Accordingly, Arctic Atlantification will intensify and shift poleward in future [Shu et al., 2021].

There is still limited knowledge about climate effect on timing of the spring phytoplankton bloom onset, its duration, and levels of quantitative development of primary producers in Arctic waters. Reduction of the area of the Arctic Ocean ice is expected to result in increased primary phytoplankton production [Kahru et al., 2011; Wassmann, 2011]. It will be facilitated by a rise in ice-free water area, a longer vegetation period, and additional carbon export to the pelagic zone from the atmosphere [Lewis et al., 2020]. All these factors can affect phenology of phytoplankton blooms in the Barents Sea [Dong et al., 2020; Oziel et al., 2017]. Seasonal variations of sea ice boundaries related to a decrease in the ice cover have already led to a shift in spring and summer phytoplankton blooms in the Barents Sea in northern and eastern directions [Oziel et al., 2017].

In the Arctic and subarctic zones of the World Ocean, most of the annual primary production is formed during spring phytoplankton blooms; all further development of the ecosystem of Arctic seas during the year is determined by the level of the spring bloom. A bloom of phytoplankton is understood as an annually recurring increase in its total biomass. In the northern Barents Sea, the onset of this process is traditionally related to the ice edge zone, and in the southeastern Barents Sea, to shallow areas and streams of the main Atlantic currents [Biological Atlas, 2022; Kuznetsov, Shoshina, 2003; Plankton morei Zapadnoi Arktiki, 1997]. The bloom onset is determined by the coincidence of several physical factors: ice melting, amount of incoming light, stratification of the water column, wind mixing, nutrient supply, *etc.* [Fujiwara et al., 2014; Park et al., 2015; Wang et al., 2018]. According to different authors, the bloom begins in March-April [Biological Atlas, 2022; Qu et al., 2006] or April-May [Kuznetsov, Shoshina, 2003; Plankton morei Zapadnoi Arktiki, 1997]. The main, prevailing species are representatives of Arctic diatoms of neritic origin [Makarevich et al., 2012]. The Barents Sea spring phytoplankton bloom reaches its maximum values in May throughout the entire ice-free water area, including the area of drifting ice, and subsides in summer. Summer phytoplankton outbreaks recorded in some

cases in the ice edge zone are of a secondary, facultative nature [Biological Atlas, 2022; Kuznetsov, Shoshina, 2003; Wassmann et al., 2006]. As a rule, *in situ* studies cover only small areas of the sea (meridional or latitudinal transects), and this does not allow to conclude on the rest of the water area. A more complete picture is provided in works based on satellite observations. However, for high latitudes, obtaining satellite data is difficult due to high cloudiness and is associated with data distortion resulting from averaging.

In March–April 2021, expeditionary research was carried out in the Barents Sea ice-free water area. The aim of the work was to identify spots of early spring phytoplankton blooms. To do this, we determined chlorophyll *a* concentration: in general, its variability can reflect variability of phytoplankton biomass and serve as an indicator of total abundance and productivity of the phytoplankton community.

MATERIAL AND METHODS

The work was carried out during the cruise of the RV “Dalnie Zelentsy” from 10 March to 12 April, 2021, and covered a vast ice-free water area of the Barents Sea. In total, 9 transects were performed in the latitudinal and meridional directions, which included 52 hydrological stations and 34 complex stations (Fig. 1). The stations and transects were numbered in accordance with the RV records.

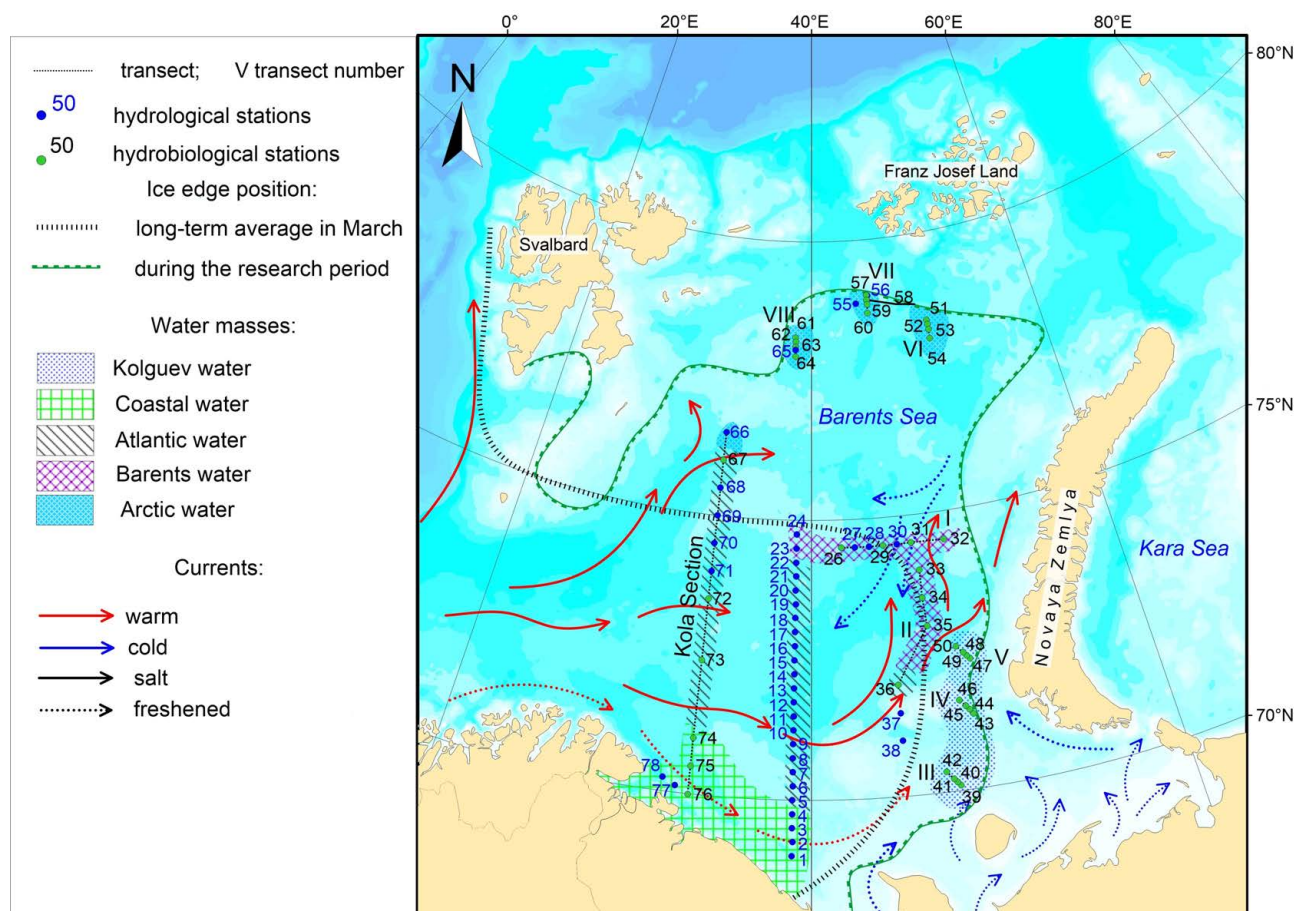


Fig. 1. Location of stations and ice conditions, the Barents Sea, March–April 2021. The ice edge location according to [EOSDIS Worldview, 2022; Johannessen et al., 2007]

To describe the hydrological structure of water masses in the studied area, material from the RV report was used [Reisovyi otchet, 2021]. At 52 stations, complex hydrological works were carried out. Water temperature and salinity were determined using SBE 19plus V2 SeaCAT Profiler (Sea-Bird Scientific, the USA). Based on the data obtained, temperature and salinity isolines along the transects were built. To isolate water masses, TS analysis was carried out [Mamaev, 1987].

For further determination of chlorophyll *a* (hereinafter Chl-*a*) concentrations ($\text{mg}\cdot\text{m}^{-3}$), seawater was sampled at horizons of 0, 25, and 50 m. Niskin bottles of 5 and 10 L were used (Hydro-Bios, Germany). A total of 114 samples were taken and processed. We followed the guideline [Aminot, Ray, 2000] based on the classic UNESCO technique for determining Chl-*a* content [Determination of Photosynthetic Pigments, 1966]. Deviations from the guideline were not allowed. Water samples of 5 L for each horizon were filtered immediately in a vacuum unit in a laboratory onboard the RV. “Vladipor” membrane filters with a diameter of 47 mm and a pore size of 0.6 μm were used. After filtration, the filters, folded in half with the sediment inward, were stored in the freezer in a desiccator with silica gel at a temperature of $-20\text{ }^{\circ}\text{C}$. Further processing of the samples was carried out in a stationary hydrochemical laboratory. The precipitate was extracted with 90% acetone. After homogenization, the samples were centrifuged at 8,000 rpm. Chl-*a* concentration in the extract was determined on a Nicolet Evolution 500 spectrophotometer (Spectronic Unicam, the UK).

To analyze the spatial distribution of Chl-*a* concentrations for the entire sea area, satellite remote sensing data and decrypted NASA images [Ocean Color NASA, 2022] were used. Daily and averaged (monthly) data were investigated. Level-3 CHL from SeaWiFS satellites (material for 1998) and MODIS-Aqua (material for 2021) were used. Data from the NASA website were imported into the ArcMAP GIS application, and raster images of Chl-*a* spatial distribution for a certain period were formed.

For hydrochemical studies, seawater was sampled at horizons of 0, 10, 25, 50, and 100 m and in the bottom layer. Dissolved oxygen (O_2) concentrations ($\text{mg}\cdot\text{L}^{-1}$) were determined using a MARK-303 portable oxygen meter (VZOR, Russia). The acid-base balance (pH) was measured in unfiltered water samples with an I-500 ionometer (Akvilon, Russia) and adjusted to *in situ* value. Inorganic dissolved phosphorus (P- PO_4) was determined by the Murphy–Riley method; dissolved silicon (Si- SiO_3), by the Korolev method; and nitrites (N- NO_2) and nitrate nitrogen (N- NO_3), by the Bendschneider–Robinson method [Chemical Methods, 1983; Methods of Seawater Analysis, 1999; Rukovodstvo po khimicheskomy analizu, 2003]. The parameters were measured on a PE-5300VI spectrophotometer (Ecroskhim, Russia).

When analyzing the data, we used the values of content of Atlantic waters (fa, %), river waters (fr, %), and waters transformed due to ice formation/melting (fi, %). These values were obtained by calculation applying the dependencies given in the work of A. Namyatov [2021a].

The dependencies were obtained by analyzing 2,200 results of parallel determinations of salinity and the isotopic parameter $\delta^{18}\text{O}$ in 1978–2014 in the Barents Sea by various authors, at different seasons of the year, and at different horizons. The justification for the possibility of using these dependencies beyond the existing series of observations of salinity– $\delta^{18}\text{O}$ was considered by A. Namyatov [2021b].

RESULTS

Water masses on the performed transects. The Barents Sea water mass. Transects I and II were performed on 21–26 March in the Central Basin area of the Barents Sea. There, the water surface does not cool as much in winter as in the southeastern sea due to the effect of warm Atlantic currents. At the stations of transect I, the water column was well mixed from the surface to the bottom and occupied by the Barents Sea water, with the temperature of 0...–0.5 °C and salinity of 34.72–34.83 PSU (Fig. 2).

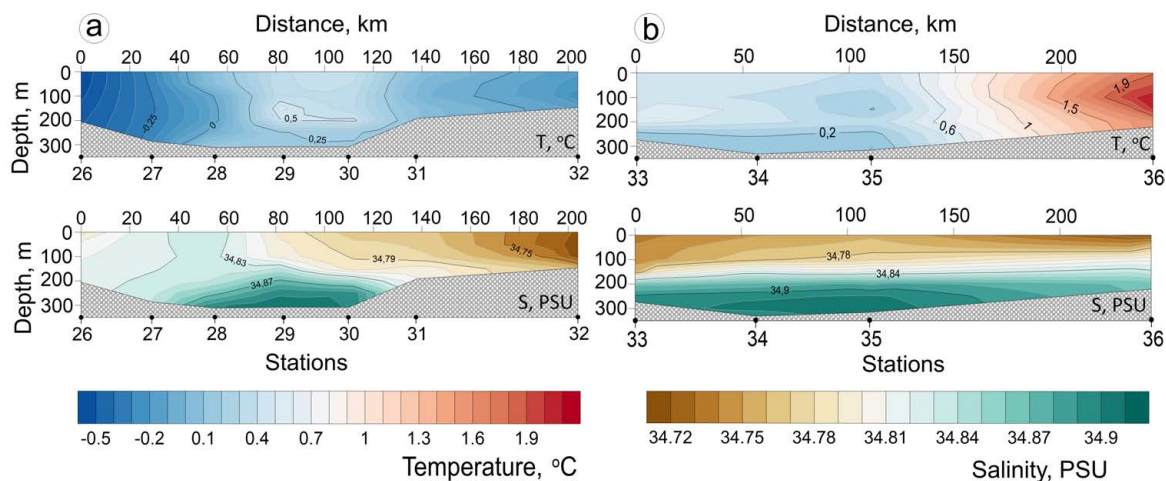


Fig. 2. Temperature (T, °C) and salinity (S, PSU) at the transects: a, transect I; b, transect II

In the deepest area of the transect (sta. 28–30) at depths of more than 150 m, there was a slight increase in temperature (up to +0.5 °C) and salinity (up to 34.91 PSU) caused by the effect of Atlantic currents. At sta. 33–35 of transect II, the mixed water layer extended to a depth of 100–150 m. Its temperature and salinity characteristics corresponded to those of the Barents Sea water. Under the mixed layer, the temperature decreased slightly, and the salinity increased. At sta. 36 at a depth of about 100 m, a warm (+2.2 °C) stream of transformed Atlantic waters of the Novaya Zemlya Current was recorded; those retained their identity only in the temperature field (not in the salinity field).

At sta. 32 of transect I, closest to the ice edge, the maximum value of dissolved oxygen saturation in water was registered, 102%. In the more western area of the transect, the value did not exceed 100%.

The Kolguev water mass. The survey with high spatial resolution (distance between stations was 5 to 10 nautical miles) was carried out near the ice edge in the northern and southeastern Barents Sea. Transects III, IV, and V were located in the southeastern sea. The White Sea Current supplies this area with the White Sea waters, with a salinity of about 33 PSU. The highest salinity in this area is noted in November–February. A decrease in salinity related to the influx of desalinated water from the White Sea begins already in March and affects not only the surface layer, but also the intermediate and even bottom ones [Ozhigin et al., 2016]. In winter months, the Barents Sea ice-free water area is intensively cooled. Under the effect of convective and wind mixing in this period, a 100–150-m thick layer is formed, relatively uniform in terms of temperature and salinity. In shallow areas of the sea, mixing can reach the bottom. The structure of the water column becomes more complex in spring since ice begins to melt. The work was carried out there on 27–29 March, when the spring ice melting had not yet begun.

At transects III and IV, temperature and salinity rose monotonically with depth. Water surface temperature was of $-1.8 \dots -1$ °C; at the bottom, temperature was close to 0 °C; and at some stations, it reached above-zero values (Fig. 3).

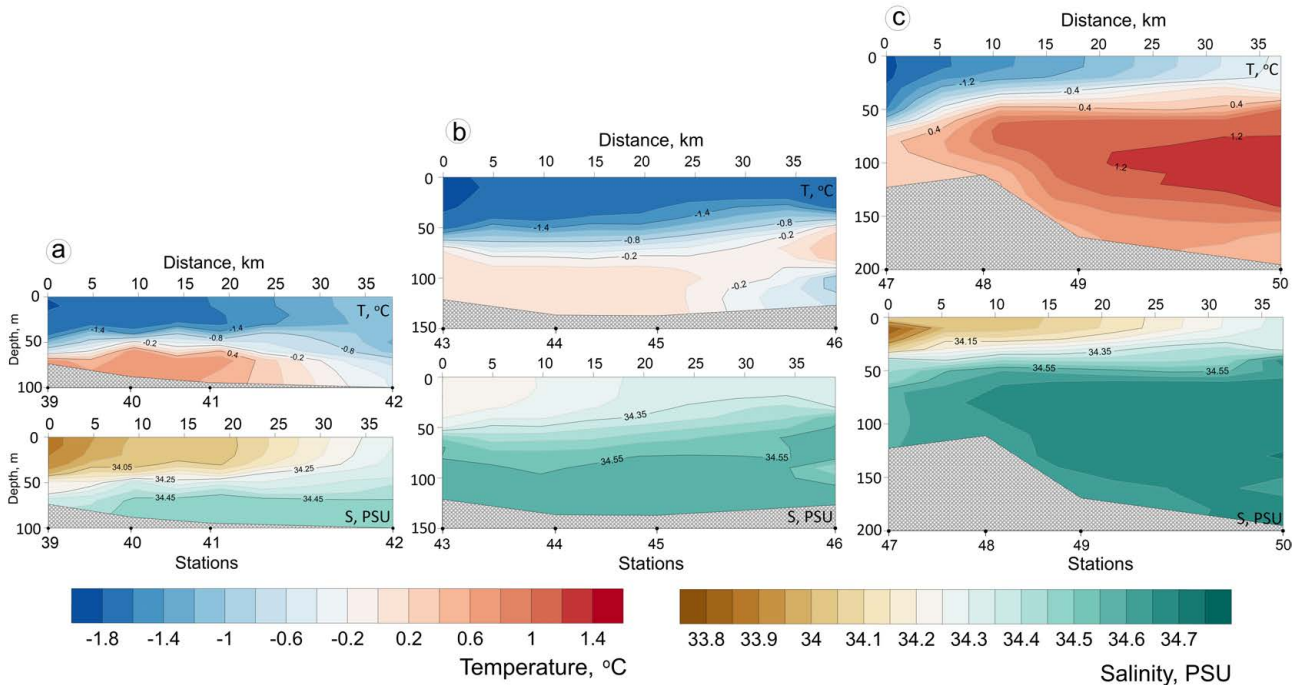


Fig. 3. Temperature (T, °C) and salinity (S, PSU) at the transects: a, transect III; b, transect IV; c, transect V

The minimum salinity value at the surface was 33.9 PSU. The maximum value at the bottom was 34.6 PSU. At transect V (sta. 49 and 50) at a depth of 100 m, a stream of warm water ($+1.4$ °C) with a salinity of 34.7 PSU was recorded. These stations are confined to the North Novaya Zemlya Trench, which is one of the routes for distribution of transformed Atlantic waters of the Novaya Zemlya Current. In general, the stations of transects III, IV, and V can be attributed to the Kolguyev structure of water masses. In the area of these transects, the characteristics and structure of the water column are determined primarily by the influx of desalinated waters from the White Sea, a large volume of river influx into the southeastern Barents Sea, and an intensive water mixing down to the bottom in autumn and winter.

The eastern stations of these transects were carried out in close proximity to the ice edge. At these stations, the dissolved oxygen saturation in water was lower than 100%. However, when moving away from the edge to the northwest, an excess of the threshold value of 100% was recorded, and this indicates the location of the first spring spots of the photosynthesis activation. At more southern transect III, this area is confined to the surface layer of sta. 42 (101%). At more northern transects IV and V, the area with the highest values was located in the 40–60-m layer. The maximums were 101 and 104%, respectively. The distribution of other nutrients across the transects was patchy.

The Arctic water mass. Transects VI, VII, and VIII were performed on 31 March – 3 April in the northern Barents Sea near the ice edge. In the study period, there was no layer of melted water. At transects VI and VII, the entire water column consisted of waters of Arctic origin. Temperature and salinity increased with depth, reaching -0.8 °C and 34.82 PSU at the bottom, respectively (Fig. 4).

At transect VIII, Arctic waters also prevailed, but at sta. 61 and 64, the effect of Atlantic waters was registered near the bottom. The temperature reached above-zero values ($+0.5\text{ }^{\circ}\text{C}$). In this area, there is a complex system of currents capable of bringing both Atlantic waters from the western border of the Barents Sea and highly transformed Atlantic waters that have passed through the Arctic Basin.

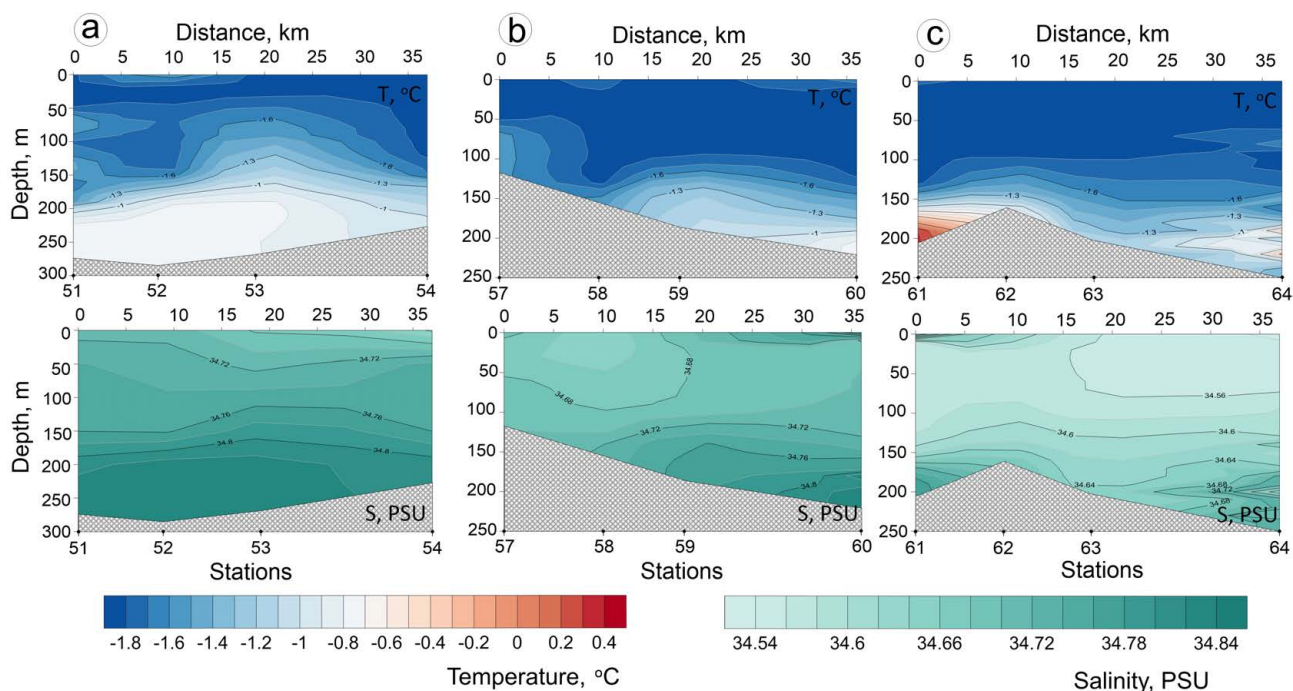


Fig. 4. Temperature (T , $^{\circ}\text{C}$) and salinity (S , PSU) at the transects: a, transect VI; b, transect VII; c, transect VIII

Excessive oxygen saturation in water was observed in the surface layer almost throughout the entire transect VIII, which is the westernmost in this group of transects. In the surface layer of its southern area, the oxygen saturation value reached 105% (sta. 64), and an excess of the threshold value of 100% in the surface layer was observed almost throughout the entire transect. In the surface layer of other, more eastern transects in this water mass, oxygen saturation was less than 100%: the values accounted for 98–99%.

Atlantic and coastal water masses. The work at the standard oceanographic transect “Kola Meridian” was carried out on 8–12 April. The transect was located on the route of distribution of warm waters of the North Cape Current and desalinated waters of the Murmansk Coastal Current. In the southern area of the transect (sta. 74–76), there was a decrease in salinity (down to 34.44–34.65 PSU) which resulted from the freshwater runoff of the rivers of Northern Norway and the Kola Peninsula, carried by the Norwegian and Murmansk currents (Fig. 5). The distribution boundary of desalinated coastal waters was determined on the sea surface between sta. 74 and 73. In the central area of the transect (sta. 67–73), Atlantic waters of high salinity (34.95 PSU) were recorded. At sta. 66, the main water column was occupied by Arctic waters, with sub-zero temperature ($-1.2\text{ }^{\circ}\text{C}$) and low salinity (34.44 PSU). At the bottom at sta. 66, a layer of warmer ($+0.8\text{ }^{\circ}\text{C}$) and more saline (34.84 PSU) transformed Atlantic water was registered.

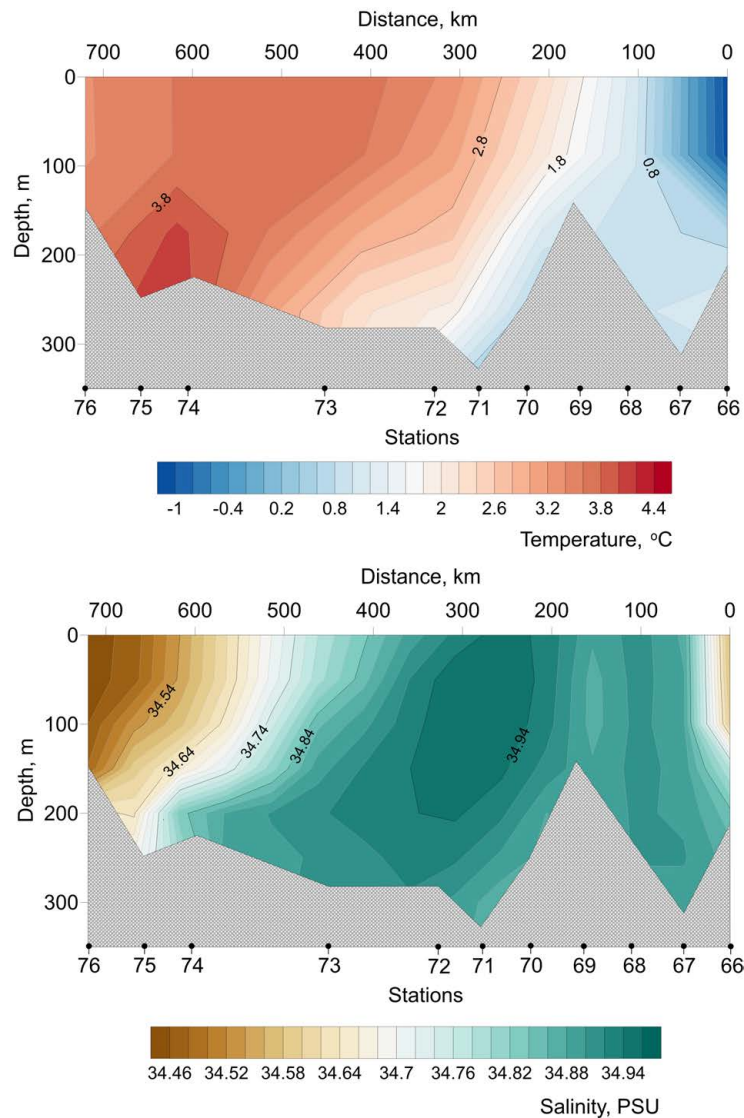


Fig. 5. Temperature (T, °C) and salinity (S, PSU) at transect “Kola Meridian”

At this transect, unlike the other ones, in the surface layer from the southern stations to northern ones, the dissolved oxygen saturation in water exceeded 100%. In the surface layer of Atlantic waters, it varied from 100 to 102%; in cold Arctic waters in the northern area of the transect, the value sharply increased to 108%.

Hydrochemical parameters of water masses. All water masses of the Barents Sea are formed by three basic waters – Atlantic ones, river ones, and waters transformed due to ice formation/melting [Namyatov, 2021a]. An alteration in the ratio of these waters throughout the year because of their advection from other water areas and vertical mixing can significantly affect the nature of the annual cycle of variability for the nutrients studied. Table 1 provides the mean values and standard deviations of concentrations of considered nutrients, temperature and salinity values, and the values of the content of Atlantic waters (fa, %), river waters (fr, %), and meltwater (fi, %) in the water masses described by us in March–April 2021.

Table 1. Mean values and standard deviations of temperature (T, °C) and salinity (S, PSU), concentrations of nutrients, and the values of the content of Atlantic waters (fa, %), river waters (fr, %), and meltwater (fi, %) in the 0–10-m layer, March–April 2021

Water mass	The Kolguyev water mass		The Barents Sea water mass		The Arctic water mass		The Atlantic water mass	The coastal water mass
	a	b	a	b	a	b	b	b
Sta. no.	39, 43, 47	40–42, 44, 46, 48–50	32	26, 29, 31	51, 57, 61, 66	52–54, 58–60, 62–64	67–73	74–76
T, °C	-1.82 ± 0.02	-1.40 ± 0.46	-0.19	-0.07 ± 0.42	-1.64 ± 0.31	-1.82 ± 0.06	2.16 ± 1.30	3.54 ± 0.05
S, PSU	34.00 ± 0.18	34.18 ± 0.14	34.72	34.8 ± 0.01	34.67 ± 0.09	34.65 ± 0.08	34.91 ± 0.04	34.49 ± 0.05
fa, %	97.0	97.5	99.1	99.2	98.9	98.8	99.6	98.4
fa, min–max, %	96.4–97.5	97.0–97.9		99.2–99.3	98.6–99.4	98.4–99.5	99.3–99.7	98.2–98.6
fr, %	2.55	2.09	0.69	0.53	0.84	0.90	0.24	1.29
fr, min–max, %	2.04–3.09	1.71–2.54		0.51–0.58	0.41–1.10	0.31–1.67	0.34–3.89	1.13–1.40
fi, %	0.49	0.43	0.23	0.21	0.26	0.29	0.16	0.33
fi, min–max, %	0.43–0.55	0.39–0.49		0.21–0.22	0.19–0.30	0.17–0.31	0.14–0.21	0.30–0.34
O ₂ , mL·L ⁻¹	8.32 ± 0.12	8.42 ± 0.09	8.16	8.02 ± 0.08	8.48 ± 0.32	8.40 ± 0.19	7.84 ± 0.42	7.42 ± 0.04
O ₂ , min–max, %	97.7–100.6	98.3–107.5	99.3–101.9	100.4	97.3–108.1	105.1	98.2–108.9	99.7–101.5
P-PO ₄ , μM	0.36 ± 0.11	0.35 ± 0.09	0.59	0.50 ± 0.10	0.53 ± 0.08	0.47 ± 0.12	0.50 ± 0.10	0.44 ± 0.10
N-NO ₃ , μM	4.61 ± 1.20	5.33 ± 0.87	7.53	8.57 ± 0.33	7.18 ± 1.58	7.14 ± 0.67	10.7 ± 0.74	7.19 ± 0.61
Si-SiO ₃ , μM	2.67 ± 0.52	1.93 ± 0.75	2.40	1.88 ± 0.41	1.95 ± 0.31	1.55 ± 0.54	3.16 ± 0.87	2.14 ± 0.33

Note: a, stations closest to the ice edge; b, stations located in open water.

A common feature of distribution of nutrients (P-PO₄, N-NO₃, and Si-SiO₃) at all the performed transects was their correspondence to the winter type, when vertical gradients of these parameters were not formed yet. The bottom layers were characterized by the lowest values of dissolved oxygen saturation in water (up to 94%) and increased concentrations of mineral forms of phosphorus, nitrogen, and silicon.

Chlorophyll *a* concentrations at the performed transects. At transects I and II (the Barents Sea waters), Chl-*a* content in the surface layer was (0.11 ± 0.05) and (0.13 ± 0.02) mg·m⁻³, respectively; at a depth of 25 m, (0.15 ± 0.04) and (0.16 ± 0.01) mg·m⁻³, respectively; and at a depth of 50 m, the absolute values were comparable to those for the surface layer (Fig. 6a, b). The only station of transect II located in Atlantic waters (sta. 36), did not differ in terms of Chl-*a* concentration from other stations carried out in the Barents Sea waters.

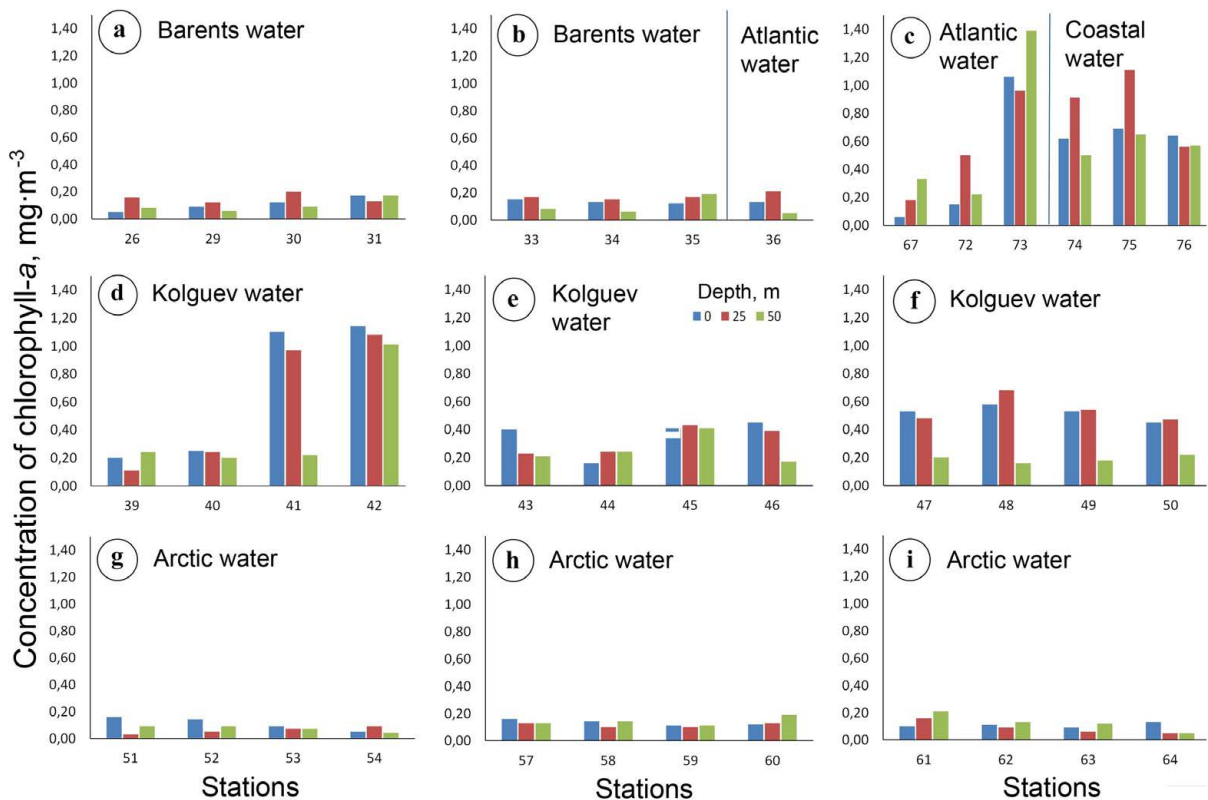


Fig. 6. Chlorophyll *a* concentrations ($\text{mg}\cdot\text{m}^{-3}$) at the transects: a, transect I; b, transect II; c, transect “Kola Meridian”; d, transect III; e, transect IV; f, transect V; g, transect VI; h, transect VII; i, transect VIII

Transects III, IV, and V (Fig. 6d, e, f) performed in the southeastern Barents Sea were affected by the Kolguyev water mass. At the stations of transect III close to the ice edge (sta. 39 and 40), Chl-*a* concentrations averaged $(0.23 \pm 0.04) \text{ mg}\cdot\text{m}^{-3}$ (0 m), $(0.18 \pm 0.09) \text{ mg}\cdot\text{m}^{-3}$ (25 m), and $(0.22 \pm 0.03) \text{ mg}\cdot\text{m}^{-3}$ (50 m) (Fig. 6d). At sta. 41 and 42, Chl-*a* content rose significantly, up to $1.14 \text{ mg}\cdot\text{m}^{-3}$ (0 m). There, the mean values were the highest for the entire Kolguyev water mass: $(0.96 \pm 0.28) \text{ mg}\cdot\text{m}^{-3}$ (0 m), $(0.87 \pm 0.27) \text{ mg}\cdot\text{m}^{-3}$ (25 m), and $(0.60 \pm 0.40) \text{ mg}\cdot\text{m}^{-3}$ (50 m) (Fig. 6d). Sta. 41 and 42 were characterized by a slight increase in surface water temperature compared to that at sta. 39 and 40. Apparently, sta. 41 and 42 were affected by the Kola Peninsula coastal waters carried by the Murmansk Current (see Fig. 1). Thus, there might be an advection of phytoplankton from the Kola Peninsula coastal waters to the area of sta. 41 and 42. This could contribute to an earlier onset of the spring phytoplankton bloom there than at other stations in the southeastern Barents Sea. At transect IV (Fig. 6e), a decrease in Chl-*a* concentrations was recorded, while content in the 0–50-m layer varied accounting for $(0.36 \pm 0.13) \text{ mg}\cdot\text{m}^{-3}$ (0 m), $(0.32 \pm 0.10) \text{ mg}\cdot\text{m}^{-3}$ (25 m), and $(0.26 \pm 0.11) \text{ mg}\cdot\text{m}^{-3}$ (50 m). At transect V (Fig. 6f), higher Chl-*a* concentrations were observed in the surface layer, $(0.52 \pm 0.05) \text{ mg}\cdot\text{m}^{-3}$, and at 25-m depth, $(0.54 \pm 0.10) \text{ mg}\cdot\text{m}^{-3}$, while at a depth of 50 m, the value decreased to $(0.19 \pm 0.03) \text{ mg}\cdot\text{m}^{-3}$.

Edge transects VI, VII, and VIII were performed in the northern water area, in Arctic waters. Low Chl-*a* concentrations, not exceeding $(0.13 \pm 0.02) \text{ mg}\cdot\text{m}^{-3}$, were distributed relatively evenly both in the water column and between stations of all three transects (Fig. 6g, h, i).

Stations of the longest transect, “Kola Meridian” (Fig. 6c), were carried out in various water masses. Specifically, sta. 74–76 were located in coastal waters. The mean Chl-*a* concentrations were quite high throughout the 0–50-m layer: $(0.65 \pm 0.04) \text{ mg}\cdot\text{m}^{-3}$ (0 m), $(0.86 \pm 0.28) \text{ mg}\cdot\text{m}^{-3}$ (25 m), and $(0.57 \pm 0.08) \text{ mg}\cdot\text{m}^{-3}$ (50 m). The maximum Chl-*a* content was recorded at a horizon of 25 m for sta. 74 and 75: the values were of 0.91 and 1.11 $\text{mg}\cdot\text{m}^{-3}$, respectively. Sta. 67, 72, and 73 were carried out in Atlantic waters. Interestingly, at sta. 73, Chl-*a* concentrations were high, with a maximum of 1.39 $\text{mg}\cdot\text{m}^{-3}$ (50 m). The proximity of this station to the area of coastal waters is noteworthy. There, the thermohaline characteristics of the water column were more consistent with those for Atlantic waters than with coastal ones. However, the salinity front on the sea surface passed between sta. 74 and 73, and the temperature front, between sta. 73 and 72. Thus, sta. 73 turned out to be located in the area of intense interaction between two types of water masses. High Chl-*a* content was not recorded in Atlantic waters. This suggests that its higher concentrations at sta. 73 result from the development of phytoplankton from coastal waters. At sta. 67 and 72, which were located in Atlantic waters beyond the frontal zone, the mean Chl-*a* content was low, no more than $(0.34 \pm 0.23) \text{ mg}\cdot\text{m}^{-3}$ (25 m).

According to our study results, in late March and early April 2021, the spatial distribution of Chl-*a* concentrations, as well as their absolute and mean values, differed significantly in the Barents Sea waters of various origin (Fig. 7). Like in previous studies [Makarevich et al., 2021, 2022], there was no linear relationship between variations in Chl-*a* content and temperature or salinity characteristics of water. Apparently, the dynamics of Chl-*a* concentration is related not to the thermohaline characteristics of water masses, but to their origin and migration routes. Chl-*a* content averaged for the 0–50-m layer was distributed fairly evenly within each of the identified water masses, with the exception of those at sta. 41, 42, and 73 (Fig. 7). Sta. 41 and 42 (Kolguev waters) and sta. 73 (Atlantic waters) are most likely to have been affected by Murmansk coastal waters.

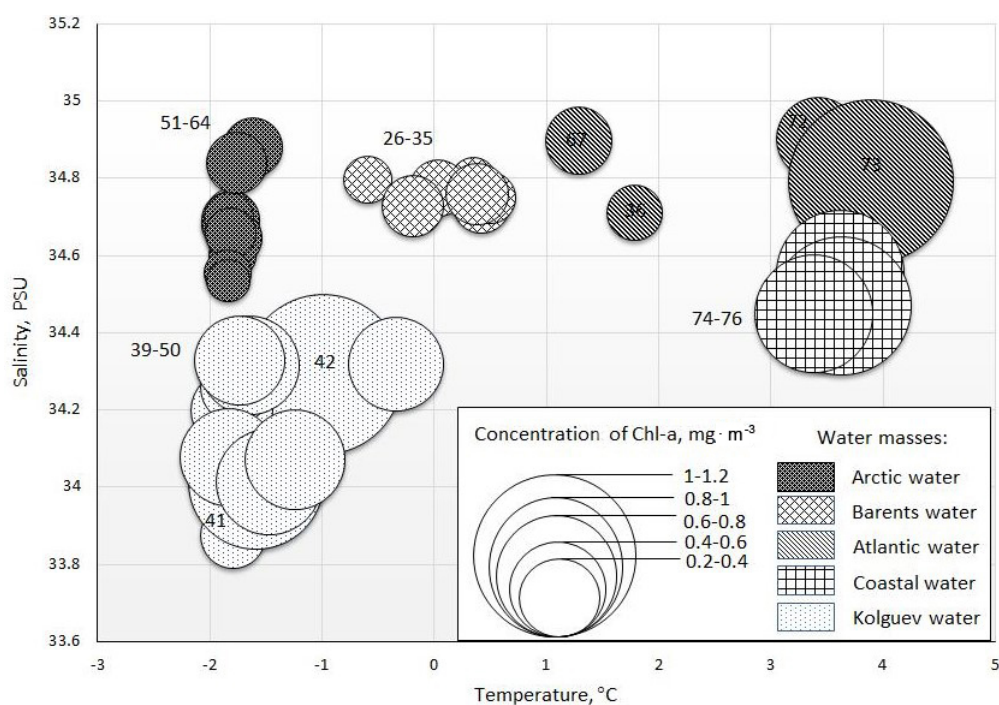


Fig. 7. Concentrations of chlorophyll *a* (Chl-*a*, $\text{mg}\cdot\text{m}^{-3}$) averaged for a seawater horizon of 0–50 m on a TS diagram

DISCUSSION

Spring phytoplankton vegetation in non-freezing areas of the Barents Sea begins in late March and early April and is primarily confined to shallow water areas of the southeastern sea and waters near the ice edge [Biological Atlas, 2022]. The spring maximum of phytoplankton development is formed mainly due to early spring arctic-boreal neritic diatoms [Makarevich et al., 2012].

Phytoplankton blooms in the Barents Sea are very sensitive to seasonal and interannual changes in sea ice area and to distribution of water masses and ocean fronts [Oziel et al., 2017]. The main environmental factors affecting the Barents Sea spring phytoplankton bloom are the rapidly increasing daily total irradiance, occurrence of maximum concentrations of nutrients in the pelagic zone, vertical mixing, and position of the polar front and boundaries of the ice cover [Kogeler, Rey, 1999; Signorini, McClain, 2009]. Meltwater is an additional mechanism that triggers spring bloom in areas of melting sea ice along the Barents Sea ice edge [Dong et al., 2020; Oziel et al., 2017]. In shallow areas of the sea, an important regulating factor in the onset of the spring phytoplankton bloom is the removal of spores and phytoplankton cells from bottom sediments, while the processes of vertical mixing of the water column can contribute to the microalgae bloom in the photic layer of the pelagic zone [Eilertsen et al., 1993]. Spring bloom is an annually recurring short-term increase in phytoplankton biomass and abundance. In the open area of the Barents Sea, one spring maximum of phytoplankton development is registered. At the onset of the spring bloom, Chl-*a* concentrations in the Barents Sea first are characterized by values of about 0.5 mg·m⁻³, and then those sharply increase. Its content can reach 6–14 mg·m⁻³ [Makarevich et al., 2022; Reigstad et al., 2002]. The maximum bloom does not last long; moreover, it is followed by a rapid decline in productivity of pelagic microalgae communities. An abundant (rapid) microalgae bloom leads to a rapid decrease in nutrient reserves in the upper layers of the pelagic zone, and the presence of sharp stratification prevents the replenishment of this reserve from underlying layers [Kuznetsov, Shoshina, 2003].

According to long-term observations, the month of the most extended ice cover for the Barents Sea is March. Usually in March, the entire eastern sea is covered with ice. In the western sea, ice extends south down to N75°. Until mid-April, the ice cover continues to increase; then, the ice edge gradually shifts to the north and east. In May, the entire central Barents Sea is ice-free; in late June and early July, the Pechora Sea and the coast of the Novaya Zemlya archipelago are ice-free [Johannessen et al., 2007]. In different years, the seasonal position of the ice edge can differ significantly from the long-term mean one. In abnormally cold years, the last of which was 1998, during the period of its maximum development, ice covered a significantly larger area of the Barents Sea and stayed longer. In such years, the southeastern sea was completely or partially covered with ice until mid-July. According to remote satellite monitoring data, low Chl-*a* content in March–April of the abnormally cold year of 1998 excluded the spring bloom stage in the phytoplankton succession cycle. Only in May, maximum Chl-*a* concentrations and active development of phytoplankton were recorded throughout the entire ice-free water area of the Barents Sea (Fig. 8). In abnormally warm years, already in late May, the Novaya Zemlya coast and the Pechora Sea can be completely ice-free. In both warm and cold years, the southwestern Barents Sea is ice-free throughout the year. In 2021, negative ice cover anomalies in the sea were registered. In May 2021, the Pechora Sea began to become ice-free; by mid-May, the Novaya Zemlya coastal waters were already completely ice-free. Data from remote satellite monitoring of Chl-*a* content for 2021 indicate as follows: in contrast to the abnormally cold year, active development of phytoplankton

was observed already in April in the southeastern Barents Sea and in certain areas of the rest of the water area. In May, the process of phytoplankton development spread in the central and northern directions and covered almost the entire sea area (Fig. 8).

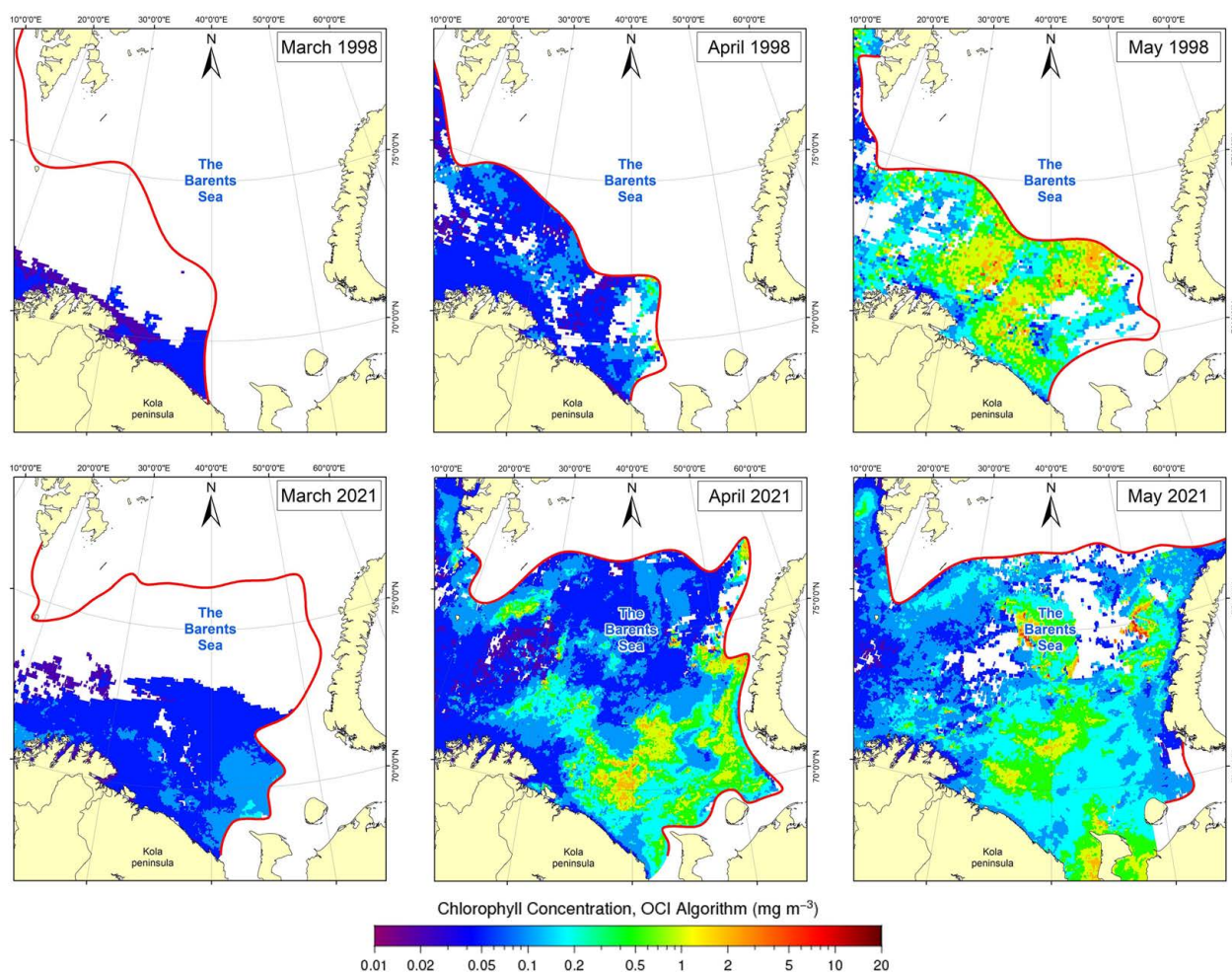


Fig. 8. Monthly averaged chlorophyll *a* concentrations ($\text{mg}\cdot\text{m}^{-3}$) according to satellite data [Ocean Color NASA, 2022]. The red line is the average position of the ice edge for the month according to [EOSDIS Worldview, 2022; Johannessen et al., 2007]

Long-term *in situ* observations of the distribution of Chl-*a* concentrations in water masses of different types in the Barents Sea allowed to systematize this material for warm years. Fig. 9 shows averaged data on Chl-*a* content in various water masses (the 0–50-m layer) of the Barents Sea in spring: March 2021; April 2016, 2018, 2019 [Makarevich et al., 2022], and 2021; May 2016 and 2018 [Makarevich et al., 2021, 2022]; and July 2017 [Vodopianova et al., 2019]. The years of 2016, 2017, 2018, and 2019 were characterized by negative ice cover anomalies, and these years are comparable to 2021.

According to our data, in years with negative ice cover anomalies, the onset of the spring phytoplankton bloom can be observed already in the third decade of March and the first decade of April. The vast ice-free water area contributes to the development of this process in several isolated areas – in the southwestern and southeastern sea. Spots of increased Chl-*a* concentrations were recorded in coastal, Atlantic, and Kolguyev waters.

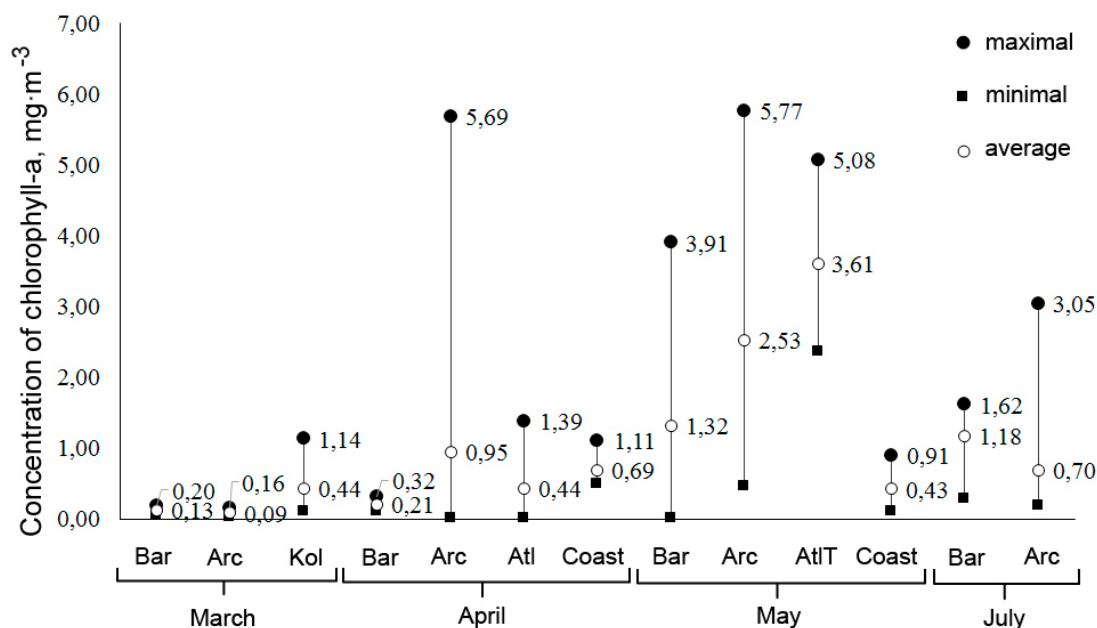


Fig. 9. Chlorophyll *a* concentrations ($\text{mg}\cdot\text{m}^{-3}$) averaged for 0–50-m layer and water masses in the Barents Sea: March 2021; April 2016, 2018, 2019 [Makarevich et al., 2022], and 2021; May 2016 and 2018 [Makarevich et al., 2021, 2022]; July 2017 [Vodopyanova et al., 2019] (Bar, Barents Sea waters; Kol, Kolguyev waters; Atl, Atlantic waters; AtlTw, transformed Atlantic waters; Arc, Arctic waters; CW, coastal waters)

Based on literature material, the Barents Sea coastal waters are characterized by occurrence of several outbreaks of phytoplankton development (3 to 4) during the vegetation period; however, the mean Chl-*a* content during the active development in the coastal area in the southwestern Barents Sea is low, about $1 \text{ mg}\cdot\text{m}^{-3}$ [Kuznetsov, Shoshina, 2003]. According to our data, in March, the mean Chl-*a* concentration in Kolguyev waters which are coastal in origin was higher than in other water masses (the mean of $0.44 \text{ mg}\cdot\text{m}^{-3}$). In April, Chl-*a* content in coastal waters in the southwestern area averaged $0.64 \text{ mg}\cdot\text{m}^{-3}$; in May, the value decreased to $0.43 \text{ mg}\cdot\text{m}^{-3}$ (Fig. 9).

In Arctic and Barents Sea waters in March, Chl-*a* concentration was very low. In the Barents Sea waters, the value averaged $0.13 \text{ mg}\cdot\text{m}^{-3}$. Equally low Chl-*a* content in the Barents Sea waters was recorded in April (the mean of $0.21 \text{ mg}\cdot\text{m}^{-3}$); only in May, it reached significant values (the mean of $1.32 \text{ mg}\cdot\text{m}^{-3}$) (Fig. 9). In March, Arctic waters were also characterized by extremely low concentrations (the mean of $0.11 \text{ mg}\cdot\text{m}^{-3}$). Already in April, a sharp increase in content was observed (the mean of $1.32 \text{ mg}\cdot\text{m}^{-3}$); in May, Chl-*a* concentrations continued to rise there (the mean of $2.53 \text{ mg}\cdot\text{m}^{-3}$). The maximum values in Arctic waters in April and May were 5.69 and $5.77 \text{ mg}\cdot\text{m}^{-3}$, respectively. By July, we noted a decrease in content of this pigment in Arctic and Barents Sea waters, but the values still remained significant, with mean of $0.70 \text{ mg}\cdot\text{m}^{-3}$ (Arctic waters) and $1.18 \text{ mg}\cdot\text{m}^{-3}$ (the Barents Sea waters).

In April, in Atlantic waters, Chl-*a* content averaged $0.44 \text{ mg}\cdot\text{m}^{-3}$ (maximum of $1.39 \text{ mg}\cdot\text{m}^{-3}$). In May, in transformed Atlantic waters, the pigment concentration was already noticeably higher (maximum of $5 \text{ mg}\cdot\text{m}^{-3}$). This month, a generally high background of content was established in water masses of all types (Fig. 9).

Our data show as follows: in March–April 2021, vertical gradients of changes in the mineral forms of phosphorus, nitrogen, and silicon, characteristic of the period of active photosynthesis, were not formed yet. Variations in nutrient content are not always directly related to changes in phytoplankton biomass or Chl-*a* concentrations. The specific nutrient content depends on the relationship between basic waters, physical factors (seawater temperature and salinity), the position of the ice edge, and the intensity of the occurring photosynthesis process (see Table 1). In the Arctic region, during the warm season, values of dissolved oxygen saturation in water exceeding 100% are traditionally related to phytoplankton development [Khimiya okeana, 1979]. The variability of this parameter in the studied water area and the values above 100% of the level of dissolved oxygen saturation in water indicated the activation of the photosynthesis process in the phytoplankton community.

Conclusion. The spatial heterogeneity of chlorophyll *a* distribution that we observed in the spring of 2021 was due to the disunity of phytoplankton bloom spots in time and space. The location and extent of areas of increased (or decreased) chlorophyll *a* concentrations were consistent with the alternation of water masses. Its local maximums were recorded in the coastal zone of central Murman and in Kolguyev shallow waters. In the waters of the northern Barents Sea, adjacent to the ice edge, chlorophyll *a* values were significantly lower than those for the southern sea. The waters of the central sea were characterized by intermediate (average) chlorophyll *a* content.

The distribution of mineral forms of phosphorus, nitrogen, and silicon in various water masses of the Barents Sea in March–April 2021 was more consistent with the winter type, when vertical gradients of their changes were not formed yet. The values of dissolved oxygen saturation in water exceeding 100% were recorded in different sites of the water area and indirectly indicated the activation of the photosynthesis process in the phytoplankton community.

There is a dependence of the localization of spots of early spring phytoplankton development on the area of ice cover. In cold years (periods with positive ice cover anomalies), active spring phytoplankton bloom occurred late, in May. In years with negative ice cover anomalies, an outbreak of spring bloom was registered in April–May in the Barents Sea coastal waters, but the onset of this process could be observed already in the third decade of March. Against the backdrop of negative ice cover anomalies, we identified several epicenters of the onset of spring development: in coastal waters along the Murmansk coast; in the southeastern Barents Sea in Kolguyev waters, which are coastal in origin; and partly in Atlantic waters – in the areas affected by the coastal water mass. At the same time, the total productivity and absolute values of chlorophyll *a* concentrations in coastal waters were lower than during subsequent outbreaks of phytoplankton development in waters of another origin.

Monitoring of spring levels of chlorophyll *a* content in the Barents Sea allows to reveal the effect of increasing Atlantification of the sea on the spring successional cycle of phytoplankton. Precisely in spring, most of the annual phytoplankton biomass is formed, and the vector of further development during the year is determined. The increase in ice-free sea area observed since 1998 makes it possible to implement several scenarios for phytoplankton development in the Barents Sea and to cover most of the areas favorable for formation of spots of early spring phytoplankton bloom. In turn, the level of phytoplankton production established in spring can affect the productivity of all other links of the Barents Sea pelagic ecosystem.

The work was carried out within the framework of MMBI state research assignment “Structural and dynamic transformations of pelagic ecosystems of Arctic marine basins under conditions of technogenic and natural environmental changes.”

Acknowledgment. The authors are grateful to the staff of the Murmansk Marine Biological Institute of the Russian Academy of Sciences for data collecting and sampling under expeditionary conditions. The authors express their deep gratitude to the reviewers for their valuable comments and suggestions.

REFERENCES

1. Aksenov P. V., Ivanov V. V. “Atlantification” as a possible cause for reducing of the sea-ice cover in the Nansen Basin in winter. *Problemy Arktiki i Antarktiki*, 2018, vol. 64, no. 1, pp. 42–54. (in Russ.). <https://doi.org/10.30758/0555-2648-2018-64-1-42-54>
2. Alekseev G. V. Development and amplification of global warming in the Arctic. *Fundamental'naya i prikladnaya klimatologiya*, 2015, vol. 1, pp. 11–26. (in Russ.)
3. Kuznetsov L. L., Shoshina E. V. *Phytoplankton of the Barents Sea (Physiological and Structural Characteristics)*. Apatity : Izd-vo KNTs RAN, 2003, 308 p. (in Russ.)
4. Mamaev O. I. *Termokhalinnyi analiz vod Mirovogo okeana*. Leningrad : Gidrometeoizdat, 1987, 296 p. (in Russ.)
5. Ozhigin V. K., Ivshin V. A., Trofimov A. G., Karsakov A. L., Antsiferov M. Yu. *The Barents Sea Water: Structure, Circulation, Variability*. Murmansk : PINRO, 2016, 260 p. (in Russ.)
6. *Plankton morei Zapadnoi Arktiki* / G. G. Matishov (Ed.). Apatity : Murmanskii morskoi biologicheskii institut, 1997, 352 p. (in Russ.)
7. *Reisovyi otchet kompleksnoi ekspeditsii na NIS “Dal'nie Zelentsy” v Barentsevo more (10.03–14.04.2021)* / P. R. Makarevich (Ed.). Murmansk : MMBI, 2021, 99 p. (in Russ.)
8. *Rukovodstvo po khimicheskomy analizu morskikh i presnykh vod pri ekologicheskom monitoringe rybokhozyaistvennykh vodoemov i perspektivnykh dlya promysla raionov Mirovogo okeana*. Moscow : VNIRO, 2003, 202 p. (in Russ.)
9. *Khimiya okeana* : [in 2 vols]. Vol. 1: *Khimiya vod okeana*. Moscow : Nauka, 1979, 518 p. (Okeanologiya). (in Russ.)
10. Aminot A., Ray F. *Standard Procedure for the Determination of Chlorophyll a by Spectroscopic Methods*. Copenhagen, Denmark : International Council for the Exploration of the Sea, 2000, 17 p. (ICES Techniques in Marine Environmental Sciences).
11. Barber D. G., Lukovich J. V., Keogak J., Baryluk S., Fortier L., Henry G. H. R. The changing climate of the Arctic. *Arctic*, 2008, vol. 61, no. 5, suppl. 1, pp. 7–26. <https://doi.org/10.14430/arctic98>
12. *Biological Atlas of the Arctic Seas 2000: Plankton of the Barents and Kara Seas* / Murmansk Marine Biological Institute, Russia ; Ocean Climate Laboratory, NODC/NOAA, USA. URL: <https://www.nodc.noaa.gov/OC5/BARPLANK/start.html> [accessed: 20.03.2022].
13. Boitsov V. D., Karsakov A. L., Trofimov A. G. Atlantic water temperature and climate in the Barents Sea, 2000–2009. *ICES Journal of Marine Science*, 2012, vol. 69, iss. 5, pp. 833–840. <https://doi.org/10.1093/icesjms/fss075>
14. *Chemical Methods for Use in Marine Environment Monitoring*. Paris : UNESCO, 1983, 53 p. (Intergovernmental Oceanographic Commission Manuals and Guides ; 12). <https://doi.org/10.25607/OBP-1419>
15. Comiso J. C., Hall D. K. Climate trends in the Arctic as observed from space. *Climate Change*, 2014, vol. 5, iss. 3, pp. 389–409. <https://doi.org/10.1002/wcc.277>
16. *Determination of Photosynthetic Pigments in Seawater*. Paris : UNESCO, 1966, 69 p. (Monographs on Oceanographic Methodology ; vol. 1).

17. Dong K., Kvile Ø. K., Stenseth N. C., Stige L. C. Associations among temperature, sea ice and phytoplankton bloom dynamics in the Barents Sea. *Marine Ecology Progress Series*, 2020, vol. 635, pp. 25–36. <https://doi.org/10.3354/meps13218>
18. Eilertsen H.-C., Hansen G. A., Svendsen H., Hegseth E. N. Onset of the spring phytoplankton bloom in the Barents Sea: Influence of changing light regime and other environmental factors. *Proceedings of SPIE : Underwater Light Measurements*, 1993, vol. 2048, pp. 20–32. <https://doi.org/10.1117/12.165507>
19. *EOSDIS Worldview* : [site]. URL: <https://worldview.earthdata.nasa.gov> [accessed: 25.03.2022].
20. Fujiwara A., Hirawake T., Suzuki K., Imai I., Saitoh S.-I. Timing of sea ice retreat can alter phytoplankton community structure in the western Arctic Ocean. *Biogeosciences*, 2014, vol. 11, iss. 7, pp. 1705–1716. <https://doi.org/10.5194/bg-11-1705-2014>
21. Johannessen O. M., Alexandrov V. Yu., Frolov I. Ye., Sandven S., Pettersson L. H., Bobylev L. P., Kloster K., Smirnov V. G., Mironov Ye. U., Babich N. G. *Remote Sensing of Sea Ice in the Northern Sea Route. Studies and Applications*. Chichester, UK : Praxis Publishing, 2007, 472 p. <https://doi.org/10.1007/978-3-540-48840-8>
22. Kahru M., Brotas V., Manzano-Sarabia M., Mitchell B. G. Are phytoplankton blooms occurring earlier in the Arctic? *Global Change Biology*, 2011, vol. 17, iss. 4, pp. 1733–1739. <https://doi.org/10.1111/j.1365-2486.2010.02312.x>
23. Kogeler J., Rey F. Ocean colour and the spatial and seasonal distribution of phytoplankton in the Barents Sea. *International Journal of Remote Sensing*, 1999, vol. 20, iss. 7, pp. 1303–1318. <https://doi.org/10.1080/014311699212740>
24. Lewis K. M., van Dijken G. L., Arrigo K. R. Changes in phytoplankton concentration now drive increased Arctic Ocean primary production. *Science*, 2020, vol. 369, no. 6500, pp. 198–202. <https://doi.org/10.1126/science.aay8380>
25. Makarevich P., Druzhkova E., Larionov V. Primary producers of the Barents Sea. In: *Diversity of Ecosystems* / A. Mahamane (Ed.). London, UK : InTech Open, 2012, pp. 367–393. <https://doi.org/10.5772/37512>
26. Makarevich P. R., Vodopianova V. V., Bula-vina A. S. Dynamics of the spatial chlorophyll-*a* distribution at the Polar Front in the marginal ice zone of the Barents Sea during Spring. *Water*, 2022, vol. 14, iss. 1, art. no. 101 (23 p.). <https://doi.org/10.3390/w14010101>
27. Makarevich P. R., Vodopianova V. V., Bula-vina A. S., Vashchenko P. S., Ishkulova T. G. Features of the distribution of chlorophyll-*a* concentration along the western coast of the Novaya Zemlya archipelago in spring. *Water*, 2021, vol. 13, iss. 24, art. no. 3648 (14 p.). <https://doi.org/10.3390/w13243648>
28. *Methods of Seawater Analysis* / K. Grasshoff, K. Kremling, M. Ehrhardt (Eds). Weinheim ; New York ; Chichester ; Brisbane ; Toronto : Wiley-VCH, 1999, 600 p. <https://doi.org/10.1002/9783527613984>
29. Namyatov A. A. $\delta^{18}\text{O}$ as a tracer of the main regularities of water mass mixing and transformation in the Barents, Kara, and Laptev seas. *Journal of Hydrology*, 2021a, vol. 593, art. no. 125813 (18 p.). <https://doi.org/10.1016/j.jhydrol.2020.125813>
30. Namyatov A. A. The relationship between geophysical processes and changes in the composition of the seawater of the Barents Sea in the course of their climatic variability. *ESS Open Archive*, 2021b, 38 p. <https://doi.org/10.1002/essoar.10507159.1>
31. *Ocean Color NASA* : [site]. URL: <https://oceancolor.gsfc.nasa.gov/l3/> [accessed: 25.03.2022].
32. Oziel L., Neukermans G., Ardyna M., Lancelot C., Tison J.-L., Wassmann P., Sirven J., Ruiz-Pino D., Gascard J.-C. Role for Atlantic inflows and sea ice loss on shifting phytoplankton blooms in the Barents Sea. *Journal of Geophysical Research Oceans*, 2017, vol. 122, iss. 6, pp. 5121–5139. <https://doi.org/10.1002/2016JC012582>

33. Park J., Kug J., Bader J., Rolph R., Kwon M. Amplified Arctic warming by phytoplankton under greenhouse warming. *The Proceedings of the National Academy of Sciences of the United States of America*, 2015, vol. 112, no. 19, pp. 5921–5926. <https://doi.org/10.1073/pnas.1416884112>
34. Qu B., Gabric A. J., Matrai P. A. The satellite-derived distribution of chlorophyll-*a* and its relation to ice cover, radiation and sea surface temperature in the Barents Sea. *Polar Biology*, 2006, vol. 29, iss. 3, pp. 196–210. <https://doi.org/10.1007/s00300-005-0040-2>
35. Reigstad M., Wassmann P., Riser C., Øygarden S., Rey F. Variations in hydrography, nutrients and chlorophyll *a* in the marginal ice-zone and the central Barents Sea. *Journal of Marine Systems*, 2002, vol. 38, iss. 1–2, pp. 9–29. [https://doi.org/10.1016/S0924-7963\(02\)00167-7](https://doi.org/10.1016/S0924-7963(02)00167-7)
36. Shu Q., Wang Q., Song Z., Qiao F.-L. The poleward enhanced Arctic Ocean cooling machine in a warming climate. *Nature Communications*, 2021, vol. 12, art. no. 2966 (9 p.). <https://doi.org/10.1038/s41467-021-23321-7>
37. Signorini S. R., McClain C. R. Environmental factors controlling the Barents Sea spring–summer phytoplankton blooms. *Geophysical Research Letters*, 2009, vol. 36, iss. 10, art. no. L10604 (5 p.). <https://doi.org/10.1029/2009GL037695>
38. Vodopyanova V. V., Vashchenko P. S., Bulavina A. S. Monitoring of chlorophyll-*a* concentration in the ice edge zone of the Barents Sea in 2017–2018. *IOP Conference Series: Earth and Environmental Science*, 2019, vol. 263, art. no. 012005 (8 p.). <https://doi.org/10.1088/1755-1315/263/1/012005>
39. Wang Y., Xiang P., Kang J.-H., Ye Y.-Y., Lin G.-M., Yang Q.-L., Lin M. Microphytoplankton community structure in the western Arctic Ocean: Surface layer variability of geographic and temporal considerations in summer. *Hydrobiologia*, 2018, vol. 811, iss. 1, pp. 295–312. <https://doi.org/10.1007/s10750-017-3500-0>
40. Wassmann P. Arctic marine ecosystems in an era of rapid climate change. *Progress in Oceanography*, 2011, vol. 90, iss. 1–4, pp. 1–17. <https://doi.org/10.1016/j.pocean.2011.02.002>
41. Wassmann P., Reigstad M., Haug T., Rudels B., Carroll M. L., Hop H., Gabrielsen G. W., Falk-Petersen S., Denisenko S. G., Arashkevich E., Slagstad D., Pavlova O. Food webs and carbon flux in the Barents Sea. *Progress in Oceanography*, 2006, vol. 71, iss. 2–4, pp. 232–287. <https://doi.org/10.1016/j.pocean.2006.10.003>
42. Zhichkin A. P. Peculiarities of interannual and seasonal variations of the Barents Sea ice coverage anomalies. *Russian Meteorology and Hydrology*, 2015, vol. 40, iss. 5, pp. 319–326. <https://doi.org/10.3103/S1068373915050052>

**ЛОКАЛИЗАЦИЯ
ЦЕНТРОВ РАННЕВЕСЕННЕГО ЦВЕТЕНИЯ ФИТОПЛАНКТОНА
В ПЕЛАГИАЛИ БАРЕНЦЕВА МОРЯ**

**П. Р. Макаревич, В. В. Водопьянова, А. С. Булавина, П. С. Ващенко,
А. А. Намятов, И. А. Пастухов**

Мурманский морской биологический институт РАН, Мурманск, Российская Федерация

E-mail: makarevich@mmbi.info

«Атлантификация» Баренцева моря приводит к уменьшению площади ледяного покрова и увеличению периода открытой воды. Этот процесс влияет на всю пелагическую экосистему Баренцева моря, где основная часть годовой первичной продукции фитопланктона формируется во время весеннего цветения. Концентрация хлорофилла *a* отражает изменения биомассы фитопланктона и может служить показателем его продукционных характеристик. Весной 2021 г.

на свободной ото льда акватории Баренцева моря были исследованы гидрологические характеристики водных масс и особенности распределения концентрации хлорофилла *a* и биогенных элементов. Этот год характеризовался отрицательными аномалиями ледовитости. Расположение и протяжённость зон повышенных (или пониженных) концентраций хлорофилла *a* совпали с чередованием водных масс. Были выявлены разобщённые центры ранневесеннего цветения — в прибрежных водах на юго-востоке и юго-западе Баренцева моря. В конце марта — начале апреля максимальные концентрации хлорофилла *a* в прибрежных водах достигали значений около $1 \text{ мг} \cdot \text{м}^{-3}$. В это же время в баренцевоморских и арктических водах максимум концентраций не превышал $0,20 \text{ мг} \cdot \text{м}^{-3}$. Распределение биогенных элементов соответствовало таковому в зимний период, когда вертикальные градиенты этих параметров ещё не сформировались. Величины насыщения вод кислородом выше уровня 100 % (в разной степени на всей исследованной акватории) характеризовали активизацию процесса фотосинтеза в фитопланктонном сообществе. Анализ многолетних данных свидетельствует, что последующее активное весеннее цветение фитопланктона в годы с отрицательными аномалиями ледовитости наступало уже во второй-третьей декаде апреля в различных типах водных масс Баренцева моря — в арктических, атлантических и прибрежных водах (максимум концентраций хлорофилла *a* достигал $5,69 \text{ мг} \cdot \text{м}^{-3}$ в арктических водах). В мае процесс весеннего цветения охватывал уже всю акваторию Баренцева моря и все типы водных масс (максимум концентраций хлорофилла *a* — $5,08\text{--}5,77 \text{ мг} \cdot \text{м}^{-3}$). В аномально холодные годы низкое положение ледовой кромки в марте — апреле ограничивало возможную область развития фитопланктона, а активная фаза его цветения (согласно спутниковым данным) наступала гораздо позже, в мае. «Атлантификация» Баренцева моря способствует распространению весеннего цветения фитопланктона на большей акватории, что может влиять на годовые продукционные показатели всей пелагиали.

Ключевые слова: хлорофилл *a*, весеннее цветение, водные массы, «атлантификация», Баренцево море

UDC 593.161.42:57.086.83

**EXPERIENCE OF GROWING THE MICROALGA
TISOCHRYSIS LUTEA (HAPTOPHYTA)
UNDER CONDITIONS OF A LABFORS BIOREACTOR
FOR THE PRODUCTION OF CAROTENOIDS AND NEUTRAL LIPIDS**

© 2024 **Zh. Markina, A. Zinov, and T. Orlova**

A. V. Zhirmunsky National Scientific Center of Marine Biology, FEB RAS, Vladivostok, Russian Federation

E-mail: zhannav@mail.ru

Received by the Editor 08.07.2022; after reviewing 06.09.2022;
accepted for publication 09.10.2023; published online 22.03.2024.

The results of the experiment on the use of a Labfors 5 Lux LED flat panel bioreactor (Infors HT, Switzerland) for *Tisochrysis lutea* (Haptophyta) cultivation are presented. During the three-week study, growth and size structure of the microalga population were assessed, and the content of chlorophyll *a*, carotenoids, and neutral lipids was estimated. The highest cell abundance, 5.3×10^4 cells·mL⁻¹, was recorded at the end of the experiment, on the 21st day. An increase in the proportion of 4–6- μ m cells was registered on the 11th day. The maximum accumulation of carotenoids occurred on the 18th day (3.3 mg·L⁻¹), and neutral lipids (Nile Red fluorescence was of 5.3×10^6), on the 14th–21st day. As revealed, Labfors 5 Lux LED flat panel bioreactor can be successfully used for cultivation of the microalga *T. lutea*.

Keywords: *Tisochrysis lutea*, biotechnology, bioreactor, carotenoids, neutral lipids

For a long time, *Tisochrysis lutea* Bendif & Probert, 2013 (Haptophyta) is widely used in algal biotechnology as a food item for larvae of invertebrates [Alkhamis, Qin, 2016; Araújo et al., 2020]. This species is the most promising producer of the prevailing carotenoid, fucoxanthin (up to 98% of the total carotenoids content) [Mohamadnia et al., 2021]. Moreover, *T. lutea* is an important producer of neutral lipids. The development of conditions for cultivation in bioreactors is the basis for biotechnological processes, and this is especially relevant for *T. lutea* [Mohamadnia et al., 2021].

For biotechnology purposes, this species is cultivated in flasks [Mohamadnia et al., 2020], but more often, *T. lutea* is cultivated in bioreactors [Falinski et al., 2018; Gao et al., 2020; Ippoliti et al., 2016; Leal et al., 2020].

To date, various modifications of bioreactors have been developed. Panel bioreactors are among the most convenient models for microalgae cultivation. Their advantages, which together ensure intensive growth of microalgae, are good mixing of an algal suspension, large area of illuminated surface, and low accumulation of oxygen in the medium [Guedes, Malcata, 2011; Tan et al., 2020].

Not only fluorescent lamps, but also light-emitting diodes (LED) are used as a light source. The benefits of LED are low energy consumption, very low heat generation during work, stable luminous flux, long lifespan, and constant luminous flux parameters over time with regular on/off cycles [Posten, 2009].

The aim of the work was to study the dynamics of population growth and the content of carotenoids and neutral lipids in *Tisochrysis lutea*, strain MBRU_Tiso-08, in the flat panel bioreactor Labfors 5 Lux LED (Infors HT, Switzerland), which was used for microalgae cultivation for the first time.

The main indicators determined in the research were cell abundance and size structure of *T. lutea* population, as well as the content of carotenoids and neutral lipids in its biomass as substances of certain interest for biotechnology. The values of optical density obtained by various methods served as additional indicators proposed for rapid assessment of *T. lutea* abundance. To better describe the physiological processes of the microalga, chlorophyll *a* was analyzed as well.

MATERIAL AND METHODS

The object of the study was the culture of the unicellular alga *T. lutea* (Haptophyta) – strain MBRU_Tiso-08 from the Marine Biobank resource collection at A. V. Zhirmunsky National Scientific Center of Marine Biology, Far Eastern Branch of the Russian Academy of Sciences (<http://marbank.dvo.ru/>). The alga was cultivated in the medium *f* [Guillard, Ryther, 1962] prepared on filtered and sterilized seawater with a salinity of 32‰ in Labfors 5 running in fed-batch mode. Seawater temperature was +20 °C. Light intensity was 50 $\mu\text{mol}\cdot\text{m}^{-2}\cdot\text{s}^{-1}$ (a LED panel served as a light source) within the range of photosynthetically active radiation. The light–dark period was 12 h : 12 h (light : dark). Air supply was 0.2 L·min⁻¹. The suspension layer in the panel was 45 mm thick. The working flask of Labfors 5 has the volume of 1.8 L and is made of carbonate glass. Out of all materials for algae cultivation, this one has the highest light permeability (95%) and high chemical resistance. It can be sterilized. Carbonate glass is inextensible, unlike polyethylene and polypropylene. It does not transmit ultraviolet radiation, like polycarbonate glass [Guedes, Malcata, 2011].

As an inoculum, a culture at the exponential growth stage was used. The initial concentration of the microalga cells in the experiment was 0.75×10^6 cells·mL⁻¹. The experiment lasted for 21 days.

A CytoFLEX flow cytometer (Beckman Coulter, the USA) was used to determine the abundance of cells and their diameter, as well as the content of neutral lipids. For analysis, 10,000 events (recorded in the particle sample) were registered during each measurement. Algal cells were selected from the total number of events recorded by the flow cytometer in accordance with chlorophyll *a* fluorescence [Hyka et al., 2013] determined on PC 5.5 channel. Cell diameter was established using calibration beads (Molecular Probes, the USA) based on direct light scattering.

Optical density (OD₇₅₀) was determined on a Spark 10M multimode microplate reader (Tecan).

In the flask of Labfors 5, optical density was established using a Dencytee sensor (Hamilton). It provides real-time measurements of the optical density of cell suspensions.

Chlorophyll *a* concentration and the total carotenoids content were determined by a standard technique of their extraction in acetone, followed by measurement of the optical density on a Spark 10M multimode microplate reader. Pigment concentrations were calculated in accordance with standard formulas [Jeffrey, Humphrey, 1975].

The content of neutral lipids was determined by the fluorescence of Nile Red fluorochrome (N3013-100MG, Sigma-Aldrich) at a concentration of 1 $\mu\text{g}\cdot\text{mL}^{-1}$; staining was carried out for 15 min at room temperature in the dark. The excitation wavelength was of 488 nm, and the emission wavelength was of 580 nm. Determination of lipid content by flow cytometry is characterized by a high speed. Moreover, its data are consistent with data obtained applying other methods which was confirmed on various microalgae [Alemán-Nava et al., 2016].

RESULTS AND DISCUSSION

The abundance of *T. lutea* cells increased with rising exposure time until the end of the experiment (Fig. 1). Cell abundance correlated with optical density data obtained by spectrophotometric method (OD₇₅₀) and by using a bioreactor sensor and analyzing changes in the turbidity of the cell suspension (see Fig. 1). Cells of 4–6 µm prevailed in the suspension, especially from the 11th day. This fact must be taken into account when planning the diet for invertebrate larvae at different stages of their development.

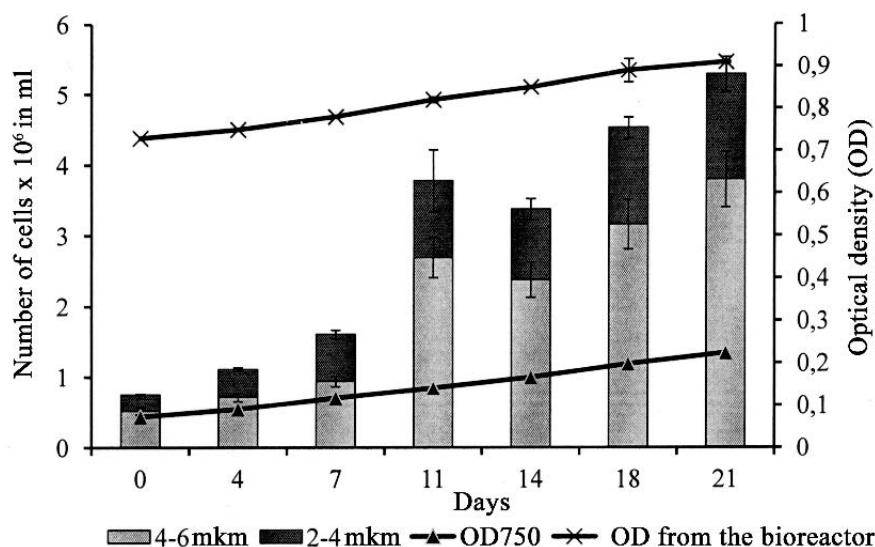


Fig. 1. Cell abundance ($\times 10^6$ cells·mL⁻¹) and optical density (μm) of *Tisochrysis lutea* culture

Similar growth dynamics was described for *T. lutea* CCAP 927/14: for this strain, an increase in cell size was also recorded. The authors explain this fact by higher rates of cell division at the beginning of the experiment [Costa et al., 2017]. In the work [Rasdi, Qin, 2015], it is noted that *Tisochrysis* culture (without specifying the strain) entered the stationary growth stage on the 6th day of cultivation. *T. lutea* from the Roscoff Culture Collection (France) entered the stationary growth stage on the 7th day of the experiment; the alga entered the dying stage on the 21st day [Gnouma et al., 2017].

In a cylindrical reactor, the abundance of *T. lutea* cells, against the backdrop of the initial concentration of 0.4×10^6 cells·mL⁻¹, accounted for only 0.45×10^6 cells·mL⁻¹ after 14 days [Falinski et al., 2018]. In a 500-L bioreactor, the abundance of cells reached its maximum, 6.92×10^6 cells·mL⁻¹, after 12 days of experiment, with the initial value of 0.2×10^6 cells·mL⁻¹ [Leal et al., 2020]. For *T. lutea* cultivated in flasks, cell abundance was higher than that for the microalga in reactors and amounted to 4.3×10^8 cells·mL⁻¹ after 4 days [Mohamadnia et al., 2020], against the backdrop of the initial concentration of 1.2×10^7 cells·mL⁻¹. In our experiment, cell abundance reached 1.1×10^6 cells·mL⁻¹ after 4 days, with the initial value of 0.75×10^6 cells·mL⁻¹. However, bioreactors allow growing microalgae on a larger scale, and this is an important advantage.

Over 14 days, the concentration of photosynthetic pigments in *T. lutea* rose slightly (Fig. 2). On the 18th day, it sharply increased, and carotenoids content became higher than chlorophyll *a* concentration.

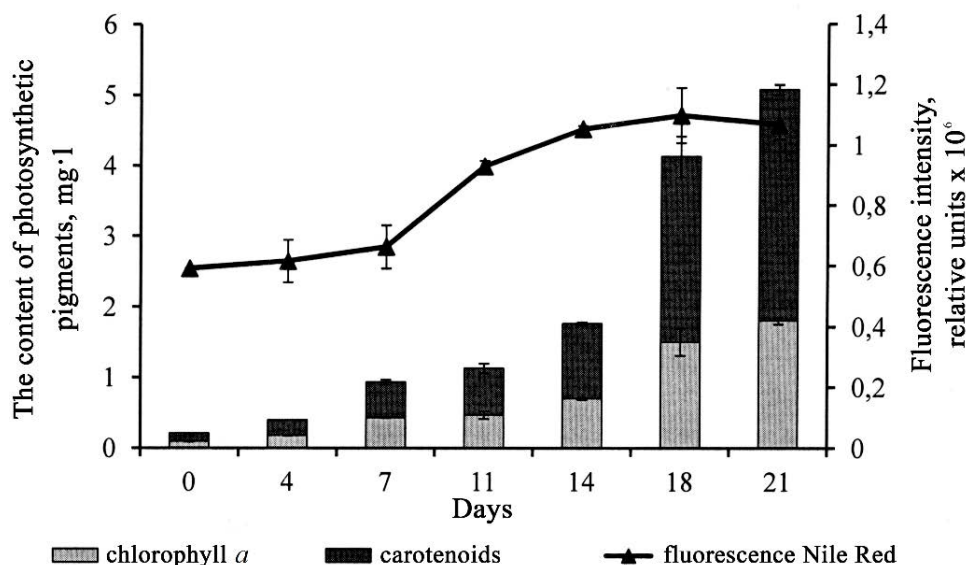


Fig. 2. Content of photosynthetic pigments and neutral lipids (Nile Red fluorescence) in *Tisochrysis lutea*

A decrease in chlorophyll *a* concentration is associated with a drop in nitrogen content during cultivation which results in a decline in the abundance of enzymes required for chlorophyll synthesis in algae cells [Costa et al., 2017]. By the 21st day, the content of pigments continued to increase but less intensely. The content of photosynthetic pigments depends on conditions of the microalga cultivation and characteristics of its physiology. Thus, in *T. lutea* CCMP 1324 cultivated under the same conditions as in this work, in a mixotrophic culture, 4,500 µg of chlorophyll *a* was recorded *per* 1 L on the 16th day of the experiment; in a heterotrophic culture, the value was 5,200 µg·L⁻¹ [Hu et al., 2018].

Until the 7th day, the content of neutral lipids increased slightly; from the 7th to 14th day, the value rose significantly; and then, it remained at the same level (see Fig. 2). An increase in the content of neutral lipids with the age of the culture is described in other works as well [Costa et al., 2017; Huang et al., 2019]. Interestingly, in most algae, reserve neutral lipids are triacylglycerides, while in *T. lutea*, along with other representatives of the family Isochrysidaceae, those are alkenones [Costa et al., 2017].

The selection of research methods is the cornerstone of scientific work; its key criteria are accuracy and ensuring the reliability of the results obtained. When assessing the state of a microalgal culture, the speed of analysis is added to the listed criteria in routine biotechnological processes. Our data show that optical density indicators can be used to analyze the dynamics of *T. lutea* population growth. Moreover, it was revealed for *Chlorella vulgaris* Beijerinck, 1890 as follows: at the lag stage and exponential growth stage, OD₇₅₀ correlates with cell abundance established by flow cytometry and by direct counting under a light microscope in a counting chamber; however, light microscopy is more accurate [Chioccioli et al., 2014].

The data obtained showed that a Labfors 5 Lux LED flat panel bioreactor can be successfully used for cultivation of the microalga *Tisochrysis lutea*.

The work was carried out within the framework of NSCMB FEB RAS state research assignment "Dynamics of marine ecosystems, adaptation of marine organisms and communities to changes in the environment" (No. 121082600038-3) and with the financial support of the Russian Science Foundation grant No. 21-74-30004.

REFERENCES

1. Alemán-Nava G. S., Cuellar-Bermudez S. P., Cuaresma M., Bosma R., Muylaert K., Ritmann B. E., Parra R. How to use Nile Red, a selective fluorescent stain for microalgal neutral lipids. *Journal of Microbiological Methods*, 2016, vol. 128, pp. 74–79. <https://doi.org/10.1016/j.mimet.2016.07.011>
2. Alkhamis Y., Qin J. G. Comparison of pigment and proximate compositions of *Tisochrysis lutea* in phototrophic and mixotrophic cultures. *Journal of Applied Phycology*, 2016, vol. 28, iss. 1, pp. 35–42. <https://doi.org/10.1007/s10811-015-0599-0>
3. Araújo R., Vázquez Calderón F., Sánchez López J., Azevedo I. C., Bruhn A., Fluch S., Garcia Tasende M., Ghaderiardakani F., Ilmjärv T., Laurans M., Mac Monagail M., Mangini S., Peteiro C., Rebours C., Stefansson T., Ullmann J. Current status of the algae production industry in Europe: An emerging sector of the blue bioeconomy. *Frontiers in Marine Science*, 2020, vol. 7, art no. 626389 (24 p.). <https://doi.org/10.3389/fmars.2020.626389>
4. Gao F., Teles I., Wijffels R. H., Barbosa M. J. Process optimization of fucoxanthin production with *Tisochrysis lutea*. *Bioresource Technology*, 2020, vol. 315, art. no. 123894 (8 p.). <https://doi.org/10.1016/j.biortech.2020.123894>
5. Guedes A. C., Malcata F. Bioreactors for microalgae: A review of designs, features and applications. In: *Bioreactors: Design, Properties and Applications* / P. G. Antolli, Z. Liu (Eds). New-York : Nova Scientist Publishers, Inc., 2011, pp. 1–52.
6. Costa F. D., Le Grand F., Quéré C., Bougaran G., Cadoret J. P., Robert R., Soudant P. Effects of growth phase and nitrogen limitation on biochemical composition of two strains of *Tisochrysis lutea*. *Algal Research–Biomass, Biofuels and Bioproducts*, 2017, vol. 27, pp. 177–189. <https://doi.org/10.1016/j.algal.2017.09.003>
7. Chioccioli M., Hankamer B., Ross I. L. Flow cytometry pulse width data enables rapid and sensitive estimation of biomass dry weight in the microalgae *Chlamydomonas reinhardtii* and *Chlorella vulgaris*. *PLoS One*, 2014, vol. 9, iss. 5, art. no. e97269 (12 p.). <https://doi.org/10.1371/journal.pone.0097269>
8. Gnouma A., Sadovskaya I., Souissi A., Sebai K., Medhioub A., Grard T., Souissi S. Changes in fatty acids profile, monosaccharide profile and protein content during batch growth of *Isochrysis galbana* (T.iso). *Aquaculture Research*, 2017, vol. 48, iss. 9, pp. 4982–4990. <https://doi.org/10.1111/are.13316>
9. Guillard R. R. L., Ryther J. H. Studies of marine planktonic diatoms: I. *Cyclotella nana* Hustedt, and *Detonula confervacea* (Cleve) Gran. *Canadian Journal of Microbiology*, 1962, vol. 8, no. 2, pp. 229–239. <https://doi.org/10.1139/m62-029>
10. Falinski K. A., Timmons M. B., Callan C., Laidley C. Response of *Tisochrysis lutea* [Prymnesiophycidae] to aeration conditions in a bench-scale photobioreactor. *Journal of Applied Phycology*, 2018, vol. 30, iss. 4, pp. 2203–2214. <https://doi.org/10.1007/s10811-018-1453-y>
11. Hyka P., Lickova S., Přibyl P., Melzoch K., Kovar K. Flow cytometry for development of biotechnological processes with microalgae. *Biotechnology Advances*, 2013, vol. 31, iss. 1, pp. 2–16. <https://doi.org/10.1016/j.biotechadv.2012.04.007>
12. Hu H., Ma L. L., Shen X. F., Wang H. F., Zeng R. J. Effect of cultivation mode on the production of docosahexaenoic acid by *Tisochrysis lutea*. *AMB Express*, 2018, vol. 8, art. no. 50 (12 p.). <https://doi.org/10.1186/s13568-018-0580-9>
13. Huang B., Marchand J., Thiriet-Rupert S., Carrier G., Saint-Jean B., Lukomska E., Moreau B., Morant-Manceau A., Bougaran G., Mimouni V. Betaine lipid and neutral lipid production under nitrogen or phosphorus limitation in the marine microalga *Tisochrysis lutea* (Haptophyta). *Algal Research–Biomass, Biofuels and Bioproducts*, 2019, vol. 40, art. no. 101506 (15 p.). <https://doi.org/10.1016/j.algal.2019.101506>
14. Ippoliti D., González A., Martín I., Sevilla J. M. F., Pistocchi R., Acien F. G. Outdoor production of *Tisochrysis lutea* in pilot-scale tubular photobioreactors. *Journal of Applied*

- Phycology*, 2016, vol. 28, iss. 6, pp. 3159–3166. <https://doi.org/10.1007/s10811-016-0856-x>
15. Jeffrey S. W., Humphrey G. F. New spectrophotometric equations for determining chlorophyll *a*, *b*, *c*₁ and *c*₂ in higher plants, algae and natural phytoplankton. *Biochemie und Physiologie der Pflanzen*, 1975, vol. 167, iss. 2, pp. 191–194. [https://doi.org/10.1016/S0015-3796\(17\)30778-3](https://doi.org/10.1016/S0015-3796(17)30778-3)
 16. Leal E., de Beyer L., O'Connor W., Dove M., Ralph P. J., Pernice M. Production optimization of *Tisochrysis lutea* as a live feed for juvenile Sydney rock oysters, *Saccostrea glomerata*, using large-scale photobioreactors. *Aquaculture*, 2020, vol. 533, art. no. 736077 (9 p.). <https://doi.org/10.1016/j.aquaculture.2020.736077>
 17. Mohamadnia S., Tavakoli O., Faramarzi M. A. Enhancing production of fucoxanthin by the optimization of culture media of the microalga *Tisochrysis lutea*. *Aquaculture*, 2021, vol. 533, art. no. 736074 (10 p.). <https://doi.org/10.1016/j.aquaculture.2020.736074>
 18. Mohamadnia S., Tavakoli O., Faramarzi M. A., Shamsollahi Z. Production of fucoxanthin by the microalga *Tisochrysis lutea*: A review of recent developments. *Aquaculture*, 2020, vol. 516, art. no. 734637 (10 p.). <https://doi.org/10.1016/j.aquaculture.2019.734637>
 19. Posten C. Design principles of photo-bioreactors for cultivation of microalgae. *Engineering in Life Sciences*, 2009, vol. 9, iss. 3, pp. 165–177. <https://doi.org/10.1002/elsc.200900003>
 20. Rasdi N. W., Qin J. G. Effect of N:P ratio on growth and chemical composition of *Nannochloropsis oculata* and *Tisochrysis lutea*. *Journal of Applied Phycology*, 2015, vol. 27, iss. 6, pp. 2221–2230. <https://doi.org/10.1007/s10811-014-0495-z>
 21. Tan J. S., Lee S. Y., Chew K. W., Lam M. K., Lim J. W., Ho S. H., Show P. L. A review on microalgae cultivation and harvesting, and their biomass extraction processing using ionic liquids. *Bioengineered*, 2020, vol. 11, iss. 1, pp. 116–129. <https://doi.org/10.1080/21655979.2020.1711626>

**ОПЫТ ВЫРАЩИВАНИЯ МИКРОВОДОРОСЛИ
TISOCHRYSIS LUTEA (НАПТОРФУТА)
В УСЛОВИЯХ БИОРЕАКТОРА LABFORS
ДЛЯ ПРОДУЦИРОВАНИЯ КАРОТИНОИДОВ И НЕЙТРАЛЬНЫХ ЛИПИДОВ**

Ж. В. Маркина, А. А. Зинов, Т. Ю. Орлова

Национальный научный центр морской биологии имени А. В. Жирмунского ДВО РАН,

Владивосток, Российская Федерация

E-mail: zhannav@mail.ru

Приведены результаты эксперимента по использованию биореактора панельного типа Labfors 5 Lux LED flat panel (Infors HT, Швейцария) для культивирования *Tisochrysis lutea* (Haptophyta). В ходе трёхнедельного исследования оценивали рост и размерную структуру популяции микроводоросли, содержание хлорофилла *a*, каротиноидов и нейтральных липидов. Максимальная численность клеток, $5,3 \times 10^4$ кл.·мл⁻¹, зафиксирована к концу эксперимента, на 21-е сутки. Увеличение доли клеток размером 4–6 мкм регистрировали на 11-е сутки опыта. Наибольшее накопление каротиноидов происходило на 18-е сутки эксперимента (3,3 мг·л⁻¹), нейтральных липидов (флуоресценция Nile Red составляла $5,3 \times 10^6$) — на 14–21-е сутки. Выявлено, что биореактор панельного типа Labfors 5 может быть успешно использован для культивирования микроводоросли *T. lutea*.

Ключевые слова: *Tisochrysis lutea*, биотехнология, биореактор, каротиноиды, нейтральные липиды

UDC 595.132(262.5)

***STYLOTHERISTUS PARAMUTILUS* SP. NOV. (NEMATODA: XYALIDAE),
A NEW NEMATODE SPECIES FROM THE BLACK SEA**

© 2024 **T. Revkova and N. Sergeeva**

A. O. Kovalevsky Institute of Biology of the Southern Seas of RAS, Sevastopol, Russian Federation
E-mail: alinka8314@gmail.com

Received by the Editor 17.07.2023; after reviewing 20.09.2023;
accepted for publication 09.10.2023; published online 22.03.2024.

Stylotheristus paramutilus sp. nov. from bottom sediments sampled in shallow-water and deep-sea habitats in the Black Sea is described and illustrated. The new species is characterized by well-developed lip region; 12 setiform cephalic sensilla in female and 16 in male; cervical setae present; spicules 0.6–0.9 anal body diameters long and expanded proximally; gubernaculum plate-like slightly curved; conico-cylindrical tail of 4.5–5.8 anal body diameters (except for one male with it equal to 12.9 anal body diameters); and 3 terminal setae. The present study provides the first *Stylotheristus* species record in the Black Sea. *S. paramutilus* sp. nov. is characterized by a wide spatial and bathymetrical (2–250-m depths) distribution in the Crimea region and the Istanbul Strait's (Bosphorus) outlet area of the Black Sea. However, in future, molecular analysis is required to confirm the identity of these specimens from different Black Sea habitats.

Keywords: Monhysterida, free-living marine nematodes, taxonomy, distribution, deep-sea, shallow-water

Free-living nematodes are among the most numerous and widespread multicellular organisms in the World Ocean. The study of meiobenthos in various areas of the Black Sea provided extensive data on the taxonomic diversity of free-living nematodes. In total, the species richness of the nematode fauna of the entire Black Sea is about 350 species and morphotypes identified only down to a genus or family level. In the region of Turkey alone, the nematode fauna includes 255 species [personal communication of PhD Derya Ürkmez]; for the Crimea region, about 230 species of nematodes are known [Sergeeva, 2003; Revkova, unpublished data].

The family Xyalidae includes 50 genera [Nemys, 2023; Venekey et al., 2014]. Out of them, 7 genera are registered in the Black Sea: *Valvaelaimus* Lorenzen, 1977, *Theristus* Bastian, 1865, *Daptonema* Cobb, 1920, *Steineria* Micoletzky, 1922, *Paramonohystera* Steiner, 1916, *Cobbia* de Man, 1907, and *Amphimonhystera* Allgén, 1929 [Mureşan, 2012, 2014; Revkova, 2015; Sergeeva, 2003; Sergeeva et al., 2021; Shnyukov, Yanko-Hombach, 2020; Vorobyova, Kulakova, 2009; Yanko et al., 2017].

Representatives of the genus *Stylotheristus* (the family Xyalidae) are widely distributed in the World Ocean: in the North and Mediterranean seas, in the Pacific, Atlantic, and Indian oceans [Nemys, 2023; OBIS, 2023], and in the Sea of Japan [our unpublished data]. Most of them were identified only down to a genus level. According to Nemys database [2023], two valid *Stylotheristus* species are known: *S. mutilus* described from the depth of 27–28 m in the North Sea and *S. multipapillatus* described from the depth of 5 m on the coast of Portugal.

In the present study, we provide a taxonomic description, illustrations, and data on distribution of a new *Stylotheristus* species for the Black Sea.

MATERIAL AND METHODS

The material was sampled in different years in the coastal and deep-sea areas of the Black Sea (Fig. 1, Table 1).

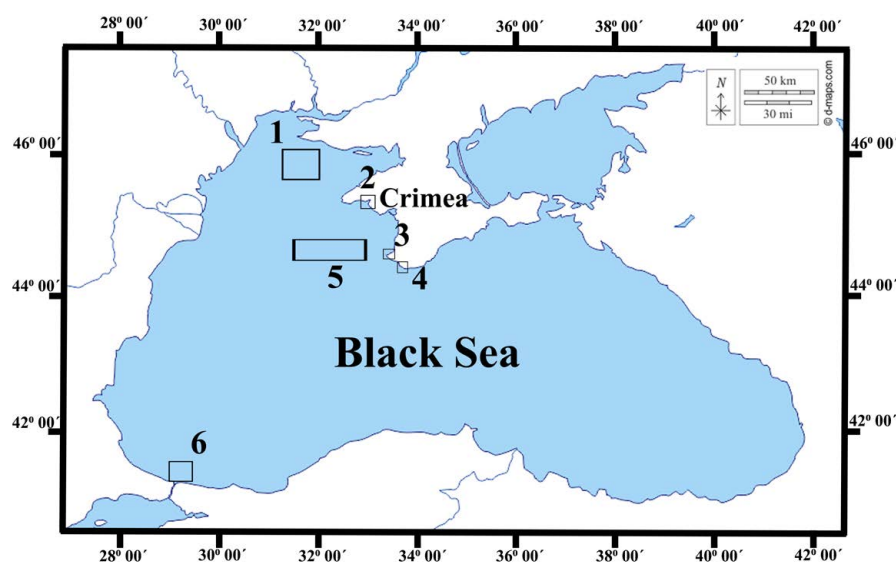


Fig. 1. The study areas where *Stylotheristus paramutilus* sp. nov. nematodes were found: 1, the Northwestern Crimea, the Zernov's *Phyllophora* Field (2010); 2, the Donuzlav Bay (2019); 3, the Kruglaya (Omega) Bay (2010); 4, the Laspi Bay (2017); 5, the Southwestern Crimea (2010); 6, the Istanbul Strait's (Bosphorus) outlet area (the Black Sea) (2009 and 2010)

To study the meiobenthos, in the coastal areas of the Crimea, the Kruglaya (Omega), Donuzlav, and Laspi bays, material was sampled at various depths using push cores (sample area of 18.1 cm²; height of 5 cm) at each station by a scuba diver. In the Kruglaya Bay, material was sampled at 1 station in different seasons in 2009–2010 [Zaika et al., 2011]; in the Donuzlav Bay, at 10 stations in its southern area in 2019 [Revkov et al., 2021]; and in the Laspi Bay, at 19 benthic stations in 2017 [Sergeeva et al., 2023]. To analyze meiofauna on the Zernov's *Phyllophora* Field, 18 sediment cores were taken by subcoring the sediment sampled with an Okean-25 bottom grab during the cruise No. 68 of the RV "Professor Vodyanitsky" in 2010. A cylindrical corer with inner diameter of 4.8 cm was used [Sergeeva et al., 2013].

In the deep-sea areas, material was sampled at the oxic/anoxic interface (82–363-m depth) in the northern Black Sea off the Crimean Peninsula during the research cruise No. 15/1 of the RV "Maria S. Merian" (Germany) (April–May 2010). In the Istanbul Strait's (Bosphorus) outlet area of the Black Sea (93–300-m depth), sampling was carried out during two research cruises: the cruise of the RV "Arar" of the Istanbul Technical University (November 2009) and the cruise No. 15/1 of the RV "Maria S. Merian" (April 2010). In the deep-sea areas, bottom sediments were sampled with a multiple corer (diameter of 9.6 cm), push corer or geological corer (diameter of 7.3 cm), and devices that provide obtaining virtually undisturbed samples. The sediment cores were sliced into 1-cm-thick layers down to a depth of 5–10 cm in order to study the vertical distribution of the fauna [Sergeeva et al., 2017, 2021].

Table 1. Station coordinates and sampling depth and time (the Black Sea)

Station No.	Latitude, N	Longitude, E	Depth, m	Date
<i>Zernov's Phyllophora</i> Field, the cruise No. 68 of the RV "Professor Vodyanitsky"				
21	45°45'24"	31°21'28"	41	13.11.2010
25	46°4'3"	31°35'5"	20	13.11.2010
The Donuzlav Bay				
1	45°18'59"	33°1'11"	2	11.07.2019
3	45°19'13"	33°0'50"	2	11.07.2019
4	45°19'27"	33°0'60"	2	11.07.2019
The Kruglaya (Omega) Bay				
5	44°36'11.0"	33°26'34.3"	8.8	28.01.2010
The Laspi Bay				
1	44°25'05"	33°41'43"	14.5	15.09.2017
15	44°25'10"	33°42'13"	9	16.09.2017
17	44°25'04"	33°42'22"	10	16.09.2017
18	44°25'04"	33°42'28"	9	16.09.2017
The Southwestern Crimea and the Bosphorus Strait outlet area, the cruise No. 15/1 of the RV "Maria S. Merian"				
235	41°29'37"	29°15'12"	159	15.04.2010
372	44°37'14"	32°53'49"	163	25.04.2010
405	44°37'21"	32°54'9"	155.5	28.04.2010
425	44°47'09"	31°58'05"	163.2	30.04.2010
The Bosphorus Strait outlet area, the cruise of the RV "Arar" (Istanbul Technical University)				
3	41°24'01.2"	29°03'12.6"	82	12.11.2009
4	41°24'01.2"	29°03'12.6"	88	15.11.2009
5	41°23'17.4"	29°12'14.4"	103	15.11.2009
7	41°26'51.6"	29°12'57"	160	15.11.2009
9	41°28'59.4"	29°15'08.4"	250	15.11.2009

All sediment sections were fixed with 75% alcohol to preserve morphological structures without distortion. In a laboratory, all sampled sediments were washed through two stacked sieves with mesh size of 1 mm and 63 µm in series and stained with rose bengal for at least 24 h.

The stained samples were placed in a Bogorov chamber; meiofaunal organisms were identified to major taxa and counted out under a binocular microscope. Nematode specimens were transferred to pure glycerin and mounted on wax–paraffin ring permanent slides [Ryss, 2002]. All measurements, photographs, and drawings were taken under Carl Zeiss Axiostar Plus and Olympus BX53 light microscopes. Holotype and paratypes were deposited in IBSS collection (Sevastopol).

Abbreviations are as follows: a, ratio of body length / maximum body diameter; b, ratio of body length / pharynx length; c, ratio of body length / tail length; c', ratio of tail length / anal body diameter; cbd, corresponding body diameter; and abd, anal body diameter.

RESULTS

Taxonomy. Order Monhysterida Filipjev, 1929. Family Xyalidae Chitwood, 1951. Genus *Stylotheristus* Lorenzen, 1977.

Diagnosis (emended from [Fonseca, Bezerra, 2014]). Cuticle transversely striated. Somatic setae usually present. Anterior sensilla arranged in two crowns with the number of setae in the second crown depending on the sex and life stage: (6 + 4) setae in juveniles; (6 + 4) or (6 + 6) in females; and (6 + 10) in males. Amphidial fovea circular or oval. Buccal cavity conical. Pharyngeal muscles

well-developed around the buccal cavity. Females with one outstretched ovary, located to the left side of intestine. Males with single anterior outstretched testis to the right or left of intestine. Spermatheca can be present. Spicules short (< 1 abd). Gubernaculum narrow, without apophysis. Precloacal supplements present or absent. Three caudal glands opening through separate pores. Tail conico-cylindrical, with three terminal setae.

Type species. *Stylotheristus mutilus* (Lorenzen, 1973) Lorenzen, 1977.

List of valid *Stylotheristus* species:

- *Stylotheristus mutilus* (Lorenzen, 1973) Lorenzen, 1977;
- *Stylotheristus multipapillatus* Pinto & Neres, 2020;
- *Stylotheristus paramutilus* sp. nov. (Figs 2, 3, 4, 5, Tables 2, 3).

Table 2. Measurements of *Stylotheristus paramutilus* sp. nov. from different areas of the Black Sea. All values are in µm unless otherwise stated, except for the ratios a, b, c, and c'. All curved structures were measured along the arc

Character	The Donuzlav Bay			The Bosphorus Strait area		The Laspi Bay
	Male holotype	Male paratype, n = 5	Female paratype, n = 4	Male paratype, n = 2	Female paratype	Male paratype
Body length	1,767	1,545–1,752	1,613–1,799	1,854–1,875	1,820	1,565
a	49.1	40.6–48.7	38.2–46.1	51.5–52.1	45.5	36.4
b	9.7	8.2–9.8	8.7–9.8	10.4–11.2	10.5	8.5
c	5.1	4.6–5.5 (12.9*)	4.8–5.7	4.5	4.5	5.8
c'	12.6	12.2–13.3 (3.3*)	12.2–14.3	12.9	16.2	9
V (%)			51.9–56.6		49.1	
Vulval body diameter			32–43		35	
Maximum body diameter	36	36–40	35–47	36	40	43
Pharynx length	181	165–188	172–196	165–180	173	184
Buccal cavity length	20	18–21	20–24	20–21	17	20
Buccal cavity diameter	15	15–20	12–14	17–20	12	19
Amphid width / cbd (%)	32	29.6–36	31.1–33.3	33.3–34.8	38.1	26.7
Amphid from anterior end	17	17–20	20–21	12–15	11	18
Nerve ring from anterior end	86	81–98	81–105	82–95	–	–
Nerve ring cbd	35	32–35	31–38	30–32	–	–
Tail length	353	317–345 (120*)	316–345	412	405	270
abd	28	26–31	22–27	29–30	25	30
Spicule length	22	17–22 (27×)		22		21
Gubernaculum length	14	10–12		12		9

Note: * denotes a male (Meib.44. N.p.) with a very short tail; × denoted a male (Meib.43. N.p.) with longer spicules.

The latter species was previously recorded in the Bosphorus Strait outlet area (the Black Sea) as *Daptonema* sp. [Sergeeva et al., 2021].

Type material. Nine males and six females. Male holotype mounted on slide Meib.39. N.h. Male paratypes mounted on slides: Meib.40. N.p. – Meib.45. N.p., Meib.50. N.p. Female paratypes in pure glycerin: Meib.41. N.p., Meib.46. N.p. – Meib.49. N.p.

Type locality. The Black Sea, the Donuzlav Bay, 45°19'13"N, 33°0'50"E, sta. 3, silt with the smell of hydrogen sulfide, sediment depth of 2 m.

Etymology. The species name means “close to *mutilus*,” “similar to *mutilus*.”

Description. Male. Body cylindrical and gradually tapering towards posterior end. Cuticle striated. Somatic setae scattered along the body, 4–11 µm long. Cervical setae thin, 9–14 µm long. Lips well developed, high. Six short inner labial conical papillae (3 µm long) and a circle with 16 cephalic setae: 12 long setae (11–18 µm long) and 4 short setae (6–9 µm long). Stoma funnel-shaped. Cheilostoma with thin, smooth walls.

Pharyngostoma funnel, with weakly cuticularized walls. Pharynx muscular, almost cylindrical. Cardia 15–21 µm long, surrounded by intestine. Amphids circular, 8–9 µm in diameter. Pharynx cylindrical, about 8.9–12.2% of total body length. Nerve ring situated near middle of pharynx (45–52.8%). Secretory-excretory pore not observed. Reproductive system monorchic. Testis outstretched, situated to the right of intestine.

Spicules short (0.6–0.9 abd), slightly curved and expanded proximally. In proximally part of spicules, visible ejacular canal. Gubernaculum plate-like, slightly curved, about 42.9–63.6% of spicule length. Sperm cells globular, 11–15 µm wide. Tail conico-cylindrical, with elongated filiform portion; three terminal setae, 8–11 µm long, on the tail tip.

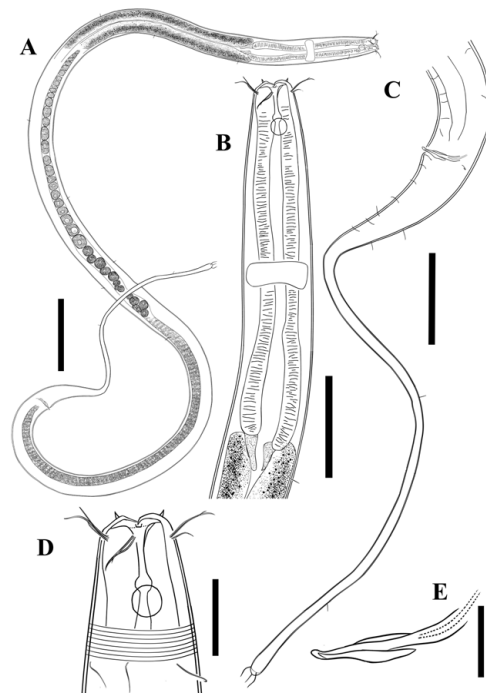


Fig. 2. *Stylotheristus paramutilus* sp. nov. Male holotype. A, general view; B, pharyngeal region; C, tail region; D, head; E, spicule. Scale bar: A, 100 µm; B, C, 50 µm; D, 20 µm; E, 10 µm

Female. Similar to male in general morphology. Cephalic sensilla arranged in a circle with 12 cephalic setae (10–18 μm long). Nerve ring at 50–57.4% of pharynx length from anterior. Reproductive system monodelphic. Ovary outstretched and on the left side of intestine. Vulva directed anteriorly, situated slightly posterior to mid-body (861–1,015 μm). Small copulatory plug visible to seal the vulva. Vagina long, with muscular walls. Spermatheca absent. Mature egg (127 \times 43 μm) and spermatozoa present in uterus. Caudal glands not visible. Tail long, with three terminal setae (8–9 μm long).

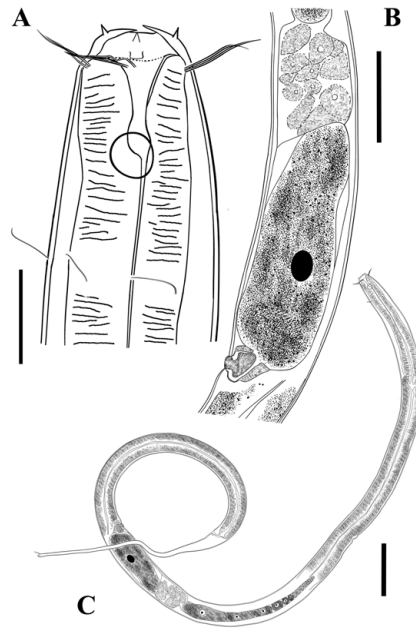


Fig. 3. *Stylotheristus paramutilus* sp. nov. Female paratype. A, head; B, vulval region; C, general view. Scale bar: A, 20 μm ; B, 50 μm ; C, 100 μm

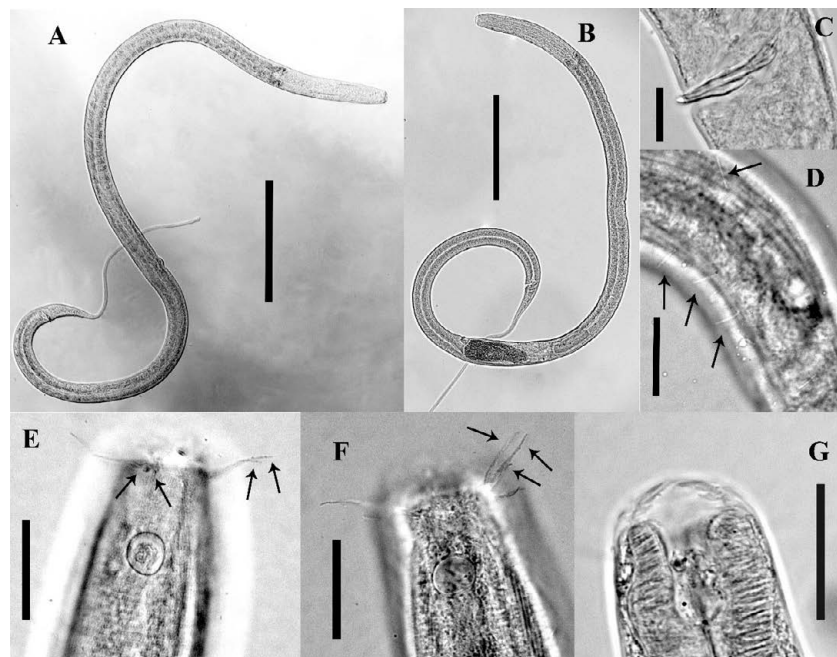


Fig. 4. *Stylotheristus paramutilus* sp. nov. A, male holotype, general view; B, female paratype, general view; C, male holotype, spicule; D, male paratype, preanal somatic setae; E, female paratype, head; F, male paratype, head; G, female paratype, buccal cavity. Scale bar: A, B, 200 μm ; C, 10 μm ; D–G, 20 μm

Diagnosis. *S. paramutilus* sp. nov. is characterized by body length of 1,545–1,875 μm ; 12 setiform cephalic sensilla in female; cervical setae present; spicules short and widening proximally; gubernaculum plate-like slightly curved; and tail 270–412 μm long (except for one male paratype, 120 μm long).

Differential diagnosis. *S. paramutilus* sp. nov. differs from all valid species (see Table 3) by number of cephalic setae in female (12 vs. 10); relatively shorter body in males (1,545–1,875 μm vs. 1,830–2,330 μm in *S. mutilus* and 1,968–2,052 μm in *S. multipapillatus*) and in females (1,657–1,820 μm vs. 1,970 μm in *S. mutilus* and 2,100–2,240 μm in *S. multipapillatus*); structure of the spicular apparatus (expand proximally vs. thin all over in *S. multipapillatus* and *S. mutilus*); and longer tail (c value of 4.5–5.8 [except for one male with 12.9] vs. 5.8–6.6 in *S. mutilus* and 6.8–8.6 in *S. multipapillatus*). *S. paramutilus* sp. nov. is similar in the body structure to *S. mutilus*, but differs from it by wider body in males (a value of 36.4–52.1 vs. 55–61). The new species differs from *S. multipapillatus* by precloacal supplements (absent vs. present).

Variability of body size and copulatory organs. Specimens from different areas of the Black Sea have significant variability in body and tail lengths; there are also slight differences in the shape and length of spicules (see Fig. 5, Table 2). Specimens from the Bosphorus Strait area are much longer and slightly slenderer than those from the Donuzlav and Laspi bays. One male (Meib.42. N.p.), from the Bosphorus Strait area, has straight spicules, and another male (Meib.41. N.p.) has proximally curved spicules (Fig. 5D, E). The third male paratype (Meib.43. N.p.), from the Donuzlav Bay, has longer spicules [27 μm (0.9 abd) vs. 17–22 μm (0.6–0.8 abd)] and ratio of spicule length to gubernaculum length (2.25 vs. 1.6–1.9) compared to other specimens (Fig. 5B). The fourth male paratype (Meib.44. N.p.), from the Donuzlav Bay, has shortened tail (3.3 abd vs. 9–13.3 abd) (Fig. 5A).

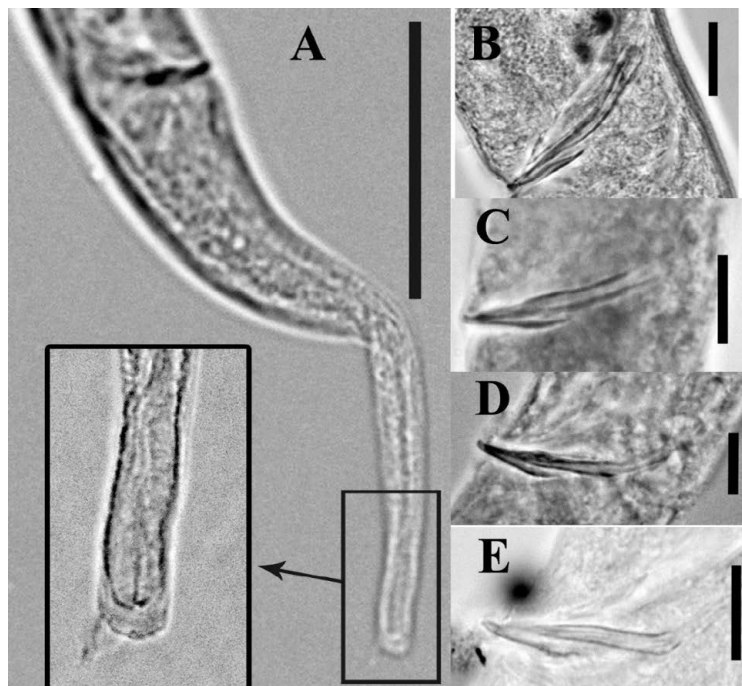


Fig. 5. *Stylotheristus paramutilus* sp. nov. A, male paratype, tail (the Donuzlav Bay); B–E, variation of shape of spicules in male paratypes: B, the Donuzlav Bay; C, the Laspi Bay; D–E, the Bosphorus Strait area. Scale bar: A, 50 μm ; B–E, 10 μm

Table 3. Morphological characters of *Stylotheristus* species. All values are in μm unless otherwise stated, except for the ratios a, b, c, and c'

Character	<i>Stylotheristus paramutilus</i> sp. nov.		<i>Stylotheristus mutilus</i>		<i>Stylotheristus multipapillatus</i>	
	males	females	males	female	males	females
Body length	1,545–1,875	1,613–1,820	1,830–2,330	1,970	1,920–2,052	2,100–2,240
a	36.4–52.1	38.2–46.1	55–61	45	56.9–68.9	43.7–56.45
b	8.2–11.2	8.7–10.5	9.2–9.6	8.7	8–9	8.2–8.9
c	4.5–5.8	4.5–5.7	5.9–6.6	5.8	7.5–8.6	6.8–7.6
c'	9–13.3	12.2–16.2	11.2	14.3	7.4–9.8	9.7–11
Number of cephalic setae	16	12	16	10	16	10
V (%)		49.1–56.6		55		57–63
Spicule length	17–22		18–20		15.5–25	
Number of supplements	absent		absent		11–15	

It can be assumed that such morphological variability is determined by the adaptation of the species to different conditions of the waterbody. On the other hand, it is possible that in future, genetic methods applied to study individuals from various habitats will show the existence of different species of *Stylotheristus* genus in the Black Sea.

This work was carried out within the framework of IBSS state research assignment “Biodiversity as the basis for the sustainable functioning of marine ecosystems, criteria and scientific principles for its conservation” (No. 124022400148-4).

Acknowledgement. The authors are grateful to Professor Antje Boetius for the invitation to cooperate in the EU FP7 project HYPOX (*In situ* monitoring of oxygen depletion in hypoxic ecosystems of coastal and open seas, and land-locked water bodies), EC Grant 226213, and to all participants of the research cruises on the RV “Maria S. Merian” and “Arar.” The authors are grateful to PhD I. Bondarev, PhD S. Mazlumyan, PhD N. Revkov, and PhD V. Timofeev (IBSS) for participating in benthic sampling.

REFERENCES

1. Fonseca G., Bezerra T. N. Order Monhysterida Filipjev, 1929. In: *Handbook of Zoology. Gastrotricha, Cycloneuralia, Gnathifera*. Vol. 2. *Nematoda* / A. Schmidt-Rhaesa (Ed.). Berlin ; Boston : De Gruyter, 2014, pp. 435–465. <https://doi.org/10.1515/9783110274257>
2. Lorenzen S. Freilebende Meersenematoden aus dem Sublitoral der Nordsee und der Kieler Bucht. *Veröffentlichungen des Instituts für Meeresforschung in Bremerhaven*, 1973, Bd. 14, pp. 103–130.
3. Lorenzen S. Revision der Xyalidae (freilebende Nematoden) auf der Grundlage einer kritischen Analyse von 56 Arten aus Nord- und Ostsee. *Veröffentlichungen des Instituts für Meeresforschung in Bremerhaven*, 1977, Bd. 16, pp. 197–261.
4. Mureşan M. Assessment of free-living marine nematodes community from the NW Romanian Black Sea shelf. *Geo-Eco-Marina*, 2012, vol. 18, pp. 133–145. <https://doi.org/10.5281/zenodo.56876>
5. Mureşan M. Diversity and distribution of free-living nematodes within periazoic level on the Romanian shelf of the Black Sea. *Geo-Eco-Marina*, 2014, vol. 20, pp. 19–28.
6. *Nemys: World Database of Nematodes* : [site], 2023. URL: <https://nemys.ugent.be> [accessed: 23.06.2023]. <https://doi.org/10.14284/366>
7. *OBIS: Ocean Biogeographic Information System* : [site]. URL: <https://obis.org/taxon/153200> [accessed: 08.07.2023].

8. Pinto T. K., Neres P. F. Four new species of free-living nematodes from shallow continental shelf of Portugal. *Zootaxa*, 2020, vol. 4722, no. 1, pp. 1–33. <https://doi.org/10.11646/zootaxa.4722.1.1>
9. Revkova T. N. Struktura taksotsena svobodnozhivushchikh nematod v bukhte Kruglaya (Omega) (Chernoje more). In: “*Pontus Euxinus – 2015*” : tezisy IX Vserossiiskoi nauchno-prakticheskoi konferentsii molodykh uchennykh (s mezhdunarodnym uchastiem) po problemam vodnykh ekosistem, posvyashchenoi 100-letiyu so dnya rozhdeniya d. b. n., prof., chl.-kor. AN USSR V. N. Greze, 17–20 Nov., 2015. Sevastopol : DigitPrint, 2015, pp. 144–145. (in Russ.). <https://repository.marine-research.ru/handle/299011/1855>
10. Revkov N. K., Boltacheva N. A., Revkova T. N., Bondarenko L. V., Schurov S. V., Lukjanova L. F. Bottom fauna of lake Donuzlav under conditions of industrial sand mining. *Ekosistemy*, 2021, iss. 27, pp. 5–22. (in Russ.). <https://doi.org/10.37279/2414-4738-2021-27-5-22>
11. Ryss A. Y. Express technique to prepare permanent collection slides of nematodes. *Zoosystematica Rossica*, 2002, vol. 11, no. 2, pp. 257–260. <http://doi.org/10.31610/zsr/2002.11.2.257>
12. Sergeeva N. G. Meiobenthos in the region with the methane gas seeps. In: *Modern Conditions of Biological Diversity in Near-shore Zone of Crimea (the Black Sea Sector)* / V. N. Eremeev, A. V. Gaevskaya (Eds). Sevastopol : Ekosi-Gidrofizika, 2003, pp. 258–267. (in Russ.). <https://repository.marine-research.ru/handle/299011/1467>
13. Sergeeva N. G., Kharkevych Kh. O., Revkova T. N. Modern structure of meiobenthos of the north-western shelf of the Black Sea. In: *From the Caspian to Mediterranean: Environmental Change and Human Response During the Quaternary (2013–2017)* : proceedings of the IGCP 610 First Plenary Conference and Field Trip, Illia State University, Tbilisi, Georgia, 12–19 October, 2013. Tbilisi : LTD “Sachino”, 2013, pp. 126–129.
14. Sergeeva N. G., Revkova T. N., Ürkmez D. Meiobenthic assemblages of the Laspi Bay (Crimea, Black Sea): Taxonomic diversity and quantitative development. *Acta Aquatica Turcica*, 2023, vol. 19, iss. 1, pp. 58–70. <https://doi.org/10.22392/actaquatr.1169181>
15. Sergeeva N. G., Ürkmez D., Dovgal I. V., Sezgin M. Protists (Ciliophora, Gromiida, Foraminifera) in the Black Sea meiobenthic communities. *Journal of the Black Sea/Mediterranean Environment*, 2017, vol. 23, no. 2, pp. 121–155.
16. Sergeeva N. G., Ürkmez D., Revkova T. N. Meiobenthic nematodes at the deep oxic/anoxic boundary of the Black Sea (Istanbul Strait Outlet Area) with new records for Turkey. *Regional Studies in Marine Science*, 2021, vol. 46, art. no. 101904 (12 p.). <https://doi.org/10.1016/j.rsma.2021.101904>
17. Shnyukov E., Yanko-Hombach V. Black Sea methane and marine biota (case study). In: *Mud Volcanoes of the Black Sea Region and Their Environmental Significance*. Cham, Switzerland : Springer, 2020, pp. 449–485. https://doi.org/10.1007/978-3-030-40316-4_11
18. Venekey V., Gheller P. F., Maria T. F., Brustolin M. C., Kandratavicius N., Vieira D. C., Brito S., Souza G. S., Fonseca G. The state of the art of Xyalidae (Nematoda, Monhysterida) with reference to the Brazilian records. *Marine Biodiversity*, 2014, vol. 44, iss. 3, pp. 367–390. <https://doi.org/10.1007/s12526-014-0226-3>
19. Vorobyova L. V., Kulakova I. I. *Contemporary State of the Meiobenthos in the Western Black Sea*. Odesa : Astroprint, 2009, 126 p.
20. Zaika V. E., Ivanova E. A., Sergeeva N. G. Seasonal changes of meiobenthos of the Sevastopol Bays with the analysis of influence of bottom hypoxia. *Morskoj ekologicheskij zhurnal*, 2011, vol. 2, sep. iss. 2, pp. 29–36. (in Russ.). <https://repository.marine-research.ru/handle/299011/1115>
21. Yanko V. V., Kravchuk A. O., Kulakova I. I. *Meiobenthos of Methane Outlets of the Black Sea*. Odesa : Feniks, 2017, 240 p. (in Russ.)

**STYLOTHERISTUS PARAMUTILUS SP. NOV. (NEMATODA: XYALIDAE),
НОВЫЙ ВИД НЕМАТОД ИЗ ЧЁРНОГО МОРЯ**

Т. Н. Ревкова, Н. Г. Сергеева

ФГБУН ФИЦ «Институт биологии южных морей имени А. О. Ковалевского РАН»,
Севастополь, Российская Федерация
E-mail: alinka8314@gmail.com

Приведены иллюстрации и описание *Stylotheristus paramutilus* sp. nov. из сборов донных осадков мелководных и глубоководных зон Чёрного моря. Новый вид характеризуется хорошо развитой губной областью, 12 щетинковидными головными сенсиллами у самки и 16 у самца; наличием шейных щетинок; спикулами (0,6–0,9 анального диаметра), расширяющимися проксимально; пластинчатым рульком, слегка изогнутым; конико-цилиндрическим хвостом, равным 4,5–5,8 анального диаметра (кроме одного самца, значение у которого составило 12,9 анального диаметра) и 3 щетинками на кончике хвоста. В настоящем исследовании описана первая находка рода *Stylotheristus* в Чёрном море. *S. paramutilus* sp. nov. характеризуется широким пространственным и батиметрическим (глубины от 2 до 250 м) распространением в Чёрном море — как в различных районах Крыма, так и на выходе из пролива Босфор. Сделано заключение о необходимости проведения в будущем молекулярного анализа для подтверждения принадлежности черноморских представителей из разных местообитаний к одному виду.

Ключевые слова: Monhysterida, свободноживущие морские нематоды, систематика, распределение, глубоководный, мелководный

UDC 582.263-11:[57.04:665.7]

**ANALYSIS OF PHYSIOLOGICAL AND BIOCHEMICAL PARAMETERS
OF ACROSIPHONIA ARCTA (DILLWYN) GAIN CELLS
AT THE EARLY STAGE OF STRESS REACTION FORMATION
UNDER THE EFFECT OF DIESEL FUEL EMULSION**

© 2024 I. Ryzhik¹, D. Salakhov¹, M. Makarov¹, and M. Menshakova²

¹Murmansk Marine Biological Institute of the Russian Academy of Sciences, Murmansk, Russian Federation

²Murmansk Arctic University, Murmansk, Russian Federation

E-mail: alaria@yandex.ru

Received by the Editor 29.07.2022; after reviewing 24.03.2023;
accepted for publication 09.10.2023; published online 22.03.2024.

Features of stress reaction formation were studied in cells of the green alga *Acrosiphonia arcta* under the effect of diesel fuel emulsion. Changes in indicators of oxidative stress (concentration of hydrogen peroxide and accumulation of products of lipid peroxidation) were analyzed; activity of antioxidant enzymes, intensity of photosynthesis, and condition of cells were investigated. As shown, during the first day of exposure to the toxicant, plasmolysis and disruption of the chloroplast structure occur in cells. The stress reaction develops in stages. At the first stage, the amount of hydrogen peroxide increases, the concentration of products of lipid peroxidation changes, and the activity of superoxide dismutase rises. At the second stage, catalase activity increases. By the end of the first day of exposure, against the backdrop of a drop in catalase activity, peroxidase activity rises (the third stage). The intensity of photosynthesis decreases by the end of the experiment. As suggested, under the effect of diesel fuel emulsion, the daily dynamics of the biological cycles of a number of enzymes may be disrupted.

Keywords: *Acrosiphonia arcta*, diesel fuel, catalase, superoxide dismutase, peroxidase, lipid peroxidation, hydrogen peroxide, photosynthesis intensity

Acrosiphonia arcta (Dillwyn) Gain, 1912 is a species of green algae widespread in the littoral zone of the Barents Sea [Malavenda, 2018], where it can form quite large thickets. It belongs to the first settlers preparing the substrate for colonization by perennial species of algae, for example, *Fucus* representatives. *A. arcta* has high adaptive capabilities: it can withstand a wide range of fluctuations in environmental factors, such as temperature, light, etc. [Sussmann, Scrosati, 2011].

With intensive industrial development, the anthropogenic load inevitably increases which includes the release of petroleum hydrocarbons into the environment [Patin, 2008]. In coastal cities, the most vulnerable zone is the near-shore area affected from both land and sea. The flora of such coastal sites is poor in terms of species composition; vegetation surviving here has mechanisms to neutralize toxicants and/or adapt to their occurrence [Malavenda, 2018; Milchakova, Shakhmatova, 2007; Shakhmatova, Milchakova, 2014]. Petroleum products slow down vegetation growth, as shown for *Ascophyllum nodosum* and *Laminaria digitata* [Bokn, 1985], and disrupt zygote formation and fucoid development [Thélin, 1981]. On the example of *Fucus* representatives, researchers also noted the lack

of significant changes in the intensity of photosynthesis and concentration of pigments under exposure to petroleum products, both long-term [Voskoboinikov et al., 2004] and short-term [Stepanyan, 2014]. However, the biochemical composition and activity of enzymes changed noticeably under their effect [Shakhmatova, Ryzhik, 2020; Voskoboinikov et al., 2004]. At the same time, when green algae are exposed to petroleum products, a decrease in photosynthesis intensity was recorded; also, significant damage and alteration in the biochemical composition of cells were registered [El Maghraby, Hassan, 2021; Klindukh et al., 2021; Pilatti et al., 2016; Ryzhik, Makarov, 2019; Voskoboinikov et al., 2018].

When an organism encounters a toxicant, several defense systems are gradually activated [Apel, Hirt, 2004; Kolupaev, 2007]. First of all, the formation of reactive oxygen species is intensified [Pokora, Tukaj, 2010; Vega-López et al., 2013] which activate the antioxidant defense system (catalase, superoxide dismutase, glutathione peroxidase, and so on) [Alscher et al., 2002]. Changes in superoxide dismutase activity were revealed for *Chlorella vulgaris* [Calderón-Delgado et al., 2019], *Phaeodactylum tricornutum* [Wang et al., 2008], and *Ulvaria obscura* [Salakhov et al., 2020]. Changes in catalase activity were recorded for *Palmaria palmata* [Voskoboinikov et al., 2020] and *Ulva* algae [Pilatti et al., 2016; Ryzhik, Makarov, 2019]. The nature of variations in activity of enzymes depends on the value and duration of the stress factor effect. Chronic exposure triggers profound changes in cycles of synthesis of proteins / amino acids, lipid metabolism (alterations in the composition of fatty acids and lipids), etc. [Nechev et al., 2002; Ramadass et al., 2015].

Antioxidant enzymes which are biomarkers can be used to detect metabolic disorders caused by xenobiotics [Díaz-Báez et al., 2004; Geret et al., 2003; Inupakutika et al., 2016; Mallick, 2004; Shakhmatova, 2004]. The speed of activation of defense systems is important for further adaptation of an organism to a toxicant.

However, issues of the rate of the stress response formation and features of the involvement of various antioxidant system components in the cell protection from oxidative stress remain poorly studied, especially for macrophytic algae inhabiting the Arctic zone. We assume as follows. Based on the intensity of the response development and changes in enzyme activity, it will be possible to conclude on the fate of vegetation: whether it will be able to adapt to effects of the toxicant or die. As noted earlier, the fate of cells will depend on the changes occurring at the moment of contact with the toxicant [Shiu et al., 2020]. Thus, analysis of the indicators of the antioxidant system and photosynthetic activity on the first day of cell contact with petroleum products is significant for understanding the mechanisms of adaptation formation.

The aim of this study is to determine the rate of activation of *Acrosiphonia arcta* antioxidant system in response to the contact of this alga with a diesel fuel emulsion. The nature of the effect will be assessed by markers of oxidative stress (concentrations of hydrogen peroxide and lipid peroxidation products) and the state of enzymes of the antioxidant system (superoxide dismutase, catalase, and peroxidase).

MATERIAL AND METHODS

Experimental work was carried out in July 2020 at the seasonal biological station of the Murmansk Marine Biological Institute (Dalnie Zelentsy village, the Barents Sea eastern coast). This area belongs to ecologically clean spots of algae growth.

The alga thalli were sampled from the littoral zone of the Dalnezelenetskaya Bay and placed in laboratory conditions: a thermostatically controlled room with irradiance of $150 \text{ W} \cdot \text{m}^{-2}$ (24 h light : 0 h dark), water temperature of $+8 \dots +10 \text{ }^\circ\text{C}$, and constant aeration of vegetation in vessels. The mode of irradiance

was chosen in accordance with features of the photoperiod (polar day) at the time of the experiment. The alga was acclimated to laboratory conditions for three days. Then, one part of the alga was placed in control vessels [pure seawater with salinity of 33‰], and another part was placed in experimental vessels [seawater with salinity of 33‰ with summer diesel fuel (state standard GOST 305-82) added at a concentration of 43 mg·L⁻¹]. In each variant of the experiment, 8 alga thalli were used (with a total mass of < 50 g). The concentration of petroleum products corresponded to the maximum noted for the Kola Bay coastal waters in 2014–2016.

The experiment lasted for one day. Indicators were measured during the day in 1, 3, 7, 10, and 24 h, in triplicate. In total, 70 samples were processed. Physiological and biochemical indicators were determined with a PE-5300VI spectrophotometer (Ecoskhim, Russia).

The content of hydrogen peroxide was established in accordance with a modified spectrophotometric method [Bellincampi et al., 2000]. It is based on the oxidation of iron Fe²⁺ with hydrogen peroxide to Fe³⁺ forming stained compounds with xylenol orange. Optical density was measured at a wavelength of 560 nm.

The level of lipid peroxidation (hereinafter LPO) was assessed by the accumulation of active products of thiobarbituric acid [Esterbauer, Cheeseman, 1990]. Measurements were carried out at 540 nm.

The supernatant for determining the activity of catalase and superoxide dismutase (hereinafter CAT and SOD, respectively) was obtained in the following way. The alga with the weight of 150–200 mg was ground on ice in a mortar, with 2,000 µL of extraction buffer added (K/Na-phosphate buffer). The homogenate was centrifuged for 5 min at 12,000 g; then, the supernatant was sampled.

CAT activity was measured by a modified spectrophotometric method [Korolyuk et al., 1988]: 2 mL of 0.03% hydrogen peroxide solution was added to 0.1 mL of the supernatant. To a blank sample, instead of the supernatant, 0.1 mL of distilled water was added. The reaction was stopped after 10 min by adding 1 mL of 4% ammonium molybdate. The intensity of the developing color was measured at a wavelength of 410 nm against a control sample to which 2 mL of water was added instead of hydrogen peroxide.

SOD activity was determined according to [Giannopolitis, Ries, 1977]. Optical density of the content of vessels was assessed at 560 nm. Activity of enzymes (CAT and SOD) was calculated on a dry weight basis.

Peroxidase activity was analyzed by the Boyarkin method [Metody, 1987]. It is based on determining the rate of benzidine oxidation in the presence of hydrogen peroxide and peroxidase. Optical density was measured at a wavelength of 590 nm every second for 120 s. The difference between initial and final optical density was taken into account. Enzyme activity was calculated on a dry weight basis.

The rate of photosynthesis was measured by the Winkler titration. The change in oxygen content in water during incubation of thalli was calculated (µg O₂ per 1 g of thallus wet weight per h). The alga in vessels without petroleum products served as the control.

The content of dry matter was determined according to a generally accepted method [Metody, 1987]. The alga thalli, after removing droplet moisture from the surface with filter paper, were weighed on a VLTE-310 scale (Gosmetr, Russia) (accuracy of 0.001 mg), dried in a desiccator for 24 h to a constant weight at +105 °C and re-weighed. Dry matter content was assessed as the proportion of dry weight to wet weight.

The state of the alga cells was analyzed by light microscopy under a Mikmed-6 microscope (LOMO, Russia) at a magnification of ×400.

The significance of differences between options was calculated for initial data by the Student's *t*-test, with a probability of 95% ($p \leq 0.05$). To assess the significance of the effect of the pollution factor, the one-way analysis of variance (ANOVA) was applied. The data obtained were processed and analyzed in MS Office Excel 2010 statistical package.

RESULTS AND DISCUSSION

State of the alga cells. Control samples remained intact until the end of the study (Fig. 1A). In experimental samples, after 3 h of exposure, perforated chloroplast structures expanded. By the end of the first day, the chloroplast decreased; in a number of cells, it acquired a granular structure. The development of plasmolysis was noted (Fig. 1B, C).



Fig. 1. *Acrosiphonia arcta* cells at the end of the experiment (24 h): A, the control; B, C, cells after exposure to water containing diesel fuel

Markers of oxidative stress. Normally, in cells, hydrogen peroxide is constantly present (its level ranges within 0.004–0.005 z^{-1} dry weight), as well as LPO products (their concentration ranges within 0.003–0.005 c. u. $\cdot g^{-1}$ dry weight). Most likely, a decrease and increase in the content of these substances in a cell are caused by the occurrence of daily rhythms of changes in the activity of physiological processes (Fig. 2A, B).

Under the effect of diesel fuel, the concentration of hydrogen peroxide in experimental samples increases by 1.5 times during the 1st hour. This rise is followed by a gradual decrease (by 2 times). The level of LPO in the experimental alga decreases during the 1st hour; by the 7th hour of exposure, it rises almost 2 times; and by the 10th hour of observation, it drops. By the end of the experiment, LPO increases.

It is worth noting as follows: changes in the level of LPO in the control and experiment are in antiphase. In 1 and 10 hours of the study, in the control, accumulation of LPO products was observed, while in the experiment, their concentration decreased significantly (Fig. 2A, B).

Activity of enzymes of the antioxidant system. In the control, SOD activity remained unchanged from the 1st to 7th hour of the study, increased by 1.3 times by the 10th hour, and did not change until the end of the experiment. Under the effect of diesel fuel, SOD activity rose by 1.5 times in the 1st hour, decreased by 2 times by the 7th hour, and became equal with the indicator in the control by the first day (Fig. 2C).

CAT activity in the control did not change during the 1st hour. By the 3rd hour, a 3.6-fold rise in activity was recorded; by the 7th hour, a 3-fold drop; and by the 10th hour, a 1.5-fold increase. Until the end of measurements, the values of CAT activity remained high. In experimental samples, there was a gradual rise in CAT activity (by 3 times) from the 1st to 7th hour. By the 10th hour, enzyme activity decreased by 2.5 times; until the end of exposure, it did not change (Fig. 2D).

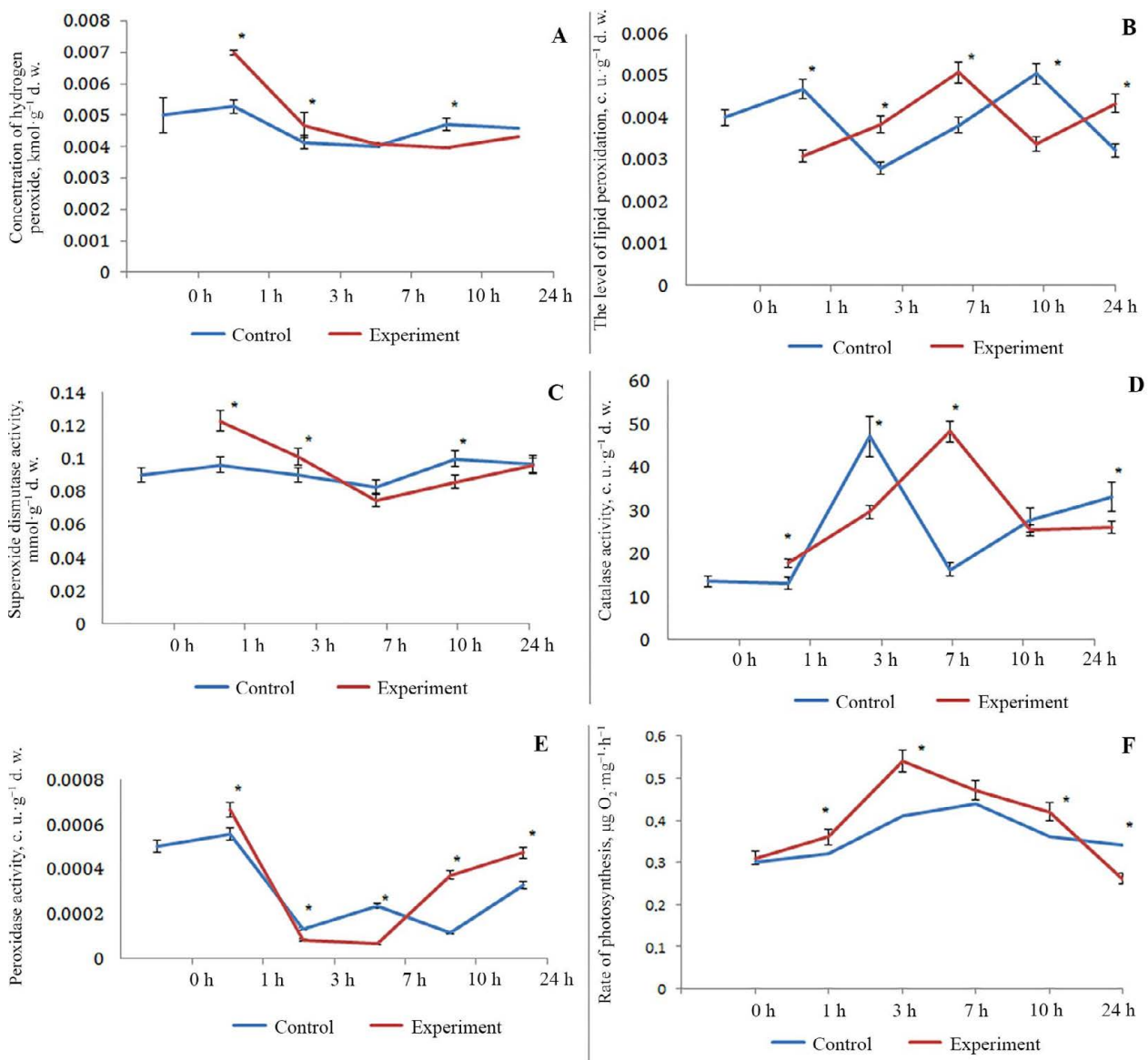


Fig. 2. Changes in the main physiological and biochemical parameters of *Acrosiphonia arcta* during the experiment: A, hydrogen peroxide concentration; B, the level of lipid peroxidation; C, superoxide dismutase activity; D, catalase activity; E, peroxidase activity; F, rate of photosynthesis. Data in the graphs are presented as arithmetic means; bars indicate standard deviation [* marks significant differences with the control ($p \leq 0.05$)]

During the experiment, peroxidase activity varied significantly in control samples and in those under exposure.

In the control, there was a wave-like change in enzyme activity. During the 1st hour, a slight increase in peroxidase activity was noted, and by the 3rd hour, there was a 6-fold drop. In the 3rd to 7th hour, activity rose by 2 times. Then, it decreased by 2 times. By the end of the experiment (the 24th hour), the value increased by 3 times compared to the previous values (Fig. 2E). In experimental samples, there were also a rise in peroxidase activity by the 1st hour (by 1.3 times) and a drop by the 3rd hour (by 7 times). At the same time, from the 7th hour of exposure, there was an increase in peroxidase activity. By the 10th hour, it rose by 5 times, and by the 24th hour, by 1.5 times compared to the previous values; it was significantly higher than peroxidase activity in the control (Fig. 2E).

Rate of photosynthesis. During the experiment, the rate of photosynthesis was measured as well (Fig. 2E). In the first hours, experimental samples were characterized by an increase in the rate of photosynthesis compared to the control. The most significant differences were observed by the 3rd hour of measurements: the values were 1.3 times higher than control ones. By the end of exposure, the rate of photosynthesis of experimental samples became 1.3 times lower than that of the control.

DISCUSSION

A change in the activity of antioxidant enzymes in response to stressors of various nature is a universal reaction of any organism [Milchakova, Shakhmatova, 2007; Regoli et al., 2002; Ryzhik et al., 2019; Sardi et al., 2016; Shakhmatova, 2004; Zhang et al., 2004]. Literature sources mainly discuss long-term effects of petroleum products and corresponding alterations in an organism. Specifically, on the example of *Hypnea musciformis*, a complex pattern of changes in various biochemical parameters was shown: a decrease in the content of chlorophyll *a*, a decline in the concentration of phenolic compounds, and an increase in the content of carotenoids. A change in cell morphology was noted as well, in particular in the structure of a cell wall surface [Ramlov et al., 2014, 2019]. As established for the microalga *Pseudokirchneriella subcapitata*, fresh and, to a greater extent, used motor oil caused a rise in the activity of antioxidant enzymes (first, SOD activity increased; then, peroxidase and CAT activity rose); thus, oxidative damage to biomolecules decreased [Ramadass et al., 2015]. In cells of green algae, with prolonged exposure to a toxicant, researchers recorded the development of plasmolysis, destruction of chloroplasts, etc. [Salakhov et al., 2021; Voskoboinikov et al., 2018].

Long-term experiments often fail to identify the true response to exposure to a toxicant. Specifically, studies on *Fucus vesiculosus* did not reveal a rise in CAT activity after prolonged (more than 10 days) contact with diesel fuel [Ryzhik et al., 2019]. However, under natural conditions, CAT activity was significantly higher in algae exposed to chronic pollution of a high level than in algae of ecologically clean spots [Shakhmatova, Ryzhik, 2020].

The current study provides data on changes in the activity of antioxidant enzymes in *A. arcta* cells in response to exposure to diesel fuel during the first day of the experiment. To date, it is established that the intensification of formation of reactive oxygen species results in an increase in the activity of antioxidant enzymes involved in the formation of long-term adaptations [Kolupaev, 2007; Kolupaev, Karpets, 2010; Migdal, Serres, 2011; Rogozhin, 2004].

According to the results of our study, stress reactions begin to form in the alga cells by the 1st hour of exposure. In particular, plasmolysis develops, and the structure of chloroplasts is disrupted.

During the first day, three blocks of rapid stress reactions can be distinguished; those are launched in stages. One of the first, implemented immediately after the beginning of exposure, is the intensification of LPO processes. Malondialdehyde and other LPO products are unique signals for enhancing the synthesis of antioxidant enzymes. After the 1st hour of the experiment, a decrease in LPO level and an increase in SOD activity were registered compared to the control. LPO processes develop at high speed; as shown on the example of higher plants (wheat sprouts), a significant accumulation of LPO products can occur already within the first 10–15 min of exposure [Rogozhin, 2004]. To neutralize them, the pool of SOD is used which was in a cell before the onset of exposure. Moreover, *de novo* synthesis begins, since SOD is an inducible enzyme. According to literature data, on the example of a study on ultraviolet radiation effect on wheat sprouts, it was revealed as follows: at the initial stages of exposure, the available supply of SOD is used to utilize reactive oxygen species; then, the synthesis of enzyme begins [Rogozhin, 2004]. In parallel, we can observe an increase in the concentration of hydrogen peroxide in *Acrosiphonia* cells. Also, during this period, CAT synthesis is activated, and its maximum activity occurs at the 7th hour of measurements (the second block of reactions).

Then, CAT concentration decreases in the studied alga, and the level of peroxidase increases (the third stage). Identified features may be a consequence of inhibition of CAT activity by high concentrations of hydrogen peroxide and/or products of the split of petroleum hydrocarbons, as well as the possible transition of this enzyme to another form allowing to perform an oxygenase function [Kolupaev, Karpets, 2010; Kolupaev et al., 2011]. At the same time, a decrease in CAT activity was accompanied by an increase in peroxidase activity. With the similarity of functions they perform, it indicates the compensatory nature of the changes. The publications of a number of researchers showed compensatory changes in some components of the antioxidant system under inhibition of the activity / reducing the content of its other components [Apel, Hirt, 2004; Miroschnichenko, 1992].

The study also revealed an increase in the rate of photosynthesis in the experimental alga in the first hours of measurements (the 1st, 3rd, 7th, and 10th) and a decrease by the end of exposure.

A rise in the rate of photosynthesis we observed within the first hours of the experiment may be due to features of the Winkler titration: to measure photosynthesis, plants are transferred to a medium without a toxicant for 30–60 min. We assume that transferring plants to clean water for measurements caused a temporary activation of photosynthesis, since toxic effect of diesel fuel was reduced. However, when plants remain in the experiment for a longer period, this effect is not observed, because irreversible changes are accumulated in cells. Apparently, a shift in prooxidant/antioxidant reactions towards LPO processes in cells of the experimental alga after a day of exposure led to a change in the structure of chloroplasts, plasmolysis, and, accordingly, a decrease in the rate of photosynthesis.

Changes in physiological parameters during the first hours of exposure to stressors were registered for various groups of organisms, and those affected not only the state of the antioxidant system, but also the protein-synthesizing and energy apparatus of a cell. For example, for microalgae and microorganisms, significant changes were shown in ratios of protein/carbohydrate and cell growth rate / survival occurring upon contact with dissolved diesel fuel during the first day of exposure [Shiu et al., 2020]. According to the results of a research on the effect of petroleum product film, with a short-term exposure (one tidal cycle), green algae experience cell plasmolysis, a decrease in the rate of photosynthesis, and an increase in the intensity of respiration [Ryzhik, Makarov, 2019].

At the same time, we established a shift in the daily cycle of CAT and LPO level in experimental samples compared to control ones. This may indicate a disruption in daily rhythms of CAT activity

and LPO processes. A number of publications provided data on the existence of biological rhythms in algae in production of antioxidants, and those are important for cell functioning [Carvalho et al., 2004]. Studies on ultraviolet radiation effect on the state of the antioxidant complex in cereal plants showed a similar result [Rogozhin, 2004]. Disruption of rhythms can negatively affect the resistance of vegetation under changing environmental conditions, and this is confirmed by data of our research.

Thus, the results of the study allowed to establish as follows. An increase in the activity of antioxidant enzymes in *Acrosiphonia arcta* cells exposed to diesel fuel occurs during the 1st hour of the experiment and is an adaptive response of the alga to a rise in the concentration of hydrogen peroxide. During exposure, different time maximums of the activity of SOD, CAT, and peroxidase were established. This corresponds to modern ideas on the sequence of the antioxidant response: SOD → CAT/peroxidase.

Importantly, the negative effect of diesel fuel is not only due to disruption of physiological processes in cells, but probably also due to biorhythms that allow organisms to adapt to periodically changing factors.

This is especially true for littoral plants exposed to periodically changing environmental factors, in particular the tidal cycle when disruption of synchronization can cause the death of algae.

The study was carried out within the framework of the Russian Science Foundation grant No. 22-17-00243 "Radiation oceanology and geoecology of the coastal shelf of the Barents and White seas. Bioinert interactions in the system bottom sediments – water – macroalgae – microorganisms; their role in the remediation of the marine coastal ecosystem during radiation and chemical pollution in the Arctic."

REFERENCES

1. Voskoboinikov G. M., Lopushanskaya E. M., Zhakovskaya Z. A., Metelkova L. O., Matishov G. G. Participation of the green algae *Ulvaria obscura* in bioremediation of sea water from oil products. *Doklady Akademii nauk*, 2018, vol. 481, no. 1, pp. 111–113. (in Russ.). <https://doi.org/10.31857/S086956520000064-3>
2. Kolupaev Yu. Ye. Reactive oxygen species in plants at stressors action: Formation and possible functions. *Visnyk Kharkivskoho natsionalnoho universytetu imeni V. N. Karazina. Serii "Biologhiia"*, 2007, iss. 3 (12), pp. 6–26. (in Russ.)
3. Kolupaev Yu. Ye., Karpets Yu. V. *Formirovanie adaptivnykh reaktivnykh rastenii na deistvie abioticheskikh stressorov*. Kyiv : Osnova, 2010, 352 p. (in Russ.)
4. Kolupaev Yu. Ye., Karpets Yu. V., Oboznyi O. I. Plants antioxidative system: Participation in cell signaling and adaptation to influence of stressors. *Visnyk Kharkivskoho natsionalnoho universytetu imeni V. N. Karazina. Serii "Biologhiia"*, 2011, iss. 1 (22), pp. 6–34. (in Russ.)
5. Korolyuk M. A., Ivanova L. I., Maiorova I. G., Tokarev V. E. Metod opredeleniya aktivnosti katalazy. *Laboratornoe delo*, 1988, no. 1, pp. 16–19. (in Russ.)
6. *Metody biokhimitskogo issledovaniya rastenii / A. I. Ermakov (Ed.) ; 3rd edition, revised & enlarged*. Leningrad : Agropromizdat, Leningradskoe otdelenie, 1987, 429 p. (in Russ.)
7. Milchakova N. A., Shakhmatova O. A. Catalase activity of the widely-distributed macroalgae of the Black Sea by gradient of the sewage pollution. *Morskoj ekologicheskij zhurnal*, 2007, vol. 6, no. 2, pp. 44–57. (in Russ.). <https://repository.marine-research.ru/handle/299011/906>
8. Miroshnichenko O. S. Biogenesis, physiological role, and properties of catalase. *Biopolimery i kletka*, 1992, vol. 8, no. 6, pp. 3–25. (in Russ.). <https://doi.org/10.7124/bc.00033C>
9. Patin S. A. *Oil Spills and Their Impact on the Marine Environment and Living Resources*. Moscow : VNIRO Publishing, 2008, 508 p. (in Russ.)

10. Rogozhin V. V. *Peroksidaza kak komponent antioksidantnoi sistemy zhivyykh organizmov*. Saint Petersburg : GIOR, 2004, 240 p. (in Russ.)
11. Stepanyan O. V. The oil film influence on photosynthesis of brown algae in the Barents Sea. *Botanicheskii zhurnal*, 2014, vol. 99, no. 10, pp. 1095–1100. (in Russ.)
12. Shakhmatova O. A. *Aktivnost' antioksidantnoi sistemy nekotorykh chernomorskikh gidrobiontov v pribrezhnoi akvatorii Sevastopolya* : avtoref. dis. ... kand. biol. nauk : 03.00.17. Sevastopol, 2004, 21 p. (in Russ.). <https://repository.marine-research.ru/handle/299011/9708>
13. Alscher R. G., Erturk N., Heath L. S. Role of superoxide dismutases (SODs) in controlling oxidative stress in plants. *Journal of Experimental Botany*, 2002, vol. 53, iss. 372, pp. 1331–1341. <https://doi.org/10.1093/jexbot/53.372.1331>
14. Apel K., Hirt H. Reactive oxygen species: Metabolism, oxidative stress, and signal transduction. *Annual Review of Plant Biology*, 2004, vol. 55, pp. 373–399. <https://doi.org/10.1146/annurev.arplant.55.031903.141701>
15. Bellincampi D., Dipierro N., Salvi G., Cervone F., De Lorenzo G. Extracellular H₂O₂ induced by oligogalacturonides is not involved in the inhibition of the auxin-regulated *rolB* gene expression in tobacco leaf explants. *Plant Physiology*, 2000, vol. 122, iss. 4, pp. 1379–1386. <https://doi.org/10.1104/pp.122.4.1379>
16. Bokn T. Effects of diesel oil on commercial benthic algae in Norway. In: *1985 Oil Spill Conference (Prevention, Behavior, Control, Cleanup)*, 25–28 February, 1985, Los Angeles, California. Washington DC : American Petroleum Institute, 1985, pp. 491–496. (International Oil Spill Conference (IOSC) proceedings ; vol. 1985, iss. 1).
17. Calderón-Delgado I. C., Mora-Solarte D. A., Velasco-Santamaría Y. M. Physiological and enzymatic responses of *Chlorella vulgaris* exposed to produced water and its potential for bioremediation. *Environmental Monitoring and Assessment*, 2019, vol. 191, iss. 6, art. no. 399 (13 p.). <https://doi.org/10.1007/s10661-019-7519-8>
18. Carvalho A. M., Neto A. M. P., Tonon A. P., Pinto E., Cardozo K. H. M., Brigagão M. R. P. L., Barros M. P., Torres M. A., Magalhães P., Campos S. C. G., Guaratini T., Sigaud-Kutner T. C. S., Falcão V. R., Colepicolo P. Circadian protection against oxidative stress in marine algae. *Hypnos*, 2004, [vol.] 1 (suppl. 1), pp. 142–157.
19. Díaz-Báez M. C., Bustos Lopez M. C., Espinosa-Ramírez A. J. *Pruebas de toxicidad acuática: fundamentos y métodos*. Bogotá, Colombia : Universidad Nacional de Colombia, 2004, 118 p.
20. El Maghraby D., Hassan I. Photosynthetic and biochemical response of *Ulva lactuca* to marine pollution by polyaromatic hydrocarbons (PAHs) collected from different regions in Alexandria city, Egypt. *Egyptian Journal of Botany*, 2021, vol. 61, no. 2, pp. 467–478. <http://dx.doi.org/10.21608/ejbo.2021.37571.1531>
21. Esterbauer H., Cheeseman K. Determination of aldehydic lipid peroxidation products: Malonaldehyde and 4-hydroxynonenal. *Methods in Enzymology*, 1990, vol. 186, pp. 407–421. [https://doi.org/10.1016/0076-6879\(90\)86134-H](https://doi.org/10.1016/0076-6879(90)86134-H)
22. Geret F., Serafim A., Bebianno M. J. Antioxidant enzyme activities, metallothioneins and lipid peroxidation as biomarkers in *Ruditapes decussatus*? *Ecotoxicology*, 2003, vol. 12, iss. 5, pp. 417–426. <https://doi.org/10.1023/A:1026108306755>
23. Giannopolitis C. N., Ries S. K. Superoxide dismutases: I. Occurrence in higher plants. *Plant Physiology*, 1977, vol. 59, iss. 2, pp. 309–314. <https://doi.org/10.1104/pp.59.2.309>
24. Inupakutika M. A., Sengupta S., Devireddy A. R., Azad R. K., Mittler R. The evolution of reactive oxygen species metabolism. *Journal of Experimental Botany*, 2016, vol. 67, iss. 21, pp. 5933–5943. <https://doi.org/10.1093/jxb/erw382>
25. Klindukh M., Dobychnina E., Makarov M., Ryzhik I. Influence of diesel fuel on the composition and content of free amino acids in the green alga *Acrosiphonia arcta*. *IOP Conference Series: Earth and Environmental Science*, 2021, vol. 937, art. no. 022010 (5 p.). <https://doi.org/10.1088/1755-1315/937/2/022010>
26. Malavenda S. V. Macroalgae's flora of the Kola Bay (the Barents Sea). *Vestnik Murmanskogo*

- gosudarstvennogo tekhnicheskogo universiteta, 2018, vol. 21, no. 2, pp. 245–252. <https://doi.org/10.21443/1560-9278-2018-21-2-245-252>
27. Mallick N. Copper-induced oxidative stress in the chlorophycean microalga *Chlorella vulgaris*: Response of the antioxidant system. *Journal of Plant Physiology*, 2004, vol. 161, iss. 5, pp. 591–597. <https://doi.org/10.1078/0176-1617-01230>
28. Migdal C., Serres M. Reactive oxygen species and oxidative stress. *Médecine/Sciences*, 2011, vol. 27, no. 4, pp. 405–412. <https://doi.org/10.1051/medsci/2011274017>
29. Nechev J. T., Khotimchenko S. V., Ivanova A. P., Stefanov K. L., Dimitrova-Konaklieva S. D., Andreev S., Popov S. S. Effect of diesel fuel pollution on the lipid composition of some wide-spread Black Sea algae and invertebrates. *Zeitschrift für Naturforschung C*, 2002, vol. 57, iss. 3–4, pp. 339–343. <https://doi.org/10.1515/znc-2002-3-401>
30. Pilatti F. K., Ramlov F., Schmidt E. C., Kreusch M., Pereira D. T., Costa C., de Oliveira E. R., Bauer C. M., Rocha M., Bouzon Z. L., Maraschin M. *In vitro* exposure of *Ulva lactuca* Linnaeus (Chlorophyta) to gasoline – biochemical and morphological alterations. *Chemosphere*, 2016, vol. 156, pp. 428–437. <https://doi.org/10.1016/j.chemosphere.2016.04.126>
31. Pokora W., Tukaj Z. The combined effect of anthracene and cadmium on photosynthetic activity of three *Desmodesmus* (Chlorophyta) species. *Ecotoxicology and Environmental Safety*, 2010, vol. 73, iss. 6, pp. 1207–1213. <https://doi.org/10.1016/j.ecoenv.2010.06.013>
32. Ramadass K., Megharaj M., Venkateswarlu K., Naidu R. Toxicity and oxidative stress induced by used and unused motor oil on freshwater microalga, *Pseudokirchneriella subcapitata*. *Environmental Science and Pollution Research*, 2015, vol. 22, iss. 12, pp. 8890–8901. <https://doi.org/10.1007/s11356-014-3403-9>
33. Ramlov F., Carvalho T. J. G., Costa G. B., de Oliveira Rodrigues E. R., Bauer C. M., Schmidt É. C., Kreusch M. G., Moresco R., Bachiega Navarro B., Cabral D. Q., Bouzon Z. L., Antunes Horta P., Maraschin M. *Hypnea musciformis* (Wulfen) J. V. Lamour. (Gigartinales, Rhodophyta) responses to gasoline short-term exposure: Biochemical and cellular alterations. *Acta Botanica Brasilica*, 2019, vol. 33, iss. 1, pp. 116–127. <https://doi.org/10.1590/0102-33062018abb0379>
34. Ramlov F., Carvalho T. J. G., Schmidt É. C., Martins C. D. L., Kreusch M. G., de Oliveira Rodrigues E. R., Bauer C. M., Bouzon Z. L., Antunes Horta P., Maraschin M. Metabolic and cellular alterations induced by diesel oil in *Hypnea musciformis* (Wulfen) J. V. Lamour. (Gigartinales, Rhodophyta). *Journal of Applied Phycology*, 2014, vol. 26, iss. 4, pp. 1879–1888. <https://doi.org/10.1007/s10811-013-0209-y>
35. Regoli F., Gorbi S., Frenzilli G., Nigro M., Corsi I., Focardi S., Winston G. W. Oxidative stress in ecotoxicology: From the analysis of individual antioxidants to a more integrated approach. *Marine Environmental Research*, 2002, vol. 54, iss. 3–5, pp. 419–423. [https://doi.org/10.1016/S0141-1136\(02\)00146-0](https://doi.org/10.1016/S0141-1136(02)00146-0)
36. Ryzhik I., Pugovkin D., Makarov M., Roleda M. Y., Basova L., Voskoboynikov G. Tolerance of *Fucus vesiculosus* exposed to diesel water-accommodated fraction (WAF) and degradation of hydrocarbons by the associated bacteria. *Environmental Pollution*, 2019, vol. 254, pt B, art. no. 113072 (6 p.). <https://doi.org/10.1016/j.envpol.2019.113072>
37. Ryzhik I. V., Makarov M. V. Effect of diesel fuel film on green algae *Ulva lactuca* L. and *Ulvaria obscura* (Kützinger) Gayral ex Bliding of the Barents Sea. *IOP Conference Series: Earth and Environmental Science*, 2019, vol. 302, art. no. 012029 (6 p.). <https://doi.org/10.1088/1755-1315/302/1/012029>
38. Salakhov D., Pugovkin D., Ryzhik I., Voskoboynikov G. The changes in the morpho-functional state of the green alga *Ulva intestinalis* L. in the Barents Sea under the influence of diesel fuel. *IOP Conference Series: Earth and Environmental Science*, 2021, vol. 937, art. no. 022059 (8 p.). <https://doi.org/10.1088/1755-1315/937/2/022059>

39. Salakhov D., Pugovkin D., Ryzhik I., Voskoboinikov G. The influence of diesel fuel on morpho-functional state of *Ulvaria obscura* (Chlorophyta). *IOP Conference Series: Earth and Environmental Science*, 2020, vol. 539, art. no. 012202 (7 p.). <https://doi.org/10.1088/1755-1315/539/1/012202>
40. Sardi A. E., Sandrini-Neto L., da S. Pereira L., Silva de Assis H., Martins C. C., da Cunha Lana P., Camus L. Oxidative stress in two tropical species after exposure to diesel oil. *Environmental Science and Pollution Research*, 2016, vol. 23, iss. 20, pp. 20952–20962. <https://doi.org/10.1007/s11356-016-7280-2>
41. Shakhmatova O., Ryzhik I. Seasonal dynamics of catalase activity in *Cystoseira crinita* (Black Sea) and *Fucus vesiculosus* (Barents Sea). *Ecological Chemistry and Engineering S*, 2020, vol. 27, iss. 4, pp. 643–650. <http://dx.doi.org/10.2478/eces-2020-0041>
42. Shakhmatova O. A., Milchakova N. A. Effect of environmental conditions on Black Sea macroalgae catalase activity. *International Journal on Algae*, 2014, vol. 16, iss. 4, pp. 377–391. <http://doi.org/10.1615/InterJAlgae.v16.i4.70>
43. Shiu R.-F., Chiu M.-H., Vazquez C. I., Tsai Y.-Y., Le A., Kagiri A., Xu C., Kamalanathan M., Bacosa H. P., Doyle S. M., Sylvan J. B., Santschi P. H., Quigg A., Chin W.-C. Protein to carbohydrate (P/C) ratio changes in microbial extracellular polymeric substances induced by oil and Corexit. *Marine Chemistry*, 2020, vol. 223, art. no. 103789 (8 p.). <https://doi.org/10.1016/j.marchem.2020.103789>
44. Sussmann A. V., Scrosati R. A. Morphological variation in *Acrosiphonia arcta* (Codiolales, Chlorophyta) from environmentally different habitats in Nova Scotia, Canada. *Rhodora*, 2011, vol. 113, no. 953, pp. 87–105. <https://doi.org/10.3119/10-06.1>
45. Th  lin I. Effets, en culture, de deux p  troles bruts et d'un dispersant p  trolier sur les zygotes et les plantules de *Fucus serratus* Linnaeus (Fucales, Phaeophyceae) = Effects in culture of two crude oils and one oil dispersant on zygotes and germlings of *Fucus serratus* Linnaeus (Fucales, Phaeophyceae). *Botanica Marina*, 1981, vol. 24, pp. 515–519. <https://doi.org/10.1515/botm.1981.24.10.515>
46. Vega-L  pez A., Ayala-L  pez G., Posadas-Espadas B. P., Olivares-Rubio H. F., Dzul-Caamal R. Relations of oxidative stress in freshwater phytoplankton with heavy metals and polycyclic aromatic hydrocarbons. *Comparative Biochemistry and Physiology Part A: Molecular & Integrative Physiology*, 2013, vol. 165, iss. 4, pp. 498–507. <https://doi.org/10.1016/j.cbpa.2013.01.026>
47. Voskoboinikov G. M., Matishov G. G., Bykov O. D., Maslova T. G., Sherstneva O. A., Usov A. I. Resistance of marine macrophytes to oil pollution. *Doklady Biological Sciences*, 2004, vol. 397, iss. 1–6, pp. 340–341. <https://doi.org/10.1023/B:DOBS.0000039711.48557.16>
48. Voskoboinikov G. M., Ryzhik I. V., Salakhov D. O., Metelkova L. O., Zhakovskaya Z. A., Lopushanskaya E. M. Absorption and conversion of diesel fuel by the red alga *Palmaria palmata* (Linnaeus) F. Weber et D. Mohr, 1805 (Rhodophyta): The potential role of alga in bioremediation of sea water. *Russian Journal of Marine Biology*, 2020, vol. 46, iss. 2, pp. 113–118. <https://doi.org/10.1134/S1063074020020108>
49. Wang L., Zheng B., Meng W. Photo-induced toxicity of four polycyclic aromatic hydrocarbons, singly and in combination, to the marine diatom *Phaeodactylum tricornerutum*. *Ecotoxicology and Environmental Safety*, 2008, vol. 71, iss. 2, pp. 465–472. <https://doi.org/10.1016/j.ecoenv.2007.12.019>
50. Zhang J. F., Sun Y. Y., Shen H., Liu H., Wang X. R., Wu J. C., Xue Y. Q. Antioxidant response of *Daphnia magna* exposed to no. 20 diesel oil. *Chemical Speciation & Bioavailability*, 2004, vol. 16, iss. 4, pp. 139–144. <https://doi.org/10.3184/095422904782775027>

**АНАЛИЗ ФИЗИОЛОГО-БИОХИМИЧЕСКИХ ПОКАЗАТЕЛЕЙ КЛЕТОК
ACROSIPHONIA ARCTA (DILLWYN) GAIN
НА РАННЕЙ СТАДИИ ФОРМИРОВАНИЯ СТРЕСС-РЕАКЦИИ
ПОД ДЕЙСТВИЕМ ЭМУЛЬСИИ ДИЗЕЛЬНОГО ТОПЛИВА**

И. В. Рыжик¹, Д. О. Салахов¹, М. В. Макаров¹, М. Ю. Меньшакова²

¹Мурманский морской биологический институт РАН, Мурманск, Российская Федерация

²Мурманский арктический университет, Мурманск, Российская Федерация

E-mail: alaria@yandex.ru

Проведено исследование особенностей формирования стрессовой реакции в клетках зелёной водоросли *Acrosiphonia arcta* на воздействие эмульсии дизельного топлива. Проанализированы изменения показателей окислительного стресса (концентрация перекиси водорода и накопление продуктов перекисного окисления липидов), активность ферментов антиоксидантной системы, интенсивность фотосинтеза и состояние клеток. Показано, что в течение первых суток воздействия токсиканта в клетках происходит развитие плазмолиза и нарушение структуры хлоропластов. Стрессовая реакция формируется поэтапно: на первом этапе увеличивается количество перекиси водорода, изменяется концентрация продуктов перекисного окисления липидов, повышается активность супероксиддисмутазы; на втором этапе происходит активизация каталазы; к концу первых суток воздействия на фоне снижения активности каталазы увеличивается активность пероксидазы (третий этап). Интенсивность фотосинтеза снижается к концу эксперимента. Выдвинуто предположение, что под воздействием эмульсии дизельного топлива может происходить нарушение суточной динамики биологических циклов ряда ферментов.

Ключевые слова: *Acrosiphonia arcta*, дизельное топливо, каталаза, супероксиддисмутаза, пероксидаза, перекисное окисление липидов, перекись водорода, интенсивность фотосинтеза

UDC 594.133-111.11:[551.464.6:546.221.1]

**MORPHOMETRIC CHARACTERISTICS OF ERYTHROID ELEMENTS
OF *ANADARA KAGOSHIMENSIS* (TOKUNAGA, 1906) HEMOLYMPH
UNDER CONDITIONS OF HYDROGEN SULFIDE LOADING**

© 2024 A. Soldatov^{1,2}, V. Rychkova¹, and T. Kukhareva¹

¹A. O. Kovalevsky Institute of Biology of the Southern Seas of RAS, Sevastopol, Russian Federation

²Sevastopol State University, Sevastopol, Russian Federation

E-mail: alekssoldatov@yandex.ru

Received by the Editor 06.12.2021; after reviewing 21.04.2022;
accepted for publication 09.10.2023; published online 22.03.2024.

The effect of hydrogen sulfide loading on the morphometric characteristics of erythroid elements of *Anadara kagoshimensis* (Tokunaga, 1906) hemolymph was studied experimentally. The work was carried out on adult molluscs with a shell height of 26–38 mm. Molluscs of the control group were kept in an aquarium with oxygen concentration of 7.0–7.1 mg O₂·L⁻¹ (normoxia). Molluscs of the experimental group were exposed to hydrogen sulfide loading created by Na₂S donor dissolving in water to a final concentration of 6 mg S²⁻·L⁻¹. A day later, the oxygen level in water amounted to 1.8 mg O₂·L⁻¹, and hydrogen sulfide was not detected. Some of molluscs were subjected to repeated hydrogen sulfide loading by Na₂S adding up to a final concentration of 9 mg S²⁻·L⁻¹. By the end of the second day, 1.9 mg S²⁻·L⁻¹ and 0.03 mg O₂·L⁻¹ (trace oxygen concentration) were recorded in water. Under conditions of short-term hydrogen sulfide loading (the first day), the population of *A. kagoshimensis* erythroid elements became more heterogeneous. In the hemolymph, the content of micro- and macrocytes increased; the number of cells with an altered shape and low content of granular inclusions in the cytoplasm rose. The number of free hematin granules in the hemolymph significantly increased. The mean cell volume (V_c) rose by more than 20%. Exposure to increased concentration of sulfides for two days led to a noticeable decrease in V_c, which is determined by a significant reduction in the population of macrocytes in the hemolymph of molluscs.

Keywords: molluscs, *Anadara kagoshimensis*, hydrogen sulfide, hemolymph, erythroid elements

The occurrence of an extensive redox zone (a chemocline zone) in the Black Sea fundamentally distinguishes this water area from other ones in the World Ocean. It is characterized by a combination of conditions of acute hypoxia with hydrogen sulfide contamination [Podymov, 2005]. The chemocline zone is usually located at depths of 100–150 m. A similar set of conditions can be formed in the shelf zone [Zaika et al., 2011]. Most often, it is a consequence of the lack of end-to-end vertical convection and the formation of local areas of decay of dead organic matter [Orekhova, Kononov, 2018]. Upwelling processes contributing to the accidental transport of hydrogen sulfide-contaminated deepwater into the coastal zone should also be taken into account [Orekhova, Kononov, 2018].

Of particular interest are organisms capable of living in conditions of hydrogen sulfide contamination and extremely low oxygen concentrations. In this regard, an invasive bivalve *Anadara kagoshimensis* (Tokunaga, 1906) stands out. First found in the Black Sea in 1968 [Kiseleva, 1992], it has become

one of the leading forms of benthos by now [Revkov, 2016]. Under experimental conditions, *A. kagoshimensis* showed high resistance not only to acute forms of hypoxia [Cortesi et al., 1992; Isani et al., 1989], but also to hydrogen sulfide loading [Miyamoto, Iwanaga, 2017; Nakano et al., 2017]. These are supposed to be the reasons for its wide distribution in the problematic water areas of the Black Sea and Sea of Azov [Revkov, 2016].

The tolerance of molluscs to acute forms of hypoxia and anoxia is well studied. It is shown to be based on the ability of their body to couple the processes of protein and carbohydrate metabolism. This is evidenced by an increase in NH_4^+ production [Chew et al., 2005], a rise in the activity of alanine and aspartate aminotransferase [Soldatov et al., 2009], a gain in processes of transamination of glutamate and alanine [Hochachka, Somero, 2002], and a formation of alanine and succinate as end-products [Buck, 2000].

The ability of molluscs to compensate for the occurrence of hydrogen sulfide in water is not fully investigated. As shown, their hemolymph contains a special protein and hemoglobins which are insensitive to hydrogen sulfide [Arp, Childress, 1981, 1983]. Moreover, it was revealed that special granular inclusions of erythrocytes containing hematin are involved in neutralizing increased concentrations of sulfides [Holden et al., 1994; Vismann, 1993]. We demonstrated the role of these inclusions in H_2S neutralization for *A. kagoshimensis* [Soldatov et al., 2018]. The present paper provides material in the development of these patterns.

The aim of the work is to study the effect of increased concentrations of hydrogen sulfide on morphological and morphometric characteristics of erythroid elements of *A. kagoshimensis* hemolymph under experimental conditions.

MATERIAL AND METHODS

The work was carried out on adult molluscs sampled in June 2021 in the Laspi Bay waters (the Crimea). The shell height (from the hinge to the valve edge) ranged within 26–38 mm.

Experimental design. Molluscs of the control group were kept in an aquarium with oxygen concentration of $7.0\text{--}7.1 \text{ mg O}_2\cdot\text{L}^{-1}$ (normoxia). *A. kagoshimensis* of the experimental group were exposed to hydrogen sulfide loading created by Na_2S donor dissolving in water to a final concentration of $6 \text{ mg S}^{2-}\cdot\text{L}^{-1}$. The exposure lasted 24 h (the first day of the experiment). The presence of sulfide ion in water resulted in its alkalization. This was compensated by adding 0.1 n HCl. The values of pH were maintained at 8.20–8.27. Sulfide ion interacted with oxygen, and it was accompanied by a decrease in the content of both gases in the aquarium water over time. After 24 h, the oxygen level in water amounted to $1.8 \text{ mg O}_2\cdot\text{L}^{-1}$, and hydrogen sulfide was not detected. From seven individuals, hemolymph was sampled from the extrapallial space. The other seven individuals were subjected to repeated hydrogen sulfide loading. Na_2S was added to the aquarium water to a final concentration of $9 \text{ mg S}^{2-}\cdot\text{L}^{-1}$. After 24 h (the second day of the experiment), trace oxygen concentration, $0.03 \text{ mg O}_2\cdot\text{L}^{-1}$, was registered in the aquarium water, and the level of hydrogen sulfide was of $1.9 \text{ mg S}^{2-}\cdot\text{L}^{-1}$. Hemolymph was sampled from these molluscs as well.

The oxygen content in water was monitored using a dissolved oxygen meter ST300D (Ohaus, the USA). The values of pH were measured on an InoLab pH 720 laboratory meter (Germany). The amount of sulfide ion in water was determined potentiometrically using a sulfide-selective sensor MSBS (the Netherlands).

Morphometric characteristics of erythrocytes. Smears were stained according to Pappenheim and analyzed under a light microscope Biomed PR2 LYUM equipped with a Levenhuk C NG Series camera. Cell diameter (C_1 and C_2) and nucleus diameter (N_1 and N_2) were measured from photographs in ImageJ 1.44p program (Fig. 1). On each smear, the indicated values were determined for 100 cells. Based on the obtained values, we calculated the mean cell volume (V_c) [Houchin et al., 1958], nucleus volume (V_n), cell thickness (h) [Chizhevsky, 1959], cell surface area (S_c) [Houchin et al., 1958], specific cell surface area (SS_c), and nuclear-cytoplasmic ratio (NCR) applying known algorithms:

$$V_c = 0.7012 \cdot \left(\frac{C_1 + C_2}{2} \right)^2 \cdot h + V_n ,$$

$$V_n = \frac{\pi \cdot N_1 \cdot N_2^2}{6} ,$$

$$h = 1.8 + 0.0915 \cdot (C_1 - 7.5) ,$$

$$S_c = 2\pi a^2 b + \frac{2\pi a b \sin(h^{-1}e)}{e} ,$$

where

$$e = \frac{\sqrt{a^2 - b^2}}{a} , \quad a = \frac{C_1 + C_2}{4} , \quad b = 0.67h , \quad SS_c = \frac{S_c}{V_c} , \quad NCR = \frac{V_n}{V_c} .$$

Simultaneously, the number of erythrocyte abnormalities was determined on hemolymph smears per 1,000 cells.

Statistical comparisons were performed using the nonparametric Mann–Whitney U test. The results are presented as ($M \pm m$). The standard Grapher package (version 11) was applied.

RESULTS

Morphometric characteristics. Erythrocytes in *A. kagoshimensis* hemolymph are large rounded cells (Fig. 1A). The longitudinal (C_1) and transverse (C_2) diameters have similar values: (18.86 ± 0.61) and (16.13 ± 0.52) μm , respectively. The mean cell volume (V_c) is (678.5 ± 52.0) μm^3 , and the cell surface area (S_c) is ($1,037.5 \pm 78.4$) μm^2 . The nucleus is compact, with a high proportion of heterochromatin which reflects the low functional activity of this structure. The shape is ellipsoidal [N_1 of (5.46 ± 0.09) μm ; N_2 of (4.11 ± 0.10) μm]. The nucleus is usually located in the cell center. The volume (V_n) is (50.1 ± 3.1) μm^3 . The nuclear-cytoplasmic ratio (NCR) is low, 0.08, which also indicates suppressed function of the cell nucleus. The cytoplasm is acidophilic, with a high hemoglobin content and a large number of small granular inclusions.

On the first day, hydrogen sulfide loading was accompanied by a significant increase in the volume of the cell and its nucleus (Fig. 2). A rise amounted to 24.3 and 30.1%, respectively, and it was statistically significant ($p < 0.05$). It is clearly visible that the growth was close. This was evidenced by the fact that NCR values retained at the level of control ones. The cell surface area rose by almost 23% ($p < 0.05$) and reached ($1,275.5 \pm 99.6$) μm^2 . At the same time, the specific cell surface area (SS_c) did not change and averaged $1.53 \mu\text{m}^{-1}$. The number of free hematin granules in the hemolymph increased.

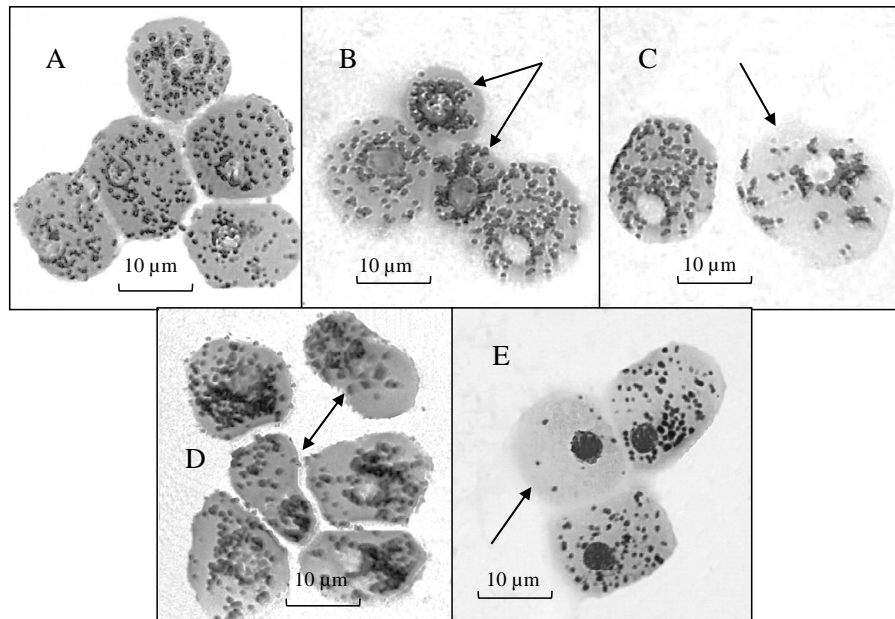


Fig. 1. Morphological types of cells in *Anadara kagoshimensis* hemolymph (A, normocytes; B, microcytes; C, macrocytes; D, cells with an altered shape; E, cells with a low number of granular inclusions)

On the second day of the experiment, the situation was the opposite. The cell volume decreased significantly (see Fig. 2): compared to control values, there was a drop by 36.4% ($p < 0.05$), and relative to the first day, by 48.9% ($p < 0.01$). The nucleus volume and erythrocyte surface area changed similarly. The changes were proportional which reflects the retention of NCR and SS_c values.

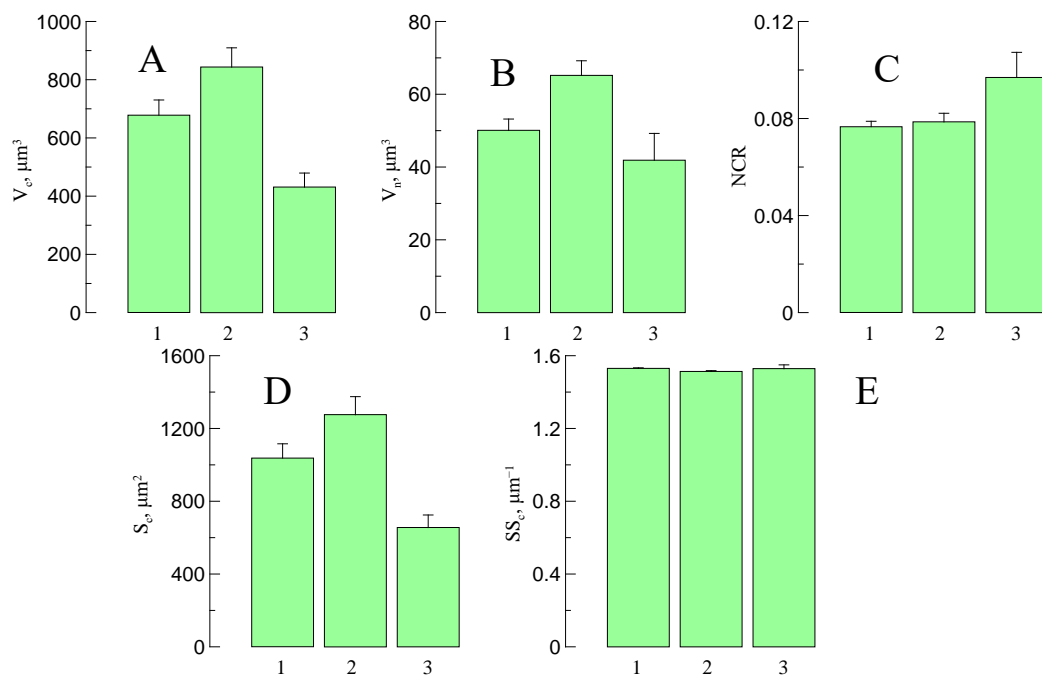


Fig. 2. Morphometric characteristics of erythroid elements of *Anadara kagoshimensis* hemolymph under conditions of hydrogen sulfide loading (A, V_c ; B, V_n ; C, NCR; D, S_c ; E, SS_c ; 1, the control group; 2, the first day of the experiment; 3, the second day of the experiment)

Morphological features. Analysis of the morphological features of erythroid cells showed a significant increase in the number of microcytes in the mollusc hemolymph under conditions of hydrogen sulfide loading (the first and second days of the experiment) (Fig. 1B, 3A). Those accounted for 6.6–7.0% of cells; it was almost three times higher than control values ($p < 0.05$). Microcytes were characterized by lower values of the transverse cell diameter (less than 15 μm). Interestingly, there was an increase in the number of macrocytes in the mollusc hemolymph on the first day by 30–32% ($p < 0.05$) (Fig. 3B). Their cell cross-section exceeded 22 μm (Fig. 1B).

Under conditions of hydrogen sulfide loading (the first day of the experiment), the number of erythrocyte abnormalities in the mollusc hemolymph rose. Cells with an altered shape and extremely low content of granular inclusions appeared (Fig. 1D, E). Their number increased by 30–50% relative to the control level (Fig. 3C, D). However, due to much individual variability in the obtained values, the differences were not statistically significant.

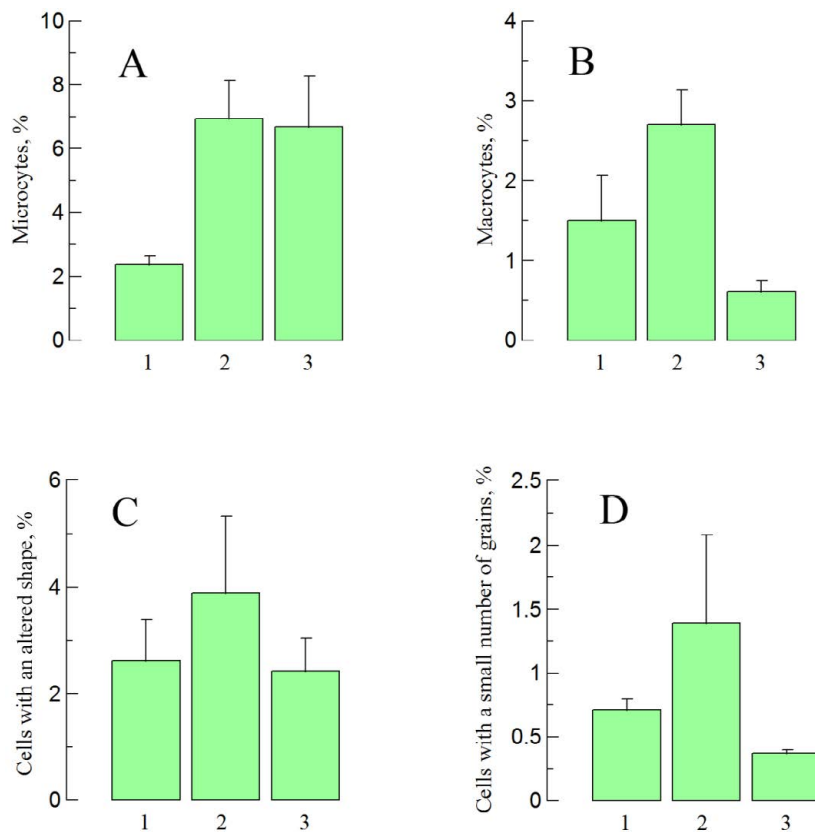


Fig. 3. Content of cells of various morphological types in *Anadara kagoshimensis* hemolymph under conditions of hydrogen sulfide loading (A, microcytes; B, macrocytes; C, cells with an altered shape; D, cells with a small number of grains; 1, the control group; 2, the first day of the experiment; 3, the second day of the experiment)

DISCUSSION

Double addition of Na_2S to the aquarium water where the molluscs were kept led to the development of an ambiguous situation:

- after the first day, moderate hypoxia occurred in water ($1.8 \text{ mg O}_2\cdot\text{L}^{-1}$), and hydrogen sulfide was not detected, which seems to be the consequence of the interaction of the latter one with oxygen;

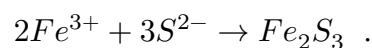
- repeated addition of Na_2S (the second day) resulted in the formation of anoxia with retention of hydrogen sulfide contamination at the level of $1.9 \text{ mg S}^{2-} \cdot \text{L}^{-1}$.

The state of the erythroid population of the mollusc cells in each case had its own specifics.

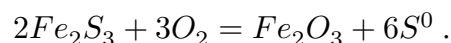
The first day of the experiment. Compared to the control, the erythroid cell population became more heterogeneous. This was evidenced by a significant increase in the content of macro- and microcytes in the hemolymph, a rise in the number of cells with an altered shape, and a reduced number of granular inclusions in the cytoplasm. The mean cell volume increased by more than 20%. A rise in V_c can be determined by several processes.

Considering that the bivalves were kept under conditions of moderate hypoxia, we can assume the development of a swelling reaction in red blood cells, which is observed in many hydrobionts, including molluscs [Holk, 1996; Jensen et al., 1998; Nikinmaa et al., 1987; Novitskaja, Soldatov, 2011]. This reaction is believed to be aimed at correcting the intracellular pH value and determined by the work of the Na^+/H^+ antiporter [Tufts, 1992]. The swelling is controlled by catecholamines (adrenaline and norepinephrine) and is implemented *via* cell β -adrenergic receptors and cAMP [Ferguson, Boutilier, 1988; Salama, Nikinmaa, 1990; Val et al., 1997]. In our case, an increase in the content of catecholamines in the mollusc hemolymph can be expected, since the transition to conditions of moderate hypoxia occurred in a relatively short period of time. However, this process can determine a growth of cell volume by no more than 5–6% [Nikinmaa et al., 1987], and this is not entirely consistent with the values of changes in V_c provided in this work ($> 20\%$). Even taking into account the higher elasticity of cell membranes of molluscs, indirectly evidenced by a wider range of osmotic resistance of their erythroid elements [Novitskaja, Soldatov, 2011], this increase can be considered as excessive.

Interestingly, there was a rise in the number of macrocytes in *A. kagoshimensis* hemolymph with the diameter exceeding $22 \mu\text{m}$. A gain in the level of these cellular forms may explain such an increase in the mean cell volume (V_c). Their occurrence in a mollusc hemolymph usually precedes the apoptosis, when a cell disintegrates into separate fragments (apoptotic bodies) [Manskikh, 2007]. In the case of *A. kagoshimensis*, this reaction has the meaning of adaptation [Soldatov et al., 2018]: when a cell is destroyed, hematin-containing granular inclusions are released in a significant amount into the hemolymph [Holden et al., 1994; Vismann, 1993]. Hematins have a high oxidizing ability and can interact with hydrogen sulfide [Vismann, 1993]. The most likely product of this interaction is ferric sulfide:



It is an unstable compound that, in the presence of oxygen, is oxidized to ferric oxide releasing atomic sulfur:



As known, some species of marine invertebrates are capable of accumulating sulfur under conditions of hydrogen sulfide contamination [Powell et al., 1980]. This allows us to assume the sequence of events discussed above. A rise in the content of erythrocytes with a reduced number of granular inclusions in *A. kagoshimensis* hemolymph under conditions of hydrogen sulfide loading also gives us the grounds to make an assumption on the ability of these cells to remove hematin granules beyond their membranes not violating their integrity.

The second day of the experiment. Distinctive features of the population of erythroid elements of *A. kagoshimensis* hemolymph on the second day were the high content of microcytes in it and a significant decrease in the mean cell volume (V_c). Apparently, the latter was determined by a drop in the number of macrocytes in the mollusc hemolymph, since the content of microcytes on the first and second days of the experiment was close. An increase in the number of microcytes in the hemolymph may be due to several processes.

The first process is fragmentation of the cytoplasm areas of red blood cells leading to the formation of schistocytes. In this case, the cell size decreases (microcytes are formed). This phenomenon was noted for organisms at various levels of organization, including humans [Bessman, 1988]. It is usually observed during the development of anemia states. It was also shown for *A. kagoshimensis* under conditions of external anoxia [Soldatov et al., 2021]. Apparently, this is the main process that results in the formation of a large number of microcytes in the mollusc hemolymph in a relatively short time.

The process close to fragmentation is direct division of highly specialized cells (amitosis), *inter alia* erythrocytes. It involves a random distribution of nucleus material [Fuller, Shields, 1998]. A particular manifestation of this process is the formation of anucleate cells and microcytes. It occurs if the nucleus, *prior* to cytokinesis (formation of a constriction), moves towards one of the cell poles. This phenomenon was described for *A. kagoshimensis* as well [Novitskaya, Soldatov, 2013]. It can also be observed in cells with an altered shape in the present work (Fig. 1D).

The formation of microcytes is also possible during intensive hematopoiesis (erythropoiesis); it is most often observed under conditions of oxygen deficiency similar to those for *A. kagoshimensis*. However, data on this issue in relation to molluscs are extremely scarce [Furuta, Yamaguchi, 2001], which does not allow us to accept this interpretation as a basis.

Conclusion. Under conditions of short-term hydrogen sulfide loading (the first day), the population of *Anadara kagoshimensis* erythroid elements becomes more heterogeneous. In the hemolymph, the content of micro- and macrocytes increases, and the number of cells with an altered shape and low content of granular inclusions in the cytoplasm rises. The number of free hematin granules in the mollusc hemolymph increases noticeably. The mean cell volume (V_c) rises by more than 20%. Staying under conditions of increased sulfide concentration within the second day results in a significant decrease in V_c , which is determined by a notable reduction in the population of macrocytes in *A. kagoshimensis* hemolymph.

This work was carried out within the framework of IBSS state research assignment "Functional, metabolic, and molecular genetic mechanisms of marine organism adaptation to conditions of extreme ecotopes of the Black Sea, the Sea of Azov, and other areas of the World Ocean" (No. 124030100137-6).

REFERENCES

1. Zaika V. E., Konovalov S. K., Sergeeva N. G. The events of local and seasonal hypoxia at the bottom of the Sevastopol bays and their influence on macrobenthos. *Morskoy ekologicheskij zhurnal*, 2011, vol. 10, no. 3, pp. 15–25. (in Russ.). <https://repository.marine-research.ru/handle/299011/1167>
2. Kiseleva M. I. Sravnitel'naya kharakteristika donnykh soobshchestv u beregov Kavkaza. *Mnogoletnie izmeneniya zoobentosa Chernogo morya*. Kyiv : Naukova dumka, 1992, pp. 84–99. (in Russ.). <https://repository.marine-research.ru/handle/299011/5644>
3. Manskikh V. N. Pathways of cell death and their biological importance. *Tsitologiya*, 2007, vol. 49, no. 11, pp. 909–915. (in Russ.)

4. Novitskaja V. N., Soldatov A. A. Erythroid elements of hemolymph in *Anadara inaequivalvis* (Mollusca: Arcidae) under conditions of experimental anoxia: Functional and morphometric characteristics. *Morskoj ekologicheskij zhurnal*, 2011, vol. 10, no. 1, pp. 56–64. (in Russ.). <https://repository.marine-research.ru/handle/299011/1138>
5. Orekhova N. A., Konovalov S. K. Oxygen and sulfides in bottom sediments of the coastal Sevastopol region of Crimea. *Okeanologiya*, 2018, vol. 58, no. 5, pp. 739–750. (in Russ.). <https://doi.org/10.1134/S0030157418050106>
6. Podymov O. I. *Kolichestvennye otsenki gidrokhimicheskikh kharakteristik redoks-sloya Chernogo morya s pomoshch'yu problemno orientirovannoi bazy dannykh* : avtoref. dis. ... kand. fiz.-mat. nauk : 25.00.28. Moscow, 2005, 21 p. (in Russ.)
7. Revkov N. K. Colonization's features of the Black Sea basin by recent invader *Anadara kagoshimensis* (Bivalvia: Arcidae). *Morskoj biologicheskij zhurnal*, 2016, vol. 1, no. 2, pp. 3–17. (in Russ.). <https://doi.org/10.21072/mbj.2016.01.2.01>
8. Chizhevsky A. L. *Strukturnyi analiz dvizhu-shcheisya krovi*. Moscow : Izd-vo AN SSSR, 1959, 474 p. (in Russ.)
9. Arp A. J., Childress J. J. Blood function in the hydrothermal vent vestimentiferan tube worm. *Science*, 1981, vol. 213, no. 4505, pp. 342–344. <https://doi.org/10.1126/science.213.4505.342>
10. Arp A. J., Childress J. J. Sulfide binding by the blood of the hydrothermal vent tube worm *Riftia pachyptila*. *Science*, 1983, vol. 219, no. 4582, pp. 295–297. <https://doi.org/10.1126/science.219.4582.295>
11. Bessman J. D. Red blood cell fragmentation: Improved detection and identification of causes. *American Journal of Clinical Pathology*, 1988, vol. 90, iss. 3, pp. 268–273. <https://doi.org/10.1093/ajcp/90.3.268>
12. Buck L. T. Succinate and alanine as anaerobic end-products in the diving turtle (*Chrysemys picta bellii*). *Comparative Biochemistry and Physiology Part B: Biochemistry and Molecular Biology*, 2000, vol. 126, iss. 3, pp. 409–413. [https://doi.org/10.1016/s0305-0491\(00\)00215-7](https://doi.org/10.1016/s0305-0491(00)00215-7)
13. Chew S. F., Gan J., Ip Y. K. Nitrogen metabolism and excretion in the swamp eel, *Monopterus albus*, during 6 or 40 days of estivation in mud. *Physiological and Biochemical Zoology*, 2005, vol. 78, no. 4, pp. 620–629. <https://doi.org/10.1086/430233>
14. Cortesi P., Cattani O., Vitali G. Physiological and biochemical responses of the bivalve *Scapharca inaequivalvis* to hypoxia and cadmium exposure: Erythrocytes versus other tissues. In: *Marine Coastal Eutrophication* : proceedings of an International Conference, Bologna, Italy, 21–24 March, 1990. Amsterdam, the Netherlands : Elsevier, 1992, pp. 1041–1054. <https://doi.org/10.1016/B978-0-444-89990-3.50090-0>
15. Ferguson R. A., Boutilier R. G. Metabolic energy production during adrenergic pH regulation in red cells of the Atlantic salmon, *Salmo salar*. *Respiration Physiology*, 1988, vol. 74, iss. 1, pp. 65–76. [https://doi.org/10.1016/0034-5687\(88\)90141-7](https://doi.org/10.1016/0034-5687(88)90141-7)
16. Fuller G. M., Shields D. *Molecular Basis of Medical Cell Biology*. Stamford, Connecticut : Appleton & Lange, 1998, 231 p.
17. Furuta E., Yamaguchi K. Haemolymph: Blood cell morphology and function. In: *The Biology of Terrestrial Molluscs* / G. M. Barker (Ed.). Wallingford, UK ; New York, USA : CABI Publishing, 2001, pp. 289–306. <http://doi.org/10.1079/9780851993188.0289>
18. Hochachka P. W., Somero G. N. *Biochemical Adaptation: Mechanism and Process in Physiological Evolution*. Oxford : Oxford University Press, 2002, 356 p.
19. Holden J. A., Pipe R. K., Quaglia A., Ciani G. Blood cells of the arcid clam, *Scapharca inaequivalvis*. *Journal of the Marine Biological Association of the United Kingdom*, 1994, vol. 74, iss. 2, pp. 287–299. <https://doi.org/10.1017/S0025315400039333>
20. Holk K. Effects of isotonic swelling on the intracellular Bohr factor and the oxygen affinity of trout and carp blood. *Fish Physiology and Biochemistry*, 1996, vol. 15, pp. 371–375. <https://doi.org/10.1007/BF01875579>
21. Houchin D. N., Munn J. I., Parnell B. L. A method for the measurement of red cell

- dimensions and calculation of mean corpuscular volume and surface area. *Blood*, 1958, vol. 13, no. 12, pp. 1185–1191. <https://doi.org/10.1182/blood.V13.12.1185.1185>
22. Isani G., Cattani O., Tacconi S. Energy metabolism during anaerobiosis and recovery in the posterior adductor muscle of the bivalve *Scapharca inaequivalvis* (Bruguère). *Comparative Biochemistry and Physiology Part B: Comparative Biochemistry*, 1989, vol. 93, iss. 1, pp. 193–200. [https://doi.org/10.1016/0305-0491\(89\)90235-6](https://doi.org/10.1016/0305-0491(89)90235-6)
 23. Jensen F. B., Fago A., Weber R. E. Hemoglobin structure and function. In: *Fish Respiration* / S. F. Perry, B. L. Tufts (Eds). San Diego, CA : Academic Press, 1998, pp. 1–40. (Fish Physiology ; vol. 17). [https://doi.org/10.1016/S1546-5098\(08\)60257-5](https://doi.org/10.1016/S1546-5098(08)60257-5)
 24. Miyamoto Y., Iwanaga C. Effects of sulphide on anoxia-driven mortality and anaerobic metabolism in the ark shell *Anadara kagoshimensis*. *Journal of the Marine Biological Association of the United Kingdom*, 2017, vol. 97, iss. 2, pp. 329–336. <https://doi.org/10.1017/S0025315416000412>
 25. Nakano T., Yamada K., Okamura K. Duration rather than frequency of hypoxia causes mass mortality in ark shells (*Anadara kagoshimensis*). *Marine Pollution Bulletin*, 2017, vol. 125, iss. 1–2, pp. 86–91. <https://doi.org/10.1016/j.marpolbul.2017.07.073>
 26. Nikinmaa M., Cech J. J., Ryhänen L., Salama A. Red cell function of carp (*Cyprinus carpio*) in acute hypoxia. *Experimental Biology*, 1987, vol. 47, iss. 1, pp. 53–58.
 27. Novitskaya V. N., Soldatov A. A. Peculiarities of functional morphology of erythroid elements of hemolymph of the bivalve mollusk *Anadara inaequivalvis*, the Black Sea. *Hydrobiological Journal*, 2013, vol. 49, iss. 6, pp. 64–71. <https://doi.org/10.1615/hydrobj.v49.i6.60>
 28. Powell E. N., Crenshaw M. A., Rieger R. W. Adaptations to sulfide in sulfide-system meiofauna. End-products of sulfide detoxification in three turbellarians and a gastrotrich. *Marine Ecology Progress Series*, 1980, vol. 2, pp. 169–177.
 29. Salama A., Nikinmaa M. Effect of oxygen tension on catecholamine-induced formation of cAMP and on swelling of carp red blood cells. *American Journal of Physiology–Cell Physiology*, 1990, vol. 259, iss. 5, pt 1, pp. C723–C726. <https://doi.org/10.1152/ajpcell.1990.259.5.c723>
 30. Soldatov A. A., Andreenko T. I., Sysoeva I. V., Sysoev A. A. Tissue specificity of metabolism in the bivalve mollusc *Anadara inaequivalvis* Br. under conditions of experimental anoxia. *Journal of Evolutionary Biochemistry and Physiology*, 2009, vol. 45, iss. 3, pp. 349–355. <https://doi.org/10.1134/S002209300903003X>
 31. Soldatov A. A., Kukhareva T. A., Andreeva A. Y., Efremova E. S. Erythroid elements of hemolymph in *Anadara kagoshimensis* (Tokunaga, 1906) under conditions of the combined action of hypoxia and hydrogen sulfide contamination. *Russian Journal of Marine Biology*, 2018, vol. 44, iss. 6, pp. 452–457. <https://doi.org/10.1134/S1063074018060111>
 32. Soldatov A., Kukhareva T., Morozova V., Richkova V., Andreyeva A., Bashmakova A. Morphometric parameters of erythroid hemocytes of alien mollusc *Anadara kagoshimensis* under normoxia and anoxia. *Ruthenica, Russian Malacological Journal*, 2021, vol. 31, no. 2, pp. 77–86. [https://doi.org/10.35885/ruthenica.2021.31\(2\).3](https://doi.org/10.35885/ruthenica.2021.31(2).3)
 33. Tufts B. *In vitro* evidence for sodium-dependent pH regulation in sea lamprey (*Petromyzon marinus*) red blood cell. *Canadian Journal of Zoology*, 1992, vol. 70, no. 3, pp. 411–416. <http://doi.org/10.1139/z92-062>
 34. Val A. L., De Menezes G. C., Wood C. M. Red blood cell adrenergic responses in Amazonian teleosts. *Journal of Fish Biology*, 1997, vol. 52, iss. 1, pp. 83–93. <https://doi.org/10.1111/j.1095-8649.1998.tb01554.x>
 35. Vismann B. Hematin and sulfide removal in hemolymph of the hemoglobin-containing bivalve *Scapharca inaequivalvis*. *Marine Ecology Progress Series*, 1993, vol. 98, pp. 115–122. <http://doi.org/10.3354/meps098115>

**МОРФОМЕТРИЧЕСКИЕ ХАРАКТЕРИСТИКИ ЭРИТРОИДНЫХ ЭЛЕМЕНТОВ
ГЕМОЛИМФЫ *ANADARA KAGOSHIMENSIS* (ТОКУНАГА, 1906)
В УСЛОВИЯХ СЕРОВОДОРОДНОГО ЗАРАЖЕНИЯ**

А. А. Солдатов^{1,2}, В. Н. Рычкова¹, Т. А. Кухарева¹

¹ФГБУН ФИЦ «Институт биологии южных морей имени А. О. Ковалевского РАН»,
Севастополь, Российская Федерация

²Севастопольский государственный университет, Севастополь, Российская Федерация
E-mail: alekssoldatov@yandex.ru

В условиях эксперимента исследовали влияние сероводородной нагрузки на морфометрические характеристики эритроидных элементов гемолимфы *Anadara kagoshimensis* (Tokunaga, 1906). Работа выполнена на взрослых особях моллюска с высотой раковины 26–38 мм. Контрольную группу моллюсков содержали в аквариуме с концентрацией кислорода 7,0–7,1 мг $O_2 \cdot л^{-1}$ (нормоксия). Экспериментальную группу подвергали действию сероводородной нагрузки, создававшейся при растворении в воде донора Na_2S до финальной концентрации 6 мг $S^{2-} \cdot л^{-1}$. Спустя сутки уровень кислорода в воде составил 1,8 мг $O_2 \cdot л^{-1}$, а сероводород не был обнаружен. Часть моллюсков подвергали повторной сероводородной нагрузке путём внесения Na_2S до финальной концентрации 9 мг $S^{2-} \cdot л^{-1}$. К концу вторых суток в воде регистрировали 1,9 мг $S^{2-} \cdot л^{-1}$ и следовую концентрацию кислорода — 0,03 мг $O_2 \cdot л^{-1}$. В условиях краткосрочной сероводородной нагрузки (первые сутки) популяция эритроидных элементов анадары становилась более гетерогенной. В гемолимфе повышалось содержание микро- и макроцитов, увеличивалось число клеток с изменённой формой и низким содержанием зернистых включений в цитоплазме. Число свободных гранул гематина в гемолимфе существенно росло. Среднеклеточный объём (V_c) увеличивался более чем на 20 %. Пребывание в условиях повышенной концентрации сульфидов в течение двух суток приводило к значительному понижению V_c , что определяется существенным сокращением популяции макроцитов в гемолимфе моллюсков.

Ключевые слова: моллюски, *Anadara kagoshimensis*, сероводород, гемолимфа, эритроидные элементы

UDC 574.58(265.57)

MARINE ALGAL FLORA OF THE SOUTHERN ISLANDS OF JAPAN

© 2024 E. Titlyanov¹, T. Titlyanova¹, O. Belous¹, and M. Tokeshi²

¹A. V. Zhirmunsky National Scientific Center of Marine Biology FEB RAS, Vladivostok, Russian Federation

²Amakusa Marine Biological Laboratory, Kyushu University, Reihoku-Amakusa, Kumamoto, Japan

E-mail: ksu_bio@mail.ru

Received by the Editor 20.01.2023; after reviewing 28.03.2023;
accepted for publication 09.10.2023; published online 22.03.2024.

In 1995–2019, marine algae were sampled in the intertidal and upper subtidal zones of the Amakusa Archipelago (Shimoshima islands) and the southern islands of the Ryukyu Archipelago (Okinawa, Sesoko, Ieshima, Akajima, Miyako, Ishigaki, Iriomote, and Yonaguni). A total of 569 species and taxonomic forms of benthic macroalgae were identified. Out of them, 57% belonged to red algae; 15%, to brown algae; and 28%, to green algae. On these islands, 153 taxa were found for the first time. During the specified period, the benthic marine flora of individual islands was analyzed with varying degrees of care. The most thoroughly studied island of the Amakusa group was Shimoshima (14 localities during all seasons), and of the Ryukyu Archipelago, Sesoko (8 localities during all seasons). The comparison of taxonomic and biogeographic characteristics of marine floras of these two archipelagos – biodiversity of species and forms, taxonomic composition of algal communities, and potential capabilities of geographic (latitudinal) distribution of taxa – give us the grounds to classify the Shimoshima Island as a warm-temperate region of the Northern Hemisphere in East Asia, and the southern islands of the Ryukyu Archipelago, as a tropical biogeographic region.

Keywords: macroalgae, Amakusa Archipelago, southern islands of the Ryukyu Archipelago, comparison of the marine flora

The southern islands of Japan are situated in warm waters of two biogeographic regions of the Northern Hemisphere – Indo-West Pacific warm-temperate region and tropical region – in geographic latitudes from 32°23'N to 24°03'N, according to the scheme of J. C. Briggs [1974] modified by K. Lüning [1990] (Fig. 1).

The benthic marine flora of the southern islands of Japan has been fairly well studied mainly by Japanese algologists since 1897 [Okamura, 1897, 1930] and during the 1930s–2000s (see Supplement 1: <https://marine-biology.ru/mbj/article/view/422/655>). Only one work was dedicated to the benthic flora of Amakusa islands [Segawa, Yoshida, 1961].

The authors of the present article initiated the research on the benthic flora of the islands of the Ryukyu Archipelago in 1995 within the framework of ecological studies of Sesoko Island coral reef ecosystem (the west of Northern Okinawa) at the Tropical Biosphere Research Center Sesoko Station of the University of the Ryukyus. In parallel to eco-physiological investigations, the study of the benthic marine flora of the Amakusa Archipelago (Shimoshima islands) and the Ryukyu Archipelago (Okinawa, Sesoko, Ieshima, Akajima, Miyako, Ishigaki, Iriomote, and Yonaguni) was carried out (Fig. 1).

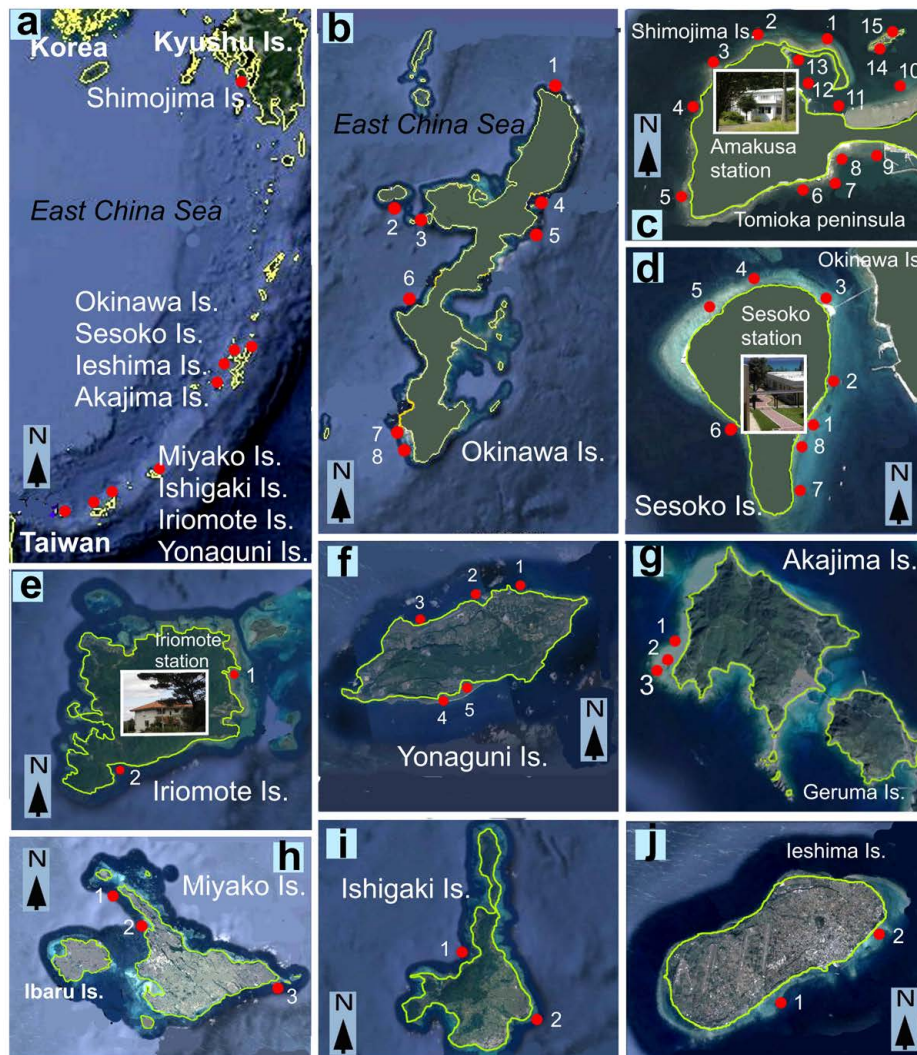


Fig. 1. Sites of algal sampling (marked with red circles) on islands of the Amakusa and Ryukyu archipelagos. A, islands where algae were sampled. B, sampling sites in Okinawa Prefecture: Cape Hedo (site 1); Ieshima Island (2); Sesoko Island (3); Oura Bay (4); Henoko point (5); Maeda coast (6); Arasaki Beach (7, 8); Ohdo coast (9). C, sampling sites along Tomioka Peninsula, Shimoshima Island: Magarizaki coast (1, 2); Akaiwa coast (3, 4); Shikizaki Bay (5); Shiraiwazaki Bay (6–8); Reihoku coast (9); Tomioka Harbor (10–13); Tsujishima Island (14, 15). D, sampling sites along Sesoko Island (1–8). E, sampling sites along Iriomote Island: Hoshidate coast (1); Kanoka coast (2). F, sampling sites along Yonaguni Island: Sonai locality (1–3); Higawa Bay (4); Tojima coast (5). G, sampling sites along Akajima Island, upper sub-tidal of the western coast (1–3). H, sampling sites along Miyako Island: Karimata coast (1, 2); Cape Higashi Hennasaki (3). I, sampling sites along Ishigaki Island: Shiraho coast (1); Kabira Bay (2). J, sampling sites along Ieshima Island, southeastern coast (1, 2)

Material partially published earlier provided the dynamics of algal growth on damaged and dead coral colonies in the sea and in aquariums of Sesoko Island [Titlyanov et al., 2008, 2010, 2018], decadal changes in algal assemblages of Yonaguni Island [Titlyanov et al., 2016], and historical changes in the marine flora of Tomioka Peninsula, Shimoshima Island [Titlyanov et al., 2019a, b]. For other islands we studied, the data are published for the first time.

The aim of this work was to present an annotated list of benthic algae in coral reef ecosystems of the Ryukyus and ecosystem of hard substrata with coral settlements of Amakusa islands, using all papers on the inventory of the benthic flora of the islands and our published and unpublished sampling data of 1995–2019. Moreover, based on a comparison of taxonomic and biogeographic characteristics

of recent benthic algal floras of the islands of these two archipelagos [diversity of species and forms, taxonomic composition of algal communities, and potential opportunities for geographical (latitudinal) distribution of taxa], we aimed at assigning them to specific biogeographic regions of the Northern Hemisphere in East Asia.

MATERIAL AND METHODS

Sampling sites and time. The study of the marine flora along the coast of Okinawa Island was carried out in November–December 2006 in the following localities: Cape Hedo, Oura Bay, Henoko point, Maeda coast, and Ohdo coast; in March 2013 and February 2014, the investigation was carried out along Arasaki Beach (Fig. 1B). In the west of Northern Okinawa, along the coast of Sesoko Island, algae were collected in 1995 (May–October), 1997 (September–December), 1998 (January–April), 2002 (October–December), 2003 (January–September), 2004 (July), 2005 (February–May), 2006 (November–December), 2007 (January), 2014 (February), and 2019 (January–February) (Fig. 1D). In December 2006, marine algae were sampled along the southeastern coast of Ieshima Island (Fig. 1J). In August 1995, algal sampling was carried out on a coral reef along the western coast of Akajima Island (the group of Kerama islands) at three localities (Kubamanohama, Kushibaru, and Hanase) (Fig. 1G), Kohama Island (the group of Yaeyama islands), and at two localities of Ishigaki Island (Kabira Bay and Shiraho Reef) (Fig. 1I). In March 2013, marine algae were sampled around Yonaguni Island (Sonai, Higawa, and Tojima bays) (Fig. 1F) and along the coast of Miyako Island (Kari-mata locality and Cape Higashi Hennasaki) (Fig. 1H). In February 2017, algal sampling was carried out along the coast of Iriomote Island (Hoshidate and Tanaka bays) (Fig. 1E). On Shimoshima Island, marine algae were sampled in November and December 2012, April and August 2013, January 2014, October and November 2015, and November 2017 at seven localities of Tomioka Peninsula: Akaiwa, Magarizaki, Shikizaki Bay, Shiraiwazaki Bay, Tomioka Harbor, Tsujishima Island, and Reihoku-cho (Fig. 1C).

Collection, conservation, and floristic analysis of samples. Macroalgae were sampled in the upper, middle, and lower intertidal and the upper subtidal (from 0.5-m to 4-m depth during low tide) zones of Ryukyu islands by T. Titlyanova, E. Titlyanov, and O. Belous; on Amakusa islands, by T. Titlyanova, E. Titlyanov, and M. Tokeshi. In the upper subtidal zone, marine plants were sampled *via* snorkeling (by T. Titlyanova) and scuba diving (by E. Titlyanov and M. Tokeshi) during low and high tides. Algae were collected from all types of substrata. The algal samples are deposited at the A. V. Zhir-munsky National Scientific Center of Marine Biology, Far Eastern Branch of the Russian Academy of Sciences (Vladivostok, Russian Federation).

Fresh and dried specimens were identified by T. Titlyanova, E. Titlyanov, and O. Belous using the data of monographic publications, floristic studies, and systematic articles cited in previous papers [Titlyanov et al., 2011; Titlyanova et al., 2012]. The systematics and nomenclature follow Algae-Base [2023]. Hierarchical classification of the phylum Rhodophyta is given according to [Saunders, Hommersand, 2004; Schneider, Wynne, 2013; Wynne et al., 2014]. The classification system of the phyla Chlorophyta and Ochrophyta is given in accordance with [Tsuda, 2003, 2006].

RESULTS

Species composition. The results of the present study are provided in Table (see Supplement 2: <https://marine-biology.ru/mbj/article/view/422/656>). It documents 569 species and taxonomic forms of benthic macroalgae sampled off the southern islands of Japan in 1995–2019; 153 species of marine

algae were new records for the Amakusa and Ryukyu archipelagos (see [Titlyanov et al., 2016, 2019a, b]). The phylum Rhodophyta (Rh in Fig. 2) was comprised of 4 classes, 17 orders, 47 families, 128 genera, and 324 species (57% of all species). The phylum Ochrophyta (Oc) was comprised of 2 classes, 10 orders, 16 families, 43 genera, and 86 species (15% of all species) belonging to the class Phaeophyceae. The phylum Chlorophyta (Ch) was comprised of 2 classes, 7 orders, 23 families, 49 genera, and 159 species (28% of all species) (Suppl. 2, Fig. 2).

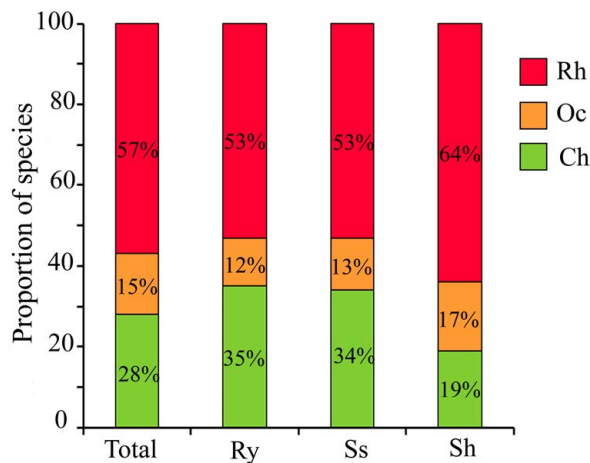


Fig. 2. Proportion of species and their taxonomic forms sampled along the islands of the Ryukyu and Amakusa archipelagos in 1995–2019. Ry, islands of the Ryukyu Archipelago; Ss, Sesoko Island; Sh, Shimoshima Island (the Amakusa Archipelago). Rh, Rhodophyta; Oc, Ochrophyta; Ch, Chlorophyta

Out of red algae, the highest number of taxa belonged to four orders: Ceramiales (129), Gigartinales (35), Corallinales (29), and Rhodymeniales (24). Brown algae were mostly represented by Ectocarpales (26), Dictyotales (22), and Fucales (23). Out of green algae, Bryopsidales (67), Cladophorales (47), and Ulvales (23) prevailed (Suppl. 2, Fig. 3A).

All species of our collection were found earlier by other authors in tropics and/or subtropics. Out of them, 79% were recorded in tropics and/or subtropic alone; 13% were registered in tropics and/or subtropics and in temperate latitudes as well; and 8% were noted in tropical and/or subtropical, temperate latitudes, and Arctic and/or Antarctic.

More than a half (58%) of all species of our collection were found in the seas of Pacific, Indian, and Atlantic oceans; 27% inhabited only the Indo-Pacific; and 15% inhabited only the seas of the Pacific Ocean (Fig. 4A).

On all investigated islands of the Ryukyu Archipelago, 428 species of marine algae were documented. Out of them, 54% were red algae, 12% were brown, and 34% were green (Suppl. 2, Fig. 2). Species of red algae belonged to 4 classes, 16 orders, 40 families, and 104 genera; species of brown algae, to 2 classes, 7 orders, 10 families, and 28 genera; and species of green algae, to 2 classes, 7 orders, 22 families, and 46 genera. In terms of species number, the richest families and orders were the following ones: out of red algae, Rhodomelaceae (50), Ceramiaceae (32), and families of Corallinales (23); out of brown algae, Dictyotaceae (17), Sargassaceae (11), and Scytosiphonaceae (6); and out of green algae, Caulerpaceae (23), Cladophoraceae (21), and Ulvaceae (13) (Suppl. 2, Fig. 3B). All species of our collection were previously found by other authors in tropics and/or subtropics. Out of them, 84% were registered only in tropical and/or subtropical latitudes; 8% were noted in temperate latitudes; and 8% were recorded in Arctic and/or Antarctic. Also, 28% of marine algae belonged to the Indo-Pacific, and 8% inhabited only the seas of the Pacific Ocean (Suppl. 2, Fig. 4B).

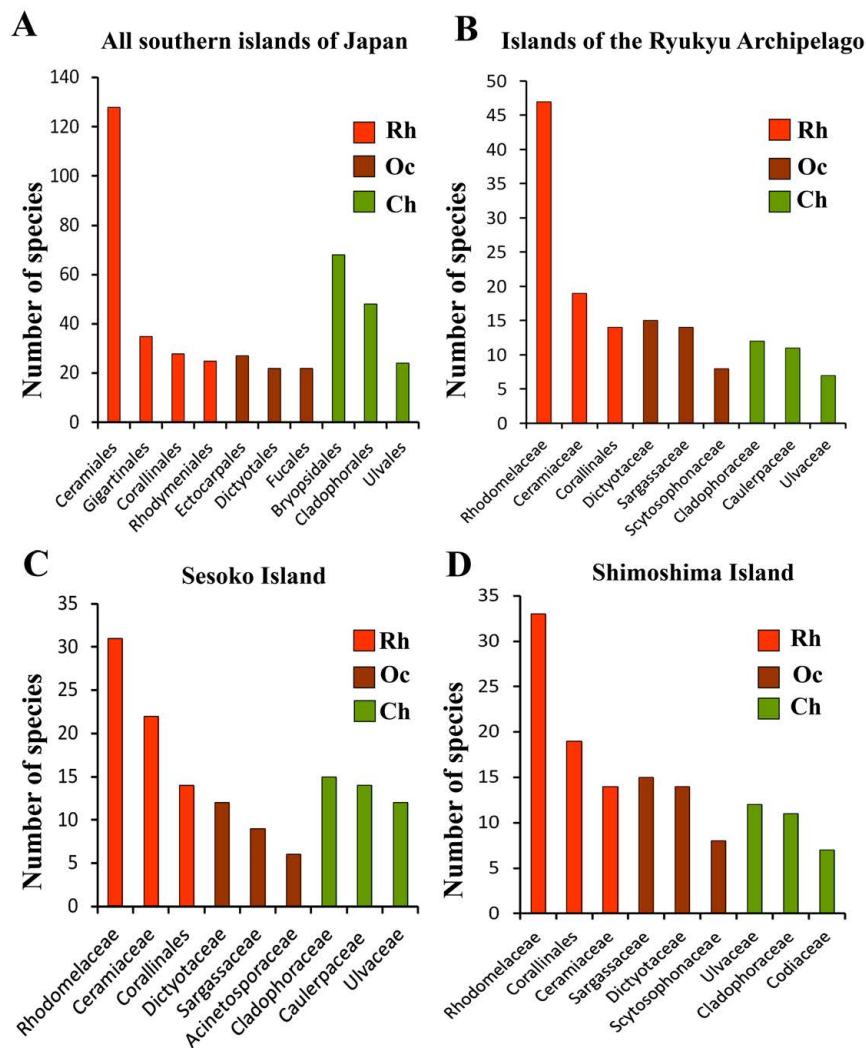


Fig. 3. Number of marine algal species in the richest taxa: A, all investigated southern islands of Japan; B, islands of the Ryukyu Archipelago; C, Sesoko Island; D, Shimoshima Island

Out of the islands of the Ryukyu Archipelago, the highest number of species (329) were sampled along the coast of Sesoko Island ($26^{\circ}38'N$, $127^{\circ}51'E$); out of them, 55% were red algae, 12% were brown, and 33% were green (Suppl. 2, Fig. 2). Species of red algae were represented by 4 classes, 16 orders, 38 families, and 94 genera; brown algae, by 2 classes, 7 orders, 10 families, and 26 genera; green algae, by 2 classes, 6 orders, 21 families, and 42 genera. The highest species richness was registered for the following orders and families. Out of red algae, Rhodomelaceae (32), Ceramiaceae (23), and families of Corallinales (14) prevailed; out of brown algae, Dictyotaceae (12), Sargassaceae (9), and Acinetosporaceae (5); and out of green algae, Cladophoraceae (14), Caulerpaceae (14), and Ulvaaceae (11) (Suppl. 2, Fig. 3C). In the collection representing Sesoko Island, 83% of all species belonged to tropics and/or subtropics alone; 8%, temperate latitudes; 9%, Arctic and/or Antarctic. Moreover, 28% of algae represented only the Indo-Pacific, and 7%, the seas of the Pacific Ocean (Suppl. 2, Fig. 4C).

Off the most northern island of investigated ones, Shimoshima (the largest island of the Amakusa Archipelago, $32^{\circ}31'N$, $130^{\circ}02'E$), located 6° north of Sesoko Island, we sampled 321 species and forms. Out of them, 63% were red algae, 17% were brown, and 20% were green (Suppl. 2, Fig. 2). Species of red algae represented 4 classes, 17 orders, 40 families, and 93 genera; species of brown algae,

1 class, 8 orders, 13 families, and 28 genera; and species of green algae, 1 class, 5 orders, 20 families, and 30 genera. The highest species richness was registered for the following families: out of red algae, Rhodomelaceae (33), families of Corallinales (20), and Ceramiaceae (13); out of brown algae, Sargassaceae (15), Dictyotaceae (14), and Scytosiphonaceae (8); out of green algae, Ulvaceae (12), Cladophoraceae (10), and Codiaceae (7) (Suppl. 2, Fig. 3D). In the collection of algae sampled off Shimoshima Island, 69% were tropical and/or subtropical species; 18% were species of temperate latitudes; and 13% were species of Arctic and/or Antarctic. Moreover, 22% inhabited only the Indo-Pacific, and 20% belonged to species inhabiting only the seas of the Pacific Ocean (Suppl. 2, Fig. 4D).

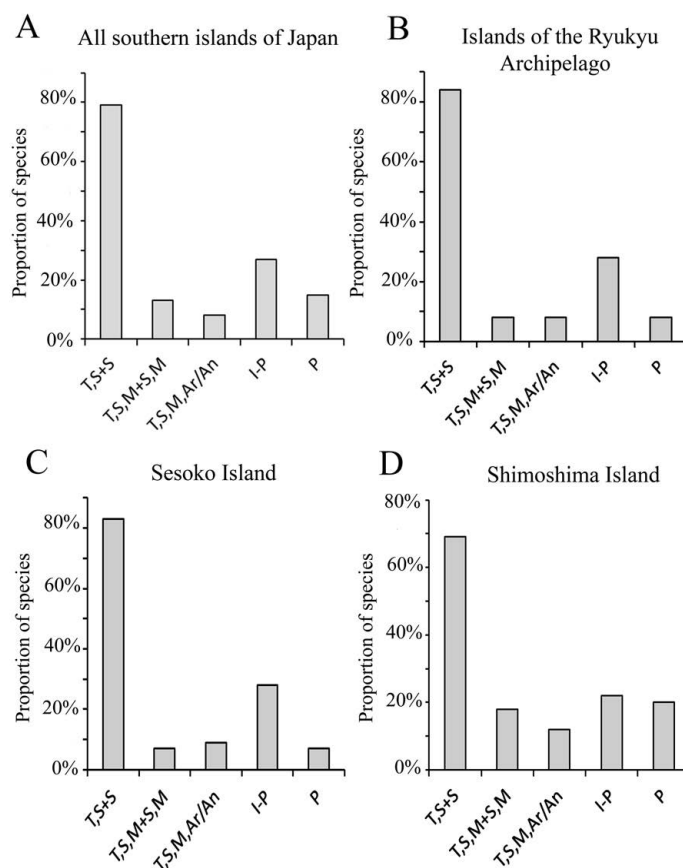


Fig. 4. Geographic distribution of marine algae off the southern islands of Japan. A, all investigated southern islands of Japan; B, islands of the Ryukyu Archipelago; C, Sesoko Island; D, Shimoshima Island. T, S + S, previously found inhabiting only the tropics and/or subtropics; T, S, M + S, M, previously found in tropical and/or subtropical and temperate latitudes; T, S, M, Ar / An, previously found in tropical and/or subtropical, temperate latitudes, and Arctic and/or Antarctic; I-P, inhabiting only the Indo-Pacific; P, found living only in the seas of the Pacific Ocean

DISCUSSION

The floristic diversity and composition of macrophytes from islands of the Ryukyu Archipelago sampled by us in 1995–2019 were close to those for other islands in the Indo-Pacific, where coral reefs are the main ecosystem, algal species richness is characterized by 400 taxa, and the floristic composition is reported to be as follows: 50–60% of red algae, 20–35% of green algae, and 10–20% of brown algae [Huisman, Borowitzka, 2003; Lewis, Norris, 1987; Silva, 1992; Silva et al., 1987, 1996; Tseng, 1983; Tsuda, 2003, 2006; Zhang, 1996].

Taxonomic diversity, species richness of above-mentioned families, a group of species, or an indicator species of coral ecosystems of the seas of Southeast Asia, and potential latitudinal distribution of marine algae of the Ryukyu Archipelago are close to those of other coral reefs studied by us in the South China and East China seas lying in tropical and subtropical latitudes [Belous et al., 2021; Titlyanov et al., 2011, 2014, 2015, 2016; Titlyanova et al., 2014].

Taxonomic characteristics of the benthic marine flora on Shimoshima Island of the Amakusa Archipelago differed significantly from those for the southern islands of the Ryukyu Archipelago. On the Amakusa Archipelago, the relative number of red algae was higher by 9%, and brown algae, by 5%. At the same time, the relative number of green algae was lower by 14% than on Ryukyu islands. Taxonomic diversity of green algae on Shimoshima Island was significantly lower than that for the southern islands of the Ryukyu Archipelago: the values were lower by 1 class, 2 orders, 2 families, 16 genera, and 82 species. Moreover, green algae of two archipelagos differed in composition of families with the highest species richness. Specifically, on Ryukyu islands, those were Cladophoraceae, Caulerpaceae, and Ulvaceae; on Amakusa islands, Ulvaceae, Cladophoraceae, and Codiaceae. Algal collections from the archipelagos differed in relative number of species belonging to various geographical zones. The collection from Shimoshima Island contains less species (by 14%) representing tropics and subtropics alone than the collection from Ryukyu islands, as well as relatively more species belonging to temperate latitudes (by 11%) and Arctic and/or Antarctic (by 3%). Also, there are 13% more species which inhabit only the seas of the Pacific Ocean.

According to the scheme of marine biogeographic regions provided by J. C. Briggs [1974] and modified by K. Lüning [1990], Kyushu Island and the Amakusa Archipelago (southern islands of Japan) are located on the border between the warm-temperate region and cold-temperate region, and the southern islands of the Ryukyu Archipelago are situated on the border between the warm-temperate region and tropical biogeographic region. Data presented by us on taxonomic diversity of marine algae on the Amakusa and Ryukyu archipelagos give the grounds to suppose that the recent benthic flora of these archipelagos belongs to two different biogeographic regions.

As known, the marine flora of biogeographic temperate regions in both hemispheres differs in species diversity and the values of R/P index (number of Rhodophyta species divided by number of Phaeophyceae species) and C/P index (number of Chlorophyta species divided by number of Phaeophyceae species) [Belous et al., 2013; Lewis, Norris, 1987; Nguyen et al., 2013; Perestenko, 1980, 1994; Pham, 1969; Santelices et al., 2009; Titlyanov et al., 2015; Titlyanova et al., 2014]. It can be summarized that an average of about 200 species of benthic macroalgae were found in the cold-temperate region, and more than 400 species were recorded in the tropical biogeographical region. Both in the Northern and Southern hemispheres, the marine flora of cold waters is enriched with brown algae, and the flora of warm waters is enriched with red and green algae. The indices R/P and C/P in a given flora are very important characteristics of biogeographic regions. Their values for the marine flora of cold waters are 1.0–2.0 and 0.3–0.8, respectively; for the marine flora of warm waters, 2.5–4.0 and 0.5–1.0, respectively; and for the marine flora of tropical waters, 3.0–4.5 and 1.0–2.0, respectively [Santelices et al., 2009].

One of key indicators of the benthic flora in the tropical biogeographic region is the richness of algal species and forms in families of the order Ceramiales (Rhodophyta) and in Caulerpaceae, Boodleaceae, and Valoniaceae (Chlorophyta) [Belous et al., 2021; Titlyanov et al., 2015]. Main identification characteristic of the benthic flora of the warm-temperate region in the Northern Hemisphere in East Asia is the most actively settling representative of the warm-water genus *Sargassum* C. Agardh, 1820 [Belous et al., 2013].

Our sampling in 2012–2017 on Shimoshima Island [Titlyanov et al., 2019a] allowed documenting more than 300 species of benthic macroalgae with a significant prevalence of red algae (63%) over brown and green algae. R/P value for sampled algae was 3.6, and C/P value was 1.1. Those correspond to the flora of warm-temperate regions and give us the grounds to classify Shimoshima Island of the Amakusa Archipelago, with its benthic flora, as part of the warm-temperate region.

On Sesoko Island, 6° south of Shimoshima Island, in 1995–2019, we recorded more than 300 species and forms of marine algae, with red and green algae prevailing. R/P value of sampled algae was 4.4, and C/P value was 2.6. All found species belonged to tropical latitudes; in these calculations, we also used material from our earlier works [Titlyanov et al., 2008, 2010, 2018, 2019b]. In the collection, species of red and green algae of tropic-specific families prevailed: Rhodomelaceae, Ceramiaceae (Rhodophyta), and Caulerpanceae (Chlorophyta).

On Yonaguni Island (southwest of Okinawa islands, 8° south of Shimoshima Island), only at three localities, we sampled about 200 species of marine algae; out of them, as well as on Sesoko Island, red (59%) and green algae (31%) prevailed. R/P value was 6.1, and C/P value was 3.2 [Titlyanov et al., 2016]. Thus, the main indicators of the taxonomic diversity of benthic floras for the most studied islands, Sesoko and Yonaguni, give us the grounds to assign the southern islands of the Ryukyu Archipelago (from N26° and south), with their benthic flora, to the tropical biogeographic region.

Conclusion. A total of 569 species of marine benthic algae were found off the southern islands of Japan; out of them, 153 species were registered for the first time. The comparison of taxonomic and biogeographic characteristics of marine floras of the Amakusa and Ryukyu archipelagos – biodiversity of species and forms, taxonomic composition of algal communities, and potential capabilities of geographic distribution of taxa – give us the grounds to classify Shimoshima Island as a warm-temperate region of the Northern Hemisphere in East Asia, and the southern islands of the Ryukyu Archipelago, as a tropical biogeographic region.

REFERENCES

1. *AlgaeBase*. World-wide electronic publication, National University of Ireland, Galway / M. D. Guiry, G. M. Guiry (Eds) : [site], 2023. URL: <http://www.algaebase.org> [accessed: 10.01.2023].
2. Belous O. S., Titlyanova T. V., Titlyanov E. A. *Morskije rasteniya bukhty Troitsy i smezhnykh akvatorii (zaliv Petra Velikogo, Yaponskoe more)*. Vladivostok : Dal'nauka, 2013, 263 p. (in Russ.). <http://www.algae.ru/350>
3. Belous O. S., Titlyanov E. A., Titlyanova T. V. Decadal comparison (1950–2020) of the benthic marine flora from Central and Southern Vietnam. *Phytotaxa*, 2021, vol. 21, no. 4, pp. 249–288. <https://doi.org/10.11646/phytotaxa.521.4.3>
4. Briggs J. C. *Marine Zoogeography*. New York, NY : McGraw-Hill, 1974, 475 p.
5. Huisman J. M., Borowitzka M. A. Marine benthic flora of the Dampier Archipelago, Western Australia. In: *The Marine Flora and Fauna of Dampier* / F. E. Wells, D. I. Walker, D. S. Jones (Eds). Perth, Western Australia : Western Australian Museum, 2003, pp. 291–344.
6. Lewis J. E., Norris J. N. *A History and Annotated Account of the Benthic Marine Algae of Taiwan*. Washington, DC : Smithsonian Institution Press, 1987, 38 p. (Smithsonian Contributions to the Marine Sciences : no. 29).
7. Lüning K. *Seaweeds. Their Environment, Biogeography and Ecophysiology*. Hoboken, NJ : John Wiley & Sons, 1990, 527 p.
8. Nguyen V. T., Le N. H., Lin S.-M., Steen F., De Clerck O. Checklist of the marine macroalgae of Vietnam. *Botanica Marina*, 2013, vol. 56, iss. 3, pp. 207–302. <https://doi.org/10.1515/bot-2013-0010>

9. Okamura K. On the algae from Ogasawara-jima (Bonin Islands). *Botanical Magazine*, 1897, vol. 11, nos 119–120, pp. 1–10, 11–17. <https://doi.org/10.15281/jplantres1887.11.en1>
10. Okamura K. On the algae from the Island Hatidyo. *Records of Oceanographic Works in Japan*, 1930, vol. 2, pp. 92–110.
11. Perestenko L. P. *Vodorosli zaliva Petra Velikogo*. Leningrad : Nauka, 1980, 232 p. (in Russ.). <http://www.algae.ru/273>
12. Perestenko L. P. *Red Algae of the Far-Eastern Seas of Russia*. Saint Petersburg : “Olga”, 1994, 330 p. (in Russ.). <http://www.algae.ru/270>
13. Pham H. H. *Marine Algae of South Vietnam*. Saigon : Center for Science and Technology, 1969, 558 p. (in Vietnamese).
14. Santelices B., Bolton J. J., Meneses I. Marine Algal Communities. In: *Marine Macroecology* / J. D. Witman, K. Roy (Eds). Chicago, IL : Chicago University Press, 2009, chap. 6, pp. 153–192. <https://doi.org/10.7208/chicago/9780226904146.003.0006>
15. Saunders G. W., Hommersand M. H. Assessing red algal supraordinal diversity and taxonomy in the context of contemporary systematic data. *American Journal of Botany*, 2004, vol. 91, iss. 10, pp. 1494–1507. <https://doi.org/10.3732/ajb.91.10.1494>
16. Segawa S., Yoshida T. *Fauna and Flora of the Sea Around the Amakusa Marine Biological Laboratory*. Pt 3. *Marine Algae*. Amakusa, Japan : Tomioka, Reihokucho-cho, 1961, 24 p. (in Japanese).
17. Schneider C. W., Wynne M. J. Second addendum to the synoptic review of red algal genera. *Botanica Marina*, 2013, vol. 56, iss. 2, pp. 111–118. <https://doi.org/10.1515/bot-2012-0235>
18. Silva P. C. Geographic patterns of diversity in benthic marine algae. *Pacific Science*, 1992, vol. 46, no. 4, pp. 429–437. <http://hdl.handle.net/10125/1869>
19. Silva P. C., Basson P. W., Moe R. L. *Catalogue of the Benthic Marine Algae of the Indian Ocean*. Berkeley ; Los Angeles ; London : University of California Press, 1996, 1280 p. (University of California Publications in Botany ; vol. 79).
20. Silva P. C., Menez E. G., Moe R. L. *Catalog of the Benthic Marine Algae of the Philippines*. Washington, DC : Smithsonian Institution Press, 1987, 179 p. (Smithsonian Contributions to the Marine Sciences : no. 27).
21. Titlyanov E. A., Titlyanova T. V., Chapman D. J. Dynamics and patterns of algal colonization on mechanically damaged and dead colonies of the coral *Porites lutea*. *Botanica Marina*, 2008, vol. 51, iss. 4, pp. 285–296. <https://doi.org/10.1515/BOT.2008.042>
22. Titlyanov E. A., Titlyanova T. V., Belous O. S. Checklist of the marine flora of Nha Trang Bay (Vietnam, South China Sea) and decadal changes in the species diversity composition between 1953 and 2010. *Botanica Marina*, 2015, vol. 58, iss. 5, pp. 367–377. <https://doi.org/10.1515/bot-2014-0067>
23. Titlyanov E. A., Titlyanova T. V., Tokeshi M. Marine plants in coral reef ecosystems of Southeast Asia. *Global Journal of Science Frontier Research—C Biology*, 2018, vol. 18, iss. C1, pp. 1–34.
24. Titlyanov E. A., Titlyanova T. V., Tokeshi M. Recent (2012–2017) seaweed flora of Tomioka Peninsula, Shimoshima Island (the East China Sea, Japan). *Coastal Ecosystems*, 2019a, vol. 6, pp. 1–21.
25. Titlyanov E. A., Titlyanova T. V., Tokeshi M., Li X. Inventory and historical changes in the marine flora of Tomioka Peninsula (Amakusa Island), Japan. *Diversity*, 2019b, vol. 11, iss. 9, art. no. 158 (15 p.). <https://doi.org/10.3390/d11090158>
26. Titlyanov E. A., Titlyanova T. V., Xia B. M., Bartsch I. Checklist of marine benthic green algae (Chlorophyta) on Hainan, a subtropical island off the coast of China: Comparisons between the 1930s and 1990–2009 reveal environmental changes. *Botanica Marina*, 2011, vol. 54, iss. 6, pp. 523–535. <https://doi.org/10.1515/bot.2011.064>
27. Titlyanov E. A., Kiyashko S. I., Titlyanova T. V., Raven J. A. $\delta^{13}\text{C}$ and $\delta^{15}\text{N}$ in tissue of coral polyps and epilithic algae inhabiting damaged coral colonies under the influence of different light intensities. *Aquatic Ecology*, 2010, vol. 44,

- iss. 1, pp. 13–21. <https://doi.org/10.1007/s10452-009-9248-5>
28. Titlyanov E. A., Titlyanova T. V., Li X. B., Hansen G. I., Huang H. Seasonal changes in the benthic macroalgae and Cyanobacteria of the intertidal zone in Sanya Bay (Hainan Island, China). *Journal of the Marine Biological Association of the United Kingdom*, 2014, vol. 94, iss. 5, pp. 879–893. <https://doi.org/10.1017/S0025315414000460>
29. Titlyanov E. A., Titlyanova T. V., Kalita T. L., Tokeshi M. Decadal changes in the algal assemblages of tropical-subtropical Yonaguni Island in the western Pacific. *Coastal Ecosystems*, 2016, vol. 3, pp. 16–37.
30. Titlyanova T. V., Titlyanov E. A., Xia B., Bartsch I. New records of benthic marine green algae (Chlorophyta) for the island of Hainan (China). *Nova Hedwigia*, 2012, Bd. 94, Heft 3–4, S. 441–470. <https://doi.org/10.1127/0029-5035/2012/0022>
31. Titlyanova T. V., Titlyanov E. A., Kalita T. L. Marine algal flora of Hainan Island: A comprehensive synthesis. *Coastal Ecosystems*, 2014, vol. 1, pp. 28–53.
32. Tseng C. K. *Common Seaweeds of China*. Beijing : Science Press, 1983, 316 p.
33. Tsuda R. T. *Checklist and Bibliography of the Marine Benthic Algae from the Mariana Islands (Guam and CNMI)*. Mangilao, Guam : University of Guam Marine Laboratory, 2003, 49 p. (Technical Report ; no. 107).
34. Tsuda R. T. *Checklist and Bibliography of the Marine Benthic Algae Within Chuuk, Pohnpei, and Kosrae States, Federated States of Micronesia*. Honolulu, Hawaii : Bishop Museum Press, 2006, 43 p. (Bishop Museum Technical Report ; no. 34). <http://pbs.bishopmuseum.org/pdf/tr34.pdf>
35. Wynne M. J., Bradshaw T., Carrington C. M. S. A checklist of the benthic marine algae of Barbados, West Indies. *Botanica Marina*, 2014, vol. 57, iss. 3, pp. 167–184. <https://doi.org/10.1515/bot-2014-0007>
36. Zhang S. The species and distribution of seaweeds in the coast of China seas. *Chinese Biodiversity Science*, 1996, vol. 4, iss. 3, pp. 139–144. <https://doi.org/10.17520/biods.1996025>

МОРСКАЯ ФЛОРА ЮЖНЫХ ОСТРОВОВ ЯПОНИИ

Э. А. Титлянов¹, Т. В. Титлянова¹, О. С. Белоус¹, М. Токеши²

¹Национальный научный центр морской биологии имени А. В. Жирмунского ДВО РАН, Владивосток, Российская Федерация

²Морская биологическая лаборатория Амаксы, Университет Кюсю, Рейкоку-Амакса, Кумамото, Япония
E-mail: ksu_bio@mail.ru

С 1995 по 2019 г. на литорали и в верхней сублиторали архипелага Амакса (остров Симосима) и южных островов архипелага Рюкю (Окинава, Сесоко, Иэдзима, Акадзима, Мияко, Исигаки, Ириомоте и Йонагуни) были собраны морские водоросли. Всего обнаружено 569 видов и таксономических форм бентосных макроводорослей, из них 57 % принадлежат к красным водорослям, 15 % — к бурым, 28 % — к зелёным. Новыми для этих островов были 153 вида водорослей. В течение указанного периода бентосную морскую флору отдельных островов анализировали с разной степенью тщательности. Среди островов архипелага Амакса самым изученным был Симосима (исследовано 14 точек во все сезоны), а среди островов архипелага Рюкю — Сесоко (8 точек во все сезоны). Сравнение таксономических и биогеографических характеристик морских флор этих двух архипелагов: биоразнообразия видов и форм, таксономического состава водорослевых сообществ и потенциальных возможностей географического (широтного) распространения видов — даёт нам основания классифицировать остров Симосима как теплоумеренный регион Северного полушария в Восточной Азии, а южные острова архипелага Рюкю — как тропический биогеографический регион.

Ключевые слова: макроводоросли, архипелаг Амакса, южные острова архипелага Рюкю, сравнение морской флоры

CHRONICLE AND INFORMATION

**ON THE ANNIVERSARY OF ILKHAM KHAYAM OGLY ALEKPEROV,
D. SC., PROFESSOR,
CORRESPONDING MEMBER OF THE AZERBAIJAN NAS**

On 20 November, 2023, a famous protistologist Ilkham Khayam ogly Alekperov, the head of the laboratory of protozoology at the Institute of Zoology of the Azerbaijan National Academy of Sciences, celebrated his 75th birthday.

Ilkham Khayam ogly Alekperov was born in Baku into a family of biologists. His father, PhD Khayam Mukhtar ogly Alekperov, was a famous mammalogist and author of many scientific articles and monographs. He worked at the Institute of Zoology of the Azerbaijan Academy of Sciences (hereinafter AAS). His mother, PhD Khalida Huseyn qizi Kulieva, worked at the Institute of Botany of AAS for many years. The specialty of Ilkham Alekperov's parents determined his choice, and after graduating from high school, he entered the biological faculty of the Azerbaijan State University (graduated in 1971).



While still a student, I. Kh. Alekperov was very interested in the study of freshwater ciliates and mastered modern cytological methods of silver impregnation of ciliate infraciliature and staining of their nuclear apparatus and other cellular structures. Even then, Ilkham Khayam ogly Alekperov published his first scientific articles and successfully made presentations at authoritative scientific meetings, which was rare in those days.

Right after graduating from the university, he entered the PhD graduate school at the Institute of Zoology of AAS. He was carrying out his PhD thesis in the laboratory of hydrobiology.

In 1977, I. Kh. Alekperov successfully defended his PhD thesis “Planktonic ciliates of the Mingachevir, Varvara, and Jeyranbatan reservoirs.” In plankton of these three reservoirs, he found 120 ciliate taxa, *inter alia* 1 new genus and 20 new species.

In 1975, Ilkham Khayam ogly Alekperov, along with several other junior researchers, was transferred by order of the Presidium of AAS to the laboratory of environmental physiology at the Institute of Physiology of AAS. He worked there until 1986. All these years, along with studying the use of certain ciliate species as test organisms and the development of methods for determining toxicity of heavy metals, oil products, insecticides, and other toxicants based on cellular physiological parameters (division rate, as well as disturbances in phagocytosis and osmoregulation), I. Kh. Alekperov continued analyzing species diversity and ecology of free-living ciliates in fresh waters of Azerbaijan.

His publications of that period, especially those containing descriptions of numerous new ciliate taxa, were actively cited by leading ciliatologists. Ilkham Khayam ogly Alekperov became a recognized authority in his field.

In 1986, he was transferred to the Institute of Zoology of AAS, to the laboratory of protozoology, as a senior researcher. In 1989, he headed this laboratory.

In 1987, I. Kh. Alekperov successfully defended his D. Sc. dissertation “Freshwater ciliates of artificial reservoirs in Azerbaijan” at the Leningrad State University. This defense was a real event, especially since the official opponents were recognized leaders in Soviet and world protozoology: corresponding member of the Academy of Sciences of the Soviet Union, Professor Yu. I. Polyansky, Professor L. N. Seravin, and Professor Ya. I. Starobogatov.

In addition to providing a detailed morphological description of 100 rare ciliate taxa, including 2 new genera and 40 new species, the dissertation was the first to provide data on the microzonal distribution of ciliates, as well as their daily migrations both in plankton and benthos. New patterns were established for colonization of sterile substrates by ciliates, sanitary characteristics were given for all the studied reservoirs, and the sources of their pollution were indicated. Moreover, an original method of obtaining live ciliate food for feeding larvae of commercially important fish was proposed, which was introduced at fish hatcheries in the Leningrad region.

In the late 1990s, Ilkham Khayam ogly Alekperov headed several biomonitoring projects aimed at assessing the effect on biodiversity of geological exploration in offshore oil field areas. In 2001–2007, he was a representative of the Azerbaijan National Academy of Sciences in the scientific research and biomonitoring group of British Petroleum Azerbaijan. In 2002–2010, I. Kh. Alekperov was a member and then chairman of the expert council of the department of biology and agriculture of the Higher Attestation Commission of Azerbaijan.

In 2007, he was elected a corresponding member of the Azerbaijan National Academy of Sciences. In 2009, by decision of the Higher Attestation Commission of Azerbaijan, he was awarded the academic rank of Professor. In 2009, Ilkham Khayam ogly Alekperov was appointed deputy director of the Institute of Zoology of the Azerbaijan National Academy of Sciences. He was elected director of this institute in 2011 and headed it until 2016.

Ilkham Khayam ogly Alekperov is the author and co-author of 4 monographs and more than 190 scientific articles. He developed several original methods for studying protozoans and biotesting techniques for assessing oil pollution. He described 5 families, about 20 genera, and about 200 new species



At the V European Congress of Protistology (Saint Petersburg, 2007). Professor Wilhelm Foissner (Salzburg, Austria) is pictured in the center



Sampling on Lake Baikal (2007). Professor Norbert Wilbert (University of Bonn) is pictured on the right

of ciliates and testate amoebae. Under his leadership, ten PhD theses and two D. Sc. dissertations were prepared and successfully defended. He participated in several major international projects and in numerous international scientific conferences. I. Kh. Alekperov serves on editorial boards of seven scientific journals, with one of them being “Biodiversity and Sustainable Development” published by IBSS. He is a reviewer for several top-rated international journals.

We congratulate dear Ilkham Khayam ogly Alekperov on his anniversary and wish him further fruitful work and success!

*I. Dovgal, N. Gavrilova, and A. Abibulaeva,
IBSS*

**К ЮБИЛЕЮ ДОКТОРА БИОЛОГИЧЕСКИХ НАУК, ПРОФЕССОРА,
ЧЛЕНА-КОРРЕСПОНДЕНТА НАН АЗЕРБАЙДЖАНА
ИЛЬХАМА ХАЙЯМ ОГЛЫ АЛЕКПЕРОВА**

20 ноября 2023 г. свой 75-летний юбилей отметил известный протистолог Ильхам Хайям оглы Алекперов — д. б. н., проф., член-корреспондент Национальной академии наук Азербайджана. И. Х. Алекперов, заведующий лабораторией протозоологии Института зоологии НАН Азербайджана, является автором и соавтором 4 монографий и более чем 190 научных статей, а также членом редколлегии 7 научных журналов.



Вниманию читателей!

*Институт биологии южных морей
имени А. О. Ковалевского РАН,
Зоологический институт РАН
издают
научный журнал*

*A. O. Kovalevsky Institute of Biology
of the Southern Seas of RAS,
Zoological Institute of RAS
publish
scientific journal*

**Морской биологический журнал
Marine Biological Journal**

**Морской биологический журнал
Marine Biological Journal**

- МБЖ — периодическое издание открытого доступа. Подаваемые материалы проходят независимое двойное слепое рецензирование. Журнал публикует обзорные и оригинальные научные статьи, краткие сообщения и заметки, содержащие новые данные теоретических и экспериментальных исследований в области морской биологии, материалы по разнообразию морских организмов, их популяций и сообществ, закономерностям распределения живых организмов в Мировом океане, результаты комплексного изучения морских и океанических экосистем, антропогенного воздействия на морские организмы и экосистемы.
- Целевая аудитория: биологи, экологи, биофизики, гидро- и радиобиологи, океанологи, географы, учёные других смежных специальностей, аспиранты и студенты соответствующих научных и отраслевых профилей.
- Статьи публикуются на русском и английском языках.
- Периодичность — четыре раза в год.
- Подписной индекс в каталоге «Пресса России» — Е38872. Цена свободная.

- MBJ is an open access, peer reviewed (double-blind) journal. The journal publishes original articles as well as reviews and brief reports and notes focused on new data of theoretical and experimental research in the fields of marine biology, diversity of marine organisms and their populations and communities, patterns of distribution of animals and plants in the World Ocean, the results of a comprehensive studies of marine and oceanic ecosystems, anthropogenic impact on marine organisms and on the ecosystems.
- Intended audience: biologists, ecologists, biophysicists, hydrobiologists, radiobiologists, oceanologists, geographers, scientists of other related specialties, graduate students, and students of relevant scientific profiles.
- The articles are published in Russian and English.
- The journal is published four times a year.
- The subscription index in the “Russian Press” catalogue is E38872. The price is free.

Заказать журнал

можно в научно-информационном отделе ИнБЮМ.
Адрес: ФГБУН ФИЦ «Институт биологии южных морей имени А. О. Ковалевского РАН», пр-т Нахимова, 2, г. Севастополь, 299011, Российская Федерация.
Тел.: +7 8692 54-06-49.
E-mail: mbj@imbr-ras.ru.

You may order the journal

in the scientific information department of IBSS.
Address: A. O. Kovalevsky Institute of Biology of the Southern Seas of RAS, 2 Nakhimov avenue, Sevastopol, 299011, Russian Federation.
Tel.: +7 8692 54-06-49.
E-mail: mbj@imbr-ras.ru.